

**Modelling of Suspended Solids
in Integrated Urban Wastewater Systems**

—

**Reliable and Efficient Data Collection,
Modelling and Optimization**

Thèse

Julia M. Ledergerber

Sous la direction de:

Peter A. Vanrolleghem, directeur de recherche
Thibaud Maruéjols, codirecteur de recherche

Résumé

Les avantages de la gestion intégrée de l'eau sont connus depuis des années, mais ces approches sont devenues plus importantes que jamais. Cela est reconnu dans l'objectif 6 des 17 objectifs de développement durable des Nations Unies. En ciblant à la fois l'eau potable et l'assainissement, cet objectif demande une approche intégrée car il reconnaît leur interdépendance. Cette thèse vise à faire progresser le domaine de la modélisation intégrée de l'eau, et en particulier en ce qui concerne les matières en suspension. Les émissions globales de l'assainissement ont gagné en intérêt puisque les normes de qualité de l'eau sont étendues de la station de récupération des ressources de l'eau au réseau d'égout. La modélisation intégrée permet d'évaluer les interactions et d'estimer les émissions en plus des mesures de la qualité de l'eau (encore) rares. Les particules peuvent être considérées comme un indicateur de la qualité de l'eau couvrant la pollution particulaire, mais aussi les matières organiques, les nutriments et les substances telles que les micro-polluants hydrophobes. L'approche de modélisation choisie est conceptuelle, pour ses calculs rapides, et basée sur la distribution de la vitesse de décantation des particules, partout où la décantation et la remise en suspension sont les processus caractéristiques. L'approche est complétée par d'autres modèles pour couvrir le système du bassin versant jusqu'à la station de récupération des ressources de l'eau.

Un modèle intégré nécessite de nombreuses données. Pour une collecte de données efficace, premièrement, une procédure est établie pour construire un modèle conceptuel d'égout à partir d'un modèle hydraulique détaillé. Deuxièmement, une méthodologie de conception expérimentale optimale est adaptée à l'environnement complexe des égouts pour une campagne de mesure de la qualité de l'eau. L'utilité de l'approche de la distribution de la vitesse de décantation des particules est ensuite démontrée en calibrant et en validant le modèle pour un site pilote. Une procédure est élaborée pour tenir compte de l'incertitude des paramètres et de la variabilité des données d'entrée afin d'identifier des points de contrôle fiables. La procédure est utilisée pour la réduction d'émission des particules, facilitée par le calcul rapide du modèle car plusieurs analyses de sensibilité sont demandées. Le dernier chapitre termine la thèse par l'évaluation pratique des stratégies visant à réduire les émissions globales. La thèse fait ainsi progresser le domaine de la modélisation intégrée des particules et fournit en même temps des procédures qui permettent de surmonter les obstacles généraux à la modélisation en mettant l'accent sur la collecte de données fiables et efficaces, la modélisation ainsi que l'optimisation.

Abstract

The advantages of integrated water management have been known for decades, but are more than ever important. This is acknowledged in goal six of the 17 sustainable development goals of the United Nations. By targeting both clean water as well as sanitation, this goal is inherently asking for an integrated approach since it recognizes their interdependence. This dissertation aims at advancing the field of integrated water systems modelling in general, and in particular with respect to suspended solids. Overall emissions from the integrated urban wastewater system have gained interest since water quality standards are increasingly extended from the water resource recovery facility to the sewer system. Integrated modelling allows evaluating interactions and estimating overall emissions complementary to the not (yet) abundant water quality measurements. For this evaluation suspended solids can be seen as an indicator for the receiving water quality covering particulate pollution as such, but also undesired organic matter, nutrients and substances such as hydrophobic micropollutants. The modelling approach chosen is conceptual, due to its rapid calculations, and based on the particle settling velocity distribution wherever settling and resuspension are the characteristic processes of suspended solids. The approach is extended with complementary models to cover the integrated system from the catchment down to the water resource recovery facility.

The development of an integrated model however requires vast data sets. First, for efficient data collection a procedure is established to build a fast conceptual sewer model from its detailed hydraulic counterpart. Second, an optimal experimental design methodology is adapted to the challenging sewer environment for the efficient planning of a water quality measurement campaign. The usability of the particle settling velocity approach is then shown by calibrating and validating the model for a case study. A procedure is developed to consider parameter uncertainty and input variability to identify reliable control handles. The procedure is applied for the abatement of total suspended solid, facilitated by the comparably low computational demand of the model, as the procedure asks for multiple global sensitivity analyses. The last chapter closes the dissertation with the practical application of evaluating different strategies to reduce the total suspended emissions to the receiving water. The dissertation thus advances the field of integrated modelling for particulates and at the same time provides procedures which overcome barriers general to modelling focusing on reliable and efficient data collection, as well as optimization.

Contents

Résumé	ii
Abstract	iii
Contents	iv
List of Tables	vii
List of Figures	viii
List of Abbreviations	x
Acknowledgements	xiii
Foreword	xv
Introduction	1
Rationale	1
Problem Statement and Objectives	3
Dissertation Outline, Contributions and Originality	9
Literature Review	10
1 Case Study Description - Clos de Hilde Catchment	23
1.1 Catchment and WRRF overview	23
1.2 Control of Chemically Enhanced Primary Treatment	27
1.3 Data from the Utility	28
1.4 Data from Measurement Campaigns	30
2 An Efficient and Structured Procedure to Develop Conceptual Catchment and Sewer Models from Their Detailed Counterparts	35
2.1 Abstract	35
2.2 Résumé	36
2.3 Introduction	36
2.4 Materials and Methods	38
2.5 Proposed Methodology	41
2.6 Results	44
2.7 Discussion	51
2.8 Conclusions	52

3	Optimal Experimental Design for Calibration of a New Sewer Water Quality Model	54
3.1	Abstract	54
3.2	Résumé	55
3.3	Introduction	55
3.4	Material and Methods	57
3.5	Results	63
3.6	Discussion	70
3.7	Conclusions	71
4	Calibration and Validation of a PSVD-based Model of TSS in Integrated Urban Wastewater Systems	73
4.1	Abstract	73
4.2	Résumé	74
4.3	The PSVD Modelling Approach	74
4.4	Description of Subsystem Models	77
4.5	Calibration and Validation Approach	89
4.6	Calibration and Validation Results	93
4.7	Illustration of Changes in PSVD Curves along the IUWS	105
4.8	Discussion and Conclusion	107
5	Selection of Effective Control Handles for Integrated Urban Wastewater Systems Management considering Parameter Uncertainty and Input Variability	113
5.1	Abstract	113
5.2	Résumé	114
5.3	Introduction	114
5.4	Proposed Procedure	116
5.5	Material and Methods	116
5.6	Results and Discussion	120
5.7	Conclusion	122
6	Integrated Modelling Study – Evaluating Scenarios Tackling the Issue of Total Suspended Solids Emission	124
6.1	Abstract	124
6.2	Résumé	125
6.3	Introduction	126
6.4	Material and Methods	127
6.5	Results	131
6.6	Conclusion	144
	Conclusions and Perspectives	147
	Conclusions	147
	Perspectives	149
A	Tabulated Performance Conceptual Models in Comparison to Detailed Models	151

B	Tabulated Parameter Values, Calibration and Validation Results	156
C	Tabulated Results Analysis Scenarios	160
	References	183

List of Tables

0.2	Minimum Requirements WRRF Performance France	22
1.1	Description Tributaries WRRF CdH	26
1.2	Overview Measurement Campaigns	30
2.1	Project Definition of Case Studies	45
2.2	Summary Calibration and Validation Results	46
2.3	Comparison Detailed and Conceptual Models	46
2.4	Comparison Model V1 and V2 for Ottawa	47
2.5	Comparison Conceptual Models with Flow Measurements	49
3.1	Evaluation OED Scenarios for NT and CdH	67
4.1	Calibration and Validation Points	90
5.1	Studied Control Handles	118
5.2	Parameter Uncertainty for Control Handle Evaluation	119
5.3	Input Variability for Control Handle Evaluation	119
6.1	Measures: Changed Capacities	129
6.2	Measures: Control RTs	129
6.3	Analyzed Scenarios for TSS Load Reduction	130
6.4	Evaluation Periods for TSS Load Reduction	131
6.5	Compliance Estimation	144
A.1	Performance Ottawa Case Study	152
A.2	Performance CdH Case Study	154
B.1	Calibrated Parameters and Values	157
B.2	Detailed Calibration Results	158
B.3	Detailed Validation Results	159
C.1	Evaluation Period RE1	161
C.2	Evaluation Period RE2	162
C.3	Evaluation Period RE3	163
C.4	Evaluation Period RE4	164
C.5	Evaluation Period RE5	165
C.6	Evaluation Period 120d	166

List of Figures

0.1	Components of Integrated Assessment	11
0.2	Interacting Effect of Measures	13
0.3	Transport Processes Sewer Sediments	20
1.1	Map of France indicating Bordeaux	24
1.2	WRRFs of the Bordeaux Urban Community	24
1.3	CdH Catchment Overview	25
1.4	CdH WRRF Layout	27
1.5	Turbidity Measurements on WRRF CdH	29
1.6	Installation Online Monitoring Station RSM30	31
1.7	Maintenance Sensors	32
1.8	Illustration Sampling at NT	33
1.9	Experimental Set-Up ViCAs	33
2.1	Map of the Ottawa Case Study	39
2.2	Map of the Bordeaux Case Study	40
2.3	Proposed Conceptual Modelling Procedure	41
2.4	Conceptualization Schema for Catchments and Sewers	43
2.5	Schema Calibration Order	45
2.6	Comparison Flow of Model V1 and V2	48
2.7	Comparison Conceptual Model with Flow Measurements	49
2.8	Comparison Recalibrated Conceptual Model with Flow Measurements	50
3.1	Potential Measurement Locations for RSM30 Station	58
3.2	Preliminary Model Validation for OED	60
3.3	OED Methodology	60
3.4	Measurement Error for TSS at NT	64
3.5	Evaluation Measurement Location	66
3.6	Evaluation Best Measurement Scenario	66
3.7	Relative Parameter Estimation Error	68
3.8	Definition Distance to Measurement	69
3.9	Comparison Parameter Location and Relative Parameter Estimation Error	70
3.10	Detailed DWF Evaluation	70
4.1	Overview Models	75
4.2	PSVDM TSS Fractionation	76
4.3	Catchment Model	77
4.4	Zone of PSVD Measurements for CdH Catchment	79
4.5	PSVD Sewer Model	81

4.6	Sigmoidal Behavior of Resuspension	82
4.7	PSVD RT Model	82
4.8	PSVD PC Model	84
4.9	PSVD GC Model	85
4.10	Effect of CEPT on PSVD	86
4.11	PSVD Curve for CF Saturation	87
4.12	Modelled Effect of CEPT	88
4.13	Simple BF Model	89
4.14	Depth-Duration-Curve for Rain Events Case Study	91
4.15	Calibration Water Quantity Model at WRRF	94
4.16	Calibration Water Quantity Model in Sewer	95
4.17	Calibration Water Quality Model	96
4.18	Validation Period 1 Water Quantity Model at WRRF	98
4.19	Validation Period 1 Water Quantity Model in Sewer	99
4.20	Validation Period 1 Water Quality Model	100
4.21	Validation Period 4 Water Quantity Model at WRRF	102
4.22	Validation Period 4 Water Quantity Model in Sewer	103
4.23	Validation Period 4 Water Quality Model	104
4.24	Location for Illustrations PSVD Curves	105
4.25	Illustration PSVD Curves in IUWS	107
4.26	Map with Location of Overflows	108
4.27	Modelled TSS Fluxes towards Receiving Water	109
4.28	Modelled TSS Fluxes including Sludge Line	109
4.29	Comparison Flow & TSS Concentration and Flow & TSS Flux	111
5.1	Procedure Evaluation Control Handles under Uncertainty	116
5.2	Map of Studied Control Handles	117
5.3	Control Handle Ranking under Uncertainty	121
5.4	SRC Values of Control Handles	122
6.1	Map of Measures and Overflows CdH	128
6.2	Outflow and By-Pass WRRF CdH	128
6.3	TSS Loads Evaluation Period RE1	132
6.4	TSS Loads Evaluation Period RE2	136
6.5	TSS Loads Evaluation Period RE5	138
6.6	TSS Loads Evaluation Period RE4	140
6.7	TSS Loads Evaluation 120 d	142

List of Abbreviations

AR	Arcins
BF	Biofilter
BP	By-pass
BT	Bastide
BOD5	5-day biochemical oxygen demand
COD	Chemical oxygen demand
CdH	Clos de Hilde
CEPT	Chemically enhanced primary treatment
CF	Coagulant, flocculant
CSO	Combined sewer overflow
CSTR	Completely stirred tank reactor
CV	Carle Vernet
DWF	Dry weather flow
FIM	Fisher Information Matrix
GC	Grit chamber
GSA	Global sensitivity analysis
IM	Integrated modelling
IUWS	Integrated urban wastewater systems
JR	Jourde
NT	Noutary
OED	Optimal experimental design
PC	Primary clarifier
PE	Person equivalents
PSVD	Particle settling velocity distribution
PSVDM	Particle settling velocity distribution model
RMSE	Root Mean Square Error
RT	Retention tank
RTC	Real time control
SA	Siphon d'ars
SE	Saint Émilion

SJ	Saint Jean
SRC	Standardized regression coefficient
TR	Thiers
TSS	Total suspended solids
ViCAs	Vitesse de chute en assainissement (settling velocity in sanitation)
WFD	Water Framework Directive
WRRF	Water resource recovery facility
WWF	Wet weather flow

Das Leben muss nicht leicht sein,
wenn es nur inhaltsreich ist.

Lise Meitner

Acknowledgements

During the last four years, I worked and discussed with, and sometimes simply enjoyed the company of wonderful, knowledgeable, and inspiring people – I am so grateful for having had this opportunity! I would like to thank all of you wholeheartedly, those mentioned by name and those who I unintentionally forgot!

I would like to thank my supervisor *Peter A. Vanrolleghem*. Peter, thank you for accepting and supporting me as one of your PhD students in your wonderful modelEAU research group. You are a visionary and a true source of inspiration to me. I would also like to thank my co-supervisor *Thibaud Maruéjols* from the *Le LyRE* team. Thibaud, thank you for having made this collaborative PhD project possible and for your insights and support all along the way, especially during the measurement campaigns.

I would also like to express my gratitude towards the members of my jury *Sophie Duchesne*, *Paul Lessard* and *Peter Krebs*, whose in-depth comments were not only very much appreciated but also greatly improved this research.

I would also like to thank *Dirk Muschalla* from TU Graz, whom I had the chance to meet on multiple occasions during my PhD. Dirk, regardless of whether we met during one of your research visits at modelEAU or at an international conference, I could not have wished for better advice.

Of course, I would also like to thank the former and the current modelEAU research team. Not only were you *Sovanna*, *Leila*, *Andreia*, *Asma*, *Bernard*, *Claudia*, *Cyril*, *Elena*, *Feiyi*, *Gamze*, *Jean-David*, *Jean-Matthieu*, *Jessy*, *Maryam*, *Maxine*, *Niels*, *Queralt*, *Rania*, *Romain*, *Sey-Hana*, *Sylvie*, *Thomas* and *all of you that I inadvertently forgot* available for a lot of research discussions, but I can say with great pleasure that we became friends.

I would also like to thank the *Le LyRE* team in general and especially *Guillaume Binet* for your support of the project and welcoming me as one of yours during my stays in Bordeaux. I would also like to thank the two interns, *Émilie Leray* and *Julie Langlois*, who were a tremendous support during the measurement campaigns. I am very well aware of the fact that our job was far from easy and still you persisted!

I would also like to thank the *CdH WRRF* team. I would like to thank particularly *Emmanuel Cottin* and *Guillaume Bain* not only for welcoming me openheartedly at your WRRF, but also for your support of the research project by answering all sorts of questions that I had and for the trust you placed in me. I would also like to thank not only those who taught and played “tarot” with me at lunch, like *Jérémy* or *Vanessa*, but also those of you of the group “belote”, like *Vincent* and *Davide*. Without you and the support of your colleagues, my work would not only have been far less pleasant, but simply impossible.

Without mentioning all of you by name, you know it in your heart, I would also like to thank my family and friends, both here and far, for not only listening to me when everything went perfect, but for your support and your understanding during the – rare but nevertheless existing – somewhat more difficult periods when I was maybe a little bit less bearable. And then there is *Alex*. Thank you, you are the best support I could ever wish for!

Foreword

This dissertation was written in the framework of the research project MOSAIQUE, the French abbreviation of ‘MODélisation du Système d’Assainissement Intégré basée sur la QUALité des Eaux’, which stands for modelling the integrated urban wastewater system based on water quality.

This research project includes both theoretical and paractical work packages. The theoretical work packages were mainly conducted at Université Laval in Québec, Canada, in the model*EAU* research group under the supervision of P.A. Vanrolleghem. The practical work was conducted at the Clos de Hilde (CdH) water resource recovery facility (WRRF) in Bordeaux, France, in collaboration with the research center Le LyRE, Suez, Talence, France, under the supervision of T. Maruéjols, the co-supervisor of this dissertation. The practical work packages consisted of the three measurement campaigns conducted during the following periods of the research project:

- September 2016
- May to August 2017
- May to July 2018

This research project was funded by a Collaborative Research and Development grant of the Natural Sciences and Engineering Research Council (NSERC) and Suez Treatment Solutions Canada. Additional important technical, financial and in-kind support was obtained from Bordeaux Metropole, Société de Gestion de l’Assainissement de Bordeaux Métropole (SGAC) and Le LyRE. Several presentations of the project were supported by CentrEau, the Quebec Water Research Centre funded by FRQNT.

The dissertation is presented in a paper format, each chapter representing one paper. One additional chapter aggregates information on the case study set-up. The presented papers were redrafted in order to avoid the repeated description of the case study in the following chapters. Only the absolutely necessary information is presented for the understanding of each chapter on its own. The papers are not presented chronologically, but ordered in a logical manner,

allowing successive chapters to build upon previous ones. The following peer-reviewed papers are included as chapters in the dissertation:

- Chapter 2: Ledergerber, J., Pieper, L., Binet, G., Comeau, A., Maruéjols, T., Muschalla, D., and Vanrolleghem, P. A. (2019). An efficient and structured procedure to develop conceptual catchment and sewer models from their detailed counterparts. *Water*, 11(10):2000.
- Chapter 3: Ledergerber, J. M., Maruéjols, T., and Vanrolleghem, P. A. (2019). Optimal experimental design for calibration of a new sewer water quality model. *Journal of Hydrology*, 574:1020-1028.
- Chapter 4: Ledergerber, J. M., Maruéjols, T., and Vanrolleghem, P. A. Calibration and validation of a PSVD-based model of TSS in integrated urban wastewater systems. *In preparation*.
- Chapter 5: Ledergerber, J. M., Maruéjols, T., and Vanrolleghem, P. A. (2019). No-regret selection of effective control handles for integrated urban wastewater systems management under parameter and input uncertainty. *Submitted to Water Science & Technology*.
- Chapter 6: Ledergerber, J. M., Maruéjols, T., and Vanrolleghem, P. A. Integrated modelling study – evaluating scenarios tackling the issue of total suspended solids emission. *In preparation*.

The authors' contributions to the publication are indicated at the beginning of the corresponding chapters.

Introduction

Rationale

The Brundtland report was published more than 30 years ago, but its definition of sustainable development as development that meets the needs of the present without compromising the ability of future generations to meet their own needs (World Commission on Environment and Development (WCED), United Nations, 1987) has neither lost any of its strength nor importance. Sustainable development still faces manifold global challenges related to poverty, inequality, climate, environmental degradation, prosperity, and peace and justice (United Nations, 2019). This is why the United Nations has adopted the 2030 Development Agenda with the 17 sustainable development goals. Goal 6 targets clean water and sanitation by 2030 (United Nations, 2019). This goal is thus at the core of this dissertation project since it inherently advocates for an integrated approach, acknowledging that clean water cannot be achieved without adequate sanitation. Holistic approaches are thus more than ever important.

The integrated approach towards water and sanitation is not novel. Nearly forty years ago Beck (1981) was already convinced that he was taking the “risk of stating the obvious” when defining the desirable attributes of water quality management:

- adaptable, flexible, integrated, and coordinated;
- an understanding of the trade-offs between and interactions among multiple objectives and problems;
- safe failure and contingency planning.

He was thus advocating holistic water quality management.

During the same period of time, the first studies started in which the interactions between different sub-systems of the urban water cycle were analyzed by evaluating the effect of a rain event on the receiving water with a vast measurement campaign throughout the system (Gujer et al., 1982). The results clearly showed the complexity and multiple interactions of the different subsystems of the integrated urban wastewater system (IUWS). The study also

pointed out that, due to the complexity of the system, multiple solutions addressing different pollutants and challenges in the environment might be necessary.

An alternative and complementary approach to extensive measurement campaigns is the modelling of the interactions of the different subsystems, known as integrated modelling (IM). The **definition of IM** applied here is based on the definition in Rauch et al. (2002), where IM is defined as “**modelling of the interaction between two or more physical systems, i.e. sewer system, treatment plant and receiving water**”. The subsystems considered for modelling in this dissertation are the catchment, the sewer system and the water resource recovery facility (WRRF). As explained in Rauch et al. (2005), IM is a holistic approach, but while it does not strive for global completeness, it includes all relevant issues regarding a particular problem and system.

The **modelling approach** chosen for this dissertation strives for a better understanding of the behavior of particulates in the IUWS. Particulates have been studied already at the time when the first major pipe installations for the transport of wastewater in the 1850s were constructed (Mattsson et al., 2015). They are known to cause operational issues, such as blockages (Ashley et al., 2004), and are widely acknowledged to be a major source of pollution (Ashley et al., 1994). The pollution of total suspended solids (TSS) is, however, not limited to particulate pollution as such, since TSS can be seen as an indicator substance, transporting also organic matter, nutrients and other pollutants such as adsorbed heavy metals and hydrophobic micropollutants (Vanrolleghem et al., 2018). The extensive research on particulates by Michelbach (1995) concluded that the settling velocity is an appropriate instrument for describing sedimentation, transport and erosion of settleable solids. The modelling approach chosen in this dissertation is thus based on the **particle settling velocity distribution (PSVD)**, a characteristic of TSS which can be obtained via the ViCAs experiment (Chebbo and Gromaire, 2009). ViCAs is the French acronym for “Vitesse de chute en assainissement” which stands for particle settling velocity in sanitation.

While the advantages of IM have been known for decades (Beck, 1976; Bach et al., 2014), IM still faces many challenges with regard to the practical application (Mollerup et al., 2013), such as submodel compatibility (Rauch et al., 2002), data availability (Langeveld et al., 2013a) and uncertainty (van Daal et al., 2017).

The dissertation strives to advance the field of integrated water quantity and quality modelling in order to better describe wastewater pollution emission to receiving waters. This is achieved by further developing the particular PSVD-based IM approach. This approach emphasizes the understanding and description of the transport, dynamics and fate of particulates in the IUWS (Vanrolleghem et al., 2018). The gained knowledge can help to prioritize between possible actions - operational changes or investment in infrastructure - for pollution abatement.

In addition, this dissertation aims at developing tools overcoming general barriers of mod-

elling, independent of the modelling approach chosen. The developed tools focus on effective data collection from either already available data in a more detailed model or by planning measurement campaigns most efficiently by applying a model-based optimal experimental design (OED) methodology. Uncertainty issues are addressed by providing a tool that allows incorporating parameter uncertainty and input variability when searching for the most efficient control handles for emission reduction, for example.

Problem Statement and Objectives

Problem Statement

The advantages of IM have been known for decades (Bach et al., 2014). In the water community, it is, however, also commonly acknowledged that not only the design but also the operation and with it the optimization of different parts of the urban wastewater system are often conducted at subsystem level rather than in an integrated approach (Mollerup et al., 2013). This entails that, for example, sewers and WRRF are usually dealt with independently (Vanrolleghem et al., 1996; Rauch et al., 2005). This is also reflected in the administrative fragmentation of the different subsystems, which is found to be a key barrier against IM (Bach et al., 2014).

However, there is a clear willingness and tendency to change. While the early phase of IM focused on the proof of concept supported by semi-empirical case studies (Vanrolleghem et al., 2005b), the more recent developments have been more applied and in some cases successfully implemented. Examples of such early adopters would be: Odenthal, Germany (Erbe et al., 2002); Odense (Fryd et al., 2010) and Copenhagen (Vezzaro and Grum, 2014), Denmark; Garriga and Granollers, Spain (Prat et al., 2012); Eindhoven, The Netherlands (Benedetti et al., 2013b) and Lemgo, Germany (Seggelke et al., 2017). This change came about thanks to the openness of both the early adopters of the operating utilities and communities and thanks to changes in legislation (for example, the Water Framework Directive, Europe; Integrated Planning and Permitting Initiative under the Clean Water Act, USA; STORM guideline, Switzerland).

Nevertheless, challenges for IM remain:

Challenge 1: Description of fate of particulates in IUWS Although understanding the behavior of particulates in the IUWS has been debated and researched since the 1850s (Mattsson et al., 2015), understanding, describing and eventually predicting the processes related to particulates remain a considerable challenge (Vanrolleghem et al., 2018). Bertrand-Krajewski (2007) concluded that the weak point of IUWS modelling studies remains the poor description of water quality models in the sewer system. It is estimated that the uncertainties associated with the water quality models are generally an order of magnitude higher than for

the water quantity models (Willems, 2008). With respect to particulates in particular, it was even found that the particulate processes occurring in the sewer system, such as sedimentation and resuspension, are a major challenge for IM (Benedetti et al., 2013a). A recent review on particulates modelling reveals that different models exist, but that they lack sufficient detail to capture the complex processes in wastewater (Murali et al., 2019).

The development of adequate modelling approaches for TSS in the IUWS is complicated by the practice that models and thus the modelling approaches of the subsystems are traditionally developed independently (Erbe et al., 2002), making the harmonization of system interfaces necessary (Schmitt and Huber, 2006). The tendency exists for the sewer system to be hydraulically analyzed in great detail (see, for example Bilodeau et al., 2018; Shishegar et al., 2019) and in advanced cases even operated with real time control (RTC), see e.g. Pleau et al. (2005); Puig et al. (2009); Andréa et al. (2013) and Männig and Lindenberg (2013), but quality aspects and especially the fate of solids are ill-described (Bertrand-Krajewski, 2007). Therefore, the assessment of sewers is often based solely on water quantity aspects. For the biological treatment on the WRRF, however, water quality models are well developed (see, for example, the ASM model family by the IWA task group: ASM1, ASM2, ASM2d and ASM3 (Henze et al., 2006)). This results in the challenge of IM that each submodel (i.e. catchment, sewer, treatment, river) uses different variables (Rauch et al., 2002). This means that the variables are incompatible and thus require reconciliation, as suggested by Fronteau et al. (1997), or require a transformation model from one submodelling approach to another submodelling approach (Benedetti et al., 2004; Vanrolleghem et al., 2005a). Lijklema et al. (1993) concluded that joint approaches including both the sewer systems and the WRRF are required, as far as this is possible. Previous research has shown that the critical phenomenon for the description of the particulates is the settling velocity (Michelbach, 1995). It is thus necessary to look at the distribution of the settling properties as an important approach to modelling the fate of particulates throughout the IUWS, which would constitute a consistent IM approach that allows quantifying both flow and TSS over the different subsystems.

Challenge 2: Data availability The last point of the previous challenge directly leads us to the challenge of data availability. Assuming that a suitable IM approach for particulates is found, obtaining the necessary data for model calibration and validation results in an additional challenge. A potential approach for modelling particulates is, for example, the one presented by Tränckner et al. (2008), using different particulate fractions depending on their size and density. Although the general applicability was shown for a virtual sewer system, its practical applicability to a real case study remained limited by the tremendous need for measurement data. This statement was formulated in a more generalized way by Bertrand-Krajewski (2007), who concluded that, compared to the present practice, collecting more and reliable data is absolutely necessary. For the further model development this entails that it should mainly focus on water quality data collection, which would not only reduce the

problems of inadequate model calibration and validation, but also fill the knowledge gaps in in-sewer processes (Willems, 2008).

While data collection for a submodel might be feasible, measurement campaigns for the parameter identification of models covering the entire IUWS become massive (Vanrolleghem et al., 1999). A fallback on already existing data is especially difficult in the field of sewer systems, since data availability is generally rare both in research and practical applications (Freni and Mannina, 2012). This is due to their labor- and cost-intensive installations, and issues with incorrect and unstable measurements are common and need to be resolved for successful IM (Seggelke et al., 2005). Langeveld et al. (2013a) even concluded that the successful applications of IM are relatively scarce due to the lack of high-quality monitoring data. They found the reason for this lack not to be the state of the art of monitoring itself, but the practical limitations which result in incomplete data-sets. Recognizing that collecting data remains challenging, we believe that it is important to develop tools which reuse already available information, collected, for instance, in a detailed submodel, in the most efficient manner and to have tools available to allocate the resources of a measurement campaign most efficiently.

Challenge 3: Model use under uncertainty As discussed previously, many studies showed successfully how IM can identify strategies that lead to improved receiving water quality (see, for example, Vanrolleghem et al., 1996; Maruéjols et al., 2011; Benedetti et al., 2013b; Vezaro and Grum, 2014; Tik et al., 2015 and Seggelke et al., 2017). Since a model is not a perfect representation of reality, uncertainty considerations are of special importance (Beck, 1987; Belia et al., 2009; Deletic et al., 2012). In the context of water quality modelling uncertainty links with the previous challenge of data availability. Mannina and Viviani (2010) concluded that, especially, with respect to water quality, data requirements are extensive, but availability is usually limited, which burdens the quality models with large uncertainties. In the theory it is known that control needs to be evaluated under uncertainty considerations (see, for example, Duchesne et al., 2001; Benedetti et al., 2012). A review of the performance of integrated RTC in practice, however, concluded that the two main deficiencies are, on the one hand, omitting the uncertainty analysis and, on the other hand, applying limited evaluation periods and thus limiting the variability of rain events (van Daal et al., 2017). However, performing an uncertainty analysis for the evaluation of different scenarios is often time consuming due to the multitude of model evaluations required (Benedetti et al., 2012).

A model covering the entire IUWS provides a wide range of potential modifications to different subsystems, named here after control handles, to improve receiving water quality. The selection of the most effective control handles among the numerous potentially available control handles remains a major challenge (Saagi et al., 2018). Multiple studies in the field of IM have used a global sensitivity analysis (GSA) to identify the most influential control handles prior to the development of scenarios (Benedetti et al., 2012; Langeveld et al., 2013b; Corominas

and Neumann, 2014; Sweetapple et al., 2014; Saagi et al., 2018). When models are used to support decision management, Refsgaard et al. (2007) have concluded that the assessment of uncertainties is of paramount importance. As van Daal et al. (2017) have found that parameter uncertainty and the evaluation period are indispensable for the evaluation of uncertainty, it can be concluded that the need remains to develop a procedure which includes these factors during the selection of the control handles. Only if these factors are included, potential deviations between model and reality are factored into the evaluation. Omitting this might result in a control handle selection that fails the expectation when implemented in reality. Thus, considering parameter uncertainty and the evaluation period already in the evaluation of the control handles will result in a no-regret selection of control handles.

Objectives

The objectives for this dissertation are manifold, but have the common driver to advance the field of IM. The first objectives are directly related to the particular IM approach adopted in this dissertation and the demonstration of its practical applicability in a case study. The approach chosen is the PSVD approach which addresses the **Challenge 1: Description of fate of particulates in IUWS** over a wide range of submodels. As described previously, the PSVD approach focuses on the settling velocity, which was found to be a key characteristic for the description of TSS behavior. The implementation of the approach in a conceptual modelling environment also addresses the **Challenge 3: Model use under uncertainty**. Conceptual models have low computational needs and thus facilitate the inclusion of uncertainty analysis in model evaluations, as they require large numbers of simulations.

The second set of objectives is related to developing tools to overcome general barriers of modelling, and are thus independent of the modelling approach chosen in this dissertation. They should thus make all types of integrated models more feasible. They address the **Challenge 2: Data availability** and the **Challenge 3: Model use under uncertainty**.

The objectives of this dissertation are formulated as follows:

1. To further advance the development of a PSVD-based integrated quantity and quality model to better describe the transport and fate of solids in the IUWS. The approach focuses on the key characteristic of the settling velocity of TSS and thus eliminates the need of transforming variables between different submodel approaches:
 - a) Extend the existing data set of the case study with a dedicated measurement campaign to obtain a full data set for PSVD modelling and adapt the maintenance protocol for online sensors from the WRRF to the sewer (Chapter 1).
 - b) Proof the usability of the PSVD concept by calibrating and validating the PSVD-based model for a “real world” case study (Chapter 4).
 - c) Verify the practical application of PSVD-based IM by evaluating different strategies to minimize the emission of particulates towards the environment for the case study during mid-sized summer storms (Chapter 6).
2. To overcome barriers general to modelling, independent of the IM approach chosen:
 - a) Make most efficient use of already available information when developing an IM by providing a procedure to develop a conceptual catchment and sewer model from its detailed counterpart (Chapter 2).
 - b) Provide a tool to collect the most information-rich data during measurement campaigns by demonstrating the feasibility of model-based OED to complex models (Chapter 3).

- c) Providing a procedure to select the most effective no-regret control handles by considering parameter uncertainty and input variability (Chapter 5).

Dissertation Outline, Contributions and Originality

This thesis is presented in a paper format. Each chapter thus presents a paper, apart from the condensed chapter for the case study description of Clos de Hilde (CdH) in Bordeaux, France. The presented papers were redrafted in order to avoid unnecessary repetition of the information regarding the case study. The chapters are ordered in a logical way, building on one another. The individual contributions of the co-authors are given at the beginning of each chapter.

Chapter 1 gives an overview of the case study and describes the measurement campaigns to obtain the necessary data for the development of the PSVD-based integrated model. This chapter as such does not provide a novel approach; the description of the case study, however, is necessary to understand the case study-related results. This chapter also includes the description of the data provided by the utility as well as the description of the collected data during the labor-intensive measurement campaigns.

Chapter 2 presents a general procedure to develop a conceptual model from its detailed counterpart. Although it is common to build a conceptual model based on the detailed model, no methodology was previously reported in the literature. The procedure is validated with two independent combined sewer case studies.

Chapter 3 adopts a model-based OED methodology to efficiently plan a measurement campaign for final model calibration and validation of a new sewer water quality model. In comparison to previous studies, the methodology considers the actual measurement error characteristics when calculating the information content of measurement data.

Chapter 4 presents the PSVD approach to assess particulate behavior in the sewer, the RTs, the grit chamber (GC) and the primary clarifier (PC). The approach is extended with a catchment and a simple biofilter (BF) model, relevant for the biological treatment at the WRRF of the case study. The approach is validated by successfully calibrating and validating the integrated model for all the described sub-systems of the case study.

Chapter 5 proposes a procedure to select control handles under parameter uncertainty and input variability. The existing methodology for selecting the most effective control handles with a GSA is extended with an approach which explicitly considers parameter uncertainty and input variability. The procedure is applied to the case study to make a no-regret selection of the control handles for the development of scenarios that permit emission reduction.

Chapter 6 evaluates different scenarios based on the previously selected control handles. This allows confirming the benefits of a practical application of PSVD-based IM for the case study.

Literature Review

This literature review addresses the overall topics of this dissertation. The literature specific to the topic of each chapter will be addressed in the introduction to the corresponding chapter and is not repeated here to avoid repetition. This section addresses the topics of Integrated Modelling, Focus on Particulates and Project-Relevant Regulations Regarding the Case Study CdH.

Integrated Modelling

Historical Development

The field of integrated modelling (IM) is vast and many different models exist – and almost as many definitions of IM. According to Bach et al. (2014), the different models found in the literature can generally be classified in four levels of integration. At the first level, the integrated component-based models, different components of the same sub-system are modelled, such as several treatment processes within a WRRF, often also referred to as plant-wide modelling. Typical examples of this subcategory are the Benchmark Simulation Models (BSMs), of which different versions have been developed (see, for example, Copp, 2002; Rosen et al., 2004; Nopens et al., 2010). Bach et al. (2014) defines the second level of integration as the integrated urban drainage models, which extend the scope of the previous category to urban drainage. The third and fourth levels extend the scope even further, to integrate across the total urban water cycle (level 3), respectively integrating across different disciplines (level 4), such as societal models, while retaining a water-centric focus. The definition of IM as modelling the interactions between catchment, sewer and WRRF as applied in this dissertation (see Rationale) corresponds to the second level of integration of Bach et al. (2014).

In the late 1970s and 1980s, the first integrated approaches were developed and the effect of the sub-systems on the entire system was questioned and studied (see, for example, Beck, 1976, 1981 and Lindholm, 1985). Figure 0.1 is one of the first graphics showing the different components of the integrated system. It is interesting to note that the first mention of the integrated approach concept referred to it as ‘operational water quality management’ actually highlighting the purpose of the approach (Beck, 1976). The first integrated physical study was carried out in Zurich, Switzerland, where measurements were simultaneously taken in the catchment, sewer, WRRF, river and groundwater during and after a rain event (Gujer et al., 1982).

Initial modelling studies confirmed the advantages of the integrated approach, such as the work presented by Lessard (1989), who modelled stormwater discharges from combined sewer overflows (CSO) and the WRRF and evaluated potential hydraulic control strategies. He found that the state of the river will strongly influence the control strategy ultimately chosen. Additional early studies confirming the positive effect of IM can be found in Lessard (1989),

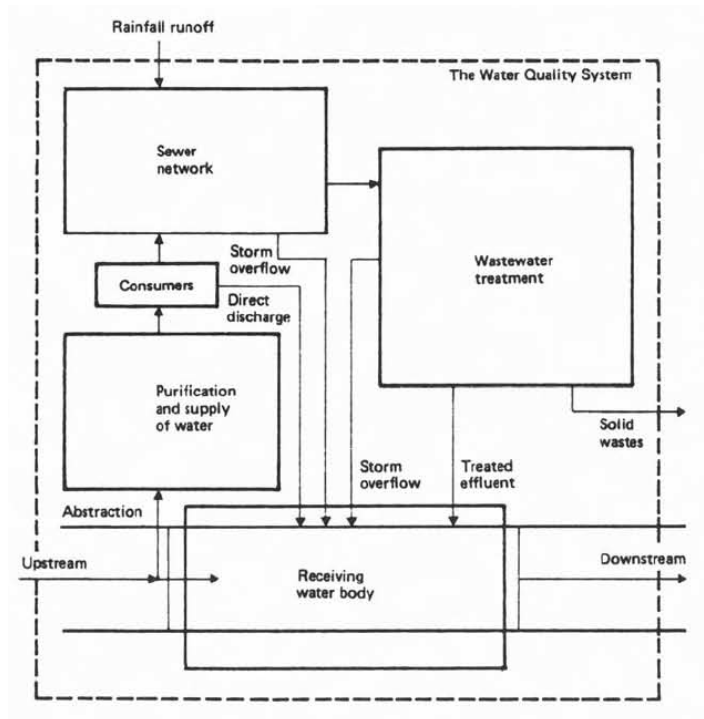


Figure 0.1: This graph published in Beck (1981) represents the different components (abstraction, purification and supply of potable water as well as the sewer network, the WRRF and the receiving water body) of integrated approaches referred to as operational water quality management.

Lessard and Beck (1990), or Beck and Reda (1994).

A second wave of IM studies appeared in the 1990s, and the idea was widely spread by different research groups who advanced the field. In comparison to the initial studies, the second wave was more applied. A case in point is Gustafsson et al. (1993), who evaluated different pumping operations for the optimal operation of the WRRF in Göteborg, Sweden. Another convincing study is the case of Brussels, Belgium, which directly considered the receiving water quality when discussing the implementation of storage tanks in the sewer system (Vanrolleghem et al., 1996). The hypothetical study by Harremoës and Rauch (1996) showed that especially for the issue of oxygen depletion in the receiving water both the CSOs and at the same time the WRRF need to be considered and that neglecting one of them conveys an erroneous impression of the behavior of the total system. And a slightly later study demonstrated the potential of optimizing the control of the IUWS in view of the receiving water quality (Schütze et al., 1999).

In the 1990s the European Union began to change the approach to its water legislation (Blöch, 1999) culminating in the Water Framework Directive (WFD). The directive was put in force in 2000 and officially imposes “integrated river basin management” and has the aim of a “good” quantitative and qualitative status of the water bodies (CEC, 2000). Rauch et al. (1998) have

stated that most efficient technical measures are designed when the wastewater discharge regulations are driven by the receiving water objectives. They also stated that this requires that the impact to the aquatic ecosystem can be predicted quantitatively by means of integrated wastewater models. This change in regulation has thus caused an increase in IM studies, among others by Erbe et al. (2002), Rauch et al. (2002), Rauch et al. (2005), Vanrolleghem et al. (2005b), Solvi (2006), Freni et al. (2008), or Muschalla (2008). Driven by the WFD, the Central European Simulation Research Group (Hochschulgruppe, HSG) presented a guideline for IM (Muschalla et al., 2009). Although water quality-based assessment has become quite wide spread, Blumensaat et al. (2012) have shown that for the actual implementation a wide range of different national protocols exist. They highlighted the considerable risk of subjective assessment due to the differences in protocols with respect to structure, complexity, assessment concept, spatial and temporal scale as well as the handling of uncertainty. The Clean Water Act (CWA) was amended in 1972, and in its current form of 2002 specifically asks for a unified wet weather approach on a watershed or sub-watershed basis (EPA, 2002). And the Canada-wide Strategy for the Management of Municipal Wastewater Effluent (CCME, 2009) indicates that monitoring at a watershed level will conform to the protection of the environment. The focus on the watershed did, in comparison to Europe, however, not lead to an increased amount of IM studies, since the central element is the river and not the urban catchment.

More recent IM studies have widened the traditional scope. An extensive study in Australia highlighted the interaction between the drinking water supply and the corrosion issues in the urban drainage system caused by sulfate. IM showed that the aluminum sulfate addition during drinking water production was a primary source of the sulfide in the sewer system and that switching to a sulfate-free coagulant in the drinking water supply would only cause minor additional costs for the drinking water production but would lead to large savings in the sewer corrosion issue (Pikaar et al., 2014). Another study looked at the interaction between the sewer system and the waterways in view of flood protection (Zhu et al., 2016). IM modelling studies have also become broader in the sense of including the estimation of the uncertainty of the runoff forecast when minimizing CSOs by RTC (Vezzaro and Grum, 2014) or they aim to enhance the resilience of water infrastructure by including failure scenarios in the planning phase (Mugume et al., 2015). In the context of climate change, modelling the greenhouse gas emissions from the IUWS has also gained importance (Mannina et al., 2018). Highlighting the importance of IM, a hypothetical, system-wide Benchmark Simulation Model has been proposed to allow objective comparisons of different control strategies in the IUWS (Saagi et al., 2017).

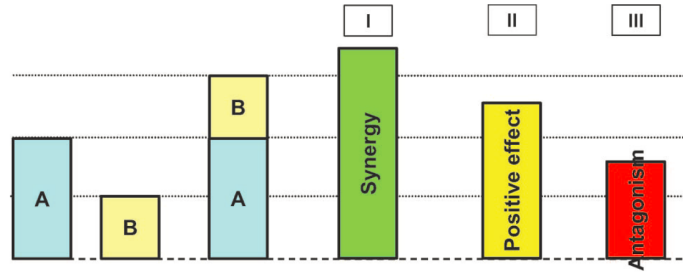


Figure 0.2: Possible interactions of combining different measure A and B. The total effect does not need to be the sum of the two single effects, but can result in either a positive (synergy) or a negative (antagonism) effect (Blumensaat et al., 2009).

Motivation for IM

IM for quantification of effect on receiving water The interaction between different sub-systems of the urban infrastructure and the effect of a rain event on the receiving water has already been analyzed in Gujer et al. (1982) with a vast measurement campaign throughout the IUWS. The study also reveals that carrying out such a measuring campaign may not always be feasible. An IM may thus provide a valid alternative to quantitatively predict the effect on the receiving water (Rauch et al., 1998). In a semi-hypothetical integrated case study it was shown that the local analysis of CSO performance evaluated via spill frequency and volume was only under certain conditions a good indicator for the receiving water quality (Lau et al., 2002). This finding was confirmed by Butler and Schütze (2005), who have been able to show that an integrated analysis is necessary since conventional design criteria, such as the limitation of overflow volumes as also used in the previous example, can result in misleading conclusions as the receiving water quality is not considered.

IM for comparison of measures and strategies The possibly interacting effects of different measures to improve water quality were studied with IM in the Ruhr area, Germany (Blumensaat et al., 2009). To assess the overall effect of different measures, a single value index was developed to summarize the set of criteria that were identified as deficits of the system. The normalized single index value was aggregating over all the criteria to permit the relative comparison between the current status of the system and the status that would be obtained by implementing the measures. Applying this index to different scenarios showed that the combined effect (index AB) of two measures A and B, with an effect index A and index B, may result in synergy (index AB is larger than index A+B), a positive effect (index AB is larger than each single index) or even antagonism, where the combination reduces the positive effect of a single measure, see Figure 0.2. This study has thus shown that a local evaluation of different measures might lead to an over- or underestimation of the effect on the water quality improvement and that the overall effect has to be assessed carefully.

An example of a study comparing different measures was conducted in Bauma, Switzerland

(Holzer and Krebs, 1998), where three different options with respect to the total ammonia impact on the receiving water from CSOs and the WRRF were compared. The options were no retention tank (RT), a RT for combined, and a RT for pure sanitary water. The model found that the sanitary RT performed better with respect to the total load emitted. The combined tank, however, performed better with respect to reduction in peak concentrations of $\text{NH}_4\text{-N}$.

Another integrated study taking into account the interactions of the sewer system and the WRRF compared three different measures to improve the system performance with respect to the water quality of the receiving water (Langeveld et al., 2002). It was found that the use of a stormwater settling tank at the inlet of the WRRF was to be preferred over the enlargement of the WRRF treatment capacity, respectively the enlargement of the hydraulic capacity of the primary treatment followed by a by-pass of the excess water.

Solvi et al. (2008) compares different measures in the IUWS, including source control, construction work, different operational strategies as well as measures in the river, such as artificial aeration to improve the receiving water quality. It was found that an upgrade of the upstream WRRFs of the considered catchment was inevitable.

An example in which different strategies are compared can be found in the analysis of the optimal dosing strategy of chemicals for the control of hydrogen sulfide in sewers (Sharma et al., 2012). A number of simulations were carried out to find the optimal location for the chemical dosing in order to ensure an optimal performance of the WRRF, since some of the added chemicals can have negative effects (e.g. nitrate and oxygen addition reduces the available carbon sources for biological nitrogen and phosphorus removal at the WRRF), while others would be beneficial (e.g. support chemical phosphate precipitation).

IM for planning Schulz et al. (2005) have shown with a hypothetical case study that IM provides a tool for planning future rehabilitation activities. The study analyzed the performance improvements of the urban wastewater system by incorporating reduced infiltration rates of the rehabilitated pipes. The improvement with respect to the receiving water quality allowed prioritizing of the rehabilitation of different sewer sections. Similarly, Benedetti et al. (2013b) have demonstrated that IM is a powerful tool for planning and decision support, as it allows evaluating the effect of different measures before implementation and thus allows striving for cost-effective solutions. In that particular case study the monitoring campaign and modelling work had a pay-back period of only 6-14 months, depending on the calculations and assumptions, and thus proved the power of IM.

IM for adaptation Another rationale for IM is provided by the constant requirement to optimize urban water infrastructure (Dominguez and Gujer, 2006). As shown in Neumann et al. (2015), infrastructure is constantly challenged with problems for which it was not devised.

Throughout its lifetime, it therefore needs to adapt constantly. IM allows re-assessing the situation by evaluating strategies for adaptation, other than the “muddling-through” strategy which was found to be pre-dominant in Neumann et al. (2015). An example for strategic, transdisciplinary planning and adaptation of the IUWS is the IM in Lima, Peru (Schütze et al., 2019), where together with stakeholders scenarios for the development of the IUWS over the next decades have been identified and evaluated under different climate change scenarios. This resulted in an action plan to which the responsible authorities of the water sector committed.

IM for control IM is also important in view of the evaluation of control strategies. An early study of Beck et al. (1991) compared different control strategies of the WRRF based on their receiving water impact, once with respect to dissolved oxygen concentrations and once with respect to ammonium. Seggelke et al. (2005) found that an integrated model predictive control of the inflow to the WRRF is able to improve the receiving water quality with respect to the reduction of $\text{NH}_4\text{-N}$ peak concentrations. Another study by Tränckner et al. (2007) showed that integrated control of the inflow to the WRRF can lead to a significant reduction of the total emission, especially for small and medium rain events. For a catchment in the north of Luxembourg fuzzy decision making did not only reduce the overflow from the sewer system, but also directed it to the less sensitive parts of the river (Regneri et al., 2010). IM also allows evaluating the effect of implementing a RTC to the sewer system on the IUWS (Schütze et al., 2018). For the given case study it was shown that the RTC reduced the overflow volume almost as much as increasing the inflow to the WRRF. Another recent case study by Kroll et al. (2018) has revealed very interesting RTC results for both the improved effluent water quality of the WRRF and energy savings during dry weather conditions. This was achieved by synchronizing sewer storage activation at pumping stations in combination with intermittent aeration at the WRRF. This strategy thus promotes variable WRRF inflow, which is in contrast to the equalization of WRRF inflow during dry weather flow (DWF). During wet weather flow (WWF), RTC reduced the overflows and decreased the sedimentation potential. What makes the results particularly interesting is that this RTC can be applied to about 50 Belgian WRRFs without any structural changes.

Software for IM

Different modelling platforms have been found valuable for IM. A list of early examples of successful implementations can be found in Erbe et al. (2002). They found that a main difference is whether all the different sub-models are implemented in the same software or whether different platforms are used and then require coupling.

According to Benedetti et al. (2013a), a main differentiation results from the type of models used in the sewer subsystems. One can distinguish between models using full hydrodynamics, namely the de Saint-Venant equations, requiring solution of partial differential equations, and models using simplified hydrodynamics, such as the tanks-in-series approach (also called

hydrological or conceptual approach), which solve ordinary differential equations. If the full hydrodynamic models are used, the software usually has to be connected to a WRRF simulator. If different modelling platforms are used for the subsystems, they need to be linked for the creation of the IM (Rauch et al., 2002). Muschalla et al. (2015a) have proposed a possible approach.

If the conceptual approach is chosen for the sewer system, different modelling software allows implementing the models on one platform. Here only those most frequently used are presented. One is SIMBA[#], which is provided by ifak system GmbH¹ and allows taking into account the sewer system, the WRRF, the sludge treatment and the river. Another is AQUASIM, provided by Eawag², which allows connecting different compartments, such as mixed reactors, biofilm reactors, plug flow reactors, river sections and lakes. Then, there is WEST by DHI³, which was initially developed for modelling of WRRFs, but thanks to its open model library and the foundation on differential and algebraic equations, different types of models can be implemented (Solvi, 2006). According to Bach et al. (2014), it is a platform that allows implementing fast models for long-term simulation.

Examples of IM Case Studies

Various case studies around the globe have already been carried out highlighting different aspects of the integrated system and each addressing distinctive challenges. This section does not strive for completeness and only highlights those studies found to be relevant to this PhD thesis as they focus on a similar scope in terms of subsystem modelled.

In order to upgrade one of its WRRFs and plan reconstruction work for its sewer system, the city of Trondheim, Norway, implemented an IM. The objective was to minimize pollutant loads from storm sewer overflows, CSOs and the WRRF (Milina et al., 1999). Two different sets of measures were compared, including extended pumping capacities, adjustment of overflows, separation of storm water runoff from the combined system, retention and real-time control of sewer storage volumes. It was shown that the hydraulic load of the WRRF could be reduced by 14% with one set of imposed measures in comparison to the other set while treating almost the same flux of pollutants.

Several IM case studies have tackled the problem of ammonia (NH₃-N) in the river. With a semi-hypothetical model based on a catchment in Tielt, Belgium, a proof of concept was given for RTC actions in the sewer and on the WRRF based on water quality measurements in the receiving water (Meirlaen et al., 2002).

The analysis of a model-based predictive controller of the sewer system and the WRRF of the

¹www.ifak.eu

²www.eawag.ch

³www.mikepoweredbydhi.com/products/west

city of Hildesheim, Germany, showed that the receiving water quality could be improved, since the ammonium peak concentrations in the receiving water could be limited (Seggelke et al., 2005).

Another case study covering the same issue was carried out in Odenthal, Germany (Erbe and Schütze, 2005). Limiting the ammonia and nitrite concentrations in the receiving water is especially important since it is a salmon-spawning river. It was found that managing the system based on the water quality variables in the WRRF and the receiving water could significantly improve the situation. It also was found that for different single events the peak concentrations could approximately be halved.

The catchment of the Congost river in Spain includes two sewer systems, their corresponding WRRFs, an interceptor which connects the two WRRFs, and the river. For this case study different scenarios were studied, a reference scenario and a number of potential emergency scenarios, such as unplanned industrial spills (Devesa et al., 2009). It was found that the use of storage tanks originally designed for preventing CSOs during rain events could significantly lower peak concentrations in the receiving water. Modelling these scenarios was conducive to gaining knowledge on how to deal with such events from a management point of view. The models were implemented in Infoworks CS, GPS-X and Infoworks RS for the sewer systems, WRRFs and stream reach, respectively and used a specifically developed software based on the Delphi programming language to connect the different models.

For the same river catchment, Prat et al. (2012) later developed an integrated model on the modelling platform WEST as a decision support tool. The following water quality components were modelled: soluble and particulate chemical oxygen demand (COD), total nitrogen, $\text{NH}_4\text{-N}$, total phosphorus and $\text{PO}_4\text{-P}$. Five scenarios were analyzed, namely a reference dry-weather flow, a Mediterranean storm, an increase of population, and two organic shock loads at different locations in the system. With the degrees of freedom, Monte Carlo simulations were carried out to find the optimal parameters for flow rates, wastage sludge flow rates and set-points of the dissolved oxygen concentration in the two WRRFs. With these simulations both the performance was improved (better effluent characteristics) and the costs were reduced for all scenarios.

In the Shezhen River Catchment, part of Shezhen City, China, an integrated model including a sewer, WRRF and receiving water was used to evaluate the expected benefits from the renovation plan (Dong et al., 2012). With the findings of the IM the effectiveness of different measures with respect to the total pollution load was quantified.

For the catchment of the Quebec City, Canada, an integrated model was developed to optimize the strategy of RT emptying and alum addition in the PC in order to reduce the overall amount of particulates released to the environment (Tik et al., 2014b).

In the city of Dresden, Germany, for more than ten years an integrated flow control of the RTs and the sewer system has been in operation. The implementation of integrated control has resulted in savings of approximately 60 million Euro which did not have to be spent on the construction of RTs. In addition to the cost savings, the integrated control also includes flood protection measures and allows for special operation modes. These special operation modes can be activated, for instance, during construction work to reduce flow in a certain part of the system, or the flow can temporarily be increased for sediment flushing purposes (Männig and Lindenberg, 2013).

One year after the implementation of an integrated RTC strategy in the city of Wilhelmshaven, Germany, the analysis of the system performance showed that the integrated approach is most effective during small and medium sized rain events. In total, 22 % of the CSO events were avoided, while the total CSO volume was reduced by 25%, without overloading the WRRF, since inflow limitation was included in the RTC strategy (Seggelke et al., 2013).

Using an integrated model in combination with a cost model proved to be a powerful tool to find cost-effective measures to increase the quality of the Dommel River in the Netherlands. With an integrated model (sewer-WRRF-river), Benedetti et al. (2013b) have shown that it is possible to reach the quality goals with different combinations of measures, but that there are substantial cost differences between the scenarios. They found that the modelling and measurement work necessary to produce these findings had a pay-back time of about 6-14 months, depending on the cost calculation.

Initially, the renovation planning of the WRRF in Lemgo, Germany, revealed the necessity for the construction of a third secondary clarifier to upgrade the existing system. Investigating an integrated approach with an IM revealed, however, that alternative optimization approaches, such as making optimal use of the storage volume in the sewer and implementing a RTC for the inflow to the WRRF, would make the construction of the third clarifier obsolete. The responsible approval authority considered the theoretical findings and has called for an 18-month test operation prior to final approval. If the test operation is successful, investments in the order of four million Euros can be avoided (Seggelke et al., 2017).

Focus on Particulates

According to Tchobanoglous et al. (2004), wastewater can be defined “as a combination of the liquid or water-carried wastes removed from residences, institutions, and commercial and industrial establishments, together with such groundwater, surface water, and stormwater as may be present”. The definition of liquid or water-carried waste shows that water pollution is commonly split in soluble and particulate compounds (Vanrolleghem et al., 2018).

Motivation for Focus on Particulates

As stated earlier, this research focuses on particulates. Particulates are widely acknowledged as a primary source of pollutants throughout the sewer system (Ashley et al., 1994). If particulate pollution reaches the receiving water, it does not only lead to visual pollution, but also to oxygen depletion since it contains considerable organic matter, and causes eutrophication since it contains nutrients (Vanrolleghem et al., 2018). Depending on the type of sediment, the particulates function not only as carriers of COD, but also of additional pollutants, such as pathogens and heavy metals and hydrophobic micro-pollutants (Ahyerre and Chebbo, 2002; Ashley et al., 2004).

Another motivation derives from operational issues caused by particulates, as they block and damage screens, cause pump abrasion, create gases and odors and reduce the hydraulic capacity of the sewer system (Ashley et al., 2004). The latter was further assessed and sediment depositions in the sewer system were found to cause minor flood events (Cherqui et al., 2015).

Excess particulate depositions in sewers constitute, however, not only an operational issue but also a problem with respect to pollution, since they can be resuspended during rain events and be released to the environment via CSOs (Murali et al., 2019). An effect related to this phenomenon is the so-called first flush, which is caused by an increasing flow in the sewer and results in an initially increased concentration of solids and other pollutants (Ashley et al., 2004). The effect of the flow increase is different for soluble and particulate concentrations, as a sudden increase in flow causes a wave propagating through the sewer. Krebs et al. (1999) have shown that the wave celerity is faster than the flow velocity of the water, implicating that the soluble concentration in the wave front originates from the water already in the sewer and thus with (increased) DWF concentrations. They conclude that the first flush of particulates is caused by the increased erosion of sewer sediments. This corresponds with the findings from a study in Paris, where it was shown that 30-80% of the mass of suspended solids during a rain event resulted from in-sewer sediments (Ahyerre and Chebbo, 2002). The more recent and quite stringent definition of the first flush, as 80% of the pollutants having to be found in the first 30% of the water flow volume, makes the first flush a complex and fairly rare phenomenon (Bertrand-Krajewski et al., 1998).

From the perspective of resource recovery the correlation between settling and organic content is interesting, as suggested by Bachis et al. (2015). The addition of coagulants and flocculants in the primary treatment can maximize the settling of organic material and thus increase biogas production. In an integrated approach, maximizing solids production does not need to be seen as maximizing waste, but rather as maximizing a resource of energy and nutrients.

Results from two case studies in Italy have shown that sewer sediments play a major role in the assessment of the impact of rain events and should be included in future assessments of the urban drainage system (Mannina and Viviani, 2010). The recent literature review by Murali

et al. (2019) concluded that further research is required to understand solids erosion, deposited bed processes, and gross solids transport. Furthermore, current modelling approaches to particulates are deemed to lack sufficient detail to capture the ongoing processes in the sewer system. Or, as Vanrolleghem et al. (2018) put it, understanding the particulate pollution in the IUWS and predicting its fate remains a considerable challenge and warrants ample further investigation.

Characterization of Particulates

Although the importance of particulates is widely acknowledged, no general definition of sewer solids is widely accepted and different definitions exist (Friedler et al., 1996). Common differentiation is made between gross solids and sewer sediments, gross solids being sewer solids with a diameter of >6 mm in any one direction and the sewer sediments being smaller (Jefferies and Ashley, 1994). In Ahyerre and Chebbo (2002) sewer sediments are further divided into three classes; Type A sediments, which represent the coarse, loose, granular sediments at the bottom of pipes, biofilms found along pipe walls and organic sediments at the water-bed interface. For the Type A sediments, a correlation between settling velocity and volatile solid content was found: The faster the sediments settle, the lower their volatile solid content. Regarding the characterization of involved transport processes for sewer sediments, a recent review by Murali et al. (2019) presented the processes illustrated in Figure 0.3: Erosion, settling, suspended transport, bedload transport and saltation.

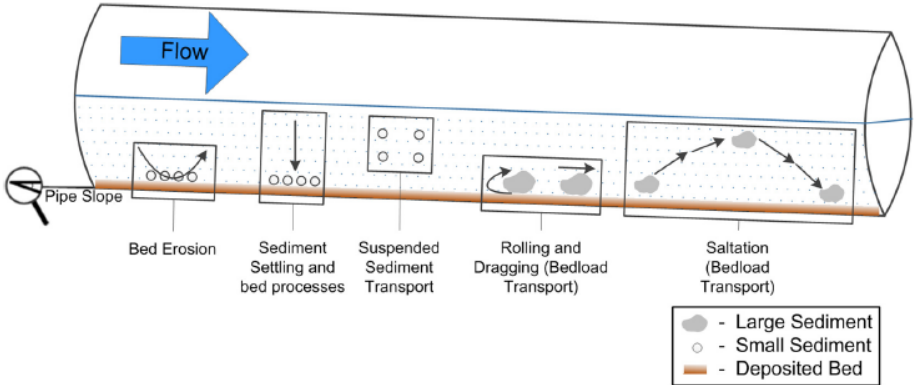


Figure 0.3: Illustration of processes affecting the transport of sewer sediments: erosion, settling, suspended transport, bedload transport and saltation (Murali et al., 2019).

Different measurements exist for the characterization of particulates. A considerable number of these focus on particle density, particle size distribution or the description of their composition, for example, with respect to COD content (Ruban et al., 2015). None of these measures is, however, described in detail, since they address the settling velocity only indirectly. Nevertheless, the settling velocity was found to be a key parameter with regard to the description of sedimentation, transport and erosion of particulates (Michelbach, 1995). Chancelier et al.

(1998) distinguish between two types of protocols for the measurement of the settling velocity: those using a homogeneous sample of a mixture between solids and the liquid phase, and those using a floating layer, i.e. a layer of solids added to the top of the liquid phase at the beginning of the experiment. According to the review by Berrouard (2010), all these measurements belong to the class of static measurements, which use a static water column. This is opposed to measurements of the settling velocity under dynamic conditions, such as the elutriation by Exall et al. (2009). Berrouard (2010) conducted an extensive study of different protocols to measure the settling velocity, such as the Aston column (Lin, 2003), a column of the UFT type (Umwelt und Fluid Technik) described by Wong and Piedrahita (2000) or the ViCAs column presented in Chebbo and Gromaire (2009). Considering different criteria, such as the possibility to measure small settling velocities without any pre-treatment of the sample, the use of a comparably small sampling volume, and the reasonable size of the sampling equipment, led to the conclusion that the ViCAs column is the most suitable for the measurement of settling velocities. This finding that the ViCAs measurement is a comparably simple, yet accurate, method to describe the settling behavior is confirmed by Tik et al. (2014a), who applied it throughout the entire IUWS. The method is presented in detail in Section 1.4.

Ongoing PSVD Modelling Developments

As stated earlier, this thesis uses the PSVD modelling approach based on the ViCAs experiment. The development of the PSVD modelling approach is a joint effort by the model EAU team from Université Laval, Quebec City, Canada. Not only has a lot of prior work already been conducted (such as Maruéjols et al., 2014; Muschalla et al., 2014; Maruéjols et al., 2015; Bachis et al., 2015; Tik et al., 2016a and Vallet et al., 2016 to name only some) but the developments are ongoing. Next to this dissertation, three complementary theses on PSVD modelling are in progress: Sovanna Tik adopts PSVD models (PSVDM) for optimizing the IUWS with RTC (see, for example, Tik et al., 2014b), Queralt Plana studies the behavior of particulates in the grid chamber via PSVD (see, for example, Plana et al., 2018) and Kamilia Haboub investigates the behavior of suspended solids in sewers, also based on PSVD (Haboub et al., 2019). This work thus forms part of a broader, concerted effort by the model EAU team to better understand and describe the fate of particulates in the IUWS.

Project-Relevant Regulations Regarding the Case Study CdH

Sewer System

The current regulation for environmental compliance of the Bordeaux sewer system is found in the “Note Technique du 7 septembre 2015 sur la conformité relative à la mise en œuvre de certaines disposition de l’arrêté du 21 juillet 2015 relatif aux systèmes d’assainissement collectif”. To assess compliance of the sewer system, three possible criteria exist, one of which has to be chosen:

- The total volume discharged during rain weather has to be smaller than 5% of the total volume produced by the catchment per year.
- The total pollutant flux discharged during rain weather has to be smaller than 5% of the total flux produced by the catchment per year.
- Less than 20 days of overflow for each overflow structure with a load exceeding 120 kg_{BOD5}/d during DWF.

The first criterion, using the volumes, is calculated using Equation 1, where volume V_{A1} represents the discharged volume within the sewer system, V_{A2} the volume by-passed at the entrance of the WRRF and V_{A3} the volume entering the WRRF for treatment. The second criterion is calculated with the same equation, exchanging volume for pollutant flux:

$$\frac{V_{A1}}{V_{A1} + V_{A2} + V_{A3}} * 100 \leq 5. \quad (1)$$

WRRF

The current legislation for the WRRFs in France was published in the “Journal officiel de la République française” in 2015 (JORF, 2015). The minimum effluent requirements for WRRFs discharging in receiving waters not considered sensitive to eutrophication are shown in Table 0.2 and depend on the loading of the 5-day biochemical oxygen demand (BOD₅) of the WRRF.

Table 0.2: Minimum requirements for WRRFs in France

Parameter	BOD ₅ Load of WRRF (kg/d)	Max. daily average effluent concentration (mg/l)	Min. daily average reduction
BOD ₅	<120	35	60%
	≥120	25	80%
COD	<120	200	60%
	≥120	125	75%
TSS	<120	–	50%
	≥120	35	90%

The WRRF of the case study is described further in Chapter 1, but has a load of approximately 24’500 kg/d, which means that the more stringent effluent conditions apply. The effluent concentrations must be met by 95% of the flow arriving at the WRRF, while for a limited amount representing no more than 5% of the flow these concentrations may be exceeded.

Chapter 1

Case Study Description - Clos de Hilde Catchment

1.1 Catchment and WRRF overview

The case study “Clos de Hilde” (CdH) is located in the city of Bordeaux, in the south-west of France, as shown in Figure 1.1. The city was founded on the banks of the Garonne river, which traverses the city from south to north. It is one of the major rivers in France, has a length of approximately 600 km and discharges to the Atlantic Ocean not much downstream of Bordeaux. The flow follows a annual pattern, with low flow in summer and autumn and high flow during winter and spring (average monthly flow in Mas-d’Agenais, approximately 100 km upstream of Bordeaux, for August: 190 m³/s and February: 1030 m³/s). At the level of Bordeaux, the river starts being influenced by the tide of the sea (“Garonne”, 2019) and has very high turbidity.

The climate in Bordeaux is a typical oceanic climate with mild winters and hot summers. Bordeaux has frequent rainfalls (approximately 1000 mm/year), which are evenly distributed throughout the year, but in summer often caused by storms (“Bordeaux”, 2019).

Figure 1.2 indicates the six water resource recovery facilities (WRRF) of the Bordeaux urban community with a total treatment capacity of almost 1 million person equivalents (PE). The historical city center is located in the Louis Fargue catchment. The catchment of the case study, CdH, is south of the city center and therefore discharges upstream of the old town into the Garonne river. It can be seen from Figure 1.2 that the catchment is located both on the east and the west banks of the river. This requires the water to be pumped from the left side to the right side, where the WRRF CdH is located.

The CdH catchment is a typical urban catchment consisting of housing, industrial and combined areas. Figure 1.3 shows that the catchment consists of both combined (hatched) and

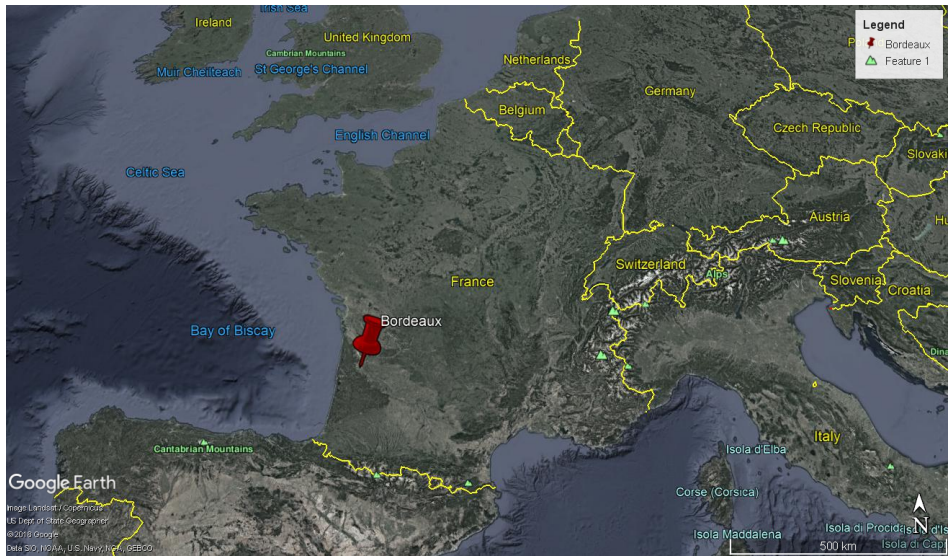


Figure 1.1: Location of Bordeaux within France.

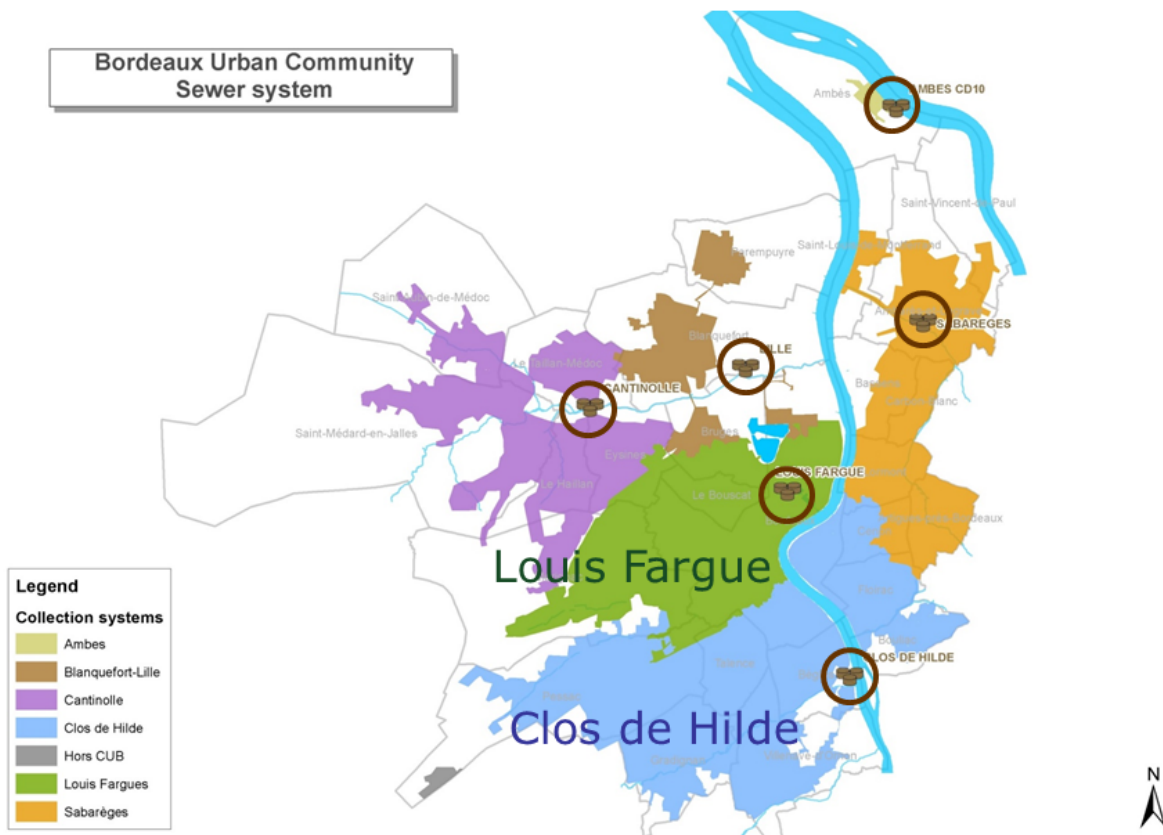


Figure 1.2: WRRFs (brown circles) and corresponding catchments of the Bordeaux urban community, with the main catchments Louis Fargue and Clos de Hilde.

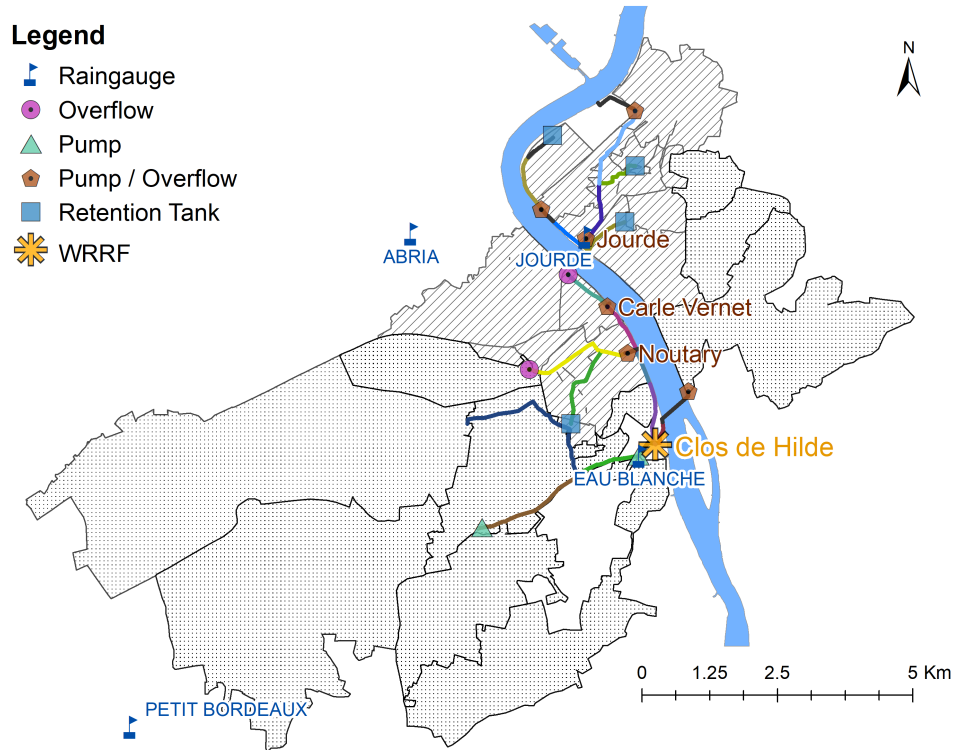


Figure 1.3: Sewer system and WRRF of the CdH catchment with an indication of the key hydraulic structures. Hatched subcatchments indicate combined, and dotted subcatchments separate sewer systems. The colored lines indicate the sewer stretches modelled (see Chapter 2). Since the river flows from south to north, the WRRF is located upstream of the catchment.

separate sewer systems (dotted). The older part of the system is mostly covered by a combined system, whereas the newer part of the system, located in the outer circle, has a separate system. The main sewer system is indicated with colored lines. This is also the sewer system that will be modelled. One color corresponds to one modelled sewer stretch. The development of the model as well as the calibration and validation of the sewer model is described in Chapter 2. A special characteristic of the CdH catchment is that the WRRF is located upstream of the catchment itself, which leads to the situation that most of the water needs to be pumped to the WRRF. To this end, several pumping stations as well as overflows are located on the river banks (see Figure 1.3). These pumping stations and overflows limit the flow to the WRRF. The figure also shows four RTs located further upstream in the catchment. All the RTs are off-line tanks and have unusually large volumes as they were built for flood protection in response to the big flood events in the 1980s (“Météo France”, 2019). The Bastide tank for example, which is located in the north of the eastern catchment area, has a volume of $9\,550\text{ m}^3$.

The WRRF has five tributaries, four tributaries from the catchment and the WRRF internal wastewater, which is comparably small. The contributions of each of the tributaries are listed

Table 1.1: Description of the five tributaries of the WRRF CdH with their respective contribution during DWF and WWF. For the calculation of the WWF contribution the later calibration event is chosen (for more detail see Chapter 4).

Tributary	Description	Sewer System	Contribution	
			DWF (%)	WWF (%)
CdH Tributary 1	Ars-Bourde	Sanitary	37	36
CdH Tributary 2	Rive Gauche	Combined	55	55
CdH Tributary 3	Blanche	Sanitary	5	5
CdH Tributary 4	Arcins	Sanitary	3	4
CdH Tributary 5	WRRF Internal	Sanitary	~	~

in Table 1.1. From the four tributaries of the catchment, two can be considered the main contributors to the flow at the WRRF. Tributary 1, the “Ars-Bourde” catchment, contributes approximately 37% of the total DWF. It is the main sanitary catchment located in the southwest of the CdH catchment. Tributary 2, also known as the “Rive Gauche” catchment, is a sanitary catchment contributing 55% of the DWF inflow to the WRRF. The name of this tributary is a bit misleading: “Rive Gauche” is French and means “left bank”, but this tributary does not only include the combined part of the left bank, but also the major part of the wastewater from the right bank of the Garonne. The map in Figure 1.3 indicates that the water from the pumping station Jourde joins the water on the left side in the outflow chamber of the pumping station Carle Vernet. To indicate the WWF contributions of the different tributaries, the rain event is chosen, for which the model will be calibrated later. This rain event has an estimated return period of approximately 3 months (for more detail, see Chapter 4). Table 1.1 indicates that the contributions do not substantially change under WWF. It should however be noted that in the Ars-Bourde catchment no major overflow exists, whereas the Rive Gauche catchment suffers from heavy overloading and multiple major overflows exist. This can also be observed on the map in Figure 1.3. Including all those overflow volumes in the analysis would thus only increase the importance of the Rive Gauche tributary.

The WRRF CdH has a treatment capacity of about 400 000 PE and a nominal flow capacity of 100 000 m³/d. The two WRRFs Louis Fargue and CdH treat together more than 70% of the wastewater and can therefore be considered as the two main WRRFs of the Bordeaux urban community. The CdH WRRF was constructed in 1994 by Degrémont and was extended from 2004 to 2007 by the same company. This two phase development is reflected in the plant layout shown in Figure 1.4. The wastewater arriving via four different sewer lines and the internally produced wastewater is pre-screened (50 mm), followed by four fine screens (16 mm). The wastewater passes the aerated GC and then additional fine screens (3 mm). After the fine screens the extension of the WRRF becomes visible: The upper part in Figure 1.4 represents the old line (from 1994) and the lower part represents the new line (from 2007). The unit processes however, stay the same: first the water is treated by chemically enhanced primary

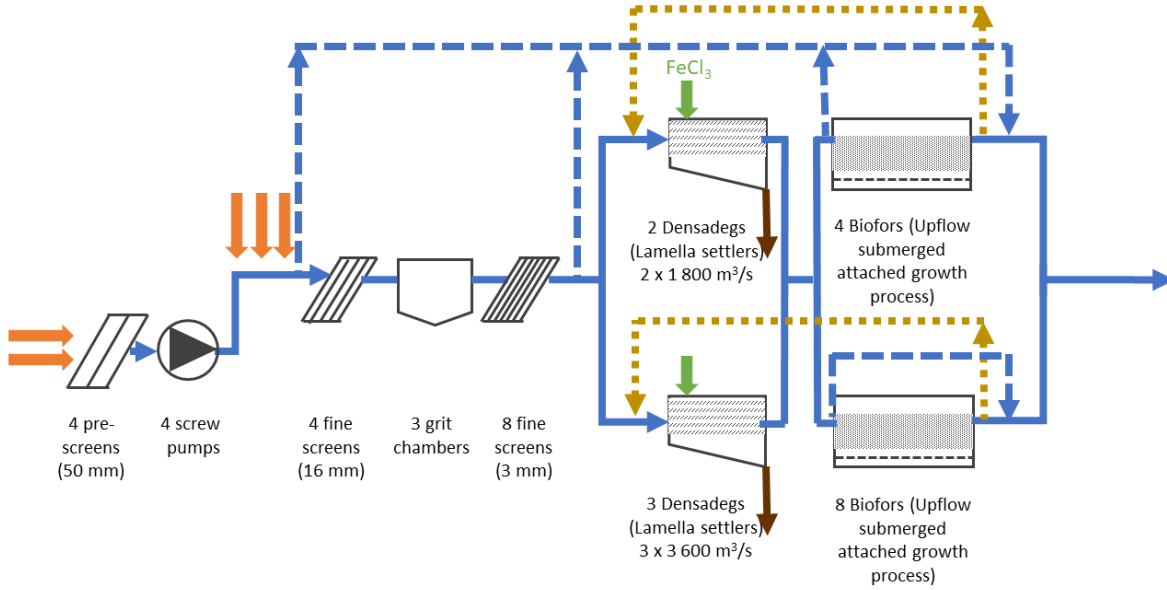


Figure 1.4: CdH WRRF layout with the main sewer lines arriving (orange), the regular water line (continuous blue), possible bypass options (dashed blue) and backwash water (dotted yellow).

treatment (CEPT). The PC installed is a lamella settler (Densadeg by Degrémont) to which iron trichloride ($FeCl_3$) is added. The control of the CEPT will be described in more detail in Section 1.2. After the primary settlers, the water is redistributed and flows through two upflow submerged attached growth processes (Biofor biofiltration by Degrémont). Due to the design of the BFs no secondary clarifier is necessary and the effluent is directly discharged to the receiving water.

1.2 Control of Chemically Enhanced Primary Treatment

The addition of the coagulant, ferric chloride $FeCl_3$, is controlled on the WRRF CdH. The control of the CEPT is described in more detail, since the control implemented on the WRRF has to be implemented in the model too.

The CEPT controller calculates the $FeCl_3$ coagulant concentration added in the PC based on the TSS concentration measurement in the inlet of the PC (TSS_{in}). Equation 1.1 shows the detailed calculation of the coagulant concentration ($FeCl_3$) and reveals that if the TSS concentration in the inlet TSS_{in} reaches a certain level TSS_{max} the coagulant concentration will increase no further and reaches its maximum $FeCl_{3,max}$. The same can be found for the minimal coagulant addition $FeCl_{3,min}$ that is reached when TSS_{in} reaches the minimum TSS concentration TSS_{min} . If the TSS_{in} concentration thus passes the boundaries of the controller

the minimal, respectively the maximal, concentration of coagulant is added.

$$FeCl_3 = FeCl_{3,max} - \frac{FeCl_{3,max} - FeCl_{3,min}}{TSS_{max} - TSS_{min}} (TSS_{max} - TSS_{in}) \quad (1.1)$$

$$FeCl_{3,min} \leq FeCl_3 \leq FeCl_{3,max} \quad (1.2)$$

where:

$FeCl_3$	Dosed $FeCl_3$ concentration	dosed	mg/l
$FeCl_{3,max}$	Maximum $FeCl_3$ concentration	45	mg/l
$FeCl_{3,min}$	Minimum $FeCl_3$ concentration	20	mg/l
TSS_{in}	TSS concentration in the inlet of the PC	measured	mg/l
TSS_{max}	TSS concentration for which maximum dosage is reached	400	mg/l
TSS_{min}	TSS concentration for which minimum dosage is reached	150	mg/l

1.3 Data from the Utility

Several measurements are regularly taken by the utility. The available data for this project are presented here. The main difference is made between water quantity measurements (precipitation/flow) and water quality measurements. For the sewer system water quantity measurements are available at different locations; water quality measurements however are only available at the WRRF.

The water quantity measurements provided in the sewer system are measured based on a 5 min interval at the following locations (also indicated in Figure 1.3):

- Precipitation measurements (tipping bucket)
 - Abria
 - Jourde
 - Eau blanche
 - Petit Bordeaux
- Flow rate measurements
 - Jourde:
 - Calculated via pump operation and opening level gate
 - Carle Vernet:
 - Calculated via pump operation
 - Noutary:
 - Calculated via height (piezometer) and velocity (ultrasound))

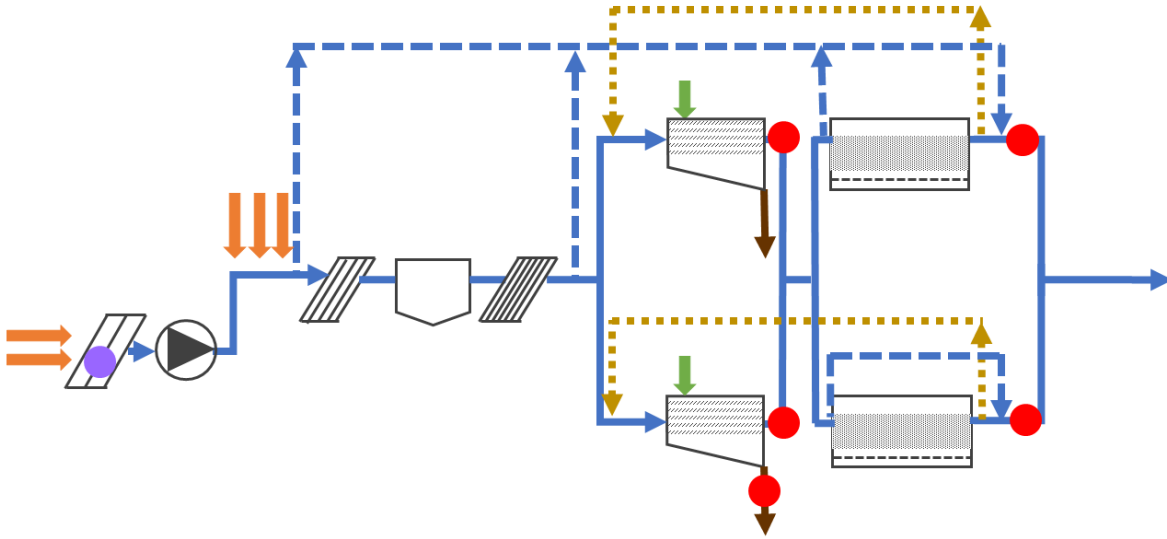


Figure 1.5: Turbidity measurements performed by the utility are indicated with a red dot and measurements collected during the project’s measurement campaign are indicated with a violet dot on the WRRF layout of CdH.

– WRRF CdH

- * Tributary 1 (Ars-Bourde):
Calculated via flow channel and velocity (ultrasound)
- * Tributary 2 (Rive Gauche):
Electromagnetic flowmeter
- * Tributary 3 (Blanche):
Electromagnetic flowmeter
- * Tributary 4 (Arcins):
Calculated via flow channel and velocity (ultrasound)

The water quality measurements available for this study are turbidity measurements (Hach, Loveland, CO, USA) located at different unit processes on the WRRF. The locations are indicated in Figure 1.5 and all data is stored based on a 5 min interval. For the control of the WRRF, a turbidity measurement is also available at the inlet of the new line of Densadegs for the control of the FeCl_3 dosing in the CEPT, see Section 1.2. Unfortunately, the data was not available for this study.

1.4 Data from Measurement Campaigns

1.4.1 Overview Measurement Campaigns

Three measurement campaigns were conducted in the course of this project, a preliminary measurement campaign and two full-scale measurement campaigns. An overview of the campaigns is given in Table 1.2. The measurements conducted during the measurement campaigns stayed the same and can be divided into online measurements and the necessary laboratory measurements for their calibration and the ViCAs experiment conducted in the laboratory to obtain the PSVD curve. The online measurements are explained in more detail in Section 1.4.2 and the ViCAS measurement in Section 1.4.3.

Table 1.2: Overview of the measurement campaigns conducted in the course of this project.

Name	Duration	Aim
Preliminary	September 2016	Installation and test of equipment Preparation laboratory
1st	May to August 2017	Online measurements Noutary and CdH ViCAs measurements Noutary and CdH
2nd	Mid-May to mid-July 2018	Online measurements Noutary and CdH ViCAs measurements Noutary and CdH ViCAs measurements primary treatment

1.4.2 Online Measurements with RSM 30 stations

For the online measurements, two RSM30 stations (Primodal Systems, Canada) were available. The RSM30 stations are flexible online monitoring stations, the vision of which has first been presented in Rieger and Vanrolleghem (2008). The key element of the vision is the station’s flexibility: both with regard to the modular system, that allows including different sensors, and the compact set-up that allows installation in different places in combination with remote access to the data.

The sensors installed at each of the two RSM30 stations during this project are a pH, a turbidity and conductivity meter of the brand WTW (Weilheim, Germany), as well as a spectro::lyser by s:can (Vienna, Austria), which is a spectrometer sensor able to measure total COD, soluble COD and TSS. The two available TSS measurements are based on different measurement principles. The turbidity meter measures the intensity of light scattered at 90 degrees as a beam of light passes through a water sample, whereas the second sensor, the spectrometer, measures the absorption spectra in the UV/vis range. The sensors are calibrated with laboratory samples.

The installation of the sensors has been developed in collaboration with Le LyRE (Le LyRE, 2016) and was presented in Ledergerber et al. (2017a). The installation aims at flexibility, which is in accordance with the vision for the RSM30 stations. The created hardware set-up

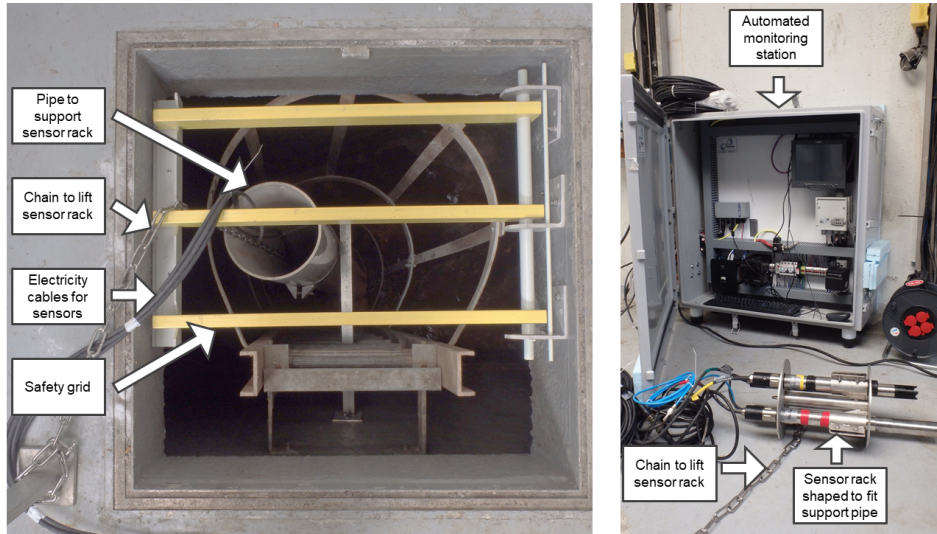


Figure 1.6: Example of installation of the RSM30 online monitoring station at the inlet of the WRRF CdH. The left-hand side shows the support pipe in which the sensor rack can be lowered and the right-hand side shows the sensors mounted on the sensor rack in front of the RSM30 station.

allows reusing the same installation at different locations. As shown for the installation at the inlet of the WRRF in Figure 1.6 it consists of two parts: the sensor rack and its support structure. The sensors are mounted on a cylindrical, re-usable sensor rack attached to a chain. To keep the sensors stable and protected, the sensor rack is placed in a pipe support structure. The chain attached to the sensor rack allows to lift them inside the support pipe for inspection and maintenance. This is necessary as for both measurement sites the sensors are installed far below ground (five respectively twelve meters).

One of the RSM30 stations was placed at the inlet of the WRRF CdH after the pre-screens (50mm), more specifically at the second tributary (Rive Gauche). The placement of the RSM30 station at this particular tributary was chosen, since, as described in Section 1.1, this is not only the biggest tributary, it is also the tributary experiencing the most important overflows during WWF. The location of the RSM30 station is also indicated in Figure 1.5. The second RSM30 station was placed at the pumping station Noutary (NT). The location of this station is indicated in Figure 1.3. This location was confirmed for the 2nd full-scale measurement campaign thanks to OED, see Chapter 3.

Building on the work of Plana (2015) for WRRFs two different maintenance protocols have been developed (Ledgergerber et al., 2017b) for sewers. They are based on the sensor's need for on-site data quality validation (pH, conductivity, turbidity) or its ability for off-site validation and calibration (spectrometer). The protocols are presented in Figure 1.7. The off-site method for the spectrometer includes standard laboratory analysis of COD, CODs and TSS. To obtain the grab samples, a portable sampler (SIGMA SD900, Hach, Loveland, CO, USA) was used

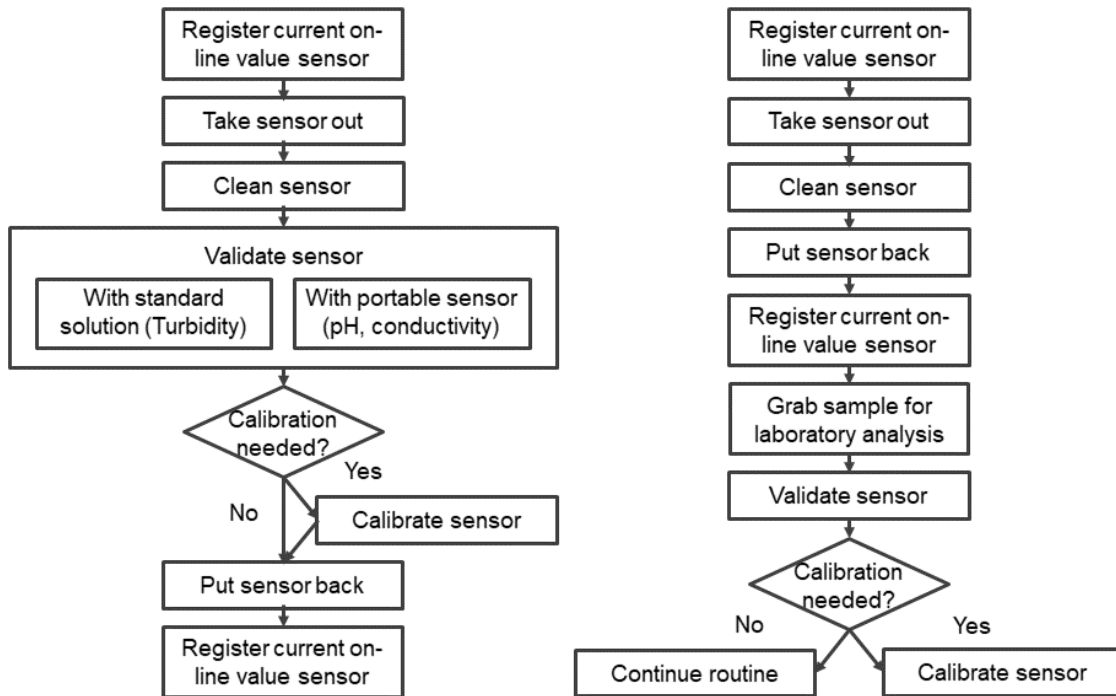


Figure 1.7: Maintenance protocol adapted from Plana (2015) for on-site (left) and off-site (right) maintenance.

for both sites. The quite special installation of the sampler at NT is shown in Figure 1.8.

The data quality of the measurements was assured by applying the univariate data quality assessment method of Alferes et al. (2013a) resulting in validated high frequency data. The resulting water quality data will be used for model calibration and validation at NT and CdH in section 4.6. The work by Philippe (2019) improved the existing method and it was found that for the TSS measurements at NT approximately 18% of the collected data points were outliers and 12% of the data points had to be rejected.

1.4.3 ViCAs Measurements

The method used to determine the characteristic PSVD of a wastewater sample is the ViCAs protocol (Chebbo and Gromaire, 2009). ViCAs is the French acronym of "vitesse de chute en assainissement" which stands for settling velocity in wastewater handling. The ViCAs protocol allows determining the static settling velocity of a wastewater sample with comparably simple equipment. The experimental set-up is shown in Figure 1.9.

A homogeneous sample is filled quickly (<5 s) into the settling column, where the particulates are subject to settling. The settled particulates are trapped in a cup that is placed underneath

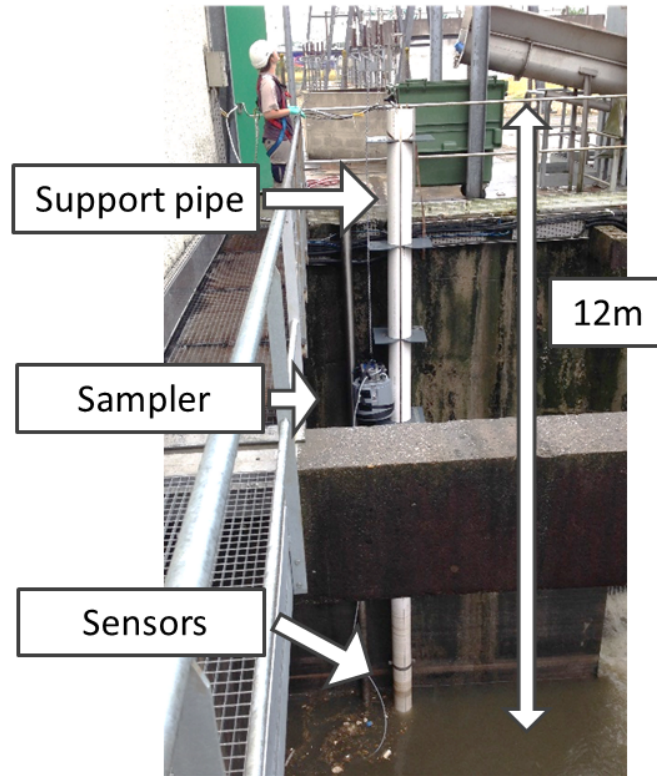


Figure 1.8: Sampling at the monitoring station RSM30 at the pumping station NT.



Figure 1.9: ViCAs experimental set-up as installed at the WRRF CdH with the settling column on the right-hand side.

the column. The cup is replaced by a series of cups that each cover a certain interval so that the ViCAs experiment captures the most relevant part of the anticipated settling time. The particulates trapped in each cup are filtered using a pore size of $1.6 \mu m$ (for filter equipment, see left-hand side of Figure 1.9), dried and then weighed. The mass settled cumulatively in the series of cups is mathematically treated and calibrated to a pre-defined function, using the second approach suggested in [Chebbo and Gromaire \(2009\)](#). The cumulative settled mass $M(t)$ is fitted to the function indicated in equation 1.3 by changing the parameters b, c and d . The resulting PSVD curve can then be used to define the particle classes in the PSVDMs, as described in Section 4.3.

$$M(t) = \frac{b}{1 + \left(\frac{c}{t}\right)^d} \tag{1.3}$$

where:

$M(t)$	Cumulative settled mass	g
b	Adjustment parameter	$b > 0$
c	Adjustment parameter	$c > 0$
d	Adjustment parameter	$1 > d > 0$

Chapter 2

An Efficient and Structured Procedure to Develop Conceptual Catchment and Sewer Models from Their Detailed Counterparts

This chapter is redrafted from the article:

Ledergerber, J., Pieper, L., Binet, G., Comeau, A., Maruéjols, T., Muschalla, D., and Vanrolleghem, P. A. (2019). An efficient and structured procedure to develop conceptual catchment and sewer models from their detailed counterparts. *Water*, 11(10):2000.

Author contributions Conceptualization, J.M.L., D.M. and P.A.V.; Funding acquisition, A.C., T.M. and P.A.V.; Investigation, J.M.L. and L.P.; Methodology, J.M.L., L.P., D.M. and P.A.V.; Project administration, G.B., A.C., T.M. and P.A.V.; Supervision, P.A.V.; Validation, J.M.L. and L.P.; Visualization, J.M.L. and L.P.; Writing—original draft, J.M.L.; Writing—review & editing, L.P., A.C., D.M. and P.A.V.

2.1 Abstract

Modelling flow rates in catchments and sewers with a conceptual, also known as hydrological, approach is widely applied if fast simulations are important. In cases where a detailed hydrodynamic model exists, it is common to start conceptualizing from this detailed counterpart. Unfortunately, no generalized procedure exists, which is surprising as this can be a complex and time-consuming task. This research work proposes a procedure that is validated with two independent combined sewer case studies. The conceptual models provide the targeted results with respect to representation of the flow rates and reduction in the computational

time. As the desired performance could be reached for different levels of model aggregation, it is concluded that the conceptual model can be tailored to the points where accurate flow rates need to be predicted. Furthermore, the comparison of the conceptual model results with flow measurements highlights the importance of analyzing and eventually compensating for the limitations of the detailed model.

2.2 Résumé

La modélisation des débits dans les bassins versants et les égouts avec une approche conceptuelle, également appelée hydrologique, est largement appliquée car les temps de simulation sont significativement réduits en comparaison avec des modèles hydrodynamiques classiques. Dans les cas où il existe un modèle hydrodynamique détaillé, il est courant de commencer à conceptualiser à partir de cette contrepartie détaillée. Malheureusement, il n'existe pas de procédure généralisée, ce qui est surprenant car cela peut être une tâche complexe et longue. Ce travail de recherche propose une procédure qui est validée par deux études de cas indépendantes sur des égouts unitaires. Les modèles conceptuels fournissent les résultats visés en ce qui concerne la représentation des débits et la réduction du temps de calcul. Étant donné que les performances souhaitées ont pu être atteintes pour différents niveaux d'agrégation du modèle, il est conclu que le modèle conceptuel peut être adapté aux points où des débits précis doivent être prévus. De plus, la comparaison des résultats du modèle conceptuel avec les mesures de débit souligne l'importance d'analyser et éventuellement de compenser les limites du modèle détaillé.

2.3 Introduction

The use of lumped conceptual models is widespread in urban drainage modelling where fast calculations are necessary for multiple model evaluations, such as sensitivity or uncertainty analysis and optimization questions (Wolfs et al., 2013), or for simulations of long timeseries with complex models, such as integrated models where multiple sub-system models are evaluated at the same time (Achleitner et al., 2007; Rauch et al., 2002). The potential beneficial use of lumped conceptual models was proven with several successful case studies over the last decades. Some examples of their application include sensitivity analysis (Gamerith et al., 2013; Vanrolleghem et al., 2015), uncertainty analysis (Mahmoodian et al., 2017), RTC and model predictive control (Meirlaen et al., 2002; Weinreich et al., 1997) or optimization and integration (Bauwens et al., 1996; Benedetti et al., 2013b; Willems, 2008).

Hydrodynamic routing, also known as distributed flow routing, calculates the flow based on a time and space component using the de Saint-Venant equations (Maidment, 1993). The evaluation of these equations is however computationally demanding and different approaches exist for simplification or emulation of hydrodynamic models (Davidsen et al., 2017; Machac

et al., 2016). Conceptual modelling, also known as hydrological or lumped modelling, is an established approach that uses time alone to calculate the flow rate at a certain location (Maidment, 1993). Conceptual models respect the conservation of mass, but conceptual relations replace the momentum equation, which makes them computationally less demanding (Achleitner et al., 2007). In comparison to hydrodynamic models no flow prediction at intermediate points is possible as the spatial component is lost and several other flow characteristics, such as velocity and water height are no longer calculated. Also, the hydraulic principles that form the basis of conceptual models are that downstream flow conditions do not influence upstream flow conditions. However, in cases where backwater conditions exist, approaches are available to properly approximate those effects (Vanrolleghem et al., 2009).

For the development of a conceptual catchment and sewer model, including runoff generation, flow concentration and routing, spatial data representing the catchment and sewer characteristics, as well as flow rate information, have to be available. If a detailed model of the catchments and full hydrodynamic model (de Saint-Venant equations) of the sewer system exist, it is a common approach to use the detailed model as a starting point for conceptualization. This allows incorporating the knowledge already available in the detailed model, thus not imposing a need for extensive collection of flow rate measurement data (Meirlaen et al., 2002). For some part of the conceptualization process, semi-automated model layout and calibration tools have been developed to speed up the process (Wolfs et al., 2013; Guo et al., 2019; Kroll et al., 2017). To the knowledge of the authors, the most complete guideline for conceptual modelling approaches is the Austrian guideline (Muschalla et al., 2015b), which provides a very good overview of conceptual modelling concepts, including different aggregation strategies for various levels of lumping (available in German only). But even given those tools, a significant amount of time and effort has to be spent developing a conceptual model (Wolfs et al., 2013; Kroll et al., 2017). It is therefore surprising that no general procedure exists to develop conceptualized catchment and sewer models from its detailed counterpart. It was even concluded that a main shortcoming of conceptual modelling is the lack of a formalized generic procedure (Wolfs, 2016).

Modellers from different disciplines of water system modelling describe that a standardized modelling protocol leads to more efficient and reproducible development of models and makes the process more transparent. Good modelling practice protocols are available for instance in integrated urban wastewater modelling (Muschalla et al., 2009), river modelling (Wolfs et al., 2015), wastewater treatment modelling (Gernaey et al., 2004; Rieger et al., 2012), and river basin and groundwater management (Refsgaard et al., 2005; Scholten et al., 2007).

This research proposes an efficient and structured procedure to develop conceptual catchment and sewer models from their detailed counterpart (Section 2.5). The proposed procedure is not automated, but certain sub-steps, such as the development of the aggregated conceptual sewer model (Kroll et al., 2017), could be automated. The conceptualization of special structures,

such as pumping stations, RTs and flow diversion structures, is not part of the developed procedure, as a general approach to conceptualization is very difficult. Special structures have to be conceptualized on a case-by-case basis. The procedure is applied to two case studies (Ottawa, ON, Canada and Bordeaux, France). Section 2.6.1 evaluates the performance of the developed conceptual models in comparison to their detailed counterpart. In Section 2.6.2 the procedure is further tested by evaluating the impact of the level of aggregation on the Ottawa case study. To do so, the initial model, where attention was paid to ensure that catchments were of similar shape and area, is compared to a maximally aggregated model. Section 2.6.3 challenges the conceptual model of Bordeaux by comparing it to actual flow rate measurements and not only to flow rate data generated by the detailed model.

2.4 Materials and Methods

2.4.1 Case Studies

Case Study 1: Ottawa, Canada

The first case study is located in the central urban area of Ottawa, ON, Canada, covering an area of approximately 6400 ha. The catchment contains sanitary, partially separated and combined sewers. In the studied area, rain data from seven rain gauges are available (Pieper, 2017). A map of the considered sewer system is shown in Figure 2.1.

Case Study 2: Bordeaux, France

The second case study is the catchment of the WRRF CdH. This case study is described in detail in Chapter 1. Relevant is that, in contrast to the first case study, flow rate measurements are also available and provided by the local utility. The relevant flow rate measurements are located at the four different tributaries of the WRRF and the pumping stations Jourde, Carle Vernet and Noutary (see Figure 2.2 for the locations of the WRRF and pumping stations).

2.4.2 Modelling Approach and Software

The catchment model to test the methodology is described in section 4.4.1 and the conceptual sewer model, based on reservoirs in series, in Section 4.4.3.

To determine the reservoir parameters, such as the number of reservoirs in series n and the residence time k , see equation 4.5, methods exist to determine them from the detailed model. Euler (1983) adapted the Kalinin-Miljukov method to define the linear reservoir parameters from the pipe characteristics. An alternative method to determine the parameters is the Muskingum method (Maidment, 1993). In the non-linear case the parameters can also be defined using the pipe characteristics from the detailed model, maximum flows and volume-outflow gradients (Mehler, 2000).

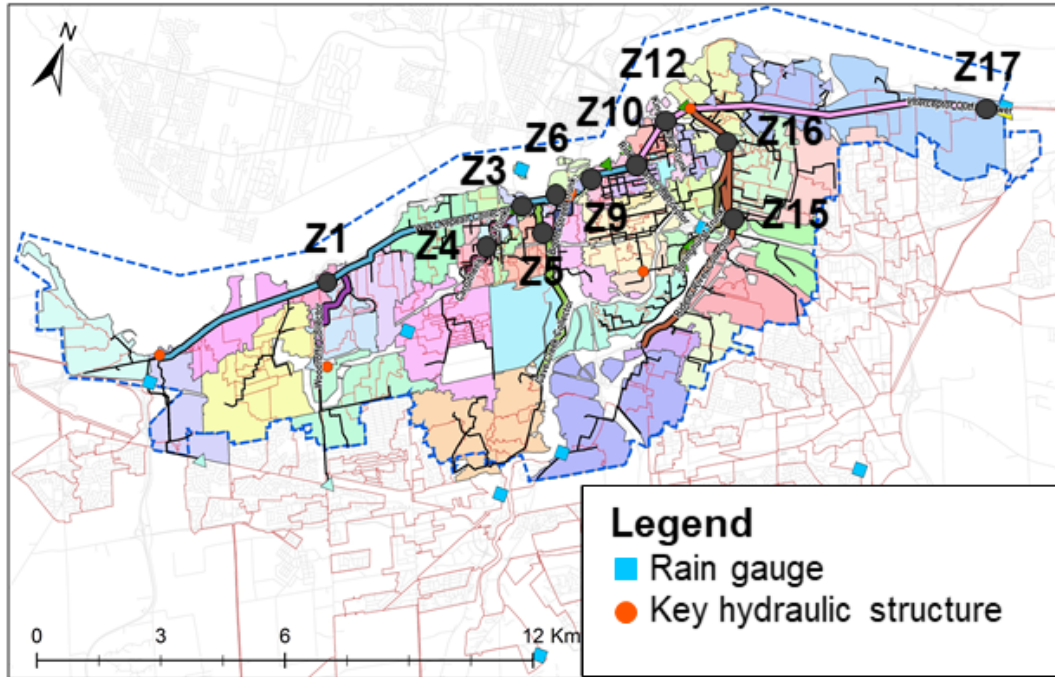


Figure 2.1: The map shows the central sewer area of Ottawa indicating rain gauges and key hydraulic structures as well as the catchments and sewer conduits of the developed conceptual model with the comparison points of the hydrodynamic and conceptual model, indicated by a Z-code (see Section 2.6.1).

2.4.3 Model Performance Criteria

The model performance criteria chosen for this study are the percent volume error (PVE) in equation 2.1, percent error in peak (PEP) in equation 2.2 and the Nash-Sutcliffe efficiency (NSE) in equation 2.3. The PVE , also known as the percent bias, measures the overall adequacy between predicted (P_i) and observed (O_i) data. The PEP characterizes the difference between the observed peak ($\max(\{O_i\})$) and the modelled peak ($\max(\{P_i\})$) for a single event but does not evaluate the timing of the peak. The NSE compares the squared residuals with the squared residuals a model written as the mean of the data (\bar{O}) would create. The optimal value equals one, zero means that the model is equally good as a mean value model and a negative value means that the model is performing worse than the mean value of the observations. Due to the squared nature of the criterion, it compares to the well-known Root Mean Square Error ($RMSE$) model performance criterion, used in other disciplines. This criterion is sensitive to extreme values (Hauduc et al., 2015).

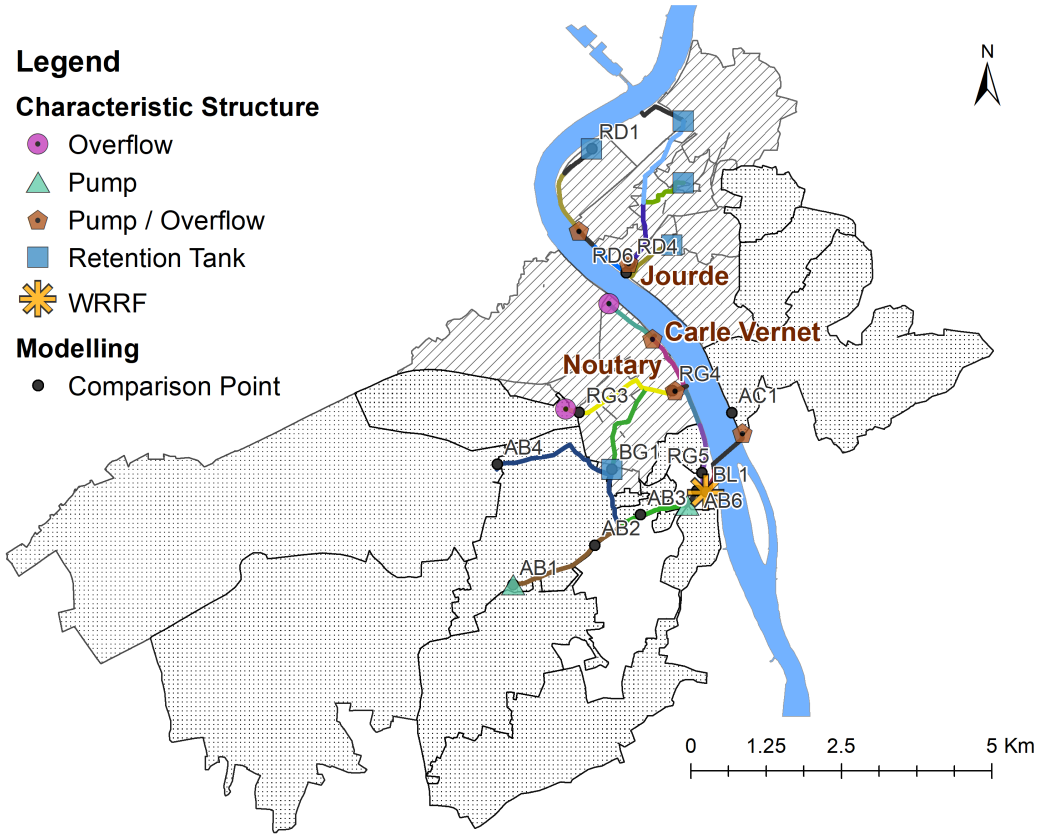


Figure 2.2: Map of the Bordeaux case study. The map shows the CdH catchment of Bordeaux with combined (hatched) and sanitary (dotted) sub-catchments of the separate system, the pumping stations with flow rate measurements (Jourde, Carle Vernet and Noutary) as well as comparison points of the hydrodynamic and conceptual model, indicated by a code of two letters and a number (see Section 2.6.1).

$$PVE = 100 \frac{\sum_{i=1}^n (O_i - P_i)}{\sum_{i=1}^n O_i} \quad (2.1)$$

$$PEP = 100 \frac{\max(\{O_i\}) - \max(\{P_i\})}{\max(\{O_i\})} \quad (2.2)$$

$$NSE = 1 - \frac{\sum_{i=1}^n (O_i - P_i)^2}{\sum_{i=1}^n (O_i - \bar{O})^2} \quad (2.3)$$

where:

P_i Predicted data

O_i Observed data

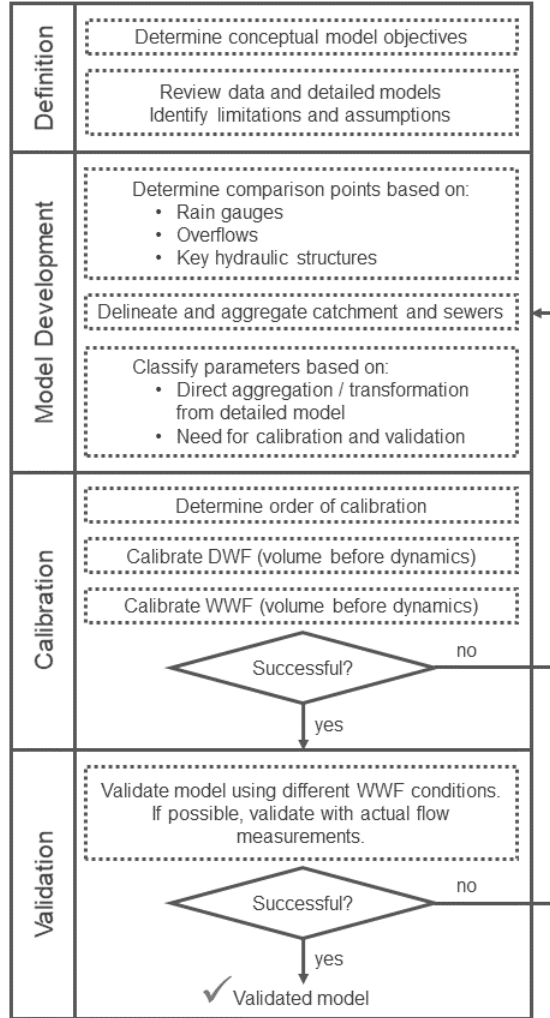


Figure 2.3: Schema for the proposed procedure for the development of a conceptual model from its detailed counterpart.

2.5 Proposed Methodology

The proposed procedure to develop a conceptual model from its detailed counterpart consists of four main stages (Figure 2.3): project definition, model development, calibration, and validation. Each of the stages will be explained in more detail in a dedicated sub-section.

2.5.1 Project Definition

In the stage of the project definition, the first step is to determine the conceptual model’s objectives. These objectives usually reveal on the one hand a certain need of model performance and on the other hand the need of fast calculations, for example for sensitivity or uncertainty analysis or model predictive control. A measure for calculation time is the speed-up factor that needs to be attained for a case study, which is calculated by dividing the simulation

time of the detailed model over the time of the conceptual model. The objectives determine whether the development of the conceptual model is an appropriate solution.

The second step is the review of the available data and the detailed hydrodynamic model from which the conceptual model can be developed. The quality of those data and the detailed model have to be assessed. Special attention should be given to the purpose for which the detailed model was built. This influences the limitations and assumptions of the detailed model and therefore also of the conceptual model. Depending on the objectives of the conceptual model, simplifications of the detailed model might be considered to facilitate conceptualization. Possible simplifications affect hydraulic structures where complexity can be reduced, for instance by replacing complex hydraulic relationships and/or RTC rules by simplified overflow structures.

2.5.2 Model Development

When developing a conceptual model, it is crucial to identify the comparison points, i.e. the points where the conceptual model should predict accurate flow rates and is therefore compared to the detailed model. To do so, it is important that locations of rain gauges, overflows and key hydraulic structures are known. Because conceptual models only predict flow rates at the outlet of a catchment or sewer conduit but not within, no aggregation of catchments and sewers should take place over the comparison points. The selected comparison points therefore have to be calibrated and validated with a corresponding point in the detailed model.

The next step is the delineation and aggregation of catchments and sewers in accordance with previously identified comparison points. The delineation of catchments and sewers has to be carried out simultaneously as they are directly linked. Figure 2.4 illustrates a simple sewer system and its conceptualization. In the example sewer system, two points are identified as comparison points where flow rates have to be predicted. The illustration shows that the local sewers (dotted lines) are represented as sewer conduits in the detailed model. In the aggregated conceptual model, however, they are no longer represented as a sewer conduit model but are incorporated in the catchment model. Only the main sewer trunk between comparison point 1 and 2 is represented in a specific sewer conduit model. Special attention must be paid to catchments through which a conceptual sewer flows as the parameters of the catchment and the sewer model cannot be calibrated independently at the downstream comparison point. In Figure 2.4, this situation corresponds to comparison point 2, where the flow rate at this point represents both the flow from the sewer conduit and catchment 2. The parameters of the sewer model can be identified by using the methods described in Section 2.4.2. Therefore, the flow rate at point 2 can be used to calibrate and validate the catchment parameters of catchment 2 after having calibrated and validated catchment 1. It might be that structural properties of the detailed catchment models are too different and do not allow for aggregation. However, if possible, it is suggested that only one conceptual catchment model is calibrated

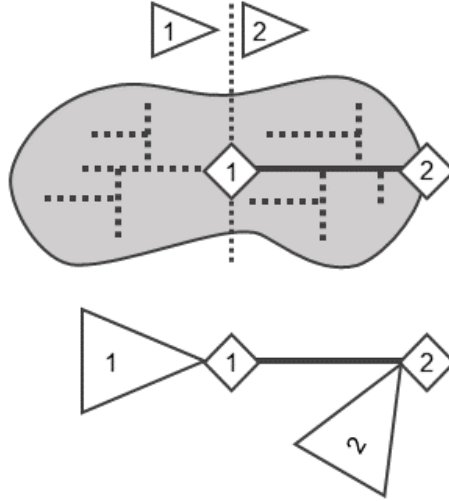


Figure 2.4: Schema illustrating a detailed model and its conceptual counterpart with two comparison points resulting in a conceptual model of two catchments and one sewer. The labeling of the comparison points indicates the calibration order.

per comparison point to avoid overparameterization. The catchments have therefore to be delineated accordingly.

2.5.3 Calibration

For the calibration of a conceptual model from a detailed model, two approaches are possible. The first is the parallel calibration of all sub-models (Wolfs et al., 2015). For each of the conceptual sub-models the detailed model results serve as input at the upstream comparison point. The parameters of the conceptual model are then calibrated at the downstream comparison point by fitting to the detailed model output. This allows independent calibration of all sub-models, which thus permits parallelisation of the calibration task. The second approach is the sequential calibration of the conceptual model, where the output of the previously calibrated upstream conceptual model serves as input to the conceptual model to be calibrated, and not the simulation results of the detailed model. For the proposed procedure, the second approach is adopted, as this approach allows for correction of inevitable model structure errors that occur during conceptualization. Even though the performance of each sub-model might be smaller due to the substitution of the detailed model's input with the upstream conceptual model, it is assumed that the overall performance at the downstream emission point is better, since upstream errors can be compensated for.

The order in which the parameters are calibrated is important and should be established prior to performing a calibration, as this will ensure that upstream model parameters are calibrated before the downstream parameters. In Figure 2.4, comparison point 1 is a first order comparison point, as it is further upstream, whereas comparison point 2 is a second

order comparison point. Assigning a calibration order for each comparison point has also the effect that it allows for parallel calibration of comparison points with the same order of calibration and therefore speeds up the calibration process.

Once the calibration order is identified the actual calibration is performed. If the catchment model is not known to the modeller, it is suggested to carry out a sensitivity analysis of the catchment model prior to calibration to determine the impact of the available model parameters. The calibration is first carried out for DWF and then for WWF, respecting the calibration order in both cases. For both DWF and WWF, the flow volume is calibrated before the flow dynamics. The previous step identified the parameters that can directly be translated from the detailed to the conceptual model. If the input and generation parameters can be translated directly, volume calibration is not necessary, but validation is recommended. The concentration and routing parameters representing the dynamics of the conceptual catchment model, however, are to be calibrated. Depending on the objective of the conceptual model, different performance criteria can be selected to assess the goodness of fit between the detailed and the conceptual model, see also Section 2.4.3. If the attained model calibration performance cannot be reached, it is suggested to go back to the previous stage of model development and refine the structure of the model.

2.5.4 Validation

In the last stage, the conceptual model is validated using a different rain time series. The rain data are used as an input to both the detailed model and the conceptual model. Comparing the flow rates at the identified comparison points with the chosen performance criteria will either validate the model or reveal that a recalibration of the conceptual model is necessary. If flow rate measurements at some points are available, it is strongly suggested to also validate the conceptual model with actual flow rate measurements. If the model validation is not successful it is suggested to go back to the stage of model development and refine the model structure.

2.6 Results

2.6.1 Developed Conceptual Models

The first stage of the project definition is summarized for both case studies in Table 2.1.

To identify the comparison points, the location of the rain gauges, overflows, and key hydraulic structures are indicated in Figure 2.1 for Ottawa and Figure 2.2 for Bordeaux. The chosen comparison points are shown in the same figures. The input and generation sub-models of the catchment were parametrized by aggregation and translation of the detailed model information. The sewer routing parameters were calculated for both cases by using the Kalinin-

Table 2.1: Project definition for case studies with objectives of conceptual models, detailed models and available data.

Step	Ottawa	Bordeaux
Objectives conceptual model	Fast conceptual model for later extension to an integrated model (including WRRF). Simulation time rain event < 1 min Calibration: NSE > 0.8 Validation: NSE > 0.65	Fast conceptual model valid over wide range of conditions to be extended with a water quality model. Simulation time rain event < 1 min. Calibration: NSE > 0.8 Validation: NSE > 0.65
Detailed models	SWMM 5 model (United States Environmental Protection Agency), built in 2013 to evaluate pipe capacities and overflows for large storm events (e.g. 100-year return period).	Mike Urban model (DHI, Horsholm, Denmark), built in 2012 to evaluate pumping capacities and overflows under WWF conditions for current and future scenarios (10 to 20 years).
Available data	7 rain gauges	4 rain gauges and 8 flow measurements

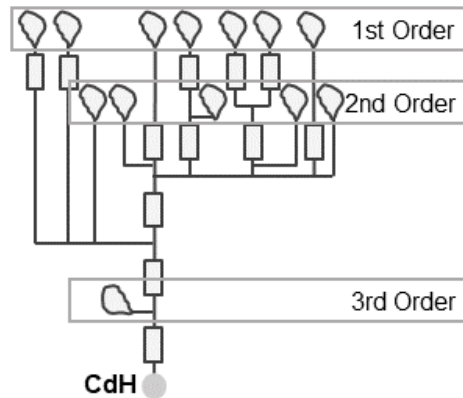


Figure 2.5: Schema of the calibration order for one of the four inlets at the WRRF of the Bordeaux case study.

Miljukov method (Euler, 1983) mentioned in Section 2.4.2. The flow concentration and routing parameters in the catchment could not be derived from the detailed model and are therefore calibrated and validated in the next stage.

As a first step in the calibration stage, the calibration order was determined for both case studies. This process is illustrated in Figure 2.5 for one of the tributaries of the Bordeaux case study. Catchments of the same order of calibration were calibrated in parallel. Following the procedure, the models were first calibrated for DWF and then for WWF. The calibration

Table 2.2: Summary of calibration and validation results. The full calibration and validation results can be found in Table A.1 and Table A.2 for Ottawa and Bordeaux, respectively.

Performance Indicator	DWF Calibration	WWF Calibration	WWF Validation
Ottawa Model V1			
Average NSE	1.00	0.96	0.95
Range NSE	0.99–1.00	0.89–0.99	0.84–1.00
Bordeaux			
Average NSE	0.93	0.95	0.87
Range NSE	0.84–1.00	0.84–1.00	0.71–0.94

Table 2.3: Comparison of detailed and conceptual models including the calculation time for the detailed and the conceptual model. Note that the conceptual model includes advective transport for water quality components in both cases.

Model		Ottawa		Bordeaux	
		Detailed	Conceptual V1	Detailed	Conceptual
Catchments	#	271	52	57	20
Conduits	#	2600	33	783	16
DWF (2 days)	(min)	8.03	0.53	7.64	0.37
Speedup factor			15		21
WWF (3 days)	(min)	30.7	0.63	10.7	0.92
Speedup factor			49		12

procedure applied was a grid search, where the best performing set of parameters was chosen if the performance objectives were met. Otherwise the grid was refined. If this did not lead to the desired results, the model structure had to be adapted. The summary of the results given in Table 2.2 shows that the calibration objective is met for all comparison points. The full results are provided in Table A.1 for Ottawa and Table A.2 for Bordeaux. For the fourth and last stage (model validation), a summary of the attainment of the objectives is also given in Table 2.2. It shows that the objective for the *NSE* is met in both case studies. The full validation results can likewise be found in Table A.1 and Table A.2. The results of the additional criteria for the simulated overall flow volume and peak flow values show that the conceptual model is not performing as well as during the calibration phase. Nevertheless, the values are still considered acceptable for the current case studies.

A summary of the developed models can be found in Table 2.3, which indicates the number of catchments and sewer conduits for both the detailed and the conceptual models, as well as the calculation time needed for the same flow rate simulations.

The speed-up factor was calculated by dividing the simulation time of the detailed over the conceptual model. It is to be noted that the conceptual model for both case studies already includes advective transport for water quality components in contrast to the detailed model, where this feature was deactivated as these models were never meant to be used for water

Table 2.4: Comparison of model V1 and V2 for Ottawa. Characteristics of sub-catchments and sewer conduits and summary of model performance.

Indicator	Attribute	Model V1	Model V2
Catchments	Number of sub-catchments	52	22
	Average/median size	146/102 ha	289/192 ha
	Size range	26–435 ha	26–732 ha
Sewers	Number of conduits	33	17
	Average/median length	1480/1280 m	2580/1490 m
	Length range	100–3000 m	770–7720 m
Speedup factor	DWF (2 days)	15	24
	WWF (3 days)	49	81
Performance	NSE DWF calibration average	1.00	1.00
	NSE DWF calibration range	0.99–1.00	1.00–1.00
	NSE WWF calibration average	0.96	0.97
	NSE WWF calibration range	0.89–0.99	0.92–0.99
	NSE WWF validation average	0.95	0.81
	NSE WWF validation range	0.84–1.00	0.68–0.91

quality. Nevertheless, a speed-up factor of over 10 could be reached for all studied flow conditions. The objective of simulating a WWF event within one minute (Table 2.1) is met for both case studies.

2.6.2 Level of Aggregation

For the Ottawa case study, the influence of the level of aggregation on model performance was evaluated. For the previously developed model (V1), it was ensured that catchments and sewer conduits were of similar size and that the aspect ratio of the catchments was not too elongated. To do so, large catchments and sewers were further subdivided to avoid a large variation in size and shape. For the further aggregated model V2, this was not considered anymore. This means that, with model V2, the maximum level of aggregation for the chosen comparison points was attained. The resulting characteristics of the catchment and sewer sub-models of the two different aggregation levels are indicated in Table 2.4. The more aggregated model V2 has approximately half the number of sub-catchments and sewer conduits than model V1 and thus shows an increased range of size and length parameters.

Sample calibrations of model V1 and V2 in comparison to the detailed model are shown in Figure 2.6. A summary of both calibration and validation results is given in Table 2.4, while the full calibration and validation results are provided in Table A.1. The validation results indicate that the performance of the model V2 is generally lower, but the validation objective for the NSE ($NSE > 0.65$) is met at all comparison points. The observation that the dynamics of the flow are generally a little less well represented in the model V2 makes sense, as the further aggregation results in a loss of resolution.

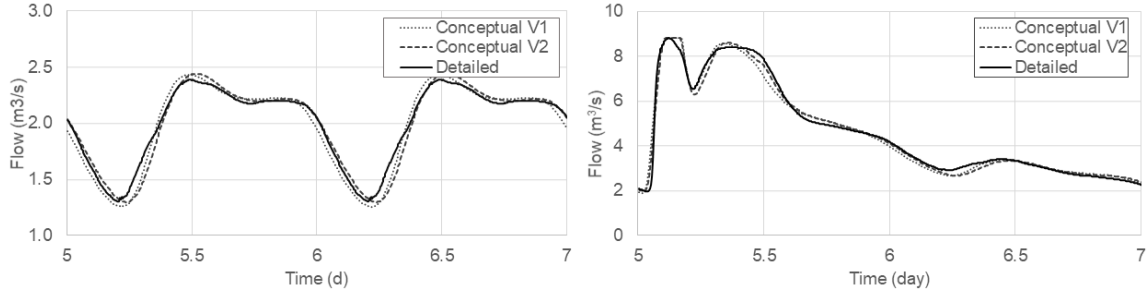


Figure 2.6: Sample flow results at selected location for DWF calibration (left-side) and WWF calibration (right-side) for the less aggregated conceptual model (V1) and the maximally aggregated model (V2).

The results of the comparison of the simulation times between both levels of aggregation are also summarized in Table 2.4. As expected, the further aggregated model V2 is faster than V1, using approximately 2/3 of the simulation time of model V1.

2.6.3 Comparison of Conceptual Model with Actual Flow Rate Data

As mentioned in Section 2.6.1, flow rate measurements are available for the Bordeaux case study. The model can thus be compared to actual measurement data and not only to simulation results of the detailed model. This was first done without any further model parameter adjustments after validation with the detailed model and is thus a true validation with respect to the model’s capability to represent reality. Figure 2.7 shows the total influent rate at the WRRF CdH inlet (left-side) and one of the four tributary branches (right-side) for 9–13 May 2017. From the left-hand side illustration, it can be concluded that the overall average DWF (DWF volume) is approximately correct, but that the dynamics are not well represented (dry weather day 8). The WWF, as such, seems underestimated (wet weather days 9–10) but this, as later will be demonstrated, is mainly due to the errors in the DWF. Furthermore, observations at one particular tributary to the WRRF CdH (right-hand side) shows that not only the dynamics do not match, but the average DWF flow for this tributary is clearly underestimated.

Table 2.5 summarizes the comparison of the conceptual model results (developed solely based on the detailed model), with the available flow rate measurements, the location of which is indicated in Figure 2.2. While the overall percentage volume error (CdH total) lies almost within an acceptable 10% error, the errors for each of the individual tributary branches at the inlet of the CdH WRRF are mostly higher. The NSE values demonstrate that the dynamics are poorly represented. Visual analysis of the results indicates that this is mainly caused by the poorly calibrated DWF volume. Good performance under DWF conditions was however never the intention of the detailed model.

As the results indicate shortcomings under DWF conditions, the DWF flow generation in the

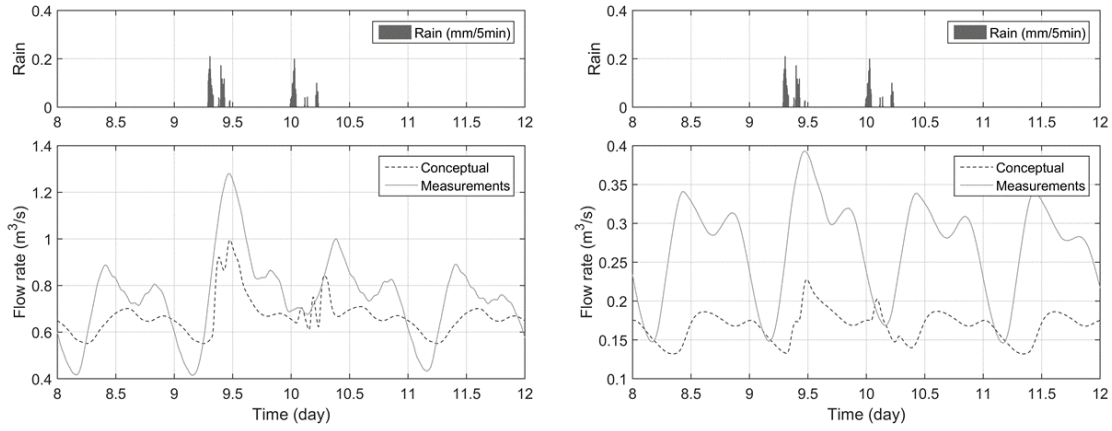


Figure 2.7: Comparison of the conceptual model built using the detailed model only with flow rate measurements for the total influent flow rate at the WRRF CdH (left-side) and one of the four tributary branches (right-side).

Table 2.5: Comparison of conceptual models with all available actual flow rate measurements. The location of the flow rate measurements is indicated in Figure 2.2. First the conceptual model built using the detailed model only is compared to the measurements and then the conceptual model with measurement based recalibrated DWF is compared to the measurements.

Comp. Point	Mea- sured Vol. (10^3 m^3)	Conceptual model calibrated on detailed model only				Conceptual model DWF recalibrated on measurements			
		Vol. (10^3 m^3)	PVE (%)	PEP (%)	NSE (-)	Vol. (10^3 m^3)	PVE (%)	PEP (%)	NSE (-)
CdH total	259	231	-11	-22	0.31	247	-5	-2	0.80
Tributary 1	93	58	-37	-42	-2.47	92	-1	2	0.85
Tributary 2	150	162	8	-10	0.59	139	-7	-3	0.69
Tributary 3	9	8	-14	-25	-0.47	10	9	5	0.65
Tributary 4	7	3	-56	-66	-1.99	6	-13	-24	0.72
Jourde Out	40	41	2	-16	0.70	38	-7	5	0.52
Jourde Over	0	3	n.a.	n.a.	n.a.	2	n.a.	n.a.	n.a.
C. Vernet Out	48	61	26	-18	-0.10	46	-5	-18	0.67
Noutary Inflow	61	59	-2	-17	0.44	55	-10	-12	0.60

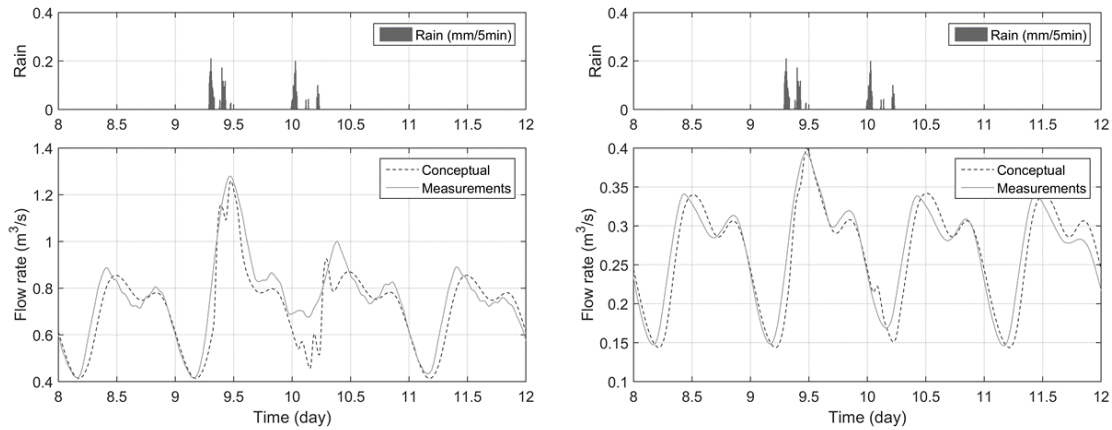


Figure 2.8: Comparison of conceptual model with recalibrated DWF contributions with actual flow rate measurements. Actual flow rate measurements were used to recalibrate the conceptual model for comparison with measured influent flows for the total influent flow rate at the WRRF CdH (left-side) and one of the four tributary branches (right-side).

catchment was recalibrated based on the available flow rate measurements. The parameters changed were the number of PE per catchment and the hourly representation of the daily DWF profile. In addition, it was recognized that some WWF pumping capacities in the system were increased in the time period between the development of the hydrodynamic model (2012) and the collection of more recent flow measurements (2017). These modelled capacities were revised to reflect current maximum pumping capacities.

The results of the recalibrated DWF model are shown in Figure 2.8 for the same validation period as in Figure 2.7. The total inflow to the WRRF CdH is shown on the left-side while the flows within one of the four tributary branches is depicted on the right-side. The example shows that both the average flow rate and the dynamics of the hydrograph are matching much better, even though shifts in time can be observed. This is due to the fact that the DWF profile in the conceptual model is now calibrated based on representative data, but the reality is that the system does not have such a consistent DWF pattern at all locations where it is applied in the model. With respect to the WWF response, one can observe that the measurements and the conceptual model simulation results match much better, even though no WWF parameters were changed.

The performance of the conceptual model with the recalibrated DWF contributions in comparison to the available flow measurements is also summarized in Table 2.5. It can be noted that the recalibration of the DWF greatly improved the performance. However, the conceptual model indicates a small overflow at Jourde, whereas the flow measurements show no such overflow. For this comparison point, the performance criteria could not be calculated (division by zero). However, the actual volume of the overflow reported by conceptual model is

comparably small.

2.7 Discussion

2.7.1 Development of Conceptual Models

The proposed procedure has been successfully tested with two independent case studies. The results demonstrated that the conceptual models represent the detailed model with the desired level of accuracy and result in considerably shorter simulation times compared to the detailed models. The question may arise why a conceptual model is better developed from a detailed model and not directly from information about the sewer system and flow rate measurements. The sewer system can be conceptualized with information about its physical properties only (see methods in Section 2.4.2), but the concentration and routing parameters in the catchment models need to be calibrated and validated on the basis of dynamic flow rate data (see the explanation in Section 2.5.2). Even though, in general, flow rate measurements can be available at several measurement points throughout the system, they are rarely available at every identified comparison point of the system. A detailed hydraulic model provides the best estimate for this non-existing data. In addition, the detailed model already and inherently contains a significant amount of characteristic data related to the catchment and the sewer system that are needed for the conceptualization, such as the PE per catchment and the physical properties of the sewer pipes. Conceptualization is thus made more efficient by the fact that this data does not need to be collected from other sources.

2.7.2 Level of Aggregation

Comparing a less aggregated conceptual model (V1) to a maximally aggregated model (V2) for the Ottawa case study showed that model V2 was still able to represent the flow dynamics of the detailed model at the comparison points (Table 2.4) although only about half the number of sub-catchments and conduits were used. This means that catchments and sewers can be aggregated to their maximum regarding the comparison points that are to be represented, as long as the special structures' locations are taken into account. While the number of sub-models was halved, the calculation time dropped only by about one third. This is due to the fixed overhead calculations (e.g. reading input files or plotting), which are independent of the number of sub-models used.

Further model aggregation results in faster simulations and less work to be spent on calibration and validation of the model. However, it comes also at a loss of information at the intermediate points that are no longer simulated and comes with the potential loss of accuracy, if the model structure is oversimplified and rain gauge influence zones are no longer respected.

2.7.3 Comparison to Flow Rate Measurement Data

Comparing the performance of a conceptual model purely built from a detailed model with real flow rate measurements highlighted two important points. First, the performance of the conceptual model with respect to replicating flow measurements is limited by the performance that the detailed model has with respect to the same flow measurements. This highlights the importance of the project definition stage, where the limitations and assumptions of the detailed model are analysed (see Section 2.5.1). For the Bordeaux case study, the detailed model was built to evaluate the sewer system under WWF conditions for current and future scenarios (see Table 2.1). Therefore, average flow rate approximation under DWF conditions was deemed sufficient. The poor performance of the conceptual model with respect to flow rate measurements was therefore caused by the purposeful omission of a DWF calibration and validation of the detailed model. These findings highlight the different purpose for which the detailed model was developed. In addition, it should be noted that the detailed model was developed in 2012, whereas the conceptual model was validated with 2017 flow rate measurements. A part of the discrepancy under DWF conditions might therefore also be caused by additional housing and industrial developments in specific sub-catchments over these 5 years. It is important to note, however, that the sewer network itself was not substantially changed or upgraded during this period.

Second, if the limitations of the detailed model are accounted for and/or rectified (in this case, the recalibration of the DWF model), the conceptual model can perform well in comparison to flow rate measurements without any further adjustments (see Table 2.5). It can therefore more generally be concluded that if the purpose of the detailed and the conceptual model are not identical, one has to carefully identify the assumptions underlying the detailed model and compensate for them when developing the conceptual model. Nevertheless, the advantages of developing the conceptual model by leveraging the modelling efforts already invested in the development of the detailed model remain very strong.

2.8 Conclusions

A four-stage modelling procedure was established to develop conceptual catchment and sewer models by maximizing the reuse of information and efforts invested in the development of a detailed hydraulic model. It was applied by different modelers on independent case studies. The procedure resulted in the successful validation of conceptual models for both cases, providing a speed-up factor of 10 to 80 for all comparison conditions. Thus, the conceptual models provide similar results to the detailed models at the selected comparison points but at a simulation rate that is at least ten times faster. It can therefore be concluded that, by applying the procedure, a faster conceptual model can be developed in a structured way. At the same time, it can be concluded that the procedure is sufficiently generic and transportable for application to

different case studies. The developed procedure follows similar stages as the Good Modelling Practice protocols reviewed for other disciplines, but is tailored to conceptualization, focusing on aggregation of catchments and sewers.

The study of additional aggregation showed the advantages and disadvantages of further aggregated models. A significant decrease in simulation time (33%) was obtained for an increased level of aggregation, but it was not found to be directly proportional to the level of aggregation. This can be expected for other case studies as well, but the reduction in simulation time is likely to depend on the modelling approach of the conceptual models and certainly also depends on the computational efficiency of the software chosen for both the detailed and the conceptual model.

From the validation of the conceptual model with actual flow rate measurements it could be concluded that the detailed and the conceptual model's objectives, and with this the modelling assumptions, need to be aligned. If they differ, they reveal where recalibration on actual measurements may be useful. The challenge of the Bordeaux model with actual flow rate data, however, also demonstrated that, if the assumptions of the detailed model are corrected, the conceptual model performs very well without further adjustments.

It is overall concluded that the proposed procedure provides a structured way to use the detailed model to develop the conceptual model. The procedure helps modelers to systematize the modelling process. The suggested procedure therefore improves the current situation in conceptual modelling, for which such a generally applicable procedure was missing.

Chapter 3

Optimal Experimental Design for Calibration of a New Sewer Water Quality Model

This chapter is redrafted from the article:

Ledergerber, J. M., Maruéjols, T., and Vanrolleghem, P. A. (2019). Optimal experimental design for calibration of a new sewer water quality model. *Journal of Hydrology*, 574:1020-1028.

Author contributions Conceptualization, J.M.L. and P.A.V.; Methodology, J.M.L. and P.A.V.; Investigation, J.M.L.; Writing – Original Draft Preparation, J.M.L.; Writing – Review & Editing, J.M.L. and P.A.V.; Visualization, J.M.L.; Supervision, T.M. and P.A.V.; Project Administration, T.M. and P.A.V.; Funding Acquisition, T.M. and P.A.V.

3.1 Abstract

Water quality data in the sewer system are indispensable for modelling, but rarely available, as measurements in sewers are challenging to conduct. Optimal experimental design is a powerful tool to identify and maximize the information content of measurement data. This chapter adopts a model-based optimal experimental design methodology to efficiently plan a measurement campaign for final model calibration and validation of a new sewer water quality model. To do so, a preliminary calibrated model of the case study is used to evaluate the information content of different potential measurement locations and scenarios for suspended solids as measured variable. The case study first demonstrates how optimal experimental design can identify the best measurement location within a complex sewer network. It secondly demonstrates that measuring the beginning of a big rain event results in the most information-rich data among all scenarios evaluated. Thirdly, it analyses in detail the information content

of dry weather flow data. In comparison to previous studies the methodology is improved by considering the actual measurement error characteristics when calculating the information content of measurement data.

3.2 Résumé

Les données sur la qualité de l'eau dans le réseau d'égout sont indispensables à la modélisation, mais rarement disponibles, car les mesures dans les égouts sont difficiles à effectuer. Le plan d'expériences optimal est un outil puissant pour identifier et maximiser le contenu d'information des données de mesure. Ce chapitre adopte une méthodologie basée sur un modèle pour planifier efficacement une campagne de mesure pour l'étalonnage final et la validation d'un nouveau modèle de la qualité de l'eau d'égout. Pour ce faire, un modèle calibré préliminaire de l'étude de cas est utilisé pour évaluer le contenu en information des différents points de mesure potentiels et des scénarios pour la matière en suspension comme variable mesurée. L'étude de cas montre d'abord comment le plan d'expériences optimal peut identifier le meilleur point de mesure dans un réseau d'égout complexe. Deuxièmement, il démontre que la mesure du début d'un épisode de pluie abondante permet d'obtenir les données les plus riches en information parmi tous les scénarios évalués. Troisièmement, il analyse en détail le contenu informatif des données de flux de temps sec. Par rapport aux études précédentes, la méthodologie est améliorée en tenant compte des caractéristiques d'erreur de mesure réelles lors du calcul du contenu informatif des données de mesure.

3.3 Introduction

Tackling the question of TSS in sewer systems goes beyond simply understanding the fate of particulates throughout the sewer system itself. TSS is known as a carrier of nutrients, but also as a carrier of heavy metals, pesticides and pathogens among others; moreover, it is the cause of organic and inorganic pollution. TSS can thus be considered an indicator substance (Vanrolleghem et al., 2018). Developing models for the prediction of the TSS flux for the control of overflow structures or the optimal management of the WRRF has therefore far-reaching benefits.

Water quality modelling for particulates remains challenging in the sewer. A main reason are the complex processes involved when it comes to TSS, as they greatly transcend mere advective transport. Particles can settle and resuspend; depending on the condition, they can flocculate, aggregate or break; and once settled, they can be consolidated on the bottom of the sewer pipes. In addition, different physical, chemical and biological processes take place both in the water phase and the sewer sediments (Ashley et al., 2004). Modelling developments are on-going, focusing on one or several processes to improve the understanding of those specific processes (e.g. for gross solids, Penn et al., 2018, or for bed load, Mohtar et al., 2018). But

even if models are currently not able to incorporate all the processes involved, they help to understand the behavior of TSS in sewer systems.

Independent of the TSS process modelled, data are indispensable for model calibration and validation. In particular, calibrating dynamic models benefits from high-resolution data as provided by online sensors. Unfortunately, these data are rarely available, as measuring in the sewer system is not very widespread and ambitious to conduct. Furthermore, they are distributed systems that may require measurements at multiple locations (Vanrolleghem et al., 1999). Measurements in sewers not only require a considerable investment in the equipment and the set-up of the measurement site, but also require a tight and intensive maintenance schedule to ensure measurements of reliable quality. The sensors need to be manually cleaned, calibrated and validated, which includes labour-intensive laboratory experiments (Ledergerber et al., 2017a). Moreover, not all data have the same information content for model calibration and validation. In order to calibrate a parameter, the parameter has to be influential during the time period when the data are collected (Dochain and Vanrolleghem, 2001). If a data set is available for calibration and validation of a complex model where overparameterization might be an issue, identifiability analysis is a method to assess the parameters that can be estimated from the given measurement data set (Freni et al., 2011). If, however, a new data set is to be collected, model-based OED can evaluate prior to the measurement campaign which potential experiment of a set of proposed experiments contains the most information for model calibration (Vanrolleghem et al., 1995). OED has mostly been applied in laboratory scale experiments and therefore in a controlled environment (see, for example, Vanrolleghem and Coen, 1995). OED utilizes a preliminary model that has been calibrated on an initial set of data: first, different experiments are proposed and simulated with the preliminary model; then simulation results are evaluated in terms of their information content (De Pauw and Vanrolleghem, 2006a). The information content of an experiment can be calculated from the Fisher Information Matrix (*FIM*), indicated in equation 3.1.

$$FIM = \sum_{k=1}^N \left(\frac{\partial y_i}{\partial \theta_j}(t_k) \right)^T Q(t_k) \left(\frac{\partial y_i}{\partial \theta_j}(t_k) \right) \quad (3.1)$$

where:

<i>FIM</i>	Fisher Information Matrix
y_i	Model output corresponding to measurements, i number of measurements
θ_j	Parameters, j number of parameters
t_k	Timestep k , with maximum timestep N
Q	Square matrix with user-supplied weighting coefficients

The *FIM* links the information content of an experiment to the sensitivity of the model output corresponding to the measurements y_i with respect to the parameters studied θ_j for the

timesteps t_k during the period of the experiment (time step 1 to N) and a square matrix Q with user-supplied weighting coefficients (De Pauw and Vanrolleghem, 2006a). Q is typically chosen as the inverse of the measurement error covariance or as the identity matrix (Vanrolleghem et al., 1995). An important characteristic of the *FIM* is the fact that the inverse of the *FIM* corresponds to the parameter estimation error covariance matrix V (Dochain and Vanrolleghem, 2001), thus allowing the direct assessment of the confidence region of the calibrated parameters. Different criteria exist to evaluate the information content of the proposed experiments, see, for example, Mehra (1974).

This chapter transcends the laboratory scale use of OED by applying it to design a second measurement campaign in a full-scale sewer environment. It studies how the potential information content of a new measurement data set can be optimized. It starts from the point that a first measurement campaign has already been conducted without OED. Those results allow calibrating and validating a preliminary model necessary for OED. It illustrates how OED can be adopted considering an approximation of the measurement error to select the best location and the best timing of the measurement for the second measurement campaign.

In the first Section 3.5.1, the measurement error is estimated with the results from the previous measurement campaign. This error approximates the weighting coefficients of the square matrix Q when calculating the *FIM*, rather than working with the identity matrix assumption as in previous studies (Vanrolleghem et al., 1995; Freni and Mannina, 2012). Then, the degrees of freedom and the constraints of the second measurement campaign are evaluated. Since the degrees of freedom include both the measurement location and the timing of the measurements, Section 3.5.2 re-evaluates the location of the RSM30 station and Section 3.5.3 studies different scenarios, thus timing of the measurements, for the chosen optimal location. In the final Section 3.5.4 DWF measurements are studied in more detail. These results allow planning the second measurement campaign in the most efficient way, making optimal use of the available budget, such as measurement equipment and working hours for maintenance.

3.4 Material and Methods

3.4.1 Case Study

Description Potential Measurement Locations

The case study CdH is described in detail in Chapter 1. Here only the relevant information for the OED is summarized. The studied sewer system is displayed in Figure 3.1 showing that pumping stations are located on both sides of the river Garonne. For the first measurement campaign, one RSM30 station was installed at the pumping station NT, and the second was installed at the inlet of the WRRF CdH. The pumping stations considered for the relocation of the RSM30 station in the sewer during the second measurement campaign are indicated

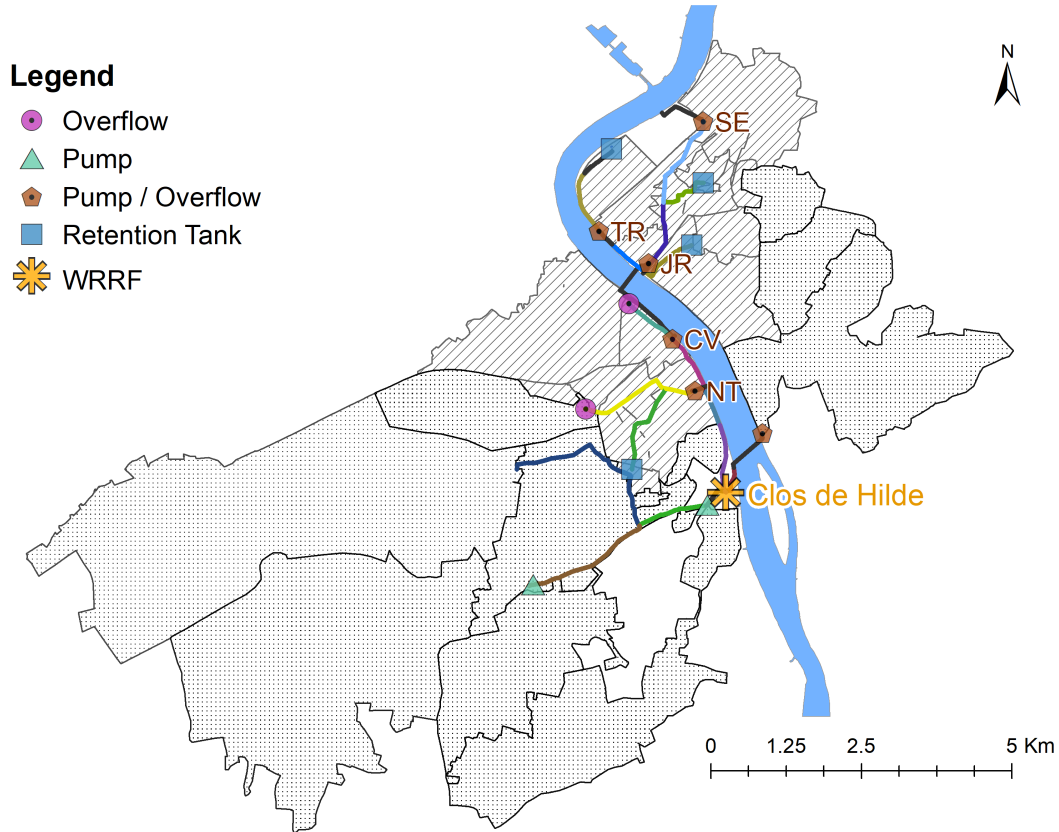


Figure 3.1: Catchment of the WRRF CdH with potential measurement locations for the RSM30 station in the sewer system indicated with a two letter code.

with a two letter code.

Available Data and Models

The data provided by the local utility is described in Section 1.3. Relevant for this chapter is, that water quantity (flow) data are available throughout the sewer system, water quality measurements however are collected by the utility only at the WRRF. In the framework of this project, a first measurement campaign to obtain an initial water quality data set for the sewer system was conducted in 2017.

In addition, a calibrated hydraulic model, implemented in Mike Urban (DHI, Denmark), is available for the water quantity calibration and validation. For further description for the conceptual model development based on the detailed model see Chapter 2.

Measurement Equipment and Installation

For this project, two RSM30 stations were available, each equipped with online TSS measurements. More detail on the measurements can be found in Section 1.4.

To collect the data for the preliminary model during the first measurement campaign, one RSM30 station was installed at the inlet of the WRRF CdH, while the other RSM30 station was installed at the major pumping chamber NT. The location of the sensors is indicated in Figure 3.1.

3.4.2 Preliminary Model

Modelling Approach

The preliminary model, with which the OED is conducted, describes the catchments and the sewer network of the WRRF CdH. The catchment model is described in detail in Section 4.4.1 and the sewer model in Section 4.4.3.

Calibration and Validation of Preliminary Model

The preliminary model for OED was calibrated for water quantity (flow) and water quality (TSS). The water quantity model for WWF was calibrated and validated (RMSE=0.058 m³/s) on the existing calibrated Mike Urban by DHI model. Only the DWF parameters had to be recalibrated on actual flow measurements, as the Mike Urban model focused on WWF. For more information on this see Section 2.6.3.

The validation period on actual flow measurements during a 4-day period, including WWF, is indicated in Figure 3.2 (left-hand side) and resulted in a RMSE of 0.064 m³/s. The preliminary water quality calibration and validation was conducted using TSS data obtained during the first measurement campaign. The time series were chosen based on an analysis of quality of the available data. A coherent measurement set was selected in which high quality data from both RSM30 station were available at the same time. The model was calibrated on a 10-day period including two rain events and was validated for the same 4-day period as the data set used for water quantity model validation, also indicated in Figure 3.2. Validation resulted in a RMSE of 58 mg TSS/l.

3.4.3 OED Methodology

Overview of Methodology

As mentioned in the previous Section 3.3, the core of OED is the calculation of the FIM and the evaluation of the experiments for a specific criterion. However, OED has to be viewed in a broader context. Figure 3.3 shows the OED methodology applied for this case study. It was inspired by many previous studies (e.g. Vanrolleghem and Coen (1995); Vanrolleghem et al.

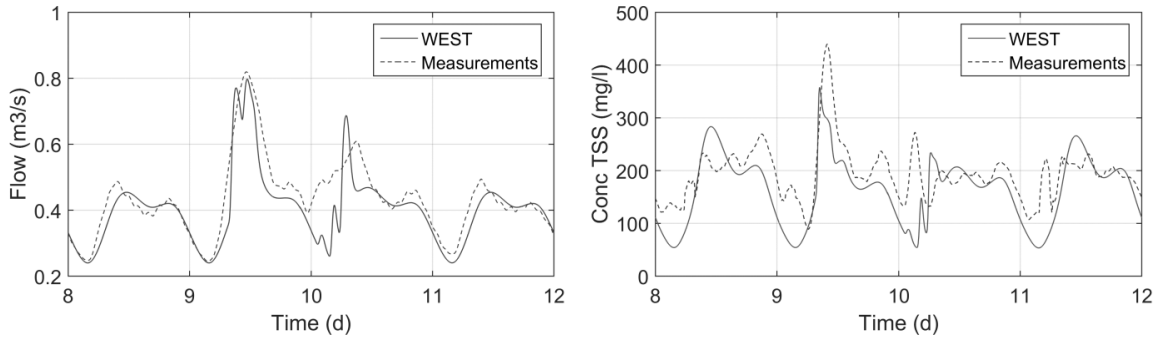


Figure 3.2: Validation of preliminary model for water quantity (left-hand side) and water quality (right-hand side) used for OED.

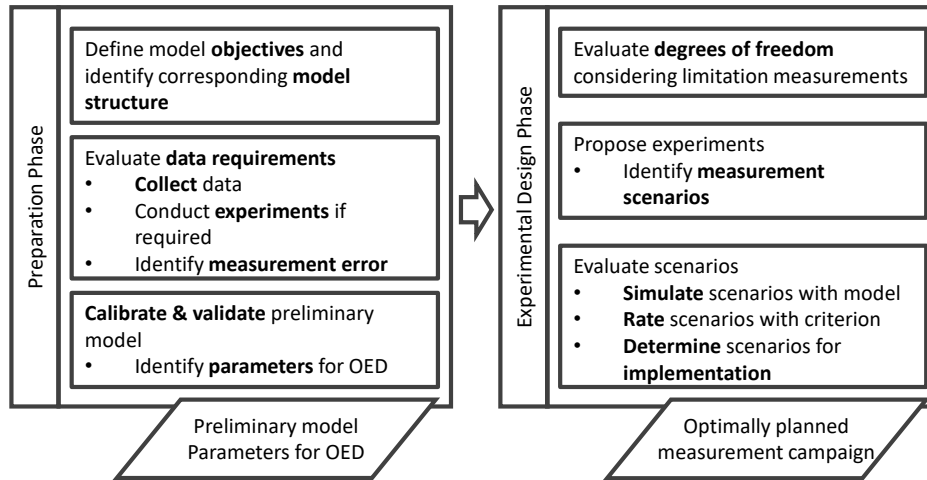


Figure 3.3: Proposed schema for the OED methodology.

(1995); De Pauw and Vanrolleghem (2006a)). The methodology is divided into two phases: the preparation phase (left) and the actual experimental design phase (right). Each phase will be described in a dedicated subsection.

Preparation Phase

The intended outcome of the preparation phase is a preliminary model, with which (a) future planned experiments can be evaluated, (b) the measurement error can be characterized, and (c) initial values can be assigned to the set of parameters for which the OED and, ultimately, the measurement campaign is conducted. The preparation phase consists of three steps, the first of which is inherent to all modelling tasks (Dochain and Vanrolleghem, 2001): identifying the

purpose of the model and with it the modelling objectives as well as the choice of corresponding model structure. The second step is to evaluate the data requirements for model calibration and validation. The data for the preliminary model have to be collected, which can include either obtaining available data or conducting a first measurement campaign if not sufficient data are available. An important aspect of this step is to analyse the measurement data and characterize the measurement error. The third step of the preparatory phase is to build, calibrate and validate the preliminary model and identify the parameter set for which the OED is conducted. Manifold references exist for calibration and validation criteria (see, for example, Hauduc et al., 2015).

Experimental Design Phase

The output of the second phase, the actual experimental design phase, is the optimally designed measurement campaign in view of recalibration of the previously identified parameters. This phase consists of three different steps. The first step is to propose experiments that could potentially be conducted. In the context of a sewer system, this step is better described as the identification of the measurement scenarios, as, unlike in laboratory conditions, the measurement conditions as such cannot be influenced, but the timing and location of the measurements can be chosen. The proposed scenarios have to be realistic with respect to the available measurement equipment, the duration of the campaign and the work required for implementation of the experiment. The second step is then to evaluate the proposed scenarios in terms of expected information content, taking the proper measurement error into account. Given the results of the OED evaluation criteria for the different scenarios proposed, the accordingly optimized measurement campaign can be implemented.

3.4.4 Additional Information Calculation

Considered Parameters for OED

As mentioned in Section 3.3 the aim of the OED for the case study is to acquire the most information-rich data for model calibration and validation of a model built for TSS predictions. Since the measurement campaign focuses on getting water quality measurements, for the OED only the parameters for water quality were considered. Water quantity parameters are constrained by the water balance and were well calibrated on the basis of the Mike Urban model and a DWF recalibration on measurement data (see Chapter 2).

The 29 parameters affecting water quality are present both in the catchment and the sewer sub-model. The parameters to be recalibrated are the following parameters: (i) in the catchment sub-model, the mean concentrations under DWF, WWF and infiltration flow, and (ii) in the sewer sub-model, the re-suspension parameters in each of the series of linear reservoirs ($r_{\text{resusp,max}}$, Q_{half} and n). For further information on the model parameters see Section 4.4. As the particle setting velocity distributions were obtained from good quality laboratory ViCAs

experiments, they were not considered as parameters to be included in the design of the second measurement campaign. Also, in contrast to other OED studies, e.g. Vanrolleghem et al. (1995), the initial conditions of all state variables of the model were not part of the OED. Indeed, they were not relevant for the simulation results as several days of warm-up were used in the simulations before the actual scenarios were simulated.

Calculation of Parameter Sensitivity

To complete the Fisher Information Matrix elements, the local sensitivity was calculated at each anticipated measurement point for the second measurement campaign as the central difference, according to equation 3.2 (De Pauw and Vanrolleghem, 2006b). The perturbation factor $\Delta\theta_j$ to calculate the sensitivity was +/- 1% of the parameter value for each of the parameters θ_j .

$$\frac{\partial y_i}{\partial \theta_j}(t) \approx \frac{y_i(t, \theta_j + \Delta\theta_j) - y_i(t, \theta_j - \Delta\theta_j)}{2\Delta\theta_j} \quad (3.2)$$

where:

- y_i Model output corresponding to measurements, i number of measurements
- θ_j Parameters, j number of parameters
- $\Delta\theta_j$ Perturbation of parameters

Definition of Measurement Error of TSS

As indicated in Section 1.4, the data obtained in the first measurement campaign of 2017 was filtered using the method developed by Alferes et al. (2013b). The comparison of the raw and the filtered data allows characterizing the measurement error $|\varepsilon|_{\text{meas,TSS}}$, which is defined as the absolute difference of the filtered ($\text{data}_{\text{filtered}}$) and the raw data (data_{raw}), as in equation 3.3.

$$|\varepsilon|_{\text{meas,TSS}}(t) = |\text{data}_{\text{filtered}}(t) - \text{data}_{\text{raw}}(t)| \quad (3.3)$$

where:

- $|\varepsilon|_{\text{meas,TSS}}$ Measurement error for TSS
- $\text{data}_{\text{filtered}}$ Filtered measurement data
- data_{raw} Raw measurement data

Evaluation Criterion for OED

For this study the D-optimal design criterion in equation 3.4 is chosen among the available scalars that can be calculated from the *FIM* (Mehra, 1974). As the *FIM* is the inverse of the parameter estimation error covariance matrix, maximising the determinant of the *FIM* results in minimizing the volume of the covariance matrix, thus minimizing the parameter estimation error (Dochain and Vanrolleghem, 2001).

$$\max [\det (FIM)] \quad (3.4)$$

3.5 Results

3.5.1 General Results

Measurement Error Estimation of TSS

Based on the assumption that the relative measurement error α does not depend on the TSS concentration ($Conc_{TSS}$), the absolute measurement error ($|\varepsilon|_{\text{meas},TSS}$), as defined in Section 3.4.4, depends linearly on $Conc_{TSS}$, as shown in equation 3.5. This relationship can be observed in Figure 3.4 for the TSS measurements at the pumping station NT.

$$|\varepsilon|_{\text{meas},TSS} = \alpha \cdot Conc_{TSS} \quad (3.5)$$

where:

$ \varepsilon _{\text{meas},TSS}$	Measurement error for TSS
α	Relative measurement error
$Conc_{TSS}$	TSS concentration

The coefficient α was obtained by fitting the above equation using least squares regression for both measurement locations: 0.09 for the inlet of the WRRF CdH and 0.18 for the pumping station NT. This difference between locations confirms the experience of the far more challenging measurement conditions in the sewer than at the WRRF.

Degrees of Freedom and Constraints for OED

In order to be able to identify the best possible experiments, hereafter named scenarios for the reasons mentioned in Section 3.4.3, the degrees of freedom of the measurement campaign had to be identified. They include the location of the RSM30 station and thus the location of the measurements as well as the timing of the measurement, differentiating between WWF and DWF and identifying different timings for both situations resulting in a two-dimensional problem.

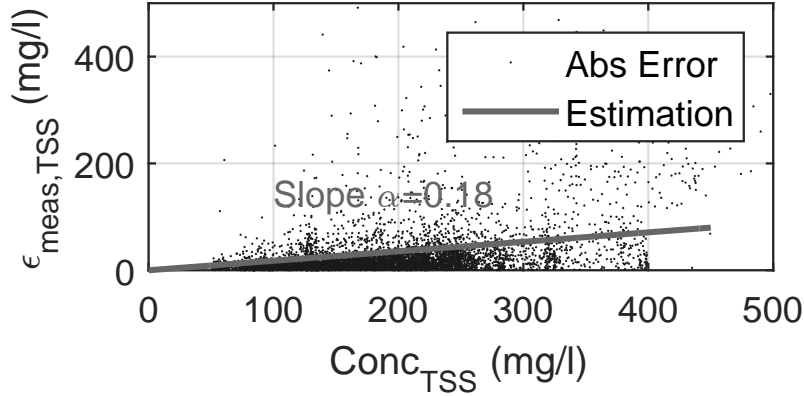


Figure 3.4: Linear dependency of absolute measurement error $|\varepsilon|_{\text{meas,TSS}}$ on TSS concentration at pumping station NT.

As mentioned initially, two RSM30 station were available for the measurement campaigns. During the first measurement campaign in 2017, which was designed based on expertise and practical experience, one RSM30 station was installed at the inlet of the WRRF CdH and the second was placed at the pumping station NT in the sewer system. The location of the RSM30 station in the sewer system was re-evaluated for the second measurement campaign, comparing eight potential locations (see Figure 3.1). The evaluated locations correspond to 7 pumping stations, respectively overflows upstream of the WRRF, the eight location CV&JR representing the confluence of two pumping stations. The first RSM30 station was always maintained at the inlet of the WRRF since this is the final outlet of the sewer system. As preliminary measurements were only available at the pumping station NT and the inlet of the WRRF CdH, the measurement error could only be estimated for those two locations. For the OED calculations, it was assumed that the measurement error found at NT was representative of the other seven locations in the sewer system.

Knowledge of the typical performance of the used measurement equipment and anticipation of different measurement conditions allow proposing measurement scenarios. The experience of the first measurement campaign showed that maintenance of the sensors is of fundamental importance and that sensors give only reliable data for a relatively short period of time after a maintenance event (Ledergerber et al., 2017a). For the given case study, it is assumed that, in the worst case, the reliable period lasts for only about 12h after a maintenance event. So, scenarios of 12h were planned with a measurement interval of three minutes, corresponding to the storage interval for the online sensors.

Different measurement scenarios were then created for the typical DWF pattern. For DWF, the day is split into day and night conditions, splitting at 09:30, respectively 21:30, assuming

that a workday starts at 09:00 at the site and sensors would have received their routine maintenance and be ready for use by 09:30. Measurement scenarios were also defined for WWF conditions, considering that, in contrast to DWF conditions, each rain event is different. To have representative rain scenarios, the proposed experiments were simulated using actual rain data of the previous measurement campaign, conducted in 2017. One big summer storm (cumulative 24h rainfall: 24.9 mm) was chosen in which multiple overflows were taking place in addition to a smaller rain event (cumulative 24h rainfall: 2.4 mm). Similar rains were observed several times over the summer of 2017. In total seven different scenarios were proposed, summarized in Table 3.1.

3.5.2 OED for Evaluation of Measurement Location

Due to the two dimensional problem (location and time), for the evaluation of the location of the RSM30 station in the sewer, scenario 6 (beginning of big rain event) was chosen. This was expected to be the best scenario independent of the location chosen, given the large TSS dynamics occurring (this will be confirmed in Section 3.5.3).

Figure 3.5 illustrates how the information content represented by value of the D-optimal criterion changes with the location of the RSM30 station in the sewer. The location of the RSM30 station at the pumping station NT, which was chosen for the first measurement campaign, ranks third among the eight identified options. The two places that rank better (CV&JR or JR) are located further upstream and contain information about the sewer system on the right bank of the Garonne, which NT lacks.

For the second measurement campaign a re-location of the RSM30 station from NT to either CV&JR or JR was therefore considered. A closer evaluation of the sites, however, revealed that those locations were no practical option, either due to the elevated risk of vandalism (JR) or accessibility (CV&JR). The location of the RSM30 station for the second measurement therefore remained at NT as it was the best possible location of those that were practically feasible.

3.5.3 OED for Evaluation of Measurement Scenarios

Most Information-rich Scenario

Since the information content (value of the D-optimal criterion) of a scenario depends on the location of the measurement station chosen, it was counted how often a scenario is evaluated as the most information-rich scenario for all eight measurement locations. The analysis was conducted once for all DWF and WWF scenarios and once for the DWF scenarios only (scenario 1 to 4, see Table 3.1). Figure 3.6 gives the results of this analysis, showing that, independent of the location chosen, the best-case scenario is always scenario 6, which corresponds to the

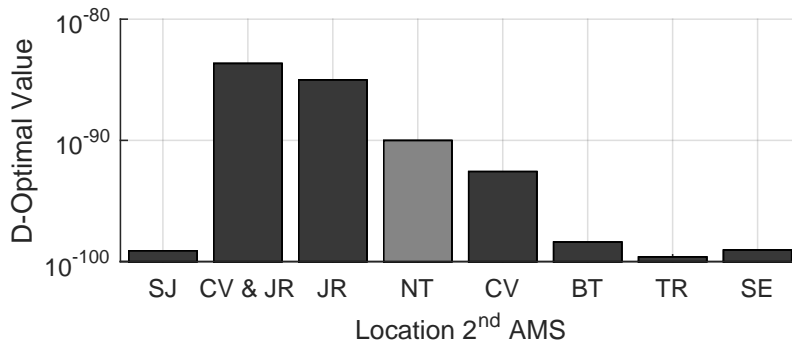


Figure 3.5: Comparison of different measurement locations for the RSM30 station in the sewer. The information content of the locations is evaluated with the D-optimal criterion for the timing of scenario 6.

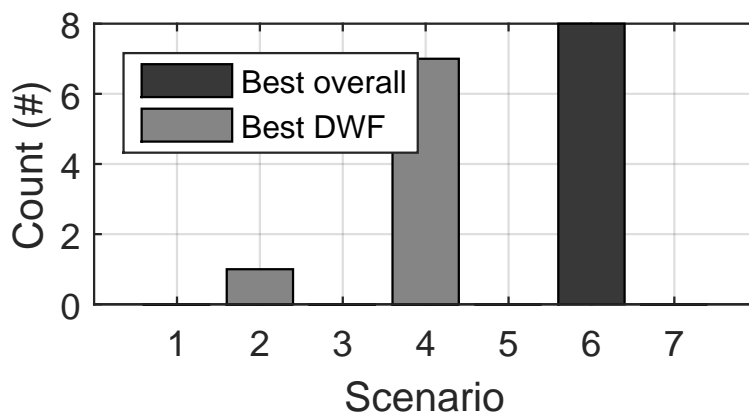


Figure 3.6: Evaluation of the best measurement scenario by counting the number of location pairs for which a scenario provided the most information content among all scenarios or all DWF scenarios.

beginning of a big rain event. This information was necessary for the previous analysis of the best measurement location in Section 3.5.2.

If the analysis is conducted for the DWF scenarios only, the results show that in seven out of the eight possible locations, scenario 4 (Night following WWF, see Table 3.1) contains the most-information rich data.

Detailed Scenario Analysis for Chosen Location

A detailed analysis of the actual information content is carried out only for the best practically feasible location combination of the RSM 30 stations, corresponding to the combination of NT

Table 3.1: Description of scenarios and resulting values of the D-optimal criterion for chosen RSM30 station location (NT and CdH).

#	Description Scenario	Characteristics	D-Opt value
1	Day long DWF period	Preceding DWF: 7 days	5.7E-142
2	Night long DWF period	Preceding DWF: 7 days	4.2E-127
3	Day following WWF	Preceding DWF: 0 days	2.6E-136
4	Night following WWF	Preceding DWF: 0 days	3.0E-127
5	Entire small rain event	24h cumulative rain: 2.4 mm	3.9E-115
6	Beginning big rain event	24h cumulative rain: 24.9 mm	9.0E-91
7	Tail big rain event	24h cumulative rain: 24.9 mm	2.7E-117

and CdH, as concluded in Section 3.5.2. The value of the D-optimal criterion for this location combination is summarized for all the scenarios in Table 3.1. One will notice that the absolute values for the D-criterion are very low in absolute terms, but this is due to the units used for the variables and parameters of the model. Optimality of the experiment does not depend on the absolute values, but on the ranking of the D-values.

For the DWF scenarios, only 28 parameters were considered, as the WWF TSS runoff concentration can only be estimated during WWF scenarios. The tabulated results show that the values of the D-criterion are by orders of magnitude higher for the WWF scenarios than for the DWF scenarios. The measurement campaign has therefore to focus on capturing wet weather conditions. It is also to be noted that the beginning of a big rain event (scenario 6) is by far richer in information than the tail of the event (scenario 7). In case of DWF-only conditions, the results show that data collected during night (21:30 – 09:30) are richer in information content than during day (09:30 – 21:30), with a longer preceding DWF period resulting in the best DWF scenario (scenario 2). A detailed analysis of the DWF is conducted in Section 3.5.4.

As the inverse of the *FIM*, V , corresponds to the parameter estimation error covariance matrix, the relative parameter estimation error of each parameter can be evaluated (the squared parameter estimation errors of the parameters j , σ_j^2 , are the diagonal elements of the matrix V). The resulting relative parameter estimation error ($\frac{\sigma_j}{\theta_j}$) is shown for three measurement scenarios in Figure 3.7, the worst-case scenario 1 (top), the best-case DWF scenario 2 (middle) and the overall best-case scenario 6. The figure clearly shows that parameter identification with only DWF measurements, even under the best conditions, is very difficult. Many parameters remain unidentifiable with a parameter estimation error much larger than the parameter value itself ($\frac{\sigma_j}{\theta_j} \gg 1$). An example for this is parameter 5, the flow at which half of the resuspension rate is reached (Q_{half}) for an upstream series of linear reservoirs. In the information-poorest scenario 1, the parameter has a parameter estimation error approximately 12 times its own value, while in the best-case DWF, this ratio is only reduced to approximately 3.

Analysing scenario 6 in Figure 3.7 shows, on the contrary, that the error on the parameter

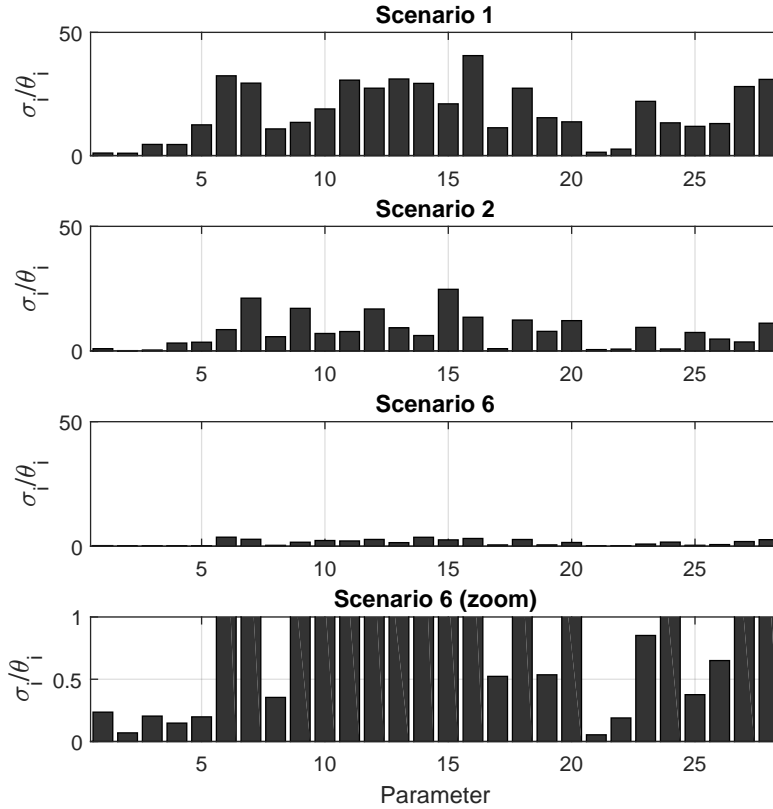


Figure 3.7: Relative parameter estimation error ($\frac{\sigma_j}{\theta_j}$) for the worst-case scenario 1 (top), the best-case DWF scenario 2 (middle) and the overall best-case scenario 6 (bottom), with a zoom on the errors for the best experiment (scenario 6).

estimation reduces dramatically for most parameters when measurements are conducted under WWF conditions. For instance, parameters 1 to 6 can now be estimated with a parameter estimation error that is less than 20% of their respective parameter value, an excellent result for water quality process parameters. It must be accepted though that some parameters remain difficult to identify, which is further studied in the next section.

Parameter Estimation Error and Distance from the Measurement Point

For the chosen location combination of the RSM30 stations and the best-case scenario 6, the parameter estimation error is studied with respect to where in the model the parameter occurs, i.e. in which sewer stretch the parameter occurs in the model. The hypothesis analysed here is that the farther the sewer stretch is from a measurement point, the lower the information content relative to the parameter occurring in that stretch is. The distance measure that is adopted here is the number of series of linear reservoirs between the sewer stretch of interest

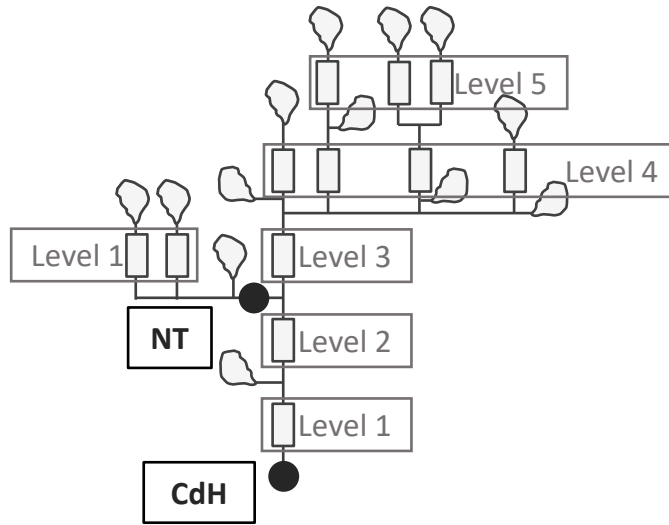


Figure 3.8: Definition of the distance from the closest measurement point, indicated as the number of series of linear reservoirs between the measurement point and the sewer stretch in which the parameter of interest occurs.

and the closest downstream measurement point. For this the layout of the case study shown in Figure 1.4 is schematized in Figure 3.8, indicating the distance from a measurement point by levels, which indicate the number of series of linear reservoirs. Global parameters are primarily the different TSS concentrations in the catchments, which determine the global mass balance and are thus considered to be “Level zero” parameters.

In Figure 3.9 the distance to the closest downstream measurement point is given for the parameters ordered with respect to their relative parameter estimation error $\frac{\sigma_i}{\theta_j}$. This figure shows a marked tendency for the parameter estimation error to increase with the distance to the closest downstream measurement point. Global parameters (Level zero) and parameters close to a measurement point can generally be better estimated.

3.5.4 OED for Optimal 12h Measurement Segment of DWF Day

Following the analysis of the different scenarios in the previous section, this last analysis tackles the question of which 12h measurement segment during stable DWF flow conditions contains the most information. Figure 3.10 shows the D-optimal value for every 12h segment following the full hour of the day. As the previous section already suggested, the information content is highly variable during the day. Figure 3.10 indicates that the information content is generally lower during measurement segments starting during day hours than during night hours. The 12h segment with the most information content starts at 02:00.

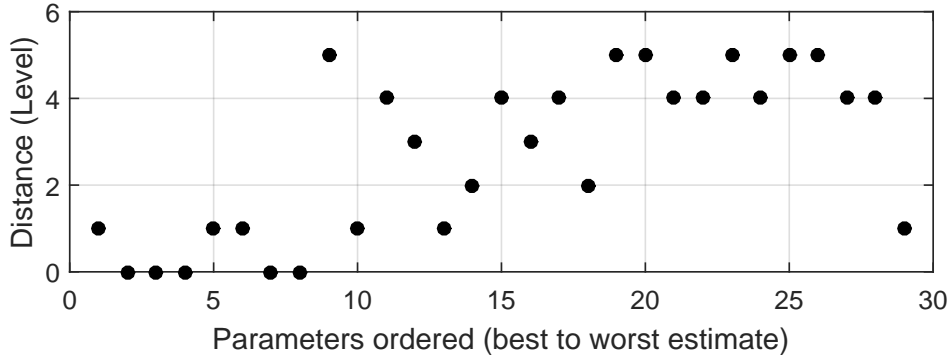


Figure 3.9: Parameters ordered from best to worst with respect to their relative parameter estimation error $\frac{\sigma_j}{\theta_j}$ in comparison to distance to the closest downstream measurement point, indicated as a level of distance.

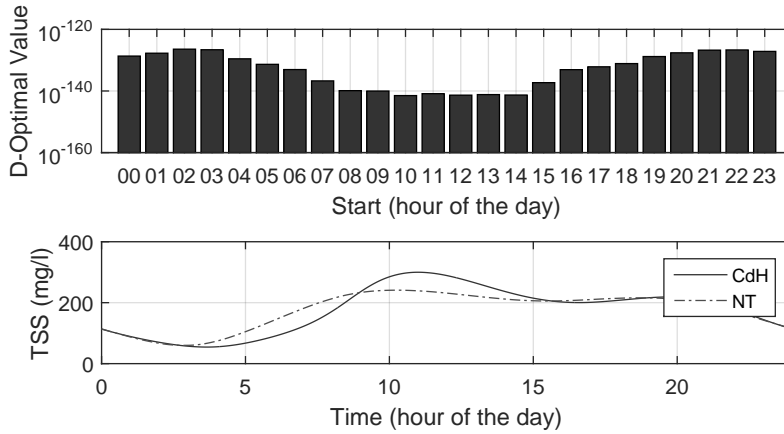


Figure 3.10: Evaluation with the D-optimal value of the information content of every 12h measurement interval starting at every full hour of the day.

3.6 Discussion

The estimation of the measurement error and the evaluation of the degrees of freedom for the second measurement campaign in Section 3.5.1 were necessary for the evaluation of the best possible set-up of the second measurement campaign.

Section 3.5.2 showed how OED can be used to identify the optimal measurement location. The results showed that the chosen location of the measurement station in the sewer, NT, ranked third. The better-ranked locations with regard to information content, CV&JR and JR, were unfortunately not feasible for practical reasons. This finding about the optimal location of the RSM 30 station is consistent with the location of the sewer stretch in which parameters occur that have a large parameter estimation error (see results Section 3.5.3). It

was demonstrated that parameters occurring in sewer stretches located at a large distance to the closest downstream measurement point (high level) are difficult to estimate. In general, those stretches are located on the right bank of the river Garonne. Moving the second RSM30 station to CV&JR or JR would indeed have allowed collecting more information about the parameters in those stretches. The current placement at NT collects information about the upstream part of the left bank of the river Garonne, as can be seen in Figure 3.1.

Section 3.5.3 evaluates different measurement timings for the best feasible measurement location (CdH and NT). It illustrates that for the same effort, i.e. a measurement campaign of 12h, data of markedly different information content can be obtained. It was shown that data collected under WWF conditions generally contain more information than those under DWF, with the beginning of a big rain event containing the most information. This is due to the important dynamics occurring during WWF conditions and the first-flush phenomenon observed for the given case study. The scenario analysis for DWF showed that the measurement campaign starting at 21:30 contains more information than the one starting at 9:30. This might be because the TSS concentrations during the night are generally lower than during daytime, which means that the measurement errors are smaller. Thus, the information content per TSS value is higher for the studied parameters.

The results in Section 3.5.4 analysed all theoretically possible 12h measurement segments starting at a full hour of a DWF day. The analysis also demonstrated that the information content of a measurement segment starting at 02:00 would contain most information, but those segments are not feasible from a practical point of view due to accessibility issues of pumping stations at night.

For the planning of the measurement campaign, it was imposed that the maintenance of the sensors must be performed prior to rain events because, if the sensors fail during a rain event, no maintenance intervention can be conducted for safety reasons. Since the beginning of the rain event is critically important, this is quite acceptable. In case DWF conditions prevail, the measurement campaign has to start late during the workday, in order to capture the information-rich night values to the fullest extent practicable. Having all of this information allows for planning a measurement campaign in its most efficient way, as it clearly indicates when the measurement campaign should be prepared and started. This ensures the optimal use of the measurement equipment and the limited resources during the campaign.

3.7 Conclusions

This research demonstrates that adaptation of model-based OED to complex sewer models is possible. It also shows that OED is a valuable tool for planning measurement campaigns in the challenging sewer environment as it allows making optimal use of the investments necessary for such a campaign. In comparison to posterior analysis of a measured data set,

OED evaluates the best location and timing for measurements prior to the actual measurement campaign. This would otherwise need to be planned by expert opinion only. OED allows to objectively rank different measurement locations with respect to their information content. This enables balancing how far upstream or downstream an RSM 30 station should be placed. With respect to the timing of the measurements, both expert opinion and OED identify WWF events as more important than DWF conditions. However, OED also differentiates between the importance of a small versus a big rain event and their beginning versus their tail. From a methodological point of view, it was demonstrated that considering the real measurement error (in this case constant relative error) affects the evaluation of the DWF scenarios. This would not have been possible without the mathematical tools provided by OED.

Chapter 4

Calibration and Validation of a PSVD-based Model of TSS in Integrated Urban Wastewater Systems

Ledergerber, J. M., Maruéjols, T., and Vanrolleghem, P. A. Calibration and validation of a PSVD-based model of TSS in integrated urban wastewater systems. *In preparation.*

Author contributions Conceptualization, J.M.L. and P.A.V.; Methodology, J.M.L. and P.A.V.; Investigation, J.M.L.; Writing – Original Draft Preparation, J.M.L.; Writing – Review & Editing, J.M.L., T.M. and P.A.V.; Visualization, J.M.L.; Supervision, T.M. and P.A.V.; Project Administration, T.M. and P.A.V.; Funding Acquisition, T.M. and P.A.V.

4.1 Abstract

Since water quality limits no longer apply only to the water resource recovery facility but are increasingly extended to the sewer system (in France since 2015), tools are necessary that allow quantifying water quality throughout the integrated urban wastewater system. These tools have to be able not only to represent the water quality at different points of interest, but should also be able to represent the interactions of the different subsystems. Only this allows to holistically describe and evaluate the integrated urban wastewater system and its subsystems. This chapter proposes the particle settling velocity distribution approach to assess the behavior of particulates throughout the integrated system. The approach is presented for the different submodels and extended with a catchment and a biofilter model, relevant for the biological treatment at the water resource recovery facility of the case study. The integrated model is successfully calibrated and validated for all the described sub-systems of the case study. The results demonstrate that the particle settling velocity distribution approach is able to represent the dynamics of both water quantity (flow) and total suspended solids at

the different validation points distributed over the integrated system. It is shown how the calibrated and validated model can be used to assess and compare the different fluxes of the particulates. It is thus concluded that the particle settling velocity distribution approach is a valuable tool to assess the water quality with respect to particulates throughout the integrated urban wastewater system.

4.2 Résumé

Comme les seuils limites de qualité de l'eau ne s'appliquent plus seulement au rejet de la station de récupération des ressources de l'eau mais sont étendues au réseau d'égout depuis l'arrêté français de 2015, des outils permettant de quantifier la qualité de l'eau sur l'ensemble du système intégré d'assainissement sont nécessaires. Ces outils doivent être capables non seulement de représenter la qualité de l'eau en différents points d'intérêt, mais aussi de représenter les interactions entre les différents sous-systèmes. Ce n'est qu'ainsi qu'il est possible de décrire et d'évaluer de manière holistique le système intégré d'assainissement et ses sous-systèmes. Ce chapitre propose l'approche de la vitesse de chute en assainissement pour évaluer le comportement des particules dans l'ensemble du système intégré. L'approche de la vitesse de chute en assainissement est présentée pour chaque sous-modèle et complétée par un modèle de bassin versant et un modèle de biofiltre pour le traitement biologique à la station de récupération des ressources de l'eau du site pilote. Le modèle intégré est calibré et validé avec succès pour tous les sous-systèmes décrits du site pilote. Les résultats démontrent que l'approche de la vitesse de chute en assainissement est capable de représenter la dynamique des débits et des concentrations en matières en suspension aux différents points de validation sur l'ensemble du système intégré. Il est montré comment le modèle calibré et validé peut être utilisé pour évaluer et comparer les différents flux de matières en suspension dans son ensemble. Il est donc conclu que l'approche de la vitesse de chute en assainissement est un outil précieux pour évaluer la qualité de l'eau en ce qui concerne les particules sur l'ensemble du système intégré d'assainissement.

4.3 The PSVD Modelling Approach

As described in the Section [Focus on Particulates](#), the PSVD is an important characteristic of particulates, when it comes to describing the behavior of the settling process. The PSVD modelling approach uses this characteristic to model the TSS throughout the integrated system where settling and resuspension are important processes to consider. The PSVD approach is thus followed throughout the sewer network, including the RTs, down to the primary treatment of the WRRF including the GC and the PC. The hypothesis is that once a particulate has a certain settling velocity assigned, this settling velocity does not change. Thus, processes such as breakage or agglomeration of particulates that could affect the PSVD are neglected.

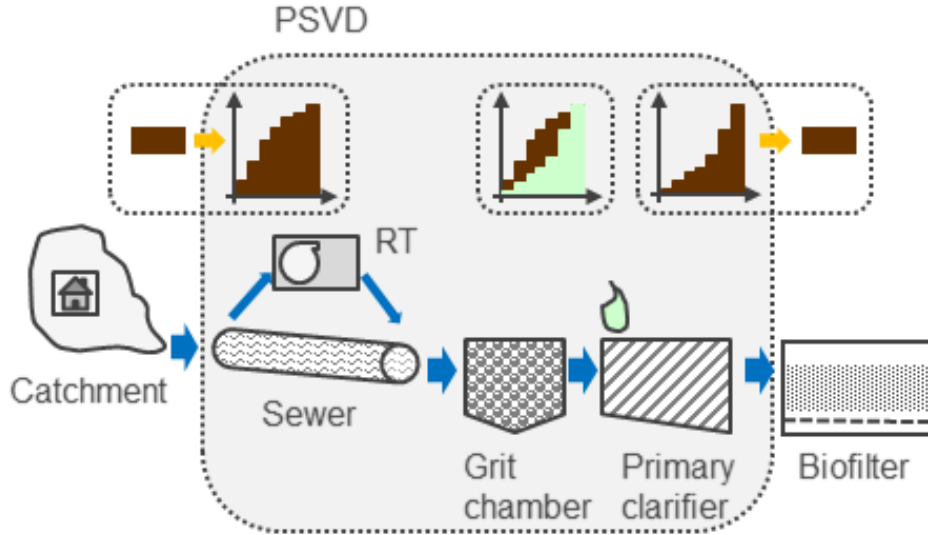


Figure 4.1: Overview of models with indication where PSVD approach is used.

The only exception is the CEPT, where the PSVD changes due to the addition of chemicals (see Section 4.4.7). For the TSS generation process in the catchment, as well as in the biological treatment of the WRRF, the PSVD characteristic is not considered. An overview of all IUWS subsystems to which the PSVD approach is applied is presented in Figure 4.1. Independent of the subsystem studied, the conceptual approach of the PSVDM stays the same. An introduction to the PSVDMs is given here.

As stated by Tik et al. (2014a), models that consider only a single, mean settling velocity for all particulates do not incorporate the heterogeneity of particulate pollution. The purpose of PSVDMs is to improve the predictive capacity of models by fractionating TSS into different particle classes. Each particle class is defined by its proper settling velocity obtained, for instance, by the ViCAs experiment (for the description of the ViCAs experiment see Section 1.4.3). Figure 4.2 illustrates how the total TSS is discretized into classes according to the cumulative settling velocity distribution (D_{TSS}) measured with the ViCAs experiment. Discretizing a function means always a loss of precision, since a certain amount of information is lost. Discretizing the settling velocity (v_s) into 10 classes ($v_{s,1}$ to $v_{s,10}$) has practically shown to give sufficient flexibility to the model to represent the PSVD from the sewer down to the PC sufficiently well. Approximating the distribution further down to a very small number of classes would not lead to a successful model application, since not all the relevant settling velocities for all specific submodels could be represented. Translating the cumulative settling velocity distribution into the density function (d_{TSS}) results in the fraction f_1 to f_{10} of the total TSS for each corresponding settling velocity class $v_{s,1}$ to $v_{s,10}$. The settling velocity $v_{s,i}$ depends on the boundary velocities of the classes chosen $v_{s,lim,i}$ and is calculated as the geometrical mean as in equation 4.1.

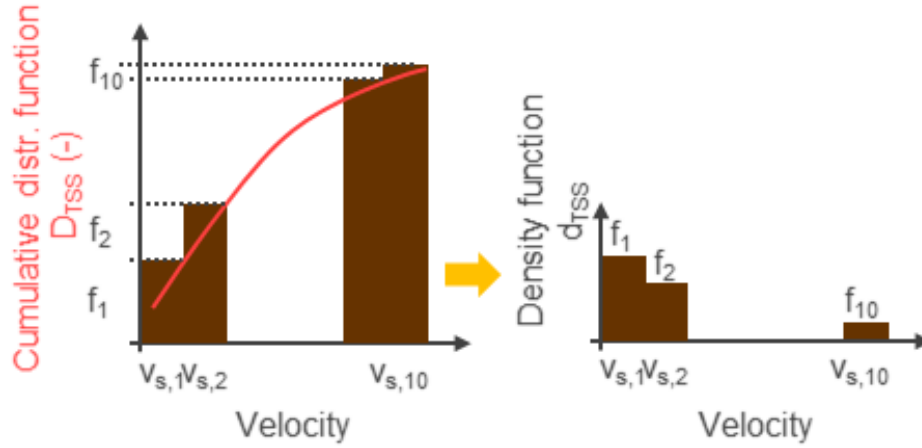


Figure 4.2: Fractionation of the total TSS into ten different classes according to the cumulative distribution of the PSVD (D_{TSS}). The corresponding density distribution (d_{TSS}) is also given.

$$v_{s,i} = \sqrt{v_{s,\text{lim},i-1} v_{s,\text{lim},i}} \quad (4.1)$$

where:

- $v_{s,i}$ Settling velocity of particle class i (L/T)
- $v_{s,\text{lim},i}$ Upper boundary velocity of class i (L/T)

The settling flux in all PSVDMs is calculated with the following assumption, that in order to be settled and no longer be in suspension, a particle class i with its mass M_i has to settle over the water height of the specific submodel with its corresponding settling velocity $v_{s,i}$. It is generally assumed that the settling process is not hindered, for example by turbulence. If the settling process is hindered, this is indicated in the specific submodel. The water height is usually calculated with the (time-varying) water volume $V(t)$ and the corresponding water surface A of the submodel. It is assumed that A is independent of the height and thus time. The settling flux can thus be calculated with equation 4.2.

$$F_{\text{sett},i}(t) = M_i(t) \frac{A}{V(t)} v_{s,i} \quad (4.2)$$

where:

- $M_i(t)$ Mass of particle class i (M)
- A Surface of submodel (L²)
- $V(t)$ Volume of submodel (L³)
- $v_{s,i}$ Settling velocity of particle class i (L/T)

The calculation of the resuspension flux is sub-model dependent, but in all submodels the resuspension rate is independent of the particle class and its settling velocity. The resuspension flux calculations will be explained for each sub-model separately.

The discretization of the TSS into the ten classes is described in Section 4.4.2 and the effect of the CEPT on the PSVD in Section 4.4.7.

4.4 Description of Subsystem Models

4.4.1 Catchment model

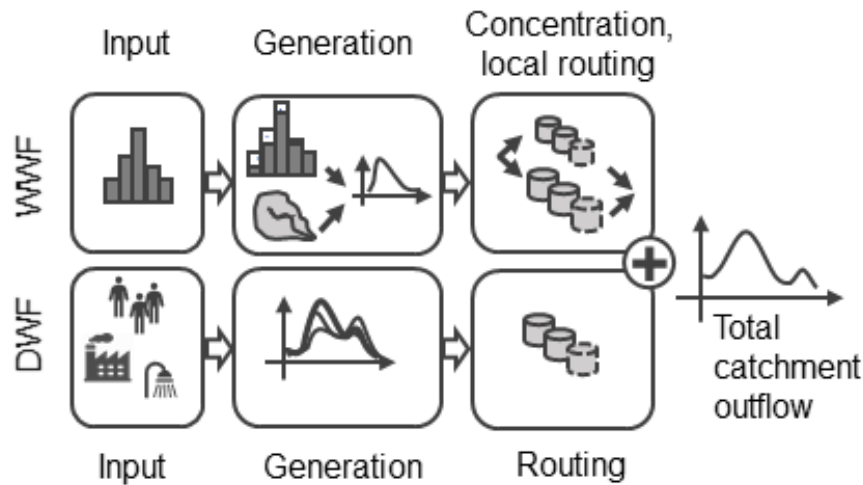


Figure 4.3: Extended KOSIM-WEST catchment model with a DWF and WWF module that includes splitting of the WWF in a fast and a slow concentration component.

The extended KOSIM-WEST model was initially described in Pieper (2017) and the description given here is extended from Ledergerber et al. (2019a).

The catchment model is based on the KOSIM model implemented in the software WEST (Meirlaen, 2002), coupling a module for WWF and a module for DWF. Figure 4.3 gives an overview of the extended catchment model and shows for both modules input, generation and routing. The input to the WWF module is rainfall information only. The flow generation takes into account different losses, such as wetting and depression losses to calculate the net rain. To generate the WWF flow, the net rain is applied over the effective area. In comparison to the original KOSIM-WEST model, the flow can be split into fast and slow flow concentration and local routing through a series of reservoirs to represent the fast and slow response characteristics of inflow and infiltration responses, respectively (Pieper, 2017). As conceptual catchments are generally aggregated over several detailed catchments, this process represents both flow concentration and local routing through the sewer network that is not modelled explicitly in a conceptual, lumped model. The input to the DWF module consists of

several information: the number of PE and their average wastewater generation rates, as well as the average wastewater production by local industry and constant groundwater infiltration to the sewer system. The DWF hydrograph is generated by applying hourly patterns over a DWF day. In comparison to the original KOSIM-WEST model, this DWF is now also routed with a series of linear reservoirs representing, as for the WWF, the flow propagation in the local sewer network (Pieper, 2017).

The water quality of the catchment for the WWF is considered with a simple event mean concentration. This concentration is applied to the runoff that is generated from the impervious surface. For the DWF the pollution is characterized with an average concentration that is distributed over the day with a relative pollution flux pattern. This means that if the pollution has the same pattern as the flow during DWF, the concentration is constant over the day. If the pollution pattern differs from the flow pattern, the concentration will vary. The constant groundwater infiltration flow is considered to have a low constant concentration of the pollutants.

4.4.2 Discretization from TSS to PSVD: the connector model

As mentioned in Section 4.3 the discretization from TSS to the PSVD classes occurs at the outlet of the catchment model, before entering the sewer system. This connector model takes the incoming TSS concentration and discretizes it into a set of ten PSVD classes with their corresponding settling velocity. Maruéjols et al. (2015) found that the PSVD of the wastewater is (linearly) depending on the TSS concentration. The correlation indicated that for low TSS concentration the particulates are settling slower than for high TSS concentrations where the particulates settle faster. A potential explanation for this correlation could be that different TSS concentration are found for different flow conditions. Different flow conditions indicate different sources of the particulates. Increased flow during DWF could increase the fraction of particulates from in-sewer sediment resuspension, whereas during increased WWF particulates from different surfaces are activated. The characteristic zone in which the PSVD curves are located was found to be site specific (Maruéjols et al., 2015).

The PSVD zone specific to the CdH catchment is indicated in Figure 4.4. The PSVD zone has two boundary curves. Those curves correspond to the measured cumulative distribution function of the highest (D_{high}) and lowest (D_{low}) measured TSS concentration. The highest curve was measured at TSS=500 mg/l and lowest at TSS=90 mg/l. The curves in Figure 4.4 indicate that at a higher TSS concentration the fraction of fast settling particulates increases in comparison to low TSS concentrations.

If the TSS concentration at the outlet of the catchment (TSS) is within those boundary concentrations ($TSS_{\text{high}}=500$ mg/l, respectively $TSS_{\text{low}}=90$ mg/l) the cumulative settling velocity distribution for that concentration ($D_{TSS,i}$) is interpolated between the two boundary curves

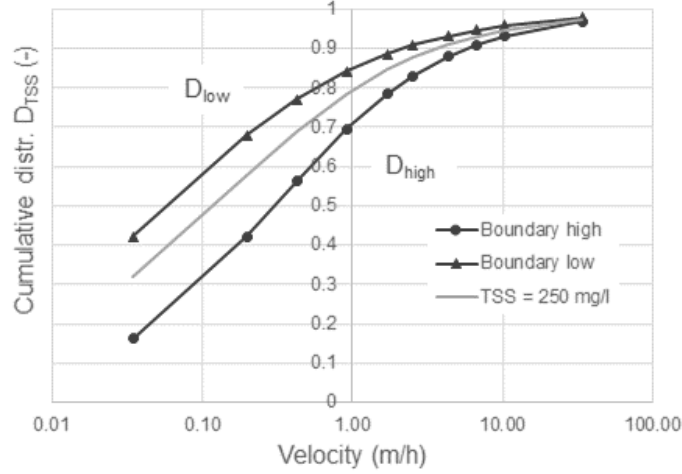


Figure 4.4: Zone of PSVD measurements in the CdH catchment. The boundary cumulative distribution D_{high} corresponds to TSS=500 mg/l and D_{low} to TSS=90 mg/l.

with equation 4.3. Figure 4.4 shows one example of an interpolated cumulative settling velocity distribution for a TSS concentration of 250 mg/l. If the TSS concentration exceeds the boundaries, the PSVD is approximated with the boundary curve itself. Another option would be the extrapolation of the highest, respectively lowest, measured PSVD curve as applied by Plana (2019). The connector model thus predicts a PSVD at each time step corresponding to the TSS concentration.

$$D_{TSS,i} = D_{\text{high},i} - (TSS - TSS_{\text{high}}) \frac{D_{\text{low},i} - D_{\text{high},i}}{TSS_{\text{high}} - TSS_{\text{low}}} \quad (4.3)$$

where:

$D_{TSS,i}$	PSVD of a TSS concentration discretized for classes i	(-)
$D_{\text{low},i}$	Boundary PSVD curve of the highest measured TSS concentration	(-)
$D_{\text{high},i}$	Boundary PSVD curve of the lowest measured TSS concentration	(-)
TSS_{low}	Lower boundary TSS concentration corresponding to 90 mg/l	(M/L ³)
TSS_{high}	Higher boundary TSS concentration corresponding to 500 mg/l	(M/L ³)
TSS	TSS concentration at the outlet of the catchment	(M/L ³)

4.4.3 PSVD Sewer Model

The PSVD sewer model is from a hydraulic perspective a conceptual model, also known as hydrological or lumped model (Maidment, 1993), that uses the approach of linear reservoirs in series. Water quality for particulates is considered with settling and resuspension within each of the reservoirs. First, the water quantity and then the water quality model will be described.

Water Quantity Model

The linear reservoir approach uses storage volumes to calculate the flow rate. The approach is based on the principle of mass conservation, shown in equation 4.4, which requires the difference of the inflow Q_{in} and outflow Q_{out} to be equal to the change of storage volume $V(t)$ of the reservoir (Maidment, 1993). The second equation of the linear reservoir approach relates the outflow to the storage volume (equation 4.5). The storage constant of the reservoir k is also known as the residence time (Maidment, 1993). If the value of the constant p equals one, equation 4.5 corresponds to a linear reservoir, otherwise it would be a non-linear reservoir (Maidment, 1993). The latter is, however, not considered for this study. If several reservoirs are placed in series, this is known as a cascade of linear reservoirs. The hydraulic principles that form the basis of the provided equations are that downstream flow conditions cannot influence upstream flow. However, in cases where backwater conditions exist, there are approaches available to properly approximate those effects (Vanrolleghem et al., 2009).

$$\frac{\partial V(t)}{\partial t} = Q_{in}(t) - Q_{out}(t) \quad (4.4)$$

$$Q_{out}(t) = \frac{1}{k}V(t)^{1/p} \quad (4.5)$$

where:

$V(t)$	Storage volume in reservoir	(L^3)
$Q_{in}(t)$	Inflow reservoir	(L^3/T)
$Q_{out}(t)$	Outflow reservoir	(L^3/T)
k	Storage constant of reservoir	(T^{-1})

Water Quality Model

To include water quality and in particular TSS, the linear reservoir approach is extended with the PSVD approach that models the fate of particulates in each of the reservoirs. The description of the sewer water quality model in this paragraph is based on Ledergerber et al. (2019d).

The PSVD sewer model consists of two compartments, the sewer compartment and the sediment compartment. Figure 4.5 shows that the sewer compartment is the compartment where the water flow takes place and thus the hydraulics are modelled. The sediment compartment however consists of sediment only and no flow is considered. The two compartments are needed to model both settling and resuspension of TSS. The TSS generated in the catchment is split into ten particle classes i before entering the sewer system. In the sewer compartment, it is assumed that the particulates are in suspension and that each class settles with its specific settling velocity $v_{s,i}$ according to the general PSVD settling assumption, given in equation 4.2.

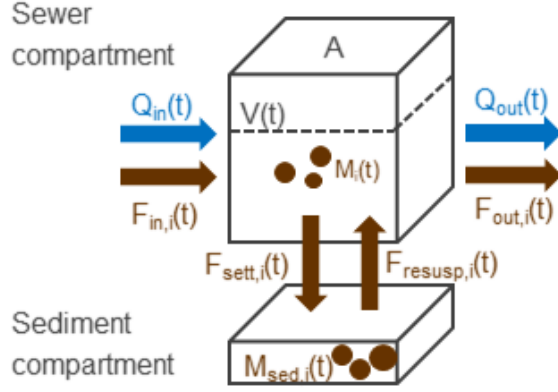


Figure 4.5: Schema of PSVD sewer water quality model

The resuspension flux $F_{\text{resusp},i}(t)$ is calculated with equation 4.6, which depends on the particle mass settled in the sediment compartment $M_{\text{sed},i}(t)$ and the resuspension rate $r_{\text{resusp}}(t)$ that is defined in equation 4.7. The resuspension is independent of the particle class i and calculated using the maximum resuspension rate $r_{\text{resusp,max}}$ and depends on the flow rate into the linear reservoir $Q_{\text{in}}(t)$ assuming a saturation function with parameters Q_{half} , the flow at which half of the maximum resuspension rate is reached, as well as the exponent n , which determines the steepness of the change around Q_{half} . This fraction represents a sigmoidal behavior, resulting in a value between 0 and 1.

$$F_{\text{resusp},i}(t) = M_{\text{sed},i}(t)r_{\text{resusp}}(t) \quad (4.6)$$

$$r_{\text{resusp}}(t) = r_{\text{resusp,max}} \frac{Q_{\text{in}}^n(t)}{Q_{\text{in}}^n(t) + Q_{\text{half}}^n} \quad (4.7)$$

where:

$F_{\text{resusp},i}(t)$	Resuspension flux for particle class i	(M/T)
$M_{\text{sed},i}(t)$	Particle mass of class i settled in the sediment compartment	(M)
$r_{\text{resusp}}(t)$	Resuspension rate	(T ⁻¹)
$r_{\text{resusp,max}}$	Maximum resuspension rate	(T ⁻¹)
$Q_{\text{in}}(t)$	Inflow to reservoir	(L ³ /T)
Q_{half}	Flow at which half of the maximum resuspension rate is reached	(L ³ /T)
n	Exponent, indication for the steepness of change around Q_{half}	(-)

The sigmoidal behavior of the fraction in equation 4.7 is illustrated in Figure 4.6. The left-hand side shows the behavior of the fraction for a varying Q_{half} , assuming a constant n . This illustrates that indeed half of the resuspension rate $r_{\text{resusp}}(t)$ is reached at Q_{half} , since the fraction of 0.5 is reached at a Q_{in} corresponding to Q_{half} . The right-hand side of Figure 4.6 shows the behavior of the fraction for varying n , assuming a constant Q_{half} . This illustrates

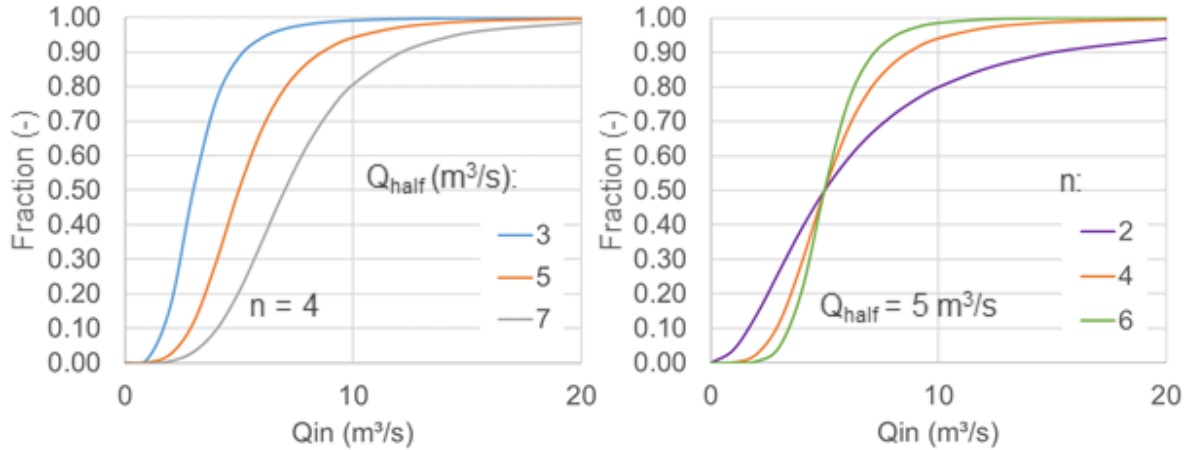


Figure 4.6: Illustration of the sigmoidal behavior of the fraction for the calculation of the resuspension rate in equation 4.7. The left-hand side shows the behavior of the fraction for varying Q_{half} , whereas the right-hand side shows the behavior for varying n .

that with increasing n , the change around Q_{half} happens faster due to the increased steepness of the function.

4.4.4 Retention tank model

The RT model is based on the off-line RT model proposed by Maruéjols et al. (2012). In order to have a fast running model, the model had to be simplified. The main change was that the separately modelled pumping chamber of the original model was removed.

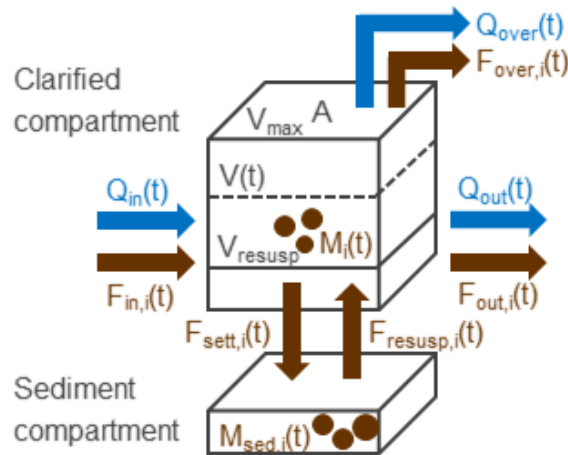


Figure 4.7: Schema of PSVD RT water quality model

The schema of the RT model in Figure 4.7 shows that it consists, as the sewer model, of two compartments: the clarified compartment, where the water can be stored, and the sediment

compartment. As for the sewer model, the hydraulics take place in the clarified compartment and the sediment compartment can be considered a storage compartment for the settled particulates.

For the water flow and with it, the advective pollution transport, three fluxes are considered: the inflow to the RT $Q_{\text{in}}(t)$, the regular outflow $Q_{\text{out}}(t)$ that generally brings the water back into the sewer system and eventually to the WRRF and an overflow $Q_{\text{over}}(t)$ that represents the security outflow when the maximum capacity of the tank is reached. For the particulates, however, two additional fluxes have to be considered: the settling and resuspension fluxes. The settling flux in the RT is calculated with the standard equation for settling in the PSVDMs (see equation 4.2). The assumption for the resuspension is that it only takes place if a cleaning mechanism in the RT is installed that is usually activated during the last emptying phase of the tank. This mechanism can be activated, for instance, by giving the fraction of remaining volume during emptying at which the cleaning mechanism is activated. The resuspension flux $F_{\text{resusp},i}(t)$ is then calculated with equation 4.8, where $M_{\text{sed},i}$ represents the particle mass settled in the sediment compartment and r_{resusp} the resuspension rate that is by default set to 10 d^{-1} (Maruéjols et al., 2012). Note that the resuspension is independent of the particle class, as it was already for the sewer water quality model.

$$F_{\text{resusp},i}(t) = M_{\text{sed},i}(t)r_{\text{resusp}} \quad (4.8)$$

where:

$F_{\text{resusp},i}(t)$	Resuspension flux for particle class i	(M/T)
$M_{\text{sed},i}(t)$	Particle mass of class i settled in the sediment compartment	(M)
r_{resusp}	Resuspension rate	(T ⁻¹)

4.4.5 Grit Chamber and Primary Clarifier Model

The GC and the PC have a very similar conceptual modelling approach and are therefore explained in the same section. In fact, the concept of the GC is an extension of the PC. Hence, the concept of the PC is explained first, so that it can later on be extended to the GC.

Primary Clarifier

The PSVDM of the PC is conceptually similar to the one-dimensional, layered settling model presented in Takács et al. (1991), which is commonly referred to as the Takács model. However, in comparison to the Takács model, where the TSS concentration is not fractionated into different classes, the PSVDM currently takes into account ten different particle classes with their settling velocities. A schematic representation of the approach is shown in left side of Figure 4.8.

The PSVDM approach, initially presented in Bachis et al. (2015), uses ten layers to model the spatial TSS gradient in the PC. For the water flow and with it, the advective pollution transport, three fluxes are considered: The inflow $Q_{in}(t)$, the outflow $Q_{out}(t)$ and the underflow $Q_{under}(t)$. The inflow $Q_{in}(t)$ is fed into the fifth layer. The clarified effluent $Q_{out}(t)$ leaves the PC from the first layer (top layer), whereas the wastage flow rate $Q_{under}(t)$ is modelled from the tenth layer (bottom layer). Therefore, it is assumed that only the feed layer and the layers above are affected by the advective flow caused by clarified effluent, which results in the pollutant flux $F_{up}(t)$. For the advective flux caused by the wastage flow rate $F_{dn}(t)$ it is correspondingly assumed that it only affects the feed layer and the layers below.

There is one additional flux that affects particulates only, the settling flux $F_{sett,i}(t)$. It is calculated for each class in each layer with the standard equation for settling in the PSVDMs (see equation 4.2).

Aerated Grit Chamber

The PSVD aerated GC model is a conceptual extension of the PC model. By comparing Figure 4.9 for the PSVD GC model with the PC model in Figure 4.8, the two main differences from a conceptual point of view can be seen: the number of layers and the additional flux $F_{air,i}(t)$ in the GC model. The number of layers in the GC is five only and the feed takes place in the fourth layer.

The additional particle flux $F_{air,i}(t)$ represents the upstream flux of particulates per surface caused by the air flow Q_{air} introduced in the GC. The effect of the air on the settling process is assumed to be decreasing with increasing height from the bottom, where it is added. The air flow is taken into account by modelling the upwards velocity v_{air} resulting from the airflow. To

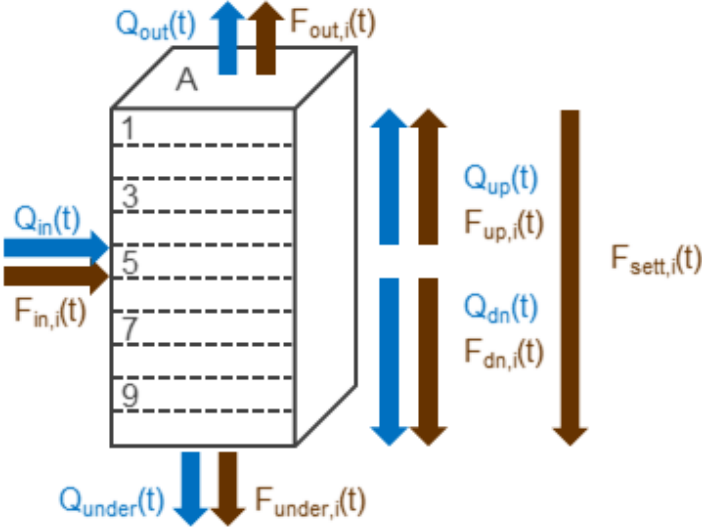


Figure 4.8: Schema of PSVD PC water quality model

model the energy dissipation from the bottom to the top, this velocity decreases over the GC height, making the velocity layer l dependent ($v_{\text{air},l}$). equation 4.9 thus calculates the velocity from the air flow as function of the layer index, taking into account the surface area of the GC A . The surface is assumed to be constant over the height of the GC. The decreasing effect of air is accounted by decreasing factor k_d . The velocity $v_{\text{air},l}$ for a specific layer l is reduced by k_d to the power of 5 (total number of layers) minus the current layer number l . This means that this induced velocity is highest in the bottom layer, i.e. layer 5, and decreases with the distance from the air source, as energy dissipates. Note that the velocity $v_{\text{air},l}$ is independent of the particle class i .

Similar to the other fluxes, the upstream flux induced by the air flow ($F_{\text{air},i,l}$) is calculated using the specific concentration of the particle class i in layer l , $TSS_{i,l}$ which is multiplied with the upstream air velocity $v_{\text{air},l}$ of the same layer, see equation 4.10.

$$v_{\text{air},l} = k_d^{5-l} \frac{Q_{\text{air}}}{A} \quad (4.9)$$

$$F_{\text{air},i,l} = v_{\text{air},l} TSS_{i,l} \quad (4.10)$$

where:

$v_{\text{air},l}$	Airflow induced upstream velocity depending on layer l	(L/T)
k_d^{5-l}	Decreasing factor for airflow induced velocity depending on layer l	(-)
Q_{air}	Upstream air flow	(L ³ /T)
A	Surface area of the GC	(L ²)
$F_{\text{air},i,l}$	Upstream flux per surface induced by the air flow	(M/L ² /T)
$TSS_{i,l}$	Concentration of the particle class i in layer l	(M/L ³)

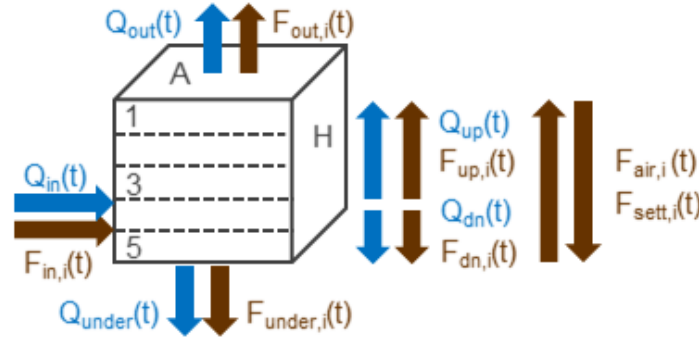


Figure 4.9: Schema of PSVD GC water quality model

4.4.6 Model of Coagulant Addition Controller

The control of the coagulant addition is modelled exactly as the controller that is implemented on the WRRF CdH. The controller has been explained extensively in Section 1.2. Therefore no further explanations are given here. How the effect of the chemical addition on the PSVD is modelled is explained in the next Section 4.4.7.

4.4.7 Transformation of PSVD characteristics due to CEPT

By performing a ViCAs experiment on samples with and without coagulant addition (for the specific study alum was used as coagulant), Bachis et al. (2015) showed that the addition of coagulants and flocculants (CF) during the CEPT changes the settling characteristics of particulates and thus the PSVD of the wastewater. Figure 4.10, which is a zoom of the overall PSVD approach Figure 4.1, shows schematically the effect of CF addition. It was found that the impact of CEPT on a wastewater sample tends to “shift” the PSVD curve to the right. This shift implies that the fractions of particulates with higher settling velocity are increased at the expense of classes with lower settling velocity (Bachis et al., 2015). Figure 4.10 also shows this shift of the PSVD curve by showing that sample without CF addition (brown) has higher fractions with lower settling velocities than the same sample with CF addition (green). The green distribution is “shifted” to the right in comparison to the brown distribution. Tik et al. (2016a) could reproduce this effect, but could additionally show that a minimum concentration of chemicals is needed to start observing such a shift of the PSVD curve. The study could similarly show that the effect of chemical addition saturates at a certain concentration. Adding more chemicals than this saturation concentration does not lead to improved settability of the particulates and thus no effect is visible on the PSVD.

This effect is taken into account in the model, by making the TSS fractionation depending on the chemical addition by using a sigmoidal representation of the PSVD change (Tik et al., 2016a). The PSVD of the sample after the addition of the CF $D_{out,i}$ is modelled with equation 4.11. It shows that $D_{out,i}$ depends on the PSVD of the inflow to the CF addition $D_{in,i}$, thus the PSVD of the sample without CF addition. The equation shows also, that $D_{out,i}$ depends on the PSVD corresponding to the saturation effect of CF addition $D_{sat,i}$. The last term of the equation basically describes how close $D_{out,i}$ is to the saturation PSVD curve $D_{sat,i}$. The parameter describing this, are the concentration of the CF added by the controller, here $CF(t)$, the exponent $expCF$, which is an indication of how fast it changes and the last parameter, CF_{half} , the concentration at which half the effect is visible. This means that if the CF concentration is comparably high to the half



Figure 4.10: Effect of CEPT on the PSVD. Comparing the same sample without (brown) and with CF addition (green).

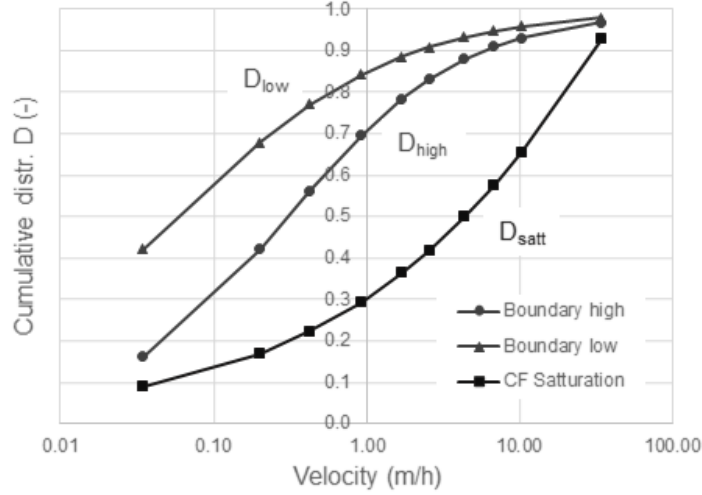


Figure 4.11: PSVD curve reached at saturation of CF addition. This curve corresponds to the PSVD measured after CF addition at a TSS concentration of approximately 400 mg/l.

effect constant CF_{half} , the outgoing PSVD curve $D_{\text{out},i}$ will correspond to the CF saturation PSVD boundary curve $D_{\text{sat},i}$.

$$D_{\text{out},i}(t) = D_{\text{in},i}(t) - (D_{\text{in},i}(t) - D_{\text{sat},i}) \frac{CF(t)^{\text{exp}CF}}{CF_{\text{half}}^{\text{exp}CF} + CF(t)^{\text{exp}CF}} \quad (4.11)$$

where:

$D_{\text{out},i}(t)$	PSVD after CF addition	(-)
$D_{\text{in},i}(t)$	PSVD before CF addition	(-)
$D_{\text{sat},i}$	PSVD curve reached at saturation, "maximum" PSVD	(-)
$CF(t)$	Dosed CF concentration	(M/L ³)
$\text{exp}CF$	Exponent indicating the fastness of change (the larger the faster)	(-)
K_{CF}	Concentration at which half the effect is visible	(M/L ³)

For the case study CdH, the saturation curve $D_{\text{sat},i}$ is assumed to correspond to the highest measured TSS concentration of a PSVD experiment (approximately 400 mg/l). This concentration coincides with the TSS concentration where the maximum dosage of coagulat is reached (see Section 1.2). This means that even if the incoming TSS concentration exceeds 400 mg/l, the controller will add no more than 45 mg/l of the CF. The saturation PSVD curve is shown in Figure 4.11, which also indicates the PSVD distribution measured prior to chemical addition (see Section 4.4.2).

Given the measured saturation curve D_{sat} , Figure 4.12 presents the modelled effect of the CF addition for the CdH case study. The effect is shown for the distribution of four illustrative TSS concentration without ("in") and with ("out") CF addition. The lowest illustrated concentration

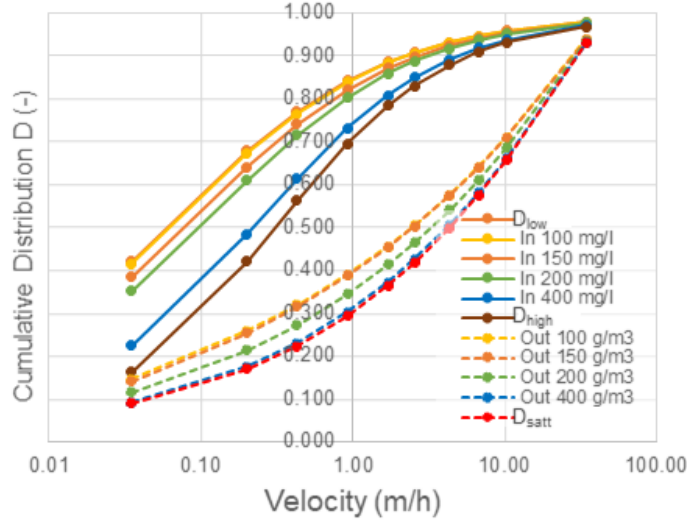


Figure 4.12: Modelled Effect of CEPT for samples with different TSS concentrations.

corresponds to 100 mg/l, whereas the highest corresponds to 400 mg/l. In Figure 4.12 it can be observed that for all the concentration the addition of CF induces a shift to the right. This means generally, that the particulates are settling faster after the addition of the CF. A second observation is that both for the distribution “in” and the distribution “out” the smaller TSS concentration have the lower settling velocity. This corresponds to the findings in Section 4.4.2.

4.4.8 Biofilter model

The simple approach for the BF model is shown in Figure 4.13. The BF is modelled with a percentage removal efficiency approach and a completely stirred tank reactor (CSTR). As usual, the inflow $Q_{in}(t)$ has a corresponding influx of particulates $F_{in}(t)$, of which a percentage fraction is directly removed. As for the GC and the PC, the removed flux is called $F_{under,i}(t)$. Since the BF is modelled with a percentage removal efficiency, the underflow of particulates $F_{under,i}(t)$ can be directly calculated with the removal efficiency RE from the influx, as given in equation 4.12. It is assumed that this flux is removed constantly from the BF. This contrasts with the common implementation of BFs where particulates are first retained in the filter and then removed intermittently via the backwash of the filters.

$$F_{under,i}(t) = RE \cdot F_{in,i}(t) \quad (4.12)$$

where:

$F_{under,i}(t)$	Underflux of reactor, removed particle flux	(M/T)
RE	Removal efficiency	(-)
$F_{in,i}(t)$	Influx of particulates	(M/T)

The remaining flux is entering a CSTR, where the particulate flux $F_{\text{out},i}(t)$ of the outflow $Q_{\text{out}}(t)$ is calculated with the standard equation for concentration and thus effluent concentration of CSTRs, given in equation 4.13. $M_i(t)$ is representing the particulate mass and V the volume of the reactor. This results in the mass balance equation of the BF model given in equation 4.14.

$$F_{\text{out},i}(t) = \frac{M_i(t)}{V} Q_{\text{out}}(t) \quad (4.13)$$

$$\frac{dM_i}{dt} = F_{\text{in},i}(1 - RE) - \frac{M_i(t)}{V} Q_{\text{out}} \quad (4.14)$$

where:

$F_{\text{out},i}(t)$	Outflow particle flux	(M/T)
$M_i(t)$	Particle mass of class i in reactor	(M)
V	Volume of reactor	(L ³)
$Q_{\text{out}}(t)$	Outflow of reactor	(L ³ /T)
$F_{\text{in},i}(t)$	Influx of particulates	(M/T)

4.5 Calibration and Validation Approach

For the calibration of the IUWS model, a step-wise approach has been chosen. This means that the model was built element-wise and that it was calibrated and validated before the model was extended with an additional submodel. The three main model elements were calibrated and validated in the following order:

1. Catchment and sewer quantity model
2. Catchment and sewer quality model

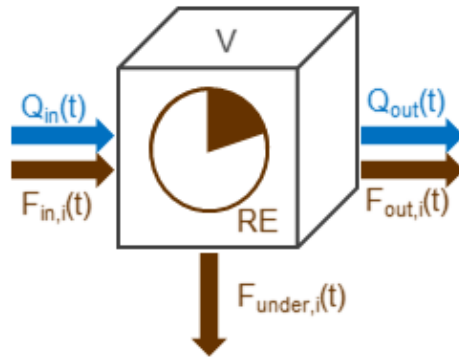


Figure 4.13: Schema of simple BF water quality model

Table 4.1: Data used for model calibration and validation with * indicating that data was collected through measurement campaign.

Abbreviation	Description	Quantity	Quality
Tributary 1	Tributary 1 of inflow WRRF CdH	yes	no
Tributary 2	Tributary 2 of inflow WRRF CdH	yes	yes*
Tributary 3	Tributary 3 of inflow WRRF CdH	yes	no
Tributary 4	Tributary 4 of inflow WRRF CdH	yes	no
JR out	Pumping station / CSO Jourde: flow to WRRF	yes	no
JR over	Pumping station / CSO Jourde: flow to Garonne	yes	no
CV out	Pumping station / CSO Carle Vernet: flow to WRRF	yes	no
NT in	Pumping station / CSO Noutary: inflow	yes	yes*
PC out	Primary clarifier outflow	no	yes
BF out	Biofilter outflow	no	yes

3. WRRF quantity and quality model

The submodel-specific calibration information will be described in a dedicated section for each element. The general calibration approach was however the same for all elements. All sub-models have been calibrated using a grid search approach with the objective function of minimizing the RMSE between the model and the measurements. The RMSE calculates a mean error penalizing greater errors more heavily and results in a value with the same units as the model results, which is useful for interpretation (Bennett et al., 2013). The model validity is evaluated with the Janus coefficient that compares the performance of the validation period in comparison to the calibration period. The coefficient is calculated by dividing the RMSE of the validation period with the RMSE of the calibration period and should be close to 1 (Sin et al., 2008).

The calibration and validation points are summarized in Table 4.1. The location of the measurement points in the sewer system are shown on the map in Figure 1.3 and measurement points on the WRRF are indicated on the plant layout in Figure 1.5.

The calibration period for all sub-models is the measurement period from day 65-75, corresponding to the calendar days July 5th to 15th 2017. This calibration period has a rain event with an estimated return period of approximately 3 months based on the rain depth-duration-curve given in Figure 4.14. This return period corresponds to the aimed size of rain events (see Problem Statement and Objectives and the evaluation in Chapter 6). Initially it was planned to recalibrate the model with data obtained during the 2nd measurement campaign in 2018, planned with OED. This was however not possible for practical reasons, as no rain event could be measured at NT during this second campaign.

The model has been validated with rain events of different magnitudes. Eight different periods were initially chosen for model validation. Only model results of validation 1 and 4 are

presented in the results Section 4.6, since they show that the model is performing well over a wide range of rainfall events. The first and slightly bigger rain event in the validation period 1 has an estimated return period <0.5 months and is thus quite a bit smaller than the rain event chosen for calibration. The rain event in validation period 4 has a return period >24 months, which is considerably bigger than for the calibration event. Unfortunately, no water quality measurements were available at NT for model validation.

4.5.1 Catchment and Sewer Quantity Model

As described in Chapter 2, the quantitative conceptual catchment and sewer model was initially built based on a detailed hydraulic model and then partially recalibrated on measurement data. The initial model development from the detailed model was an important step, since it defined the level of aggregation of the catchment and the sewer stretches. As described in Section 2.6.1, the water quantity sewer parameters were directly identified from the detailed model using the Kalinin-Miljukov method (Euler, 1983). Since this method is purely based on the sewer characteristics, the flow information from the detailed model at the comparison points could be used to calibrate and validate the catchment parameters that could not be directly aggregated from the detailed model. As described in Section 2.5.2, the catchment parameters regarding water quantity were directly aggregated from the detailed hydraulic model, whereas parameters regarding the dynamics were calibrated with the flow data from the detailed model.

For the sewer water quantity model, several real flow measurements were available. Table 4.1 gives an overview of the flow measurements used for the recalibration of the conceptual model on flow measurements. The comparison of the developed model based only on the detailed

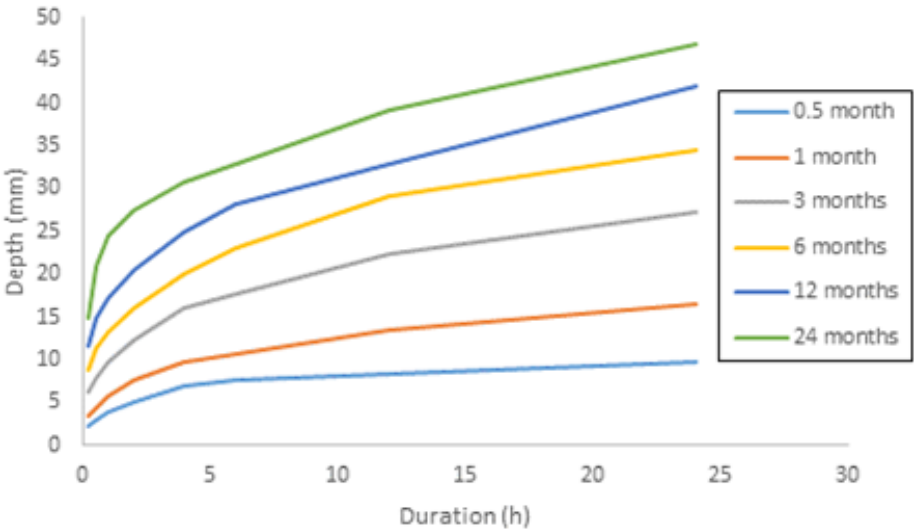


Figure 4.14: Depth-duration-curve for Bordeaux to estimate the return periods of rain events.

model with those data showed the need for recalibration in Section 2.6.3. The comparison with the measurement data highlighted at first the need for recalibration of the DWF quantity, thus the amount flow generated, and dynamics, meaning the flow distribution over the day and revealed later on some slight adjustments for WWF dynamics. Even though the flow measurements in Table 4.1 were available, they were less than the identified comparison points in the detailed model. Thus, several catchment models had to be recalibrated based on a single flow measurement location. For the recalibration of the DWF generation, the necessary adjustments regarding PE and thus the DWF generated, were distributed proportionally between all upstream catchments of a flow measurement. The assumption regarding the DWF profile was that all catchments upstream of one measurement point have the same flow profile. This was a necessary assumption since no more detailed information was available. In a later step, the WWF dynamics of the catchment model were slightly adjusted, since it was found that the catchments were reacting slower than suggested by the detailed model. The flow generation parameters, however, needed no change.

The parameters regarding the sewer model were not changed from the initial development with the Kalinin-Miljukov method.

4.5.2 Catchment and Sewer Quality Model

For the water quality aspects, no prior model was available. The water quality had thus to be calibrated and validated directly on the measurements for both DWF and WWF. For the DWF it was assumed that the pollution concentration is constant over the day, meaning that the pollution flux has the same pattern as the flow. Table 4.1 shows that two measurement points for water quality in the sewer were available: NT in and Tributary 2, with NT being a subcatchment of Tributary 2 of the WRRF. The calibration process started furthest upstream, thus calibrating the catchments and sewers upstream of NT, before calibrating the remaining catchments and sewers upstream of Tributary 2 with the measurement at this tributary. For the calibration of the catchments and sewers upstream of Tributary 1, 3 and 4, where no water quality measurements were available, it was assumed that the characteristics of Tributary 2 were representative for these tributaries. It was for example assumed that the TSS generation per PE was the same.

4.5.3 WRRF Quantity and Quality Model

For the WRRF no prior model was available and the models had thus to be built, calibrated and validated based on the measurements.

Since no water is lost or generated on a WRRF, the water quantity flowing in the WRRF should be equal the water flowing out the WRRF. The flow measurements at the inlet and at the outlet however showed a discrepancy of $\sim 10\%$. According to the operators a 10% difference, however, lies within the error of the measurements and is considered sufficiently

accurate. It was assumed that the four flow measurements at the inlet of the WRRF were correct and that the one at the outlet was off by 10%.

The water quality model of the WRRF was also calibrated in a step-wise approach. Once a specific sub-model was calibrated and validated, the next sub-model was calibrated using the previous model output as input. This holds for all sub-models apart from the BF model that was calibrated using the detailed input data available. This was made possible by the fact that inflow measurements, corresponding to the outflow measurements of the PC, were available, which was not the case for the other sub-models of the WRRF. The overview in Table 4.1 indicates that no measurements were available for the calibration of the GC model. For the GC an average performance of 7.5% TSS removal was assumed (Qasim, 2017).

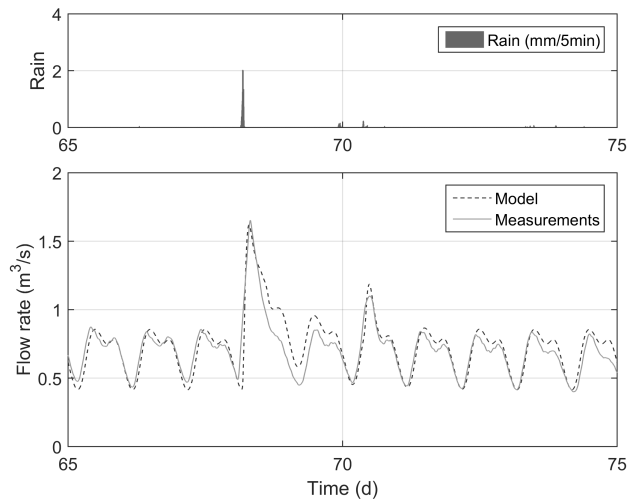
4.6 Calibration and Validation Results

4.6.1 Calibration

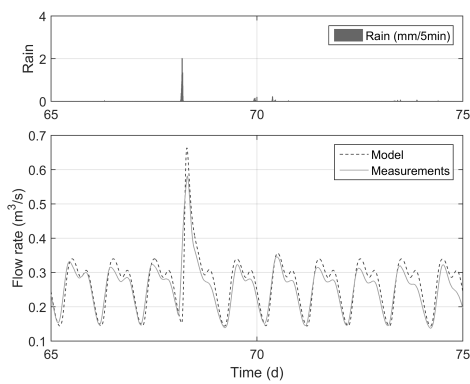
The model calibration results for water quantity are shown in Figure 4.15 for the different tributaries of the WRRF, respectively in Figure 4.16 for the available measurements in the sewer system. The calibration results for water quality are indicated in Figure 4.17. The calibrated water quality parameters and their values are indicated in the Appendix, Table B.1. Detailed performance criteria of the RMSE and the relative RMSE with respect to the measurements are summarized in the Appendix, Table B.2.

Visual inspection of the calibration results shows that the model is able to represent both the quantity and the dynamics of the total inflow of the WRRF CdH well (Figure 4.15a). The measured average flow of $0.71 \text{ m}^3/\text{s}$ is well met by the $0.74 \text{ m}^3/\text{s}$ of the model. Also, the peak flow caused by the rain event at day 68 is well represented, with an error less than 1%. Note that the total inflow has not been calibrated directly, but was calibrated indirectly by calibrating the four tributaries shown in Figure 4.15b to 4.15e. From the results it is visible that Tributary 1 and Tributary 2 are the two main contributors. Tributary 1 has a measured mean flow of $0.26 \text{ m}^3/\text{s}$ that compares to $0.27 \text{ m}^3/\text{s}$ in the model. Tributary 2 has an even bigger measured mean flow of $0.40 \text{ m}^3/\text{s}$ in comparison to $0.42 \text{ m}^3/\text{s}$ in the model. Tributary 3 and Tributary 4 have a lower performance with a relative RMSE of approximately 20%, but since their contribution is comparably small (together not even 10% of the first two tributaries) this is considered acceptable.

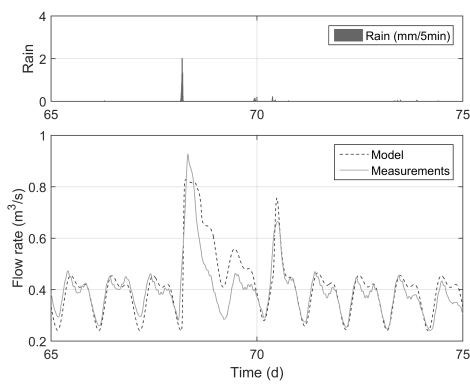
The pumping stations and overflows with available flow measurements are all located upstream of Tributary 2 and the calibration results are shown in Figure 4.16a to 4.16d. The dynamics of the overflows are generally less stable than at the inflow of the WRRF and thus more difficult to model. Nevertheless, the model is generally able to approximate the magnitude and timing of the peaks. It should be noted, however, that the quantity of water is overestimated at CV



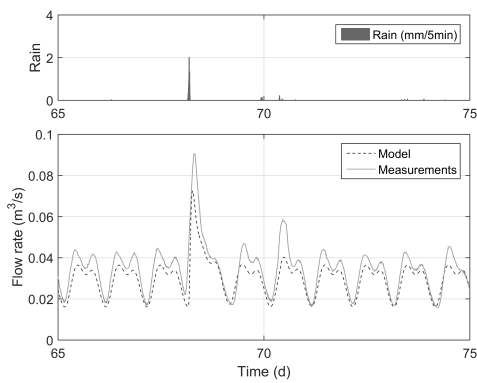
(a) Total inflow WRRF CdH



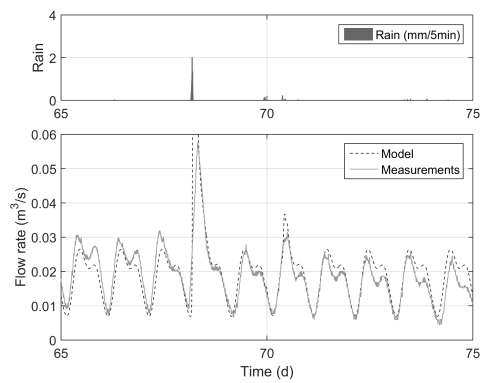
(b) Tributary 1



(c) Tributary 2



(d) Tributary 3



(e) Tributary 4

Figure 4.15: Calibration of water quantity model for all available calibration points at the inlet of the WRRF. The description of the points is given in Table 4.1.

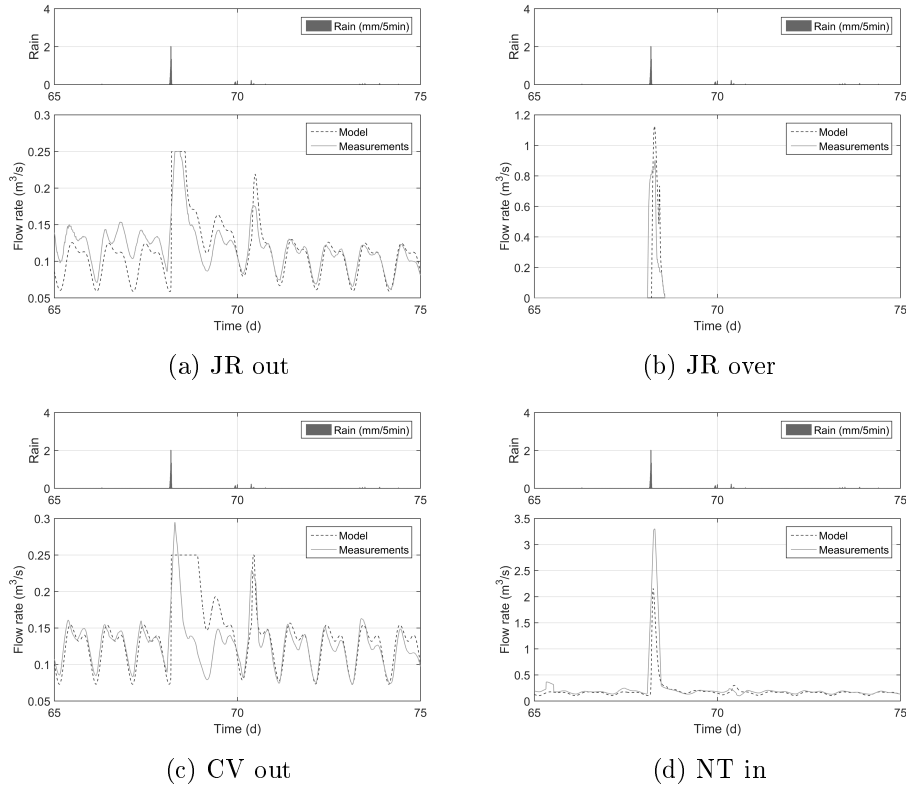


Figure 4.16: Calibration of water quantity model for all available calibration points in the sewer system. The description of the points is given in Table 4.1.

(Figure 4.16c) most likely due to the complex interactions with the upstream overflow and that quantity of water is underestimated at NT during the calibration period (Figure 4.16d). As the later model validation will show, it seems that the chosen calibration event was more of an exception. It was thus concluded not to adjust the water quantity parameters originally obtained from the detailed model.

As indicated in Table 4.1 only four locations are available for the calibration of the water quality model. Two of them are located in the sewer system, one of them being at the inlet of the WRRF (Tributary 2) and two of the points are in the WRRF. Figure 4.17 shows that the model is able to capture the variations of TSS concentrations throughout the system. The performance with regard to the measurements is, however, smaller than for the water quantity model with a relative RMSE of 22% to 35%. This is due to several different reasons. First of all, the water quality performance is limited by the performance of the water quantity model. If a deviation of the model with respect to the measurements is present for water quantity, this deviation will as a consequence also influence the performance of the water quality model. A second reason is the higher variation of the water quality measurements. While the water quantity measurements are quite stable and show, for instance, during DWF a high level of repetitiveness, this seems to be less the case for water quality measurements. A third reason is

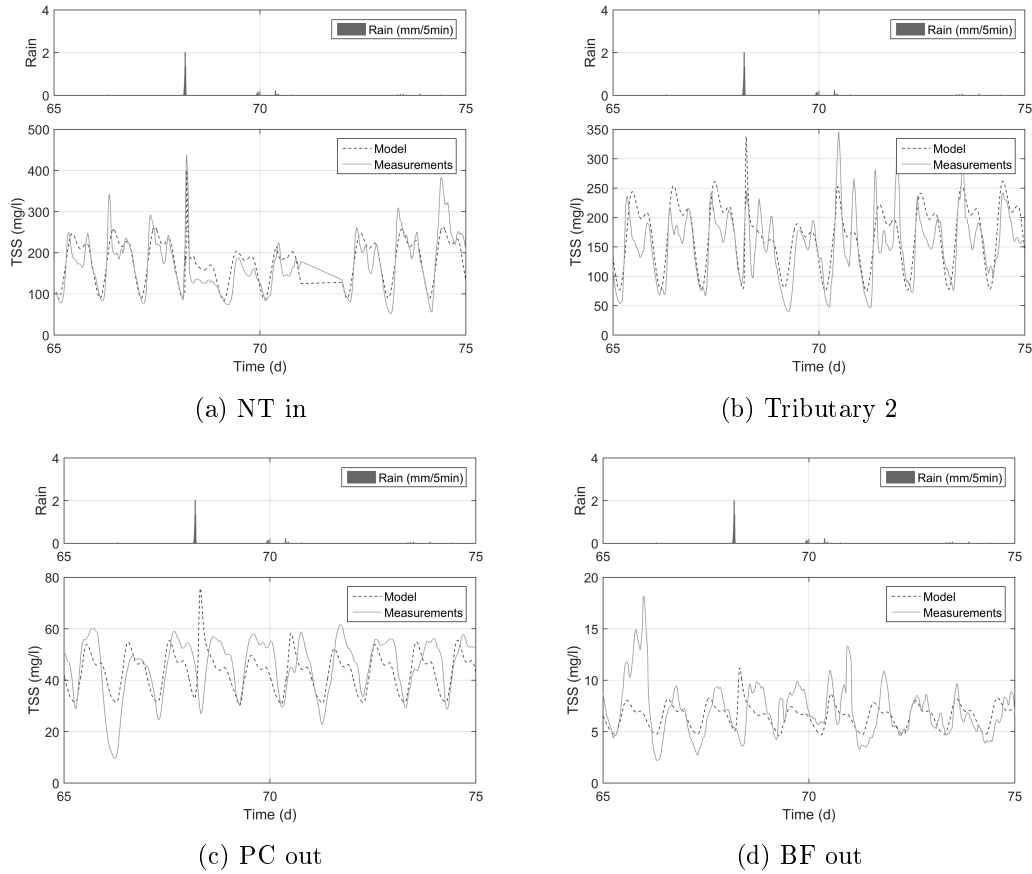


Figure 4.17: Calibration of water quality model for all the available calibration points. The description of the points is given in Table 4.1.

that the water quality measurements are less accurate than the water quantity measurements, which is passed on to the model performance. Nevertheless, also the quantitative assessment of the model performance in Table B.2 indicate that the model is able to represent the water quality throughout the IUWS. Please note that the water quality measurements at NT were failing during day 71, see Figure 4.17a. This day was excluded from model calibration.

The power of the PSVD sewer model is highlighted with respect to two observations. The first observation is that the WWF concentrations in the catchment can be modelled with the relatively simple approach of the event mean concentration (see Section 4.4.1). The model is, however, able to simulate the TSS peaks observed at the beginning of a rain event. This is due to the PSVD sewer model that is able to capture the increased resuspension during high flow. During DWF the resuspension capacity is quite low and TSS has the tendency to settle in the sewer pipes. When the flow is increasing, the resuspension capacity is increasing and the settled TSS is resuspended. The equation for the resuspension flux (equation 4.7), however, shows that the flux is not only depending on the resuspension rate, but also on the TSS mass settled in the sewer. Once this “reservoir” is emptied, the resuspension flux decreases, even if

the resuspension capacity is still high due to the high flow.

The second note worthy observation is, that the PSVD sewer model is able to capture the trend of increasing TSS concentration for longer DWF period. As described in Section 4.4.1, the DWF generation is based on profiles both for water quantity and water quality. Thus, every DWF day “generated” in the catchment looks identical at its outlet. Nevertheless, an increase of the concentration can be observed over a longer DWF period (see, for example, day 71 to 75 at tributary 2 in Figure 4.17b). This is again due to the capacity of the PSVD sewer model. After a rain event, the sewer sediment compartment has ‘lost’ a lot of particulates stored in the sediment compartment. During the DWF the reservoir is gradually filled, meaning that even if the DWF is identical every day, the resuspension flux is increasing since more particulates have settled in the sediment compartment over time.

The PC model also shows a good match between the model and the measurements in Figure 4.17c with a relative RMSE of 22%. The model, however, underestimates the performance of the clarifier at the beginning of a rain event.

Even though the BF model is quite simple, it is able to capture the trends. The mean concentration of 7 mg/l is met with a RMSE of 2 mg/l. The initially increased TSS concentration at the outflow (day 65 in Figure 4.17d) has to come from non-modelled BF internal processes, since this increase could not be seen at the outlet of the PC. Internal processes that influence the water quality dynamics during DWF are for example backwash activities or clogging phenomena that are not considered in the model.

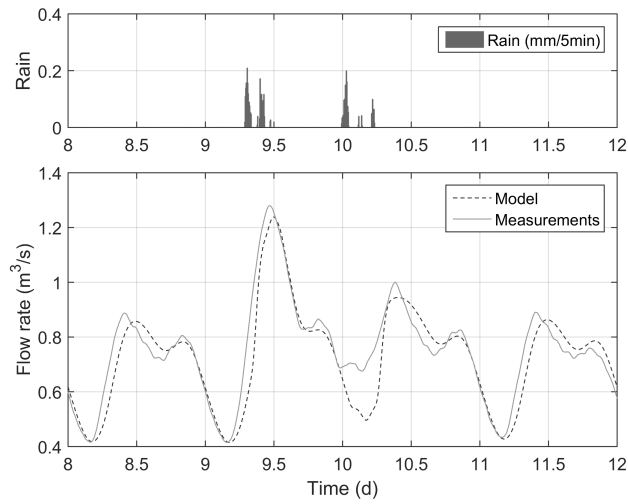
4.6.2 Validation

Validation Period 1

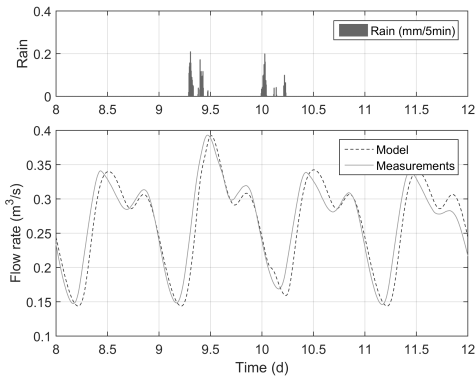
The results for the first validation period are shown for water quantity at the WRRF in Figure 4.18 and in the sewer system in Figure 4.19. The available points for water quality validation are shown in Figure 4.20. As for the calibration, the quantitative model performance is detailed in the appendix, Table B.3.

Looking at the overall performance of the water quantity model at the inlet of the WRRF in Figure 4.18a shows that the model is able to simulate this rain event, even if its magnitude differs quite importantly from the calibration event. This validation rain event has a return period smaller than every half a month, whereas the calibration event had a probability of happening every three months. The modelled mean flow corresponds to $0.73 \text{ m}^3/\text{s}$, whereas the measured mean flow is $0.75 \text{ m}^3/\text{s}$ with a relative RMSE of 10%.

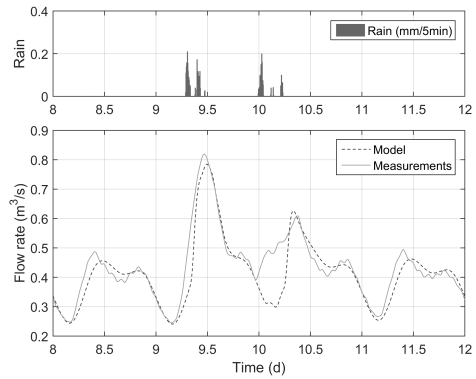
Regarding the peak flows of the rain events: the model is able to represent the peak of the first rain event (start of rain event at day 9.3 approximately) as well as the peak of the second rain event (approximately day 10.3). The model, however, misses the initial high flow of the



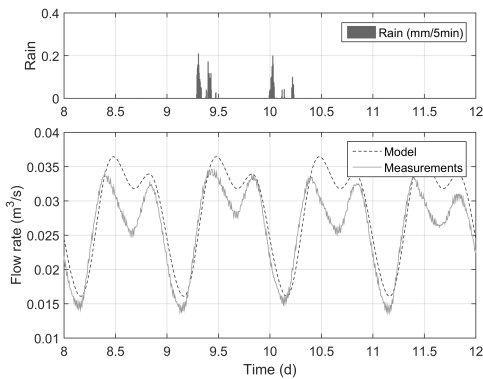
(a) Total inflow WRRF CdH



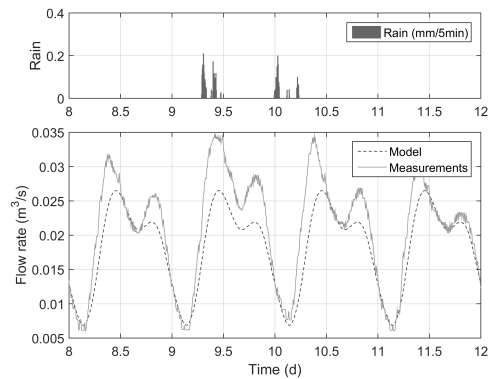
(b) Tributary 1



(c) Tributary 2



(d) Tributary 3



(e) Tributary 4

Figure 4.18: Validation period 1 of water quantity model for all available validation points at the inlet of the WRRF. The description of the points is given in Table 4.1.

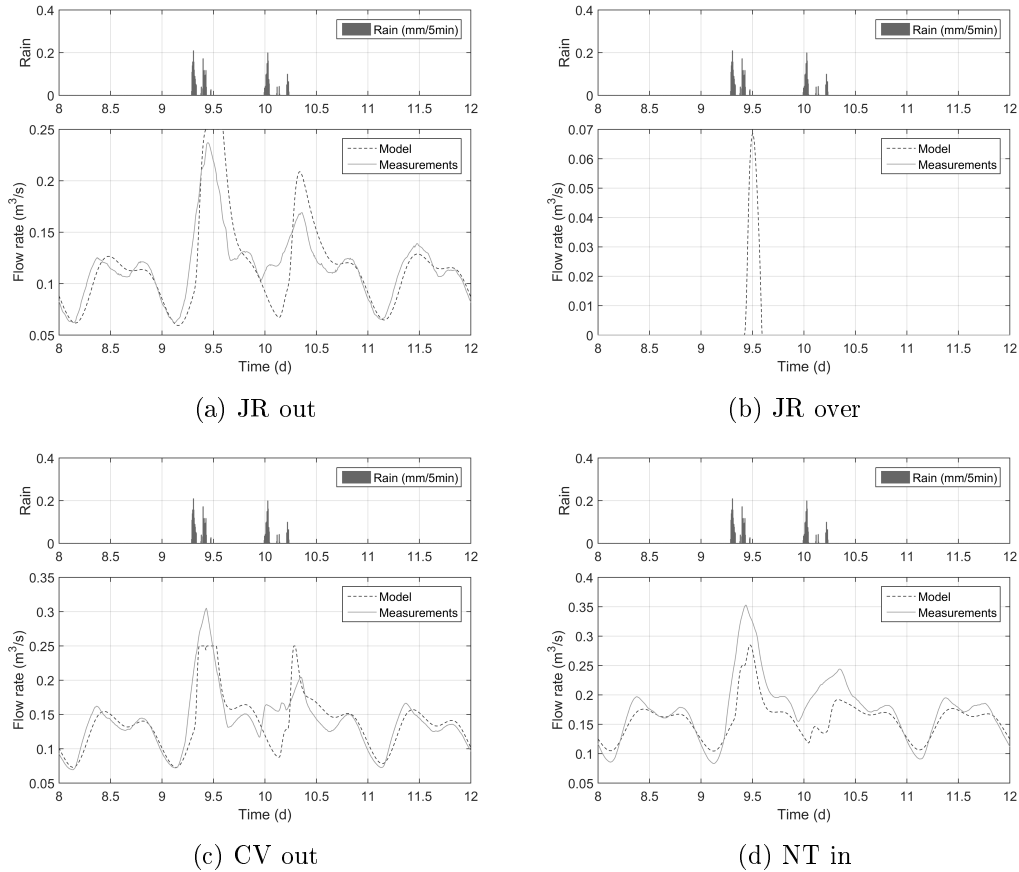
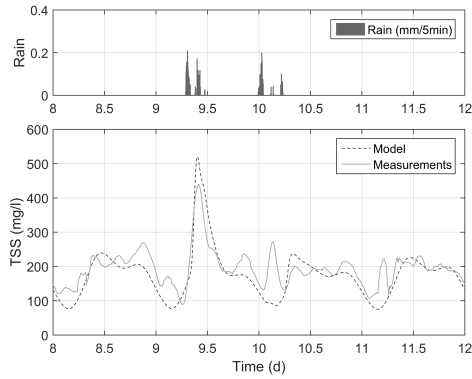


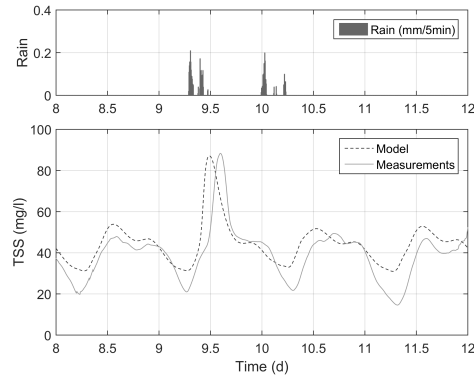
Figure 4.19: Validation period 1 of water quantity model for all available validation points in the sewer system. The description of the points is given in Table 4.1.

second rain event at the beginning of day 10. A more detailed analysis of the single tributaries shows that the increased flow at the inlet of the WRRF was mainly caused by Tributary 2 (see Figure 4.18c). A reason for this deviation between model and measurements might be the distributed characteristic of this rain event. It is likely that the main allocated rain gauge for the upstream catchments was not indicating any rain, when there actually was.

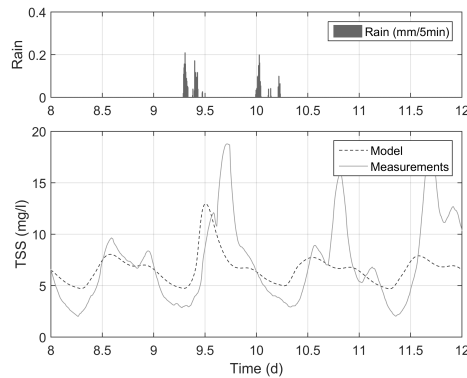
Special attention should also be given to the model validation at the pumping station and CSO JR. The model indicates an overflow at JR where none has been measured (see Figure 4.19b). The amount of overflow modelled shows that the maximum overflow corresponds only to $0.07 \text{ m}^3/\text{s}$. It can thus be considered a minor overflow, caused for example by minor deviations between the measured and the actual rain. Figure 4.19a shows that the water pumped towards the WRRF is well modelled, with the modelled and measured average corresponding to $0.12 \text{ m}^3/\text{s}$ and a RMSE of $0.023 \text{ m}^3/\text{s}$. The performance is considered acceptable. The previously measured, but not modelled increased flow around day 10 at Tributary 2 (see Figure 4.18c) can indeed be observed again in the two upstream overflows JR (Figure 4.19a), respectively CV (Figure 4.19c).



(a) Tributary 2



(b) PC out



(c) BF out

Figure 4.20: Validation period 1 of water quality model for all the available calibration points. The description of the points is given in Table 4.1.

Visual inspection of the results of the first validation period of the water quality model at the second Tributary in Figure 4.20a shows that the main dynamics are captured apart from two exceptions. The missing flow during the night of day 10 is the reason for the bad performance of the water quality model during the same period, since due to the low flow, the resuspension is not sufficiently active. This increased flow and thus resuspension most likely created the increased TSS concentration during this period. Another increased measured concentration can be observed during the night of day 11. The model, however, does not represent that peak. This increased concentration must be due to phenomena not incorporated in the model. Since, in comparison to the previous concentration increase during the night of day 10, no increased flow can be observed during this period. A potential explanation could be the activation, respectively deactivation of one of two screw pumps right after the installed TSS measurements. It could be observed that changes in the pumping activities have an effect on the TSS measurements due to the changed flow conditions and thus settling and resuspension activities. This effect is discussed in detail for another case studies in Sharma et al. (2013) and Plana (2019). The overall performance of the model at Tributary 2 is considered good,

with a relative RMSE of 24% over the whole period. This is confirmed with a Janus coefficient of 1.2, comparing the RMSE of the validation period with the calibration period (see Section 4.5).

The model is also able to capture the dynamics at the outlet of the PC (see Figure 4.20b). While, in comparison to the measurement data, the peak concentrations induced by the rain event arrive too early, the concentration profile as such matches well and the error in the peak concentration is only about 1%. With 25% the relative RMSE is similar to the performance at the inlet of the WRRF. The performance of the validation period can be considered equally good as the performance of the calibration period, since the Janus coefficient corresponds to 1, see Table B.3.

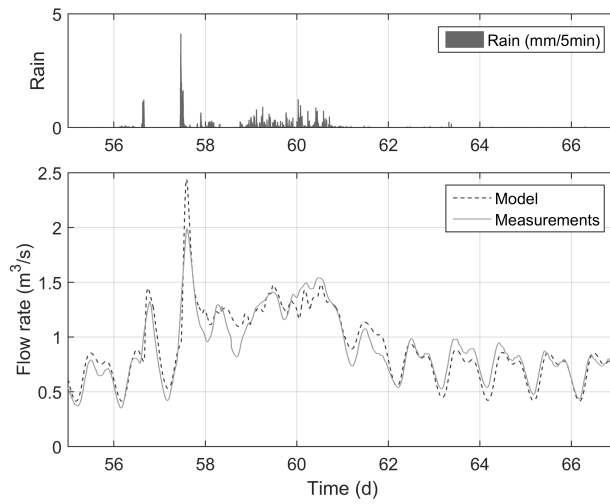
The model performance at the outlet of the BF is clearly lower than for the previous sub-models (see Figure 4.20c). A main reason for this is certainly the comparably simple BF model presented in Section 4.4.8. This means that the effluent concentration dynamics highly resembles the influent dynamics, which can be observed by comparing Figure 4.20b and Figure 4.20c. Due to the simplicity of the model, it is thus not able to represent peaks caused by inner dynamics of the BF, such as the peaks approximately at days 10.8 and 11.8. Such peaks could be caused by mechanisms such as the back washing of the BFs and the corresponding switches of activated BFs. Nevertheless, the average mean concentration of 7 mg/l modelled corresponds to the mean concentration measured. The Janus coefficient indicates with a value of 1.5 that the validation is meaningful in comparison to the calibration. The overall removal efficiency is thus considered to be well represented.

Validation Period 4

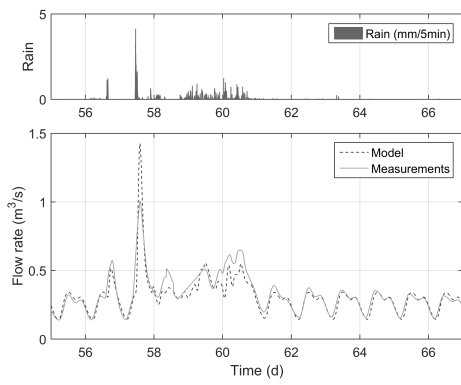
The results of the validation period 4 with the exceptionally heavy rain event (return period >24 months) allow evaluating not only the flow towards the WRRF, but provide an especially interesting validation period to evaluate the overflows, since they are activated during this event. The results are shown for water quantity at the inlet of the WRRF in Figure 4.21 and in the sewer system and thus the overflows in Figure 4.22. The results for water quality are indicated in Figure 4.23. As previously, the detailed model performance is given in Table B.3.

Figure 4.21a shows that the model is able to represent the dynamics at the inlet of the WRRF during this major rain event, although it has been calibrated to a rain event with a considerably smaller return period (~ 3 months). The mean modelled flow of $0.92 \text{ m}^3/\text{s}$ corresponds well with the measured mean flow of $0.90 \text{ m}^3/\text{s}$, with a relative RMSE over the whole period of only 12%. Also, looking at the tributaries individually reveals that the flow is quite well represented (Figure 4.21b to 4.21e) with a slight underestimation of the flow in the last tributary. However, that flow is comparably small.

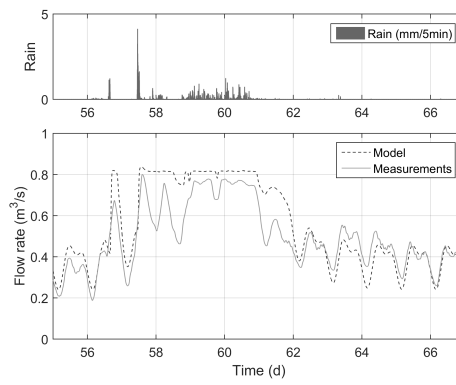
Comparing model and measurements in the sewer system in Figure 4.22 reveals that the



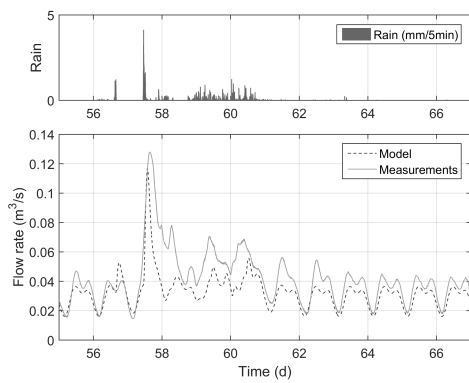
(a) Total inflow WRRF CdH



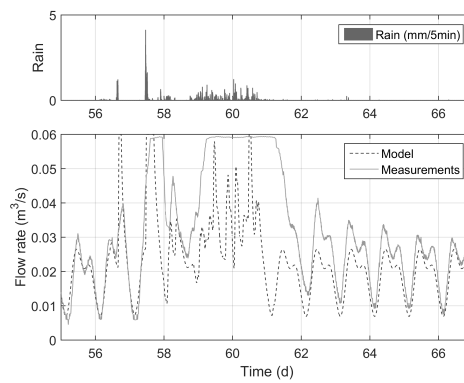
(b) Tributary 1



(c) Tributary 2



(d) Tributary 3



(e) Tributary 4

Figure 4.21: Validation period 4 of water quantity model for all available validation points at the inlet of the WRRF. The description of the points is given in Table 4.1.

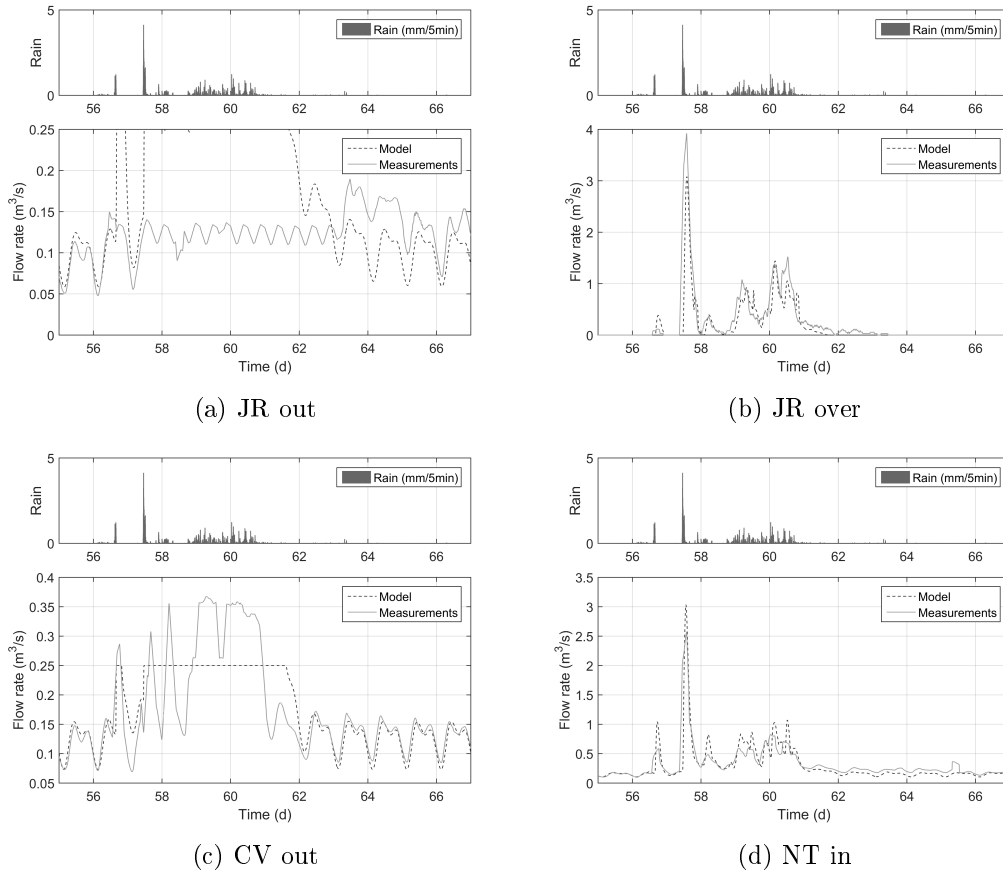


Figure 4.22: Validation period 4 of water quantity model for all available validation points in the sewer system. The description of the points is given in Table 4.1.

model seems to have some issues at the pumping station JR, see Figure 4.22a. According to the measurement data, the pumping station was only working at half capacity ($0.12 \text{ m}^3/\text{s}$) pumping the water to the WRRF, whereas the actual installed pumping capacity towards the WRRF corresponds to $0.25 \text{ m}^3/\text{s}$. The model assumes that during such a major rain event, the pumping capacity would be fully activated, whereas the measurements indicate that only half the capacity is used, even though quite important overflows were happening during this period (JR over in Figure 4.22b). Those measures and activation of pumping capacity seems especially doubtful, as during validation period 1, corresponding to a much smaller rain event, the pumping capacity was fully activated. Even though the model thus performs quite badly with a relative RMSE of almost 70%, the model performance is still accepted, since it is considered to be the realistic behavior of the pumping station during such rain event. In addition, Figure 4.22b shows that the overflow modelled at JR corresponds quite well to the overflow measured. From a mass balance perspective the measurements can thus be doubted. At the outflow of CV towards the WRRF (Figure 4.22c) the model assumes a constant high pump activity, whereas the measurements show some on-off-behavior. At the inflow to the

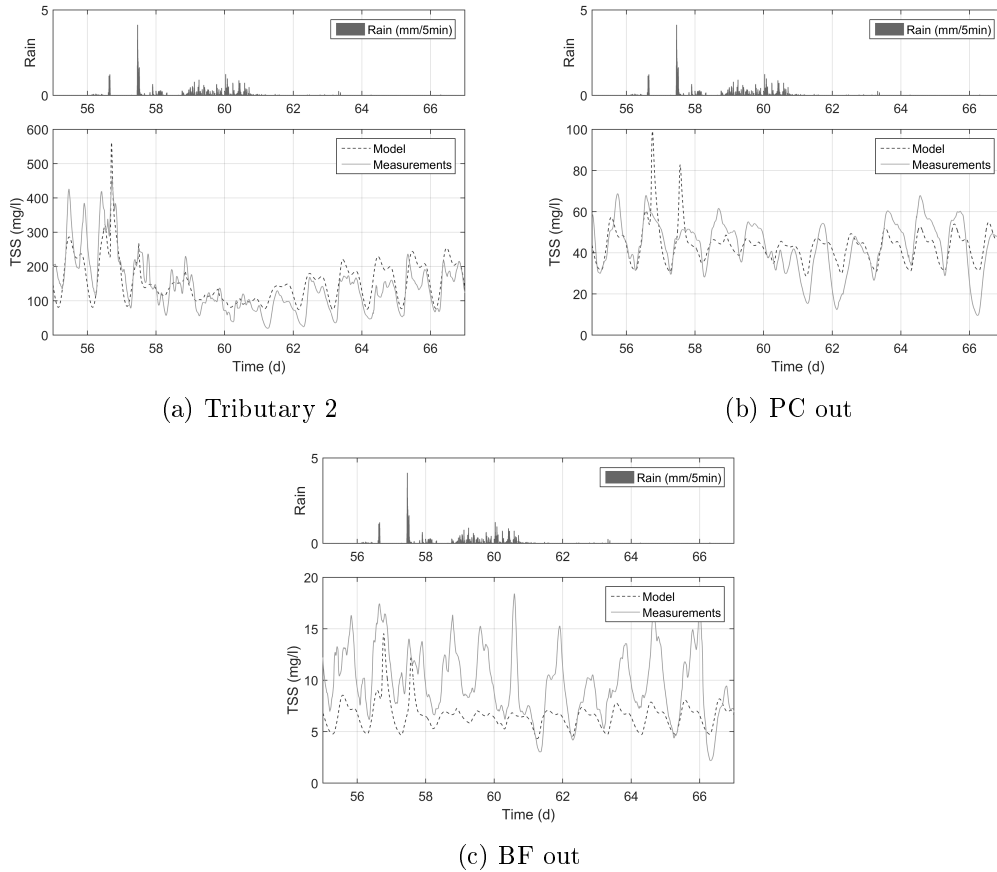


Figure 4.23: Validation period 4 water quality model for all the available calibration points. The description of the points is given in Table 4.1.

pumping station NT (Figure 4.22d), the model captures the dynamics quite well. However, the second rain peak (starting around day 10) is missed, which means that the main rain gauge allocated to the catchments upstream of NT was not indicating any, receptively insufficient, rainfall intensity.

The performance of the water quality model is presented in Figure 4.23. The especially good match between model and measurements should be noted at the inlet of Tributary 2 in Figure 4.23a. A highlight is that the model is not only able to represent the dilution effects during the rain event, but also, how well the model is able to predict the slowly increasing DWF TSS concentration after such a major rain event (see Figure 4.23a day 62 to 67). As explained previously, this good performance is due to the PSVD sewer model that is able to represent the increased resuspension flux thanks to the accumulated sediment in the sewer compartment. This enables to model the increased flux for the same resuspension rate, since the resuspension flux increases as the sewer sediment compartment becomes slowly filled during DWF periods. Wit a Janus coefficient of 1.3 in comparison to the calibration period, the performance is considered meaningful. The model is also able to capture the dynamics after the PC indicated

in Figure 4.23b. As for the previous events, the model is underestimating the PC performance for the initial peak concentrations of the rain event (day 56 and 57). The model is also not able to represent the unusually low night concentrations in the effluent during day 61, 62 and 68. One might, however, also question the measurements, since the values are unexceptionally low, even for nights (below 20 mg/l). The performance of the BF model shows that the modelling results at the effluent can give only a rough approximation of the effluent concentration. The model indicates a mean concentration of 7 mg/l in comparison to the 10 mg/l measured, thus overestimating the performance during this heavy rain event. Due to the simplicity of the BF model, effects such as clogging of the BF that can occur during such rain events, cannot be represented and the highly dynamic effluent concentration can not be explained with the model (see Figure 4.23c). It should, however, also be noted that the BF is the last submodel of a series of submodels, thus accumulating all prior errors. The performance of the model should thus be seen in the context of the whole integrated model: It should be remembered that the TSS modelled here is generated at the catchment level and has thus been transported over a long distance including different processes in all subsystem, such as the conversion due to CEPT. Incorporating a BF model seems especially useful, as it allows estimating the overall flux of TSS towards the environment which would not have been possible without this approximate model. Additionally, with a Janus coefficient of 1.7 the validation can be considered reasonable in comparison to the calibration.

4.7 Illustration of Changes in PSVD Curves along the IUWS

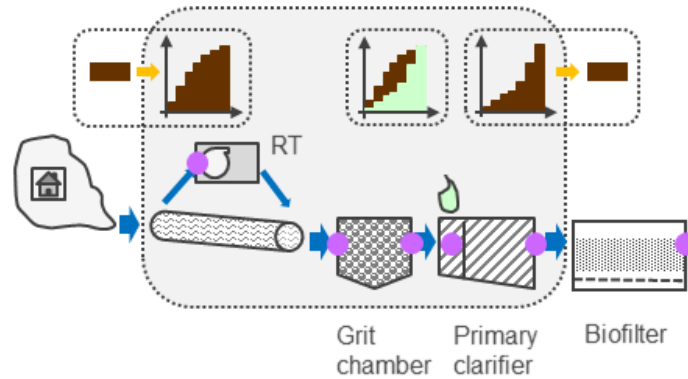


Figure 4.24: Location of the illustration of the different PSVD curves along the IUWS: the inlet of a RT, the inlet of the WRRF, after the GC, after the addition of the CF, after the PC and at the outlet of the WRRF

As described previously, the water quality model has been calibrated and validated on the TSS concentrations and thus the total of all PSVD classes (see Section 4.6). How the discretization of the TSS into the ten classes was performed is described in Section 4.4.2 and how the CEPT affects the PSVD in Section 4.4.7. Nevertheless, for a better understanding of the PSVD

approach, it is illustrated how the fractions of the TSS classes change along the IUWS.

For a typical DWF day, day 65, corresponding to the first day of the calibration period, the behavior of the PSVD curves at different points along the IUWS is demonstrated. The six points chosen for this illustration are shown in Figure 4.24: the inlet of a RT, namely NT, the inlet of the WRRF, after the GC, after the addition of the CF, after the PC and at the outlet of the WRRF, corresponding to the outlet of the BF. For this day, all the observed PSVD curves (at a 5 min interval) are plotted at the given locations, thus indicating the evolution of PSVD curves in the IUWS.

The corresponding illustration of the PSVD curves is presented in Figure 4.25 with a common color coding, where dark indicates high TSS concentration. Comparing the different PSVD distributions along the IUWS highlights several interesting points. The first being the obvious: since at the WRRF TSS is removed, the TSS concentrations get smaller towards the outflow of the WRRF. This is clearly visible by the gradually lighter shade of the PSVD curves from Figure 4.25b to Figure 4.25f.

In Section 4.4.2 it was described that the TSS is discretized into the different classes by considering the total TSS concentration, with the higher concentrations settling faster. This is the second effect that can be observed in Figure 4.25 even long after the discretization (at the outlet of the catchment) took place. Indeed, the darker curves are generally more to the right, indicating a faster settling behavior.

Analyzing Figure 4.25 in more detail highlights in addition how the different subsystems work. Comparing for example Figure 4.25b with Figure 4.25c, indicates the particle fractions removed in the GC. In Section 4.5 it was described that the GC has been calibrated on a 7.5% TSS removal. Comparing the two Figures shows that only the fastest settling particulates are removed, which is visible by remarking that the total distribution (equal 1) is reached at a lower velocity after the GC in comparison to the inlet of the WRRF. This indeed means that the fastest settling particulates were removed.

Comparing Figure 4.25c and Figure 4.25d demonstrates the drastic effect of CF addition on the PSVD distributions. The concentrations at the outlet of the GC (Figure 4.25c) and after the addition of CF (Figure 4.25d) are totally identical since no particulates are removed between the two processes. The distribution of the curves, however, changes drastically. As to be expected, the particulates settle faster after the addition of the CF, which is clearly visible, since the curves move to the right.

At the PC a large portion of the particulates is removed, which is indicated by the very light gray of the PSVD curves corresponding to low concentrations in Figure 4.25e. In addition, it can be observed that the particulates remaining in the water line have very low settling velocities.

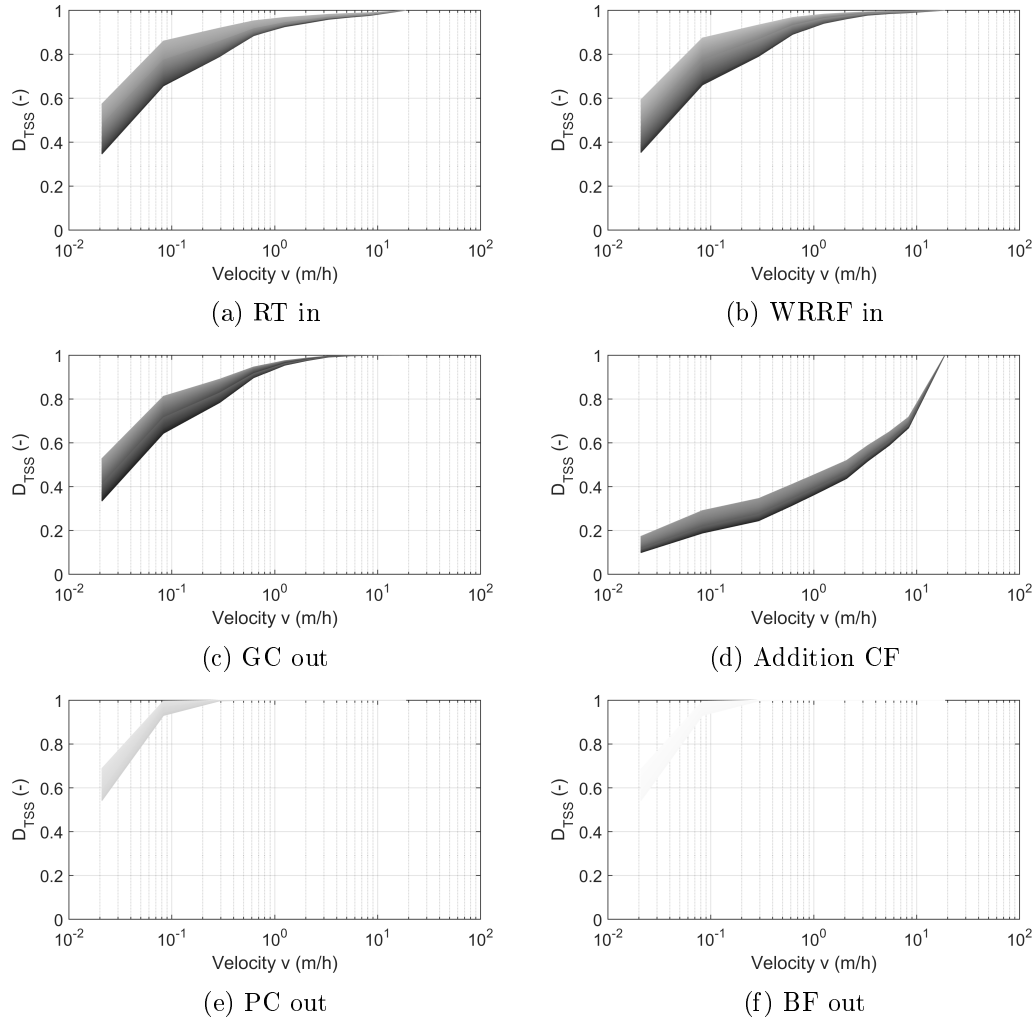


Figure 4.25: Illustration of the PSVD curves at different points in the IUWS for a typical DWF day (day 65). The color indicates the total TSS concentration with dark representing high (400 mg/l) and light representing low (5 mg/l) TSS concentrations.

As presented in the BF model description in Section 4.4.8, the BF model makes no longer use of the PSVD characteristics. The removal efficiency is defined independently of the PSVD distribution, removing an equal fraction of all classes. This is visible when comparing Figure 4.25e and Figure 4.25f. Both figures have exactly the same PSVD distribution, the only change is the shade of gray, indicating that the concentrations are lower at the effluent of the BF. This demonstrates that the TSS is removal is modelled independent of the class.

4.8 Discussion and Conclusion

The calibration and validation of the model for the case study in Section 4.6 showed that the PSVD approach extended with a catchment and BF model is a powerful tool for accurately

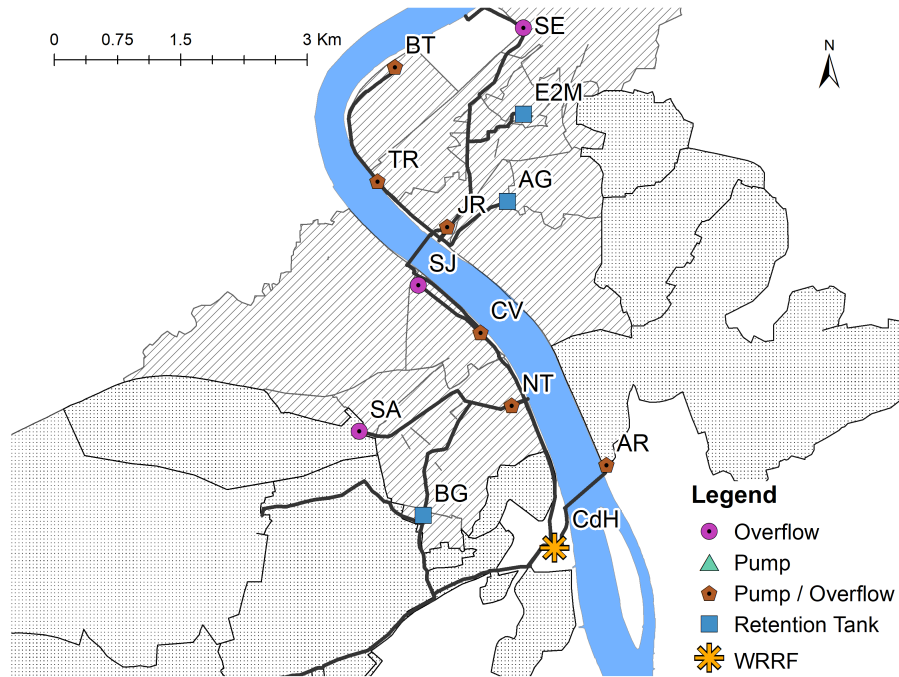


Figure 4.26: Map of the case study CdH indicating the location of the modelled TSS fluxes towards the receiving water.

representing the flow and TSS concentrations throughout the entire integrated system. Such a model thus allows also assessing the TSS fluxes towards the environment over the CSOs, the by-pass (BP) and the effluent of the WRRF, corresponding to the effluent of the BF. The CSOs are namely: Arcins (AR), Bastide (BT), Carle Vernet (CV), Jourde (JR), Noutary (NT), Siphon d'ars (SA), Saint Émilion (SE), Saint Jean (SJ) and Thiers (TR). The location of the overflows as well as the WRRF is indicated in Figure 4.26.

A comparison of all fluxes towards the receiving water over a period of 120 d (May to August 2017) is presented in Figure 4.27. This allows for instance comparing the TSS flux at the effluent of the WRRF, mainly influenced by the DWF performance of the WRRF, with the TSS fluxes during WWF at CSOs. This comparison reveals quite interesting results. For the given case study, it can be seen for example that the WRRF discharges are non-negligible contributions of TSS to the receiving water (over 50 t), although the TSS concentration at the effluent of the BF is very low (~ 10 mg/l). However, since the effluent of the WRRF is constantly discharging, this adds up over the four months. Nevertheless, it can also be observed the the sum of all overflows, that discharge only during WWF, is after all bigger than the flux over the BFs. The figure also reveals quite important differences in flux for the different CSOs. The flux resulting from the CSO NT (over 40 t) represents more than two thirds of the flux from the BFs, although only active during WWF, while other CSOs cause fluxes quite small in comparison to the effluent of the BF, for example AR, SA and BT.

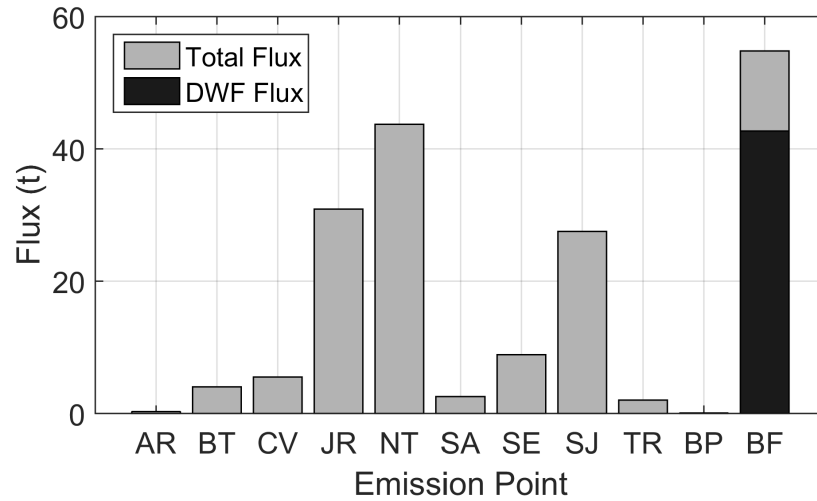


Figure 4.27: Modelled TSS fluxes towards the receiving water over 120 d (May to August 2017).

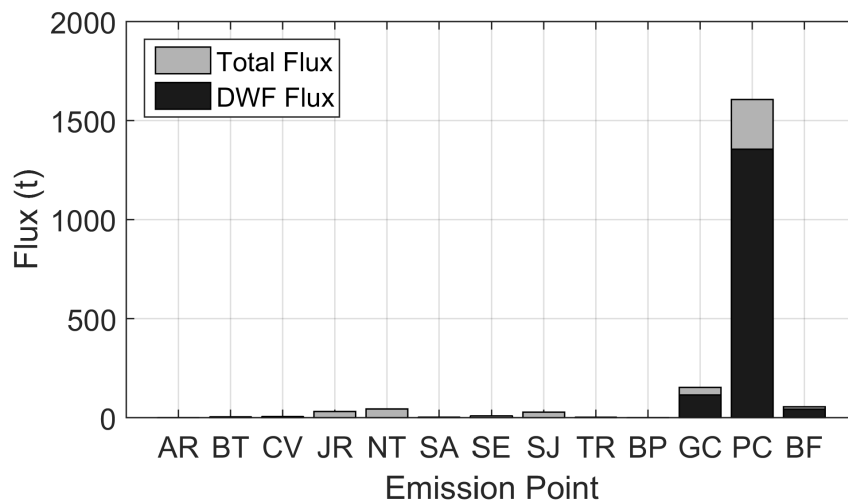


Figure 4.28: Modelled TSS fluxes over 4 months (May to August 2017) including the sludge line of the WRRF with the underflow of the GC and the PC.

Figure 4.28 is basically an extension of the previous Figure 4.27 and a powerful demonstration of the importance of the WRRF in the integrated system. Because, in comparison to the previous figure, the fluxes resulting from the sludge line are now also included as outputs of the system, namely the underflow of the GC and the PC. This demonstrates quite impressively the importance of the WRRF, since it can be seen that by far the biggest part of the particulate flux is actually removed at the WRRF, in particular at the PC. The sum of the GC and PC flux is actually the flux that is prevented to reach the receiving water thanks to the WRRF.

Figure 4.29 illustrates the power of water quality modelling in comparison to water quantity

modelling only. At different locations in the IUWS the flow and the TSS concentration, respectively the flow and the TSS flux are compared. The period indicated in Figure 4.29 corresponds to the validation period 4, since, due to the size and distribution of the rain event, this period includes multiple interesting phenomena. The sites for illustration are the CSO at JR and NT, the inlet of the WRRF CdH and the outflow of the BF.

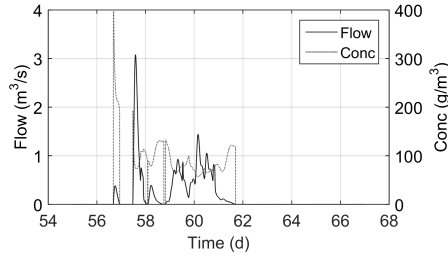
Both overflows show very high TSS concentrations during the first part of the overflow (day 56.6). At JR the TSS concentration rises to approximately 400 mg/l (Figure 4.29a) and at NT to approximately 900 mg/l (Figure 4.29c). When the second part of the overflow starts (day 57.5), with higher flows than during the first part of the overflow, the concentration rises only to approximately 200 mg/l at JR, respectively 400 mg/l at NT. Comparing the resulting TSS fluxes for the first (day 56.6) and the second (day 57.5) period reveals different behavior at JR than at NT. At JR, although the first part in concentration is higher than the second peak, the resulting TSS flux is higher for the second part. Figure 4.29b shows a peak flux of approximately 0.1 kg/s for the first part and an increased flux of over 0.2 kg/s for the second part. Even though the TSS concentrations at NT show similar behavior at JR with higher concentrations for the first than the second peak, the TSS peak flux shows a different behavior. Contrary to JR, at NT it decreases from over 0.4 kg/s to under 0.4 kg/s (Figure 4.29d).

At the inlet of the WRRF the concentration for the first peak (day 56.6) is clearly higher than for the second peak (day 57.5), but since the flow shows the reversed behavior (see Figure 4.29e), the resulting TSS flux of both peaks is around 0.7 kg/s (see Figure 4.29e). The model allows the evaluation of flow, concentration and flux showing that those do not necessarily coincide. For the studied period at the outflow of the BF however, flow and flux are behaving quite proportionally (see Figure 4.29h).

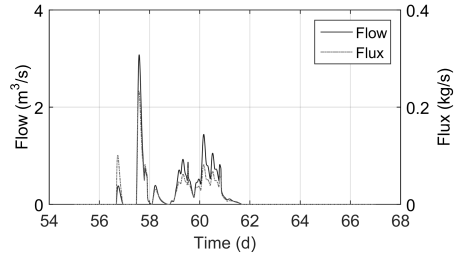
These figures clearly demonstrate that for a given location, equal peaks in flow do not necessary lead to equal peaks in pollution. Assuming that a RT is available, the fraction retained would depend on the objective. If the the aim would be for example to reduce the flow for flood protection, a different volume would be retained in the RT, than with the aim of the reduction of the TSS flux for environmental protection. A purely flow-based analysis could not come to such conclusions.

These figures also show that each CSO has its own characteristic and needs to be evaluated independently. A conclusion for one CSO, for example, about which fraction of an event would need to be retained for environmental protection, is not automatically transferable to another CSO.

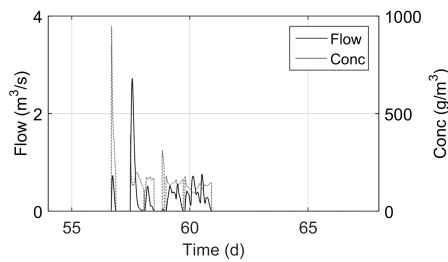
With respect to the WRRF, the model allows to draw conclusions about the flow, concentration and flux, which is important, since different subsystems at the WRRF react differently to the same rain event. For the given case study, the CEPT for instance is highly depending on the



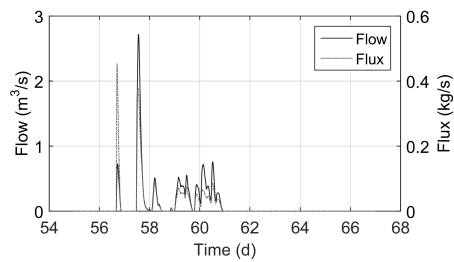
(a) JR over, Flow/Conc



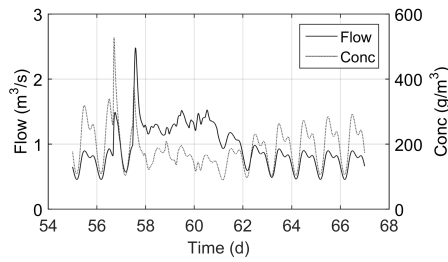
(b) JR over, Flux/Flow



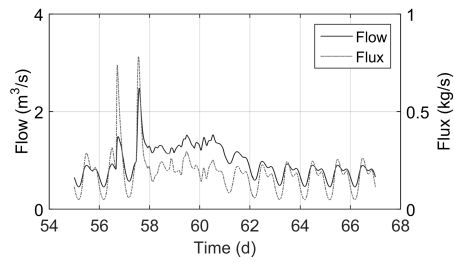
(c) NT over, Flow/Conc



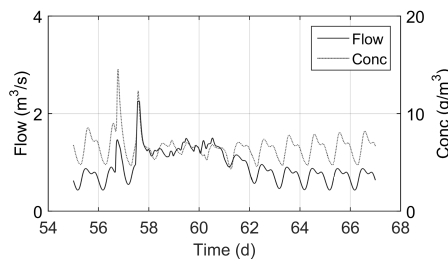
(d) NT over, Flux/Flow



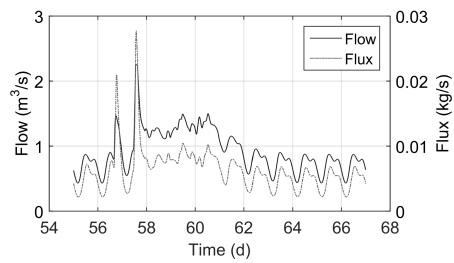
(e) CdH in, Flow/Conc



(f) CdH in, Flow/Flux



(g) BF out, Flow/Conc



(h) BF out, Flow/Flux

Figure 4.29: Comparison of flow and TSS concentration, respectively TSS flux at various locations in the IUWS during validation period 4.

TSS concentration, since the CF addition is controlled by it. Activation of the BP is however based on flow and for the evaluation of potential BF clogging, the TSS flux would be the most important value.

As indicated earlier (see, for example, Chapter 2), the advantage of conceptual models is the low computational demand and thus the fast calculations. For the given case study, 1 day is approximately simulated in 1 min, calculated from the simulation time needed for the 120 d evaluation. This approximation thus includes a mixture of DWF and WWF days. Such speedy calculations have the advantage that the model can also be used in applications that require a large number of simulations. Only thanks to this characteristic, OED could be conducted with the help of this model (see Chapter 3), the control handles can be evaluated considering uncertainty (see Chapter 5) and different scenarios can be evaluated requiring multiple model evaluation with different sets of parameters (see Chapter 6).

This chapter demonstrated the usability of the PSVD modelling approach throughout the integrated system by the calibration and validation of the CdH case study (Section 4.6). The calibration and validation results also revealed that future research should focus on the WWF behavior of both PC and BF to further increase model performance. Section 4.7 showed how the PSVD characteristics change over the different subsystems and how they can explain the functioning of those subsystem. The chapter closed with a discussion of the power and the potential uses of the developed integrated PSVDM.

Chapter 5

Selection of Effective Control Handles for Integrated Urban Wastewater Systems Management considering Parameter Uncertainty and Input Variability

This chapter has been restructured allowing to give some additional explanations from the following article:

Ledergerber, J. M., Maruéjols, T., and Vanrolleghem, P. A. (2019). No-regret selection of effective control handles for integrated urban wastewater systems management under parameter and input uncertainty. In *Proceedings of the 10th IWA Symposium on Modelling and Integrated Assessment (Watermaterx 2019)*, Copenhagen, Denmark, September 1-4 2019.

Author contributions Conceptualization, J.M.L. and P.A.V.; Methodology, J.M.L. and P.A.V.; Investigation, J.M.L.; Writing – Original Draft Preparation, J.M.L.; Writing – Review & Editing, J.M.L., T.M. and P.A.V.; Visualization, J.M.L.; Supervision, T.M. and P.A.V.; Project Administration, T.M. and P.A.V.; Funding Acquisition, T.M. and P.A.V.

5.1 Abstract

Water quality regulations are extended from the wastewater resource recovery facility (WRRF) to the sewer system. It is thus necessary to properly integrate those systems for the evaluation of the overall emissions to the receiving water. The integration of sewer system and the WRRF however leaves us with multiple potential options to reduce overall emissions. The proposed

approach builds on previous research using global sensitivity analyses (GSA) as a screening method for available control handles. It considers parameter and input uncertainty to select control handles that generate large benefits even if the model differs from reality (no-regret selection). While model structure uncertainty is not considered in this work, the procedure could be applied as well, through the evaluation of model structure scenarios. Results on a real-life case study indicate that the three top-rated handles are comparably effective for all considered uncertainty scenarios. But the results also showed that this does not apply to lower-rated handles.

5.2 Résumé

Les limites réglementaires de qualité de l'eau sont étendues des stations de récupération des ressources de l'eau au réseau d'égout. Il est donc nécessaire d'intégrer correctement ces systèmes pour l'évaluation des émissions globales dans les eaux réceptrices. L'intégration du réseau d'égout et de la station de récupération des ressources de l'eau nous laisse cependant de multiples options potentielles pour réduire les émissions globales. L'approche proposée s'appuie sur des recherches antérieures utilisant des analyses de sensibilité globale comme méthode de dépistage pour les points de contrôle disponibles. Elle tient compte de l'incertitude des paramètres et des entrées pour sélectionner les points de contrôle qui génèrent d'importants avantages même si le modèle diffère de la réalité (sélection sans regret). Bien que l'incertitude de la structure du modèle ne soit pas prise en compte dans ce travail, la procédure pourrait également être appliquée, par l'évaluation des scénarios de structure du modèle. Les résultats d'une étude de cas réelle indiquent que les trois points les mieux cotés sont similairement efficaces pour tous les scénarios d'incertitude considérés. Mais l'analyse d'incertitude a montré que pour les points de qualité inférieure, une analyse plus poussée est nécessaire.

5.3 Introduction

As highlighted in the Section [Integrated Modelling](#), IM is a powerful tool for the evaluation of the interactions between different sub-systems (Rauch et al., 2002).

Such integrated evaluation is of increasing interest, as water quality standards no longer apply to the WRRF only, but are expanded to the sewer system, in particular to CSO. An example is France, where each utility has to choose one out of three compliance criteria. One of the three choices includes water quality limits for CSOs: the overflow pollutant flux has to be smaller than 5% of the total pollutant flux per year (JORF, 2015). Integrated modelling covering the sewer system as well as the WRRF is therefore more important than ever. By assessing the overall pollutant emission to the natural environment, it allows evaluating the compliance with regulations for both the sewer system and the WRRF. An integrated model also allows

evaluating potential strategies to reduce these emissions considering the effects on the entire catchment instead of conducting a local analysis of, for instance, one particular CSO.

If the objective is to improve the quality of the receiving water, an integrated approach, however, leaves us with plenty of potential modifications to different subsystems, named hereafter control handles. Since all of those control handles could be used to reduce the overall emissions, it seems reasonable to concentrate the efforts on the most effective ones. It is therefore useful to use a screening technique of all potential control handles and identify the best handles. Only once the set of handles is selected with the proposed procedure, the development of the strategies, for example to reduce the emissions, starts.

GSA has been proposed as a model-based tool to perform such control handle ranking (Benedetti et al., 2012; Langeveld et al., 2013b; Corominas and Neumann, 2014; Sweetapple et al., 2014; Saagi et al., 2018), as it allows to identify the most influential parameters for a given objective. For the ranking of the control handles, these studies conducted a GSA on the settings of the control handles, basically a specific subset of model parameters, which allows ranking them. The current research builds on these approaches for ranking the control handles. However, in comparison to previous studies, the methodology is extended to consider uncertainty via an uncertainty scenario analysis. It is thus possible to include different areas of uncertainty, if they can be expressed with scenarios. A potential list of these uncertainties is presented by Belia et al. (2009). This is important as the model is not a perfect representation of reality and the control authority may depend on the particular reality modelled. Such considerations gain of importance when costly infrastructure decisions are based on the model results. To account for potential deviation between model and reality, variable model input and parameter uncertainty have to be considered. The proposed procedure allows working towards a no-regret selection of the control handles by accepting only those handles that will work effectively for a wide range of parameter and input conditions and can thus be implemented in practice with more confidence.

The proposed procedure is validated with a case study considering parameter and input uncertainty. For the case study application, model structure uncertainty is not addressed, but it could be included by developing scenarios with different model structures. As mentioned in the Section *Integrated Modelling*, one of the three compliance criteria for the case study limits to the pollutant emission towards the receiving water with respect to TSS. It is thus of interest to identify the most effective control handles that reduce the TSS flux to the receiving water. Since a well-performing model is by far not a perfect representation of the reality and the model input is variable, it is important to consider this, when selecting control handles. This will help to avoid regret decisions, such as investing in a wrongly ranked handle.

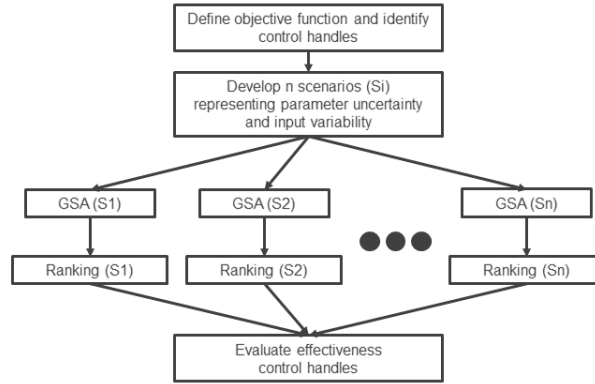


Figure 5.1: Procedure to evaluate control handles under parameter and input uncertainty.

5.4 Proposed Procedure

The proposed procedure to evaluate control handles under parameter uncertainty and input variability is presented in Figure 5.1. As in the approaches proposed in literature, the first step is to define the objective function allowing to evaluate the potential of the control handles and then identify the control handles to be studied.

Instead of directly ranking the control handle with the calibrated and validated model, in the second step n different scenarios are developed representing parameter uncertainty and input variability. The scenarios are created based on prior knowledge of the modeller resulting from developing, calibrating and validating the model.

In the third step, a GSA is carried out for each of the scenarios. For each of the GSA, the control handles are ranked according to the GSA results.

This then allows evaluating the consistency of the ranking of the control handles in the last step, by comparing the results from the different scenarios representing parameter and input uncertainty.

5.5 Material and Methods

The case study CdH is described in detail in Section 1.1. Relevant for this section is, that major pumping stations, CSOs and RTs exist on both sides of the Garonne river (see Figure 5.2). These represent all potential control handles for the reduction of TSS emission to the Garonne. Regulations for the WRRF include TSS, COD and BOD_5 and, importantly, potentially contain for the first time CSO water quality standards that cities will have to comply by 2020 (JORF, 2015).

The integrated model of the case study covers the system starting at the catchments down

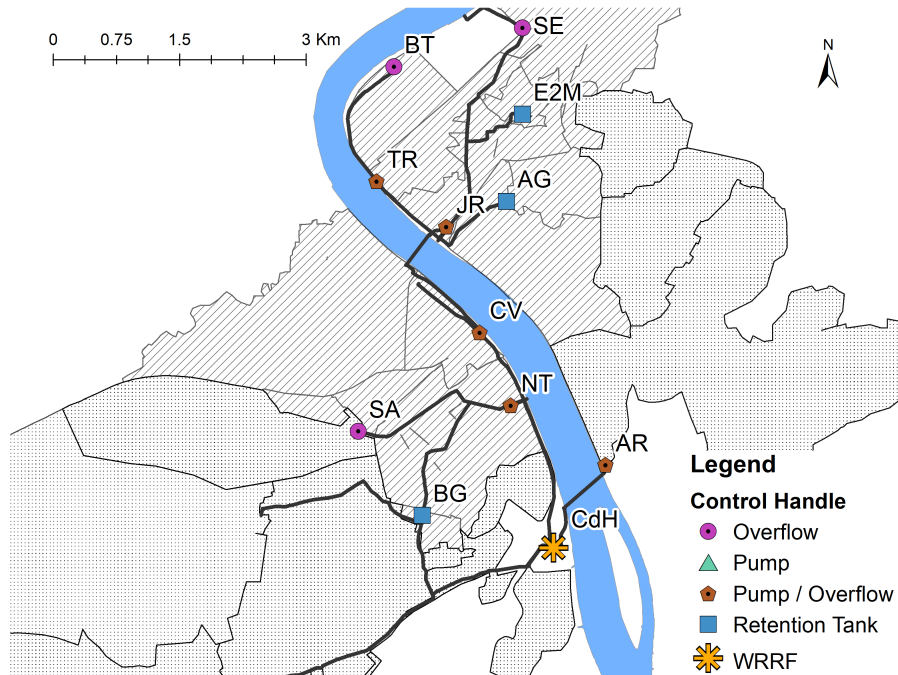


Figure 5.2: Map of the case study CdH indicating the studied control handle with a two letter code.

to the effluent of the PCs. It is a conceptual model using the PSVD approach for water quality modelling of TSS (Maruéjols et al., 2015). A detailed description of the submodels is given in Section 4.4. It is important to note that this conceptual approach is very efficient from a computational point of view: the evaluation of the whole integrated urban wastewater system has on average a simulation time of less than one minute for a whole day of simulation (including WWF).

The aim of the proposed methodology is to select control handles that can be included in scenarios to reduce TSS emission in comparison to the current default situation. The control handles are thus ranked based on their influence on total TSS flux. The potential control handles to be evaluated are mainly pumping and throttle capacities that limit the flow to the WRRF at pumping stations and overflows. Increasing a pumping, respectively a throttling, capacity towards the WRRF will reduce the overflow at the particular CSO. These modifications will require either the installation of new pumps or modifications of the throttle device. The additional control handles are related to the three RTs: the flow rates at which the filling of the RT starts, and the emptying flow rate. To change the filling of the RT, the crest of the weir will have to be modified, whereas for the emptying flow rate the currently installed pumps will need to be controlled differently. The locations of the control handles are shown in Figure 5.2. Table 5.1 summarizes the control handles with their currently implemented values and the range over which they will be studied in the GSA. The range generally corresponds

Table 5.1: Studied control handles for TSS flux reduction to the receiving water with currently implemented values and upper and lower limits for the GSA evaluation.

Abbr.	Description	Value (m ³ /d)	Lower limit (m ³ /d)	Upper limit (m ³ /d)
QP,AR	Max. pumping capacity at Arcins	5 182	2 590	7 770
QP,BT	Max. pumping capacity at Bastide	840	420	1 260
QP,CV	Max. pumping capacity at Carle Vernet	21 600	10 800	32 400
QP,JR	Max. pumping capacity at Jourde	21 600	10 800	32 400
QP,NT	Max. pumping capacity at Noutary	26 957	13 500	40 400
QEmpt,AG	Emptying flow rate RT Alfred Giret	65 000	19 500	65 000
QEmpt,BG	Emptying flow rate RT Bergonié	4 320	2 160	4 320
QEmpt,E2M	Emptying flow rate RT Entre deux mers	38 000	4 320	38 000
QT,SA	Throttle capacity at Siphon d'Ars	38 880	19 400	58 300
QFill,AG	Flow filling RT Alfred Giret	95 000	9 500	95 000
QFill,BG	Flow filling RT Bergonié	5 000	2 500	7 500
QFill,E2M	Flow filling RT Entre deux mers	5 900	2 950	8 850
QP,SE	Max. pumping capacity at St. Émilion	7 344	3 670	11 000
QP,TR	Max. pumping capacity at Thiers	3 456	1 730	5 180

to +/- 50% of the currently implemented value with the exception of the RT control handles. For those parameters, only smaller values than the currently implemented values were studied. Currently, the RTs are exclusively filled for flood protection control and are thus only very rarely in use. The operators however want to extend their service to the control of CSOs. Thus, lowering those values allows operating the RTs also for smaller rain events. The lower limits are selected in such a manner that the installed pumps could handle the flow.

For the development of the scenarios representing parameter uncertainty, the model parameters considered are listed in Table 5.2. The parameters are all related to the water quality model: the mean TSS concentration for DWF generation in the catchment (ConcTSS(DWF)) and event mean TSS concentration for WWF (ConcTSS(WWF)) for the two available measurement points in the sewer system, CdH and NT respectively. These measurement points are also indicated in Figure 5.2. The last three parameters are related to the TSS propagation in the sewer model and affect the resuspension function of the TSS (rresusp,max, fQhalf, nresusp). The catchment and the sewer model are described in more detail in Section 4.4. For the development of the uncertainty scenarios, the values of the parameters are varied by $\pm 20\%$ of their calibrated value, as indicated in Table 5.2.

The inputs to the model are the rain intensity time series. Thus, to represent the variability of the input, different rain events are chosen. The characteristics of the chosen rain events are given in Table 5.3. Since the overall goal is to reduce the TSS flux towards the receiving water, rain events are chosen with a return period for which CSO control is typically targeted (events appearing several times over a summer). An additionally quite heavy rain event (expected

Table 5.2: Default parameter values and its variation values representing parameter uncertainty for the development of the different scenarios.

Parameter	Unit	Default	Var 1	Var 2
ConcTSS(DWF,CdH)	mg/l	350	420	218
ConcTSS(DWF,NT)	mg/l	440	528	352
ConcTSS(WWF,CdH)	mg/l	50	60	40
ConcTSS(WWF,NT)	mg/l	80	96	64
rresusp,max(CdH)	1/d	24	29	19
rresusp,max(NT)	1/d	48	58	38
fQhalf(CdH)	-	1.4	1.7	1.1
fQhalf(NT)	-	1.5	1.8	1.2
nresusp(CdH)	-	4	5	3
nresusp(NT)	-	8	10	6

Table 5.3: Rain events representing input variability for the development of the different scenarios.

Input Rain Event	Start date (dd.mm.yy)	End date (dd.mm.yy)	Cumulative rain (mm)	Duration (h)	Return period (months)
RE 1	01.05.17	04.05.17	19.2	14.0	2
RE 2	17.05.17	21.05.17	37.3	24.6	8
RE 3	29.05.17	01.06.17	7.5	7.7	0.5
RE 4	27.06.17	02.07.17	105.0	46.3	> 24
RE 5	14.06.17	16.06.17	4.0	2.4	0.5

less than every other year) is chosen to push the boundaries.

The resulting scenarios of the case study are thus the following: The first scenario analysed is the default scenario, combining the default rain event (RE1) with the default model parameter values. An additional 20 scenarios are evaluated to consider parameter uncertainty. For all of the ten indicated parameters a scenario is run by combing the lower, respectively upper variation (Var 1 and 2) of a specific parameter with the other default parameters and the default rain event. The last four scenarios are run to consider input variability. For this, the default parameters are combined with the four additional rain events chosen (RE 2 to 5). This means, that a total of 25 scenarios is analysed, resulting in the evaluation of 25 GSA.

In contrast to Saagi et al. (2018), the standardized regression coefficient (SRC) method (Saltelli et al., 2008) is preferred over the Morris method for the GSA, as convergence problems are known with the latter (Vanrolleghem et al., 2015). The ranking of each control handle is evaluated using the absolute value of the obtained SRC. For the control handles, a uniform distribution with generally $\pm 50\%$ of the currently implemented limit is tested (Table 5.1). Quality control of the GSA was performed by evaluating the quality of the regression ($R^2 > 0.7$; Cosenza et al. (2013)) and the Variance Inflation Factor ($VIF < 5$; Rogerson (2014)).

5.6 Results and Discussion

For each of the 25 uncertainty scenarios a GSA was conducted and the calculation of the absolute SRC value allowed ranking the control handles according to their effectiveness. Since 25 different GSAs were conducted, 25 different rankings are available. This allows studying the effect of uncertainty and variability, represented as scenarios, on the ranking. An option to visualize the control handle ranking under uncertainty and variability is to count how often a control handle takes a specific rank. Figure 5.3 indicates this for the case study, where 14 different control handles were studied, thus resulting in 14 different ranks. Since 25 scenarios were analysed, each handle can take 25 positions. If the rank of a handle is indifferent to the uncertainty scenario analysed, it will take 25 times the same position. If, however, the ranking of a handle depends quite heavily on the scenario chosen, the 25 counts will be distributed over a wide range of ranks. The ranking distributions of the top three control handles (QP,NT, QP,CV, QP,JR) are highlighted in green. The distributions are narrow, meaning that these control handles are ranked high constantly, i.e. irrespective of the uncertainty scenario analysed. Figure 5.3 also shows that some of the control handles have a very wide distribution of their rankings. QP,TR and QFill,BG, for example, show ranks between 7-14, respectively 5-13 (highlighted in blue). This means, that depending on the scenario studied, the control handle can be quite important, respectively unimportant. Interesting are also control handles that show two fairly opposed peaks, meaning that, depending on the uncertainty scenario, they are rather effective or rather ineffective control handles. Examples of this distribution (QP,SE and QP,AR) are highlighted in orange in Figure 5.3. An analysis of the results in more detail showed that they have the tendency to take opposing ranks in the same scenario, meaning that if QP,SE is ranked high, QP,AR is usually ranked low.

Figure 5.4 gives the values of the SRCs of each control handle for every uncertainty scenario evaluated. The results indicate a wide range of absolute SRC values ($2 \cdot 10^{-4}$ to 0.86) meaning that the potential impact of the control handles on receiving water quality improvement varies over a wide range. The results also show that the three highest rated control handles (QP,NT, QP,CV, QP,JR) have an average (0.78, 0.46 and 0.26) which is considerably higher than the fourth highest average of QT,SA (0.07). Comparing these findings with the currently implemented capacities at the pumping stations in Table 5.1 shows that the installed pumping capacity at NT is highest. It is however interesting to note that the same increase of the pumping capacity at CV would have a more important effect than at JR, since those pumping stations have currently the same pumping capacity installed (see Table 5.1).

Figure 5.4 also shows whether the SRC values are positive or negative. A positive, respectively a negative SRC value gives an indication in which direction a control handle needs be changed to reduce the overall TSS flux to the environment. For the three highest rated control handle the SRC value is negative, which means that increasing the pumping capacity towards the WRRF will reduce the TSS flux to the Garonne (because the TSS can be removed at the

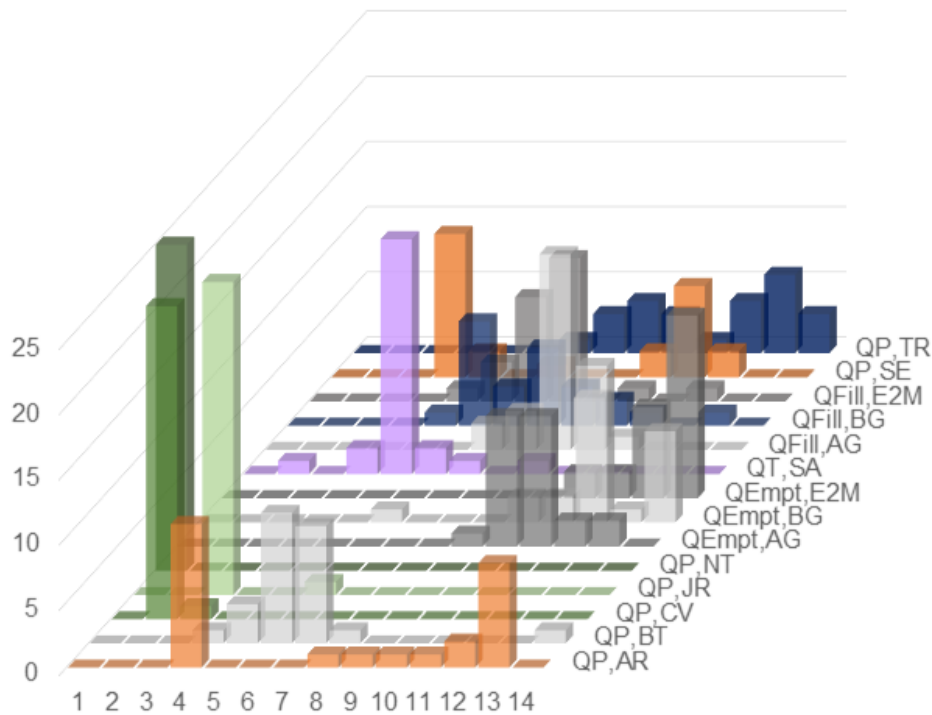


Figure 5.3: Evaluation of the control handle ranking distribution resulting from the 25 scenarios representing parameter uncertainty and input variability.

WRRF). This is, however, not the case for the limiting throttle capacity towards the WRRF of the fourth control handle QT,SA. In this case, the limiting capacity to the WRRF would need to be decreased, meaning that locally more overflow is created (!), to overall reduce the TSS emission. Figure 5.2 shows that SA is located upstream of the highly used pumping station NT. The catchment upstream SA is mainly influence by WWF and the more polluted DWF plays only a minor role. This means that it is favourable to overflow the less polluted water at SA instead of further transporting it to NT, where it is mixed with more polluted water and might cause a highly loaded overflow.

Finally, plotting the SRC values as in Figure 5.4 also allows evaluating whether a control handle switches from positive to negative values depending on the scenario. This means that depending on the actual model parameter values and the specific rain event, an increase of the value of the control handle either increases or decreases the TSS flux to the environment. Depending on the unknown reality, such a control handle can thus have the desired or the unwanted effect. For the given case study, this only occurred for control handles with generally very low SCR values and thus quite unimportant control handles, such as QP,TR, QFill,E2M or QFill,BG.

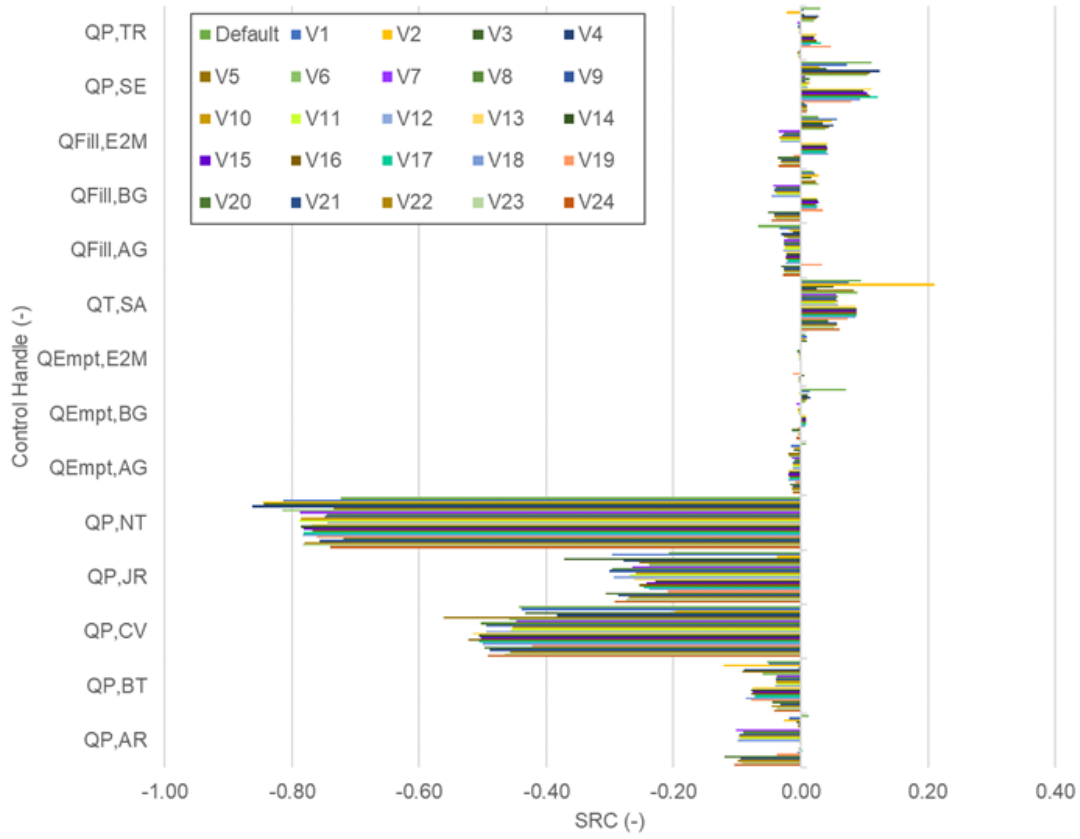


Figure 5.4: SRC values of all studied control handles for the scenarios representing parameter uncertainty and input variability.

5.7 Conclusion

The proposed methodology based on multiple GSAs of control handles conducted for a limited set of uncertainty scenarios allows studying the sensitivity of the control handle ranking to potential deviations between model and reality. In this work, the deviations evaluated parameter and input uncertainty, but the methodology can easily be extended with other sources of uncertainty (e.g. model structure uncertainty) as long as they can be expressed in scenarios to be run.

The results of the case study indicate that the three control handles that are on average ranked highest are keeping their rank for a wide range of scenarios. They are thus probably part of a no-regret decision on the system upgrade since it means that developing scenarios for reduction of the TSS flux to the natural environment based on these handles will not only have the largest impact, but will also be robust with respect to deviations between model and reality. Focusing on the lower ranked control handles would not only have a smaller positive impact on the environment and (assuming comparable investments) seems therefore

less sensible. Even worse, depending on the actual parameter values and the specific rain event occurring, these control handles might even increase the TSS flux to the environment. The evaluation of multiple GSAs representing parameter and input uncertainty showed that their effect changes from positive to negative under certain conditions. This would not have been visible in a static GSA with only one parameter set and one rain event, which might have led to a regret-decision.

This methodology provides a tool to help urban wastewater system operators and stakeholders to decide about the most effective control handles to include in the further development of their management strategies. Even though uncertainty and variability considerations were included in the selection of the control handles, these considerations should also be included in the next step, the evaluation of different management strategies using the selected control handles.

Chapter 6

Integrated Modelling Study – Evaluating Scenarios Tackling the Issue of Total Suspended Solids Emission

Ledergerber, J. M., Maruéjols, T., and Vanrolleghem, P. A. Integrated modelling study – Evaluating scenarios tackling the issue of total suspended solids emission. *In preparation*.

Author contributions Conceptualization, J.M.L., T.M. and P.A.V.; Methodology, J.M.L. and P.A.V.; Investigation, J.M.L.; Writing – Original Draft Preparation, J.M.L.; Writing – Review & Editing, J.M.L., T.M. and P.A.V.; Visualization, J.M.L.; Supervision, T.M. and P.A.V.; Project Administration, T.M. and P.A.V.; Funding Acquisition, T.M. and P.A.V.

6.1 Abstract

Integrated modelling studies have successfully tackled various issues in the integrated urban wastewater system. An integrated model has been developed for the case study of the Clos de Hilde catchment in Bordeaux, France. The modelling approach chosen, the particle settling velocity distribution approach, allows describing the fate of particulates as they move along the different subsystems. A previous study (Chapter 5) identified the most effective control handles to reduce total suspended solids emission to the receiving water, the “Garonne” river. In addition to the four most effective control handles, a simple control of the three available retention tanks is implemented as an additional measure. In this work, the measures are combined in different scenarios and evaluated for periods including rain events of different intensity. This allows studying under which conditions which measures are most effective. The smallest rain events have a return period smaller than 0.5 months, whereas the biggest

rain event has a return period of over 24 months. The size of the rain events were selected in the order of magnitude where most impact is desired by the different measures. In addition, the scenarios are evaluated over the entire summer period of 2017. This shows that scenarios with single measure implementation are able to reduce the overall load by roughly 5% to 10% of the initial total suspended solids load. Scenarios combining multiple measures however are able to reduce the overall load by 25% to 30% depending on the measures chosen. The analysis showed that multiple options are available for Noutary and Jourde, whereas for the overflow Carle Vernet the options are limited, since the upstream catchment is a completely combined catchment and no upstream retention volume is available.

6.2 Résumé

De nombreuses études de modélisation intégrée ont permis de s'attaquer avec succès à divers problèmes du système intégré d'assainissement. Un modèle intégré a été développé pour le site pilote du bassin versant du Clos de Hilde à Bordeaux, France. L'approche de modélisation choisie, l'approche de la vitesse de chute en assainissement, est capable de décrire le devenir des particules sur les différents sous-systèmes. Une analyse préalable a permis d'évaluer les points de contrôle les plus efficaces pour réduire les émissions globales de matières en suspension dans les eaux réceptrices, la rivière Garonne. Les quatre points de contrôle les plus efficaces sont sélectionnés pour la mise en œuvre des mesures visant à améliorer la qualité de l'eau de la rivière. En plus des quatre points de contrôle les plus efficaces, un simple contrôle des trois réservoirs de rétention disponibles est mis en œuvre comme mesure supplémentaire. Les mesures sont combinées dans différents scénarios et évaluées pour des périodes comprenant des événements pluvieux de différentes tailles. Cela permet d'étudier les conditions dans lesquelles les mesures sont efficaces. Les plus petites pluies ont une période de retour inférieure à 0,5 mois, alors que la plus forte pluie a une période de retour supérieure à 24 mois. L'ampleur des précipitations est choisie dans l'ordre de grandeur où un impact des mesures est souhaité. Les scénarios sont évalués sur l'ensemble de la période estivale 2017. Pour l'évaluation de l'ensemble de la période estivale, l'analyse montre que les scénarios avec une seule mesure permettent de réduire le flux global d'environ 5% à 10% du flux total initial. Les scénarios qui combinent plusieurs mesures permettent toutefois de réduire le flux global de 25% à 30% selon les mesures choisies. L'analyse a montré que de multiples mesures sont disponibles pour Noutary et Jourde, alors que pour le déversoir Carle Vernet les mesures sont limitées, puisque le bassin versant en amont est un bassin versant complètement unitaire et aucun volume de rétention n'est disponible en amont.

6.3 Introduction

This chapter aims at closing the loop of the thesis and can be seen as a summary chapter for the case study. It builds on the results found in previous chapters in multiple ways.

Section Literature Review summarized successful IM studies. Integrated modelling has been proven successful for planning (e.g. Schulz et al. (2005)), for the development of RTC (Tränckner et al., 2007; Kroll et al., 2018; Schütze et al., 2018) or for decision support as found for example by Benedetti et al. (2013b).

The case study CdH is driven by the recent developments in legislation (JORF, 2015), where water quality criteria also apply to the sewer system and no longer only to the WRRF. The receiving water, the river “Garonne”, has a very high turbidity, is influenced by tidal dynamics and is not classified as a sensitive water body and nutrients are thus not addressed. The issue of particulate pollution needs to be tackled though (see Section 1.1). For this reason an integrated model of the case study, including the catchments, sewer and WRRF, has been developed, calibrated and validated with data collected in 2017 (see Section 4.6). The PSVD modelling approach was chosen for its capability to address the issue of the case study: describe the fate of particulates in the IUWS.

During DWF the IUWS of the case study shows no major issues and is performing well. During WWF, however, major overflows occur. The aim of the case study is to tackle the issue of TSS emissions during WWF. In order to do so, different measures are proposed to reduce them. The results of the evaluation of the effectiveness of various potential control handles in Section 5.6 are considered. For the development of different measures, the four most effective control handles are selected and a simple control of the RTs is suggested as an additional measure. The different measures are combined to scenarios. The calibrated and validated integrated model of the case study of the IUWS in 2017 (see Section 4.6) is representing the default scenario. The model allows implementing the measures and estimating the overall TSS load to the receiving water. The scenarios are evaluated for different evaluation periods, including rain events of different magnitudes. This allows evaluating under what conditions (rain events) scenarios are most effective. Harremoës and Rauch (1996) found that the analysis of scenarios under short-term periods is not sufficient to replace longer simulations. For the case study long term simulations are made possible thanks to the fast running conceptual model (see Chapter 4). This allows evaluating the different scenarios also for the entire summer period of 2017 (4 months). For the case study CdH this is the relevant period, since this is the period where the most intense storm events generally occur (see Section 1.1).

6.4 Material and Methods

6.4.1 Case Study Description

The case study CdH is described in detail in Chapter 1. Only a short summary is given here to make the case study accessible for the current chapter. A map of the CdH catchment in Figure 6.1 shows that the catchment is located on both sides of the river Garonne. Since the WRRF CdH is located upstream of the catchment, major pumping stations are located along the river. The pumping stations serve at the same time also as CSOs. Once the maximum pumping capacity towards the WRRF is reached, the overflow is activated. Two RTs are located upstream of the pumping station / overflow JR and one RT is located upstream of the pumping station / overflow NT. As mentioned in section 1.1 the RTs were built for flood protection and are currently only activated during major rain events.

The map in Figure 6.1 does not provide sufficient detail to note one particularity of the sewer system: The combination of the water from the right side of the Garonne, pumped towards the WRRF via JR, and water from the left side of the Garonne, pumped towards the WRRF via CV, is only combined in the outflow of the pumping station CV. This means that the water pumped at JR does not have to be re-pumped at CV. It also means that a change of the pumping capacity at JR does not influence the overflow at CV, since the overflow at CV occurs in the inflow of the pumping chamber and not the outflow.

The fluxes contributing to the overall flux to the receiving water can be differentiated in fluxes resulting from CSOs in the sewer system and fluxes resulting from the WRRF. The fluxes in the sewer system are from the following CSOs: AR, BT, JR, SA and TR on the right bank and SE, SJ, CV and NT on the left bank, all indicated in Figure 6.1. The two fluxes towards the receiving water from the WRRF are the BP flux after the primary treatment and the effluent of the WRRF, BF. The fluxes from the WRRF are shown in Figure 6.1.

6.4.2 Modelling Approach

The modelling approach chosen is the PSVD approach, able to address the issue of TSS emission to the receiving water. The modelling approach is described for all the submodels in Section 4.3 and the calibrated and validated model of the case study is discussed in Section 4.6. The model is implemented in the software WEST (Wastewater treatment plant Engine for Simulation and Training) by DHI, Hørsholm, Denmark.

6.4.3 Definition of Measures and Scenarios

The scenarios analyzed to reduce the overall load of TSS towards the receiving water build upon the evaluation of the control handles in Chapter 5. In accordance with the findings in Section 5.6, the four most efficient control handles are chosen, namely: the maximum pumping

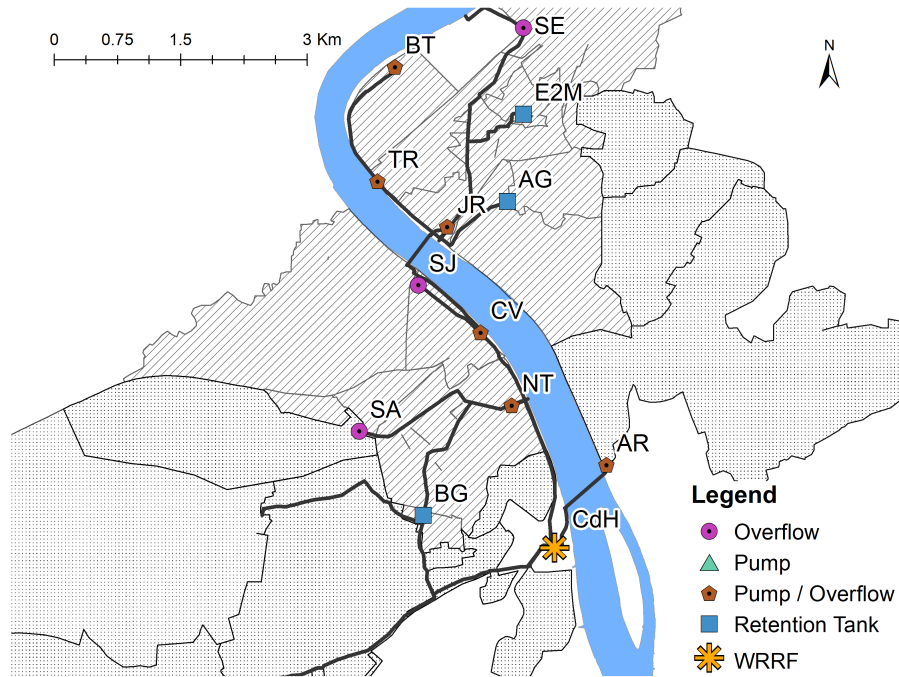


Figure 6.1: Map of the case study CdH indicating the selected measures as well as the overflows and the WRRF, representing the flux towards the receiving water.

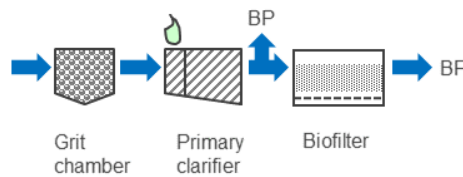


Figure 6.2: Modelled WRRF of the case study CdH indicating the two flows towards the receiving water: the by-pass (BP) after the PCF and the outflow of the BF.

capacity towards the WRRF at the three pumping stations NT, CV and JR, as well as the throttle capacity SA, limiting the flow towards the WRRF. In addition, a simple control of the RTs is implemented. These represent different potential measures to improve the water quality of the receiving water.

For the pumping capacities and the throttle capacity, the default values as well as the values for the implementation of the measures are presented in Table 6.1. Whenever a value is declared as ‘default’, it corresponds to the value implemented in the model in Chapter 4 and thus the value corresponding to the calibrated and validated model of the case study. When defining the values for the measures, the results from the control handle evaluation in Section 5.6 were considered. The results of that study indicated that the pumping capacities need to be increased whereas the throttle capacity must be decreased for a decrease in the total TSS

flux towards the receiving water. The measures assume an increase, respectively a decrease, of the default values by 50%. The resulting values are indicated in Table 6.1.

Table 6.1: Measures to improve the receiving water quality based on capacities of pumping stations and throttle devices.

Abbr. Measure	Description of measure	Values	
		Default (m ³ /d)	Measure (m ³ /d)
Q _{NT}	Increased capacity towards WRRF at NT	26 957	40 400
Q _{CV}	Increased capacity towards WRRF at CV	21 600	32 400
Q _{JR}	Increased capacity towards WRRF at JR	21 600	32 400
Q _{SA}	Decreased capacity towards WRRF at SA	38 880	19 400

In the default model, the RTs are filled based on the flow in the sewer next to the RT and the pumps emptying the RTs are activated based on the stored volume, respectively the water height in the tank. The implemented simple control of the RTs is based on the flow in the adjoining sewer stretch, summarized in Table 6.2. As in the default scenario, the filling of the RTs is still based on the flow. In this case, however, they are activated for comparably small rain events. The filling starts once a flow in the adjoining sewer stretch of three times (RT₃), respectively twice (RT₂), the maximum DWF is reached. The exception is the RT BG that starts being filled for both scenarios at twice the DWF due to its large retention volume with respect to the upstream catchment. The emptying of the RTs is no longer based on the volume already stored, but takes into consideration the flow in the sewer next to the RT. The emptying of the RTs only starts once the flow is decreased to 1.2 times the DWF.

The different measures can be analyzed separately or in different combinations resulting in the scenarios. All the measures are evaluated as a single measure to quantify the individual

Table 6.2: Measures to improve the receiving water quality based on modified control of RTs. The measure RT₃ indicates that the RTs generally start being filled at 3 times the DWF flow and for the measure RT₂ at twice the DWF in the sewer next to the RT.

RT	Parameter	Abbr.	Measure RT ₃		Measure RT ₂	
			Value (m ³ /d)	Approx. (-)	Value (m ³ /d)	Approx. (-)
BG	Flow sewer filling	Q _{SweFill,BG}	1 000	2xDWF	1 000	2xDWF
	Emptying flow rate	Q _{Empt,BG}	2 000	4xDWF	2 000	4xDWF
	Flow sewer emptying	Q _{SewEmpt,BG}	600	1.2xDWF	600	1.2xDWF
AG	Flow sewer filling	Q _{SweFill,AG}	4 500	3xDWF	3 000	2xDWF
	Emptying flow rate	Q _{Empt,AG}	6 000	4xDWF	6 000	4xDWF
	Flow sewer emptying	Q _{SewEmpt,AG}	1 800	1.2xDWF	1 800	1.2xDWF
E2M	Flow sewer filling	Q _{SweFill,E2M}	2 400	3xDWF	1 600	2xDWF
	Emptying flow rate	Q _{Empt,E2M}	3 200	4xDWF	3 200	4xDWF
	Flow sewer emptying	Q _{SewEmpt,E2M}	960	1.2xDWF	960	1.2xDWF

Table 6.3: Combination of different measures resulting in the analyzed scenarios for overall TSS load reduction. The measures regarding modified capacities are described in Table 6.1 and the measures regarding the control of the RTs in Table 6.2.

Abbr.	Scenario description	Measures					
		Q _{NT}	Q _{CV}	Q _{JR}	Q _{SA}	RT ₃	RT ₂
Default	No measures (calibrated model)						
Q _{NT}	Increased capacity NT	✓					
Q _{CV}	Increased capacity CV		✓				
Q _{JR}	Increased capacity JR			✓			
Q _{SA}	Decreased capacity SA				✓		
Q _{NT,SA}	Capacities modified NT & SA	✓			✓		
Q*	All capacities modified	✓	✓	✓	✓		
RT ₃	Control of RTs (3xDWF)					✓	
RT ₂	Control of RTs (2xDWF)						✓
Q*&RT ₂	Mod. capacities & RT ₂	✓	✓	✓	✓		✓

effect of that measure. In addition, several measures are combined and for one scenario it is assumed that all measures are implemented. The scenarios evaluated are summarized in Table 6.3 indicating the implemented measures of each of the scenarios with a ✓. The scenario named Q_{NT}, for example, is the scenario where the pumping capacity towards the WRRF is increased at NT. This is indicated by a ✓ in the column of the measures. Since the scenario RT₂ will prove more successful than RT₃ (see Section 6.5), the scenario implementing all modifications of the pumping capacities is combined with the control RT₂ in the scenario named Q*&RT₂.

6.4.4 Definition of Evaluation Period

In order to understand under what conditions certain measures are effective, various periods are simulated to evaluate the effect of the measures on the total TSS load to the receiving water. The aim is to reduce TSS emissions due to rain events occurring multiple times over the summer period. The evaluation periods are thus chosen accordingly. One evaluation period includes a major rain event, beyond the typically addressed magnitude. This allows to estimate how the scenarios perform during heavier rain events than what they were initially planned for. To facilitate the comparison with the previous Chapter 5, identical evaluation periods have been used with identical abbreviations. Since storage and later release of water in RTs prolongs the period of increased water flow at the WRRF due to WWF, certain evaluation periods had however to be prolonged to capture all the WWF-induced flow. As mentioned in Section 6.3, it is however also important to evaluate the scenarios on a long-term basis. That is the reason for the addition of the evaluation of the different scenarios over 120 days. The chosen evaluation periods are listed in Table 6.4.

Although it is the aim to evaluate the different scenarios during WWF conditions, the chosen

Table 6.4: Evaluation periods of scenarios to reduce the overall TSS load to the receiving water.

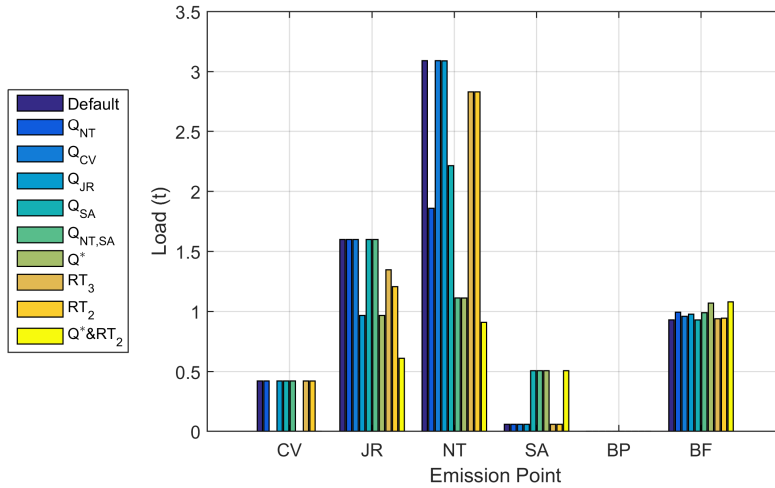
Abbr.	Start date (dd.mm.yy)	End date (dd.mm.yy)	Cumulative rain (mm)	Duration (h)	Return period (months)
RE 1	01.05.17	04.05.17	19.2	14.0	2
RE 2	17.05.17	21.05.17	37.3	24.6	8
RE 3	29.05.17	01.06.17	7.5	7.7	0.5
RE 4	27.06.17	02.07.17	105.0	46.3	> 24
RE 5	14.06.17	16.06.17	4.0	2.4	0.5
120d	01.05.17	28.08.17	271.2	165.2	N/A

evaluation periods in Table 6.4 all include a certain amount of DWF time. This is important to ensure that the entire rain event is covered all over the IUWS and that, thus, the overall impacts of a rain event, including the delayed impacts, are covered. During DWF conditions, the only TSS flux towards the receiving water is the flux resulting from the effluent of the WRRF, corresponding to the BF flux. To not compromise the evaluation of the total load towards the environment by the duration of the DWF period, the DWF from BF is thus excluded from the evaluation. In the calculation of the TSS load from the BF, only the load at the BF resulting from a flow bigger than a certain threshold ($0.9 \text{ m}^3/\text{s}$) is included. For the analysis of the loads on the WRRF, the loads including the DWF period are analyzed.

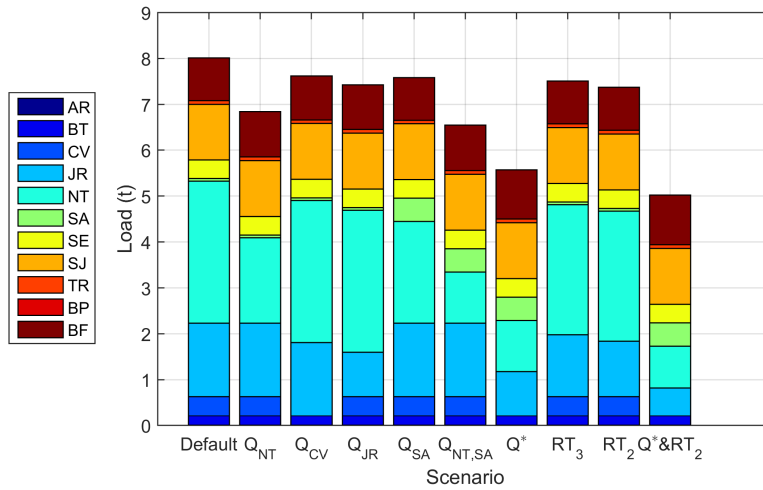
6.5 Results

The results are mostly presented in a visual format, the numerical values, however, are also available in tabulated format in Appendix C. The tabulated results are available for every evaluation period. For each period, the TSS load towards the receiving water for every overflow as well as the total TSS load are indicated. This allows calculating the performance of each scenario in comparison to the default scenario. The performance of a scenario is calculated by dividing the emitted load of the scenario over the emitted load of the default scenario. A value <1 thus indicates an improvement in comparison to the default scenario. The performance is calculated for every individual overflow as well as the total load.

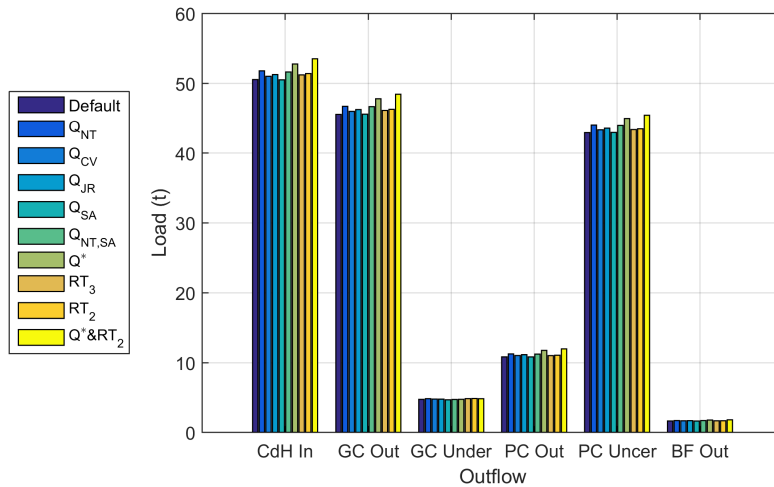
All the evaluation periods are evaluated focusing first on the effect of the scenarios on selected, individual emission points, second on the the overall load towards the receiving water and third on the effect on the loads at the WRRF.



(a) Single loads at selected locations



(b) Total TSS load for scenarios



(c) TSS load at WRRF

Figure 6.3: Total TSS loads for evaluation period RE1. The description of the scenarios is given in Table 6.3.

6.5.1 Analysis for Rain Event RE1, Return Period 2 months

Analysis Selected Emission Points

Figure 6.3a shows the total TSS loads for different overflows for all evaluated scenarios. For simplification, not all overflows are plotted, but only those potentially affected by the measures. The overflows upstream of any measure are thus not visualized (for location of overflows on map see Figure 6.1).

The most positive effect of certain scenarios in terms of TSS load reduction can be observed at NT. The increased pumping capacity (scenario Q_{NT}) decreases the load from approximately $3.1 t_{TSS}$ in the default scenario to $1.9 t_{TSS}$, which means a reduction of almost 40%. The decreased throttle capacity at SA in scenario Q_{SA} obviously increases the overflow at SA (from $0.058 t_{TSS}$ to $0.51 t_{TSS}$), but is at the same time able to reduce the load at NT from $3.1 t_{TSS}$ to $2.2 t_{TSS}$, which leads to a net positive effect. As already found in the previous Chapter 5 this is due to the fact that SA is highly influenced by WWF, with a small DWF component. This makes it more favorable to overflow the less charged water at SA, than mixing the water with the higher charged water downstream which then causes an overflow at NT. Combining the two individual measures in scenario $Q_{NT,SA}$ reduces the load at NT to only approximately 36% of the original load. Adding the control RT_2 only adds a comparably small improvement (29% of default TSS load).

The increase of the pumping capacity by 50% at CV (Q_{CV}) is able to totally eliminate the TSS load of approximately $0.4 t_{TSS}$ in the default scenario. As the map in Figure 6.1 indicates, there are no RTs upstream of CV, and, thus, implementing an improved control of the RTs does not reduce the load at this particular overflow.

The same relative and absolute increase of the pumping capacity at JR (Q_{JR}) decreases the overflow from $1.6 t_{TSS}$ to $0.97 t_{TSS}$, which represents approximately 60% of the original TSS load. Since two RTs are located upstream of JR, lowering the filling value to approximately 3xDWF (RT_3), respectively 2xDWF (RT_2), results in a load representing 84%, respectively 74%, of the original load. These measures thus have a relatively bigger impact on JR than on NT.

Since most measures send more wastewater to the WRRF, more TSS reaches the environment over the effluent than in the default case. But due to the high efficiency of the WRRF, this increase is marginal in comparison to the “saved” TSS at the overflows. The maximum increase of all scenarios amounts to $0.2 t_{TSS}$, which represents an increase by 20% in effluent load. In addition, it should also be noted that none of the scenarios activated the BP after the primary treatment. Thus, all the water reaching the WRRF is biologically treated.

Analysis Overall Impact on TSS Emissions

Figure 6.3b shows the total TSS load towards the receiving water as the sum of all individual components. This allows comparing the overall performance of the different scenarios. For the default scenario, the model estimates a total TSS load of $8.0 t_{TSS}$ towards the receiving water caused by the rain event RE1. The evaluation of the affected overflows leads to remarkable improvements for certain scenarios. As only the emission points with potential improvements were analyzed, it is to be expected that the overall performance of the different scenarios is somewhat lower since also the overflows upstream of any measures are included. Since their emission is identical for all the scenarios they decrease the overall performance. Figure 6.3b reveals that the best case scenario is the implementation of all measures ($Q^* \& RT_2$), which leads to a total TSS load corresponding to approximately 63% of the default load. Implementing only all modifications in the capacities (scenario Q^*) is, however, also performing quite well with 70% of the default values. The scenarios with the implementation of only one measure perform approximately equally well, with one exception with a bigger impact: the increase of the pumping capacity at NT that leads to a reduction to 85% of the default scenario.

Analysis TSS Loads on WRRF

As clearly illustrated in Figure 6.3b, implementing measures generally decreases the load to the receiving water. This implies that the TSS load prevented to reach the environment is mostly removed at the WRRF. Figure 6.3c shows the detailed TSS loads at the WRRF over the entire evaluation period RE1, including the DWF. The loads shown are the inload to the WRRF (CdH In), the load out of the GC to the PC (GC Out), the underload of the GC (GC Under), the load out of the PC to the BF (PC Out), the underload of the PC (PC Under) and load out of the BF (BF Out). First, it should be noted that these loads are approximately an order of magnitude larger than the loads towards the environment in Figure 6.3a. As anticipated, indeed, Figure 6.3c shows that the loads towards the WRRF are increased for all scenarios. The Figure also shows that the additional load is passing the GC and is then mostly removed at the PC, which can be seen by the increased PC underload. The increase of maximally $0.2 t_{TSS}$ in the effluent of the BF (see Figure 6.3a) is basically invisible when analyzing the loads on the WRRF with inclusion of the DWF load, due to the difference in order of magnitudes.

Three observations are interesting to note. First, it is impressive to see that the WRRF is able to treat the major share of the additional load caused by the implementation of different measures for all scenarios. Second, it is impressive to note that the most of the additional load is removed at the PC and third, that the relative overall emission reduction is high in comparison to the relative increase of TSS load removed at the PC. The overall TSS emission reduction, for example, of scenario $Q^* \& RT_2$ was almost 40% (see Figure 6.3b) whereas the increase in the underload of the PC is in the single digits. This effect is mainly caused

by the fact that the loads at the WRRF are highly influenced by the DWF, which puts the absolute additional removal at the PC into perspective.

For this evaluation period all tabulated results can be found in Table C.1.

6.5.2 Analysis for Rain Event RE2, Return Period 8 months

Analysis Selected Emission Points

In comparison to the rain event RE1 (return period 2 months), the RE2 (return period 8 months) almost doubles the total TSS emissions towards the receiving water to $18 t_{TSS}$. Comparing the previous distribution of the single loads in Figure 6.3a with the current Figure 6.4a, shows that the relative distribution is quite similar, with increased loads though.

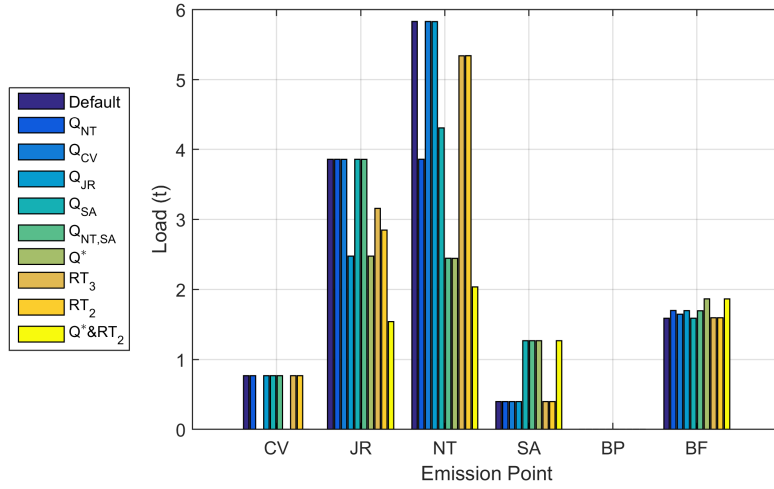
At NT, also the combination of the decreased capacity at SA and the increased capacity at NT itself (scenario $Q_{NT,SA}$) creates a big reduction of TSS load. A total of $3.4 t_{TSS}$ is prevented at NT to reach the receiving water. The addition of the simple RT control removes an additional $0.4 t_{TSS}$. The implementation of a simple control only seems less interesting since only approximately $0.5 t_{TSS}$ in total are prevented to reach the receiving water. The implementation of a simple RT control is however more favorable at JR, where the implementation almost reaches the effect of the increased pumping capacity. As for the overflow at NT and JR, also the other overflows show quite a similar picture as during the less intense rain event RE1. It should be noted that even for this rain event (return period 8 months) the BP of the BF is not yet activated for any of the scenarios.

Analysis Overall Impact on TSS Emissions

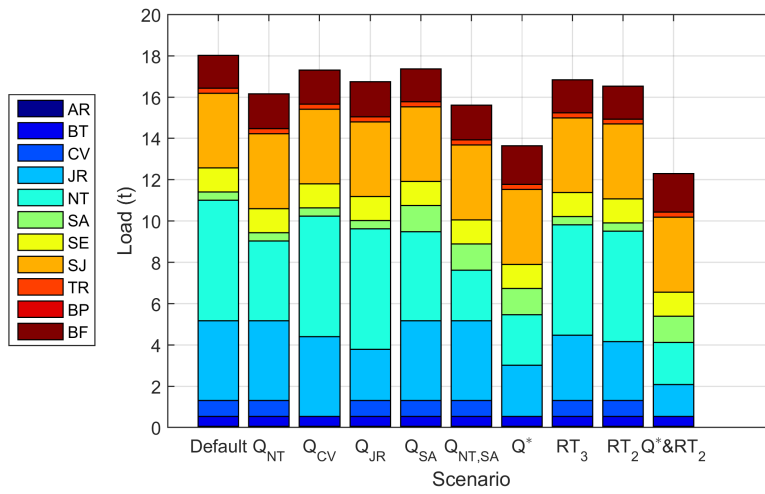
Looking at the overall performance of the different scenarios in Figure 6.4b shows that the total TSS load of $18 t_{TSS}$ is reduced to $17 t_{TSS}$ in the worst case and in the best case to $12 t_{TSS}$, which represents 68% of the default load. As this rain event is already quite remarkable, several overflows where no measures are implemented start to contribute significantly and thus lower the overall effectiveness.

Analysis TSS Loads on WRRF

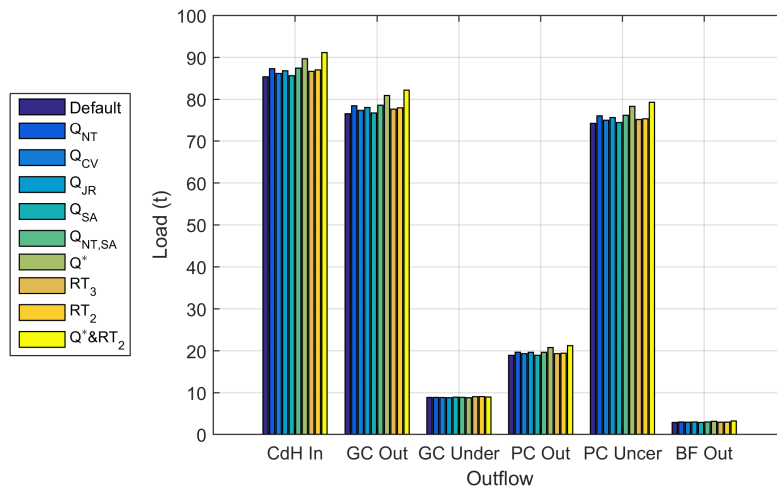
Figure 6.4c indicates the TSS loads at the WRRF. As for the previous rain event RE1, also for RE2, the same tendency can be observed. The more measures implemented to reduce the TSS load to the environment, the more TSS reaches the WRRF. In the default scenario a load of $85 t_{TSS}$ arrives at the WRRF (CdH In). Depending on the scenario an additional load of approximately $1 t_{TSS}$ (e.g. Q_{CV}) to $6 t_{TSS}$ ($Q^* \& RT_2$) reaches the WRRF. Those numbers correspond well with the numbers in the previous Figure 6.4b of the overall emission reduction. For example, for scenario $Q^* \& RT_2$, $6 t_{TSS}$ overall emission reduction was achieved, leading to an improvement of approximately 30%. According to the model, those $6 t_{TSS}$ “saved” reach



(a) Single loads at selected locations



(b) Total TSS load for scenarios



(c) TSS load at WRRF

Figure 6.4: Total TSS loads for evaluation period RE2. The description of the scenarios is given in Table 6.3.

the WRRF, leading to an inload of $91 t_{TSS}$. This same absolute amount of TSS, however, leads only to an increase of 7% at the influent of the WRRF.

Independent of the scenario, most of the additional TSS is removed at the PC, enabling the comparably small increase in TSS load at the effluent of the WRRF (BF Out) already observable in Figure 6.3a.

For this evaluation period all tabulated results can be found in Table C.2.

6.5.3 Analysis for Rain Events RE3 and RE5, Return Period <0.5 months

Since both RE3 and RE5 have quite small return periods, they are analyzed in the same subsection. The results found individually in Table C.3 for RE3 and in Table C.5 for RE5 show that the overall performances are comparable. Since the rain event in RE3 was mainly occurring on the left bank of the Garonne and mostly no, respectively only very little (BT), overflow was occurring on the right bank, the discussion of measures on the right side is obsolete. The analysis of the results thus focuses on the analysis of RE5.

Analysis Selected Emission Points

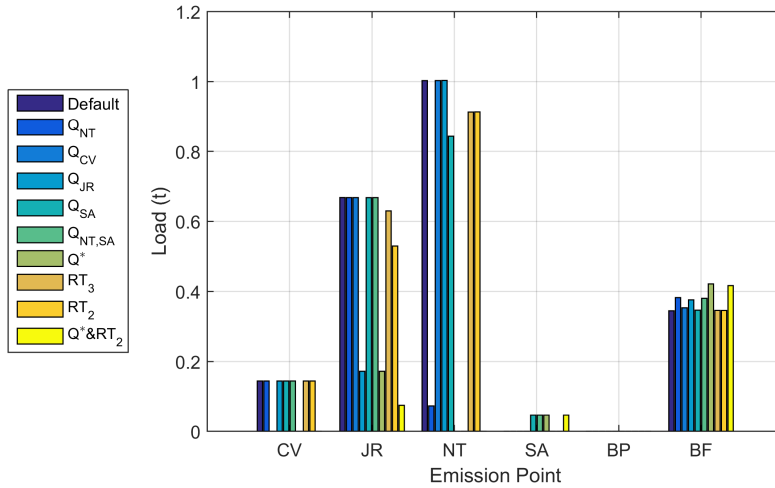
Figure 6.5a shows the most remarkable effect of certain scenarios in terms of TSS load towards the receiving water at NT. The increased pumping capacity (scenario Q_{NT}) decreases the load from approximately $1 t_{TSS}$ to $0.07 t_{TSS}$. The decreased throttle capacity at SA imposes an overflow at SA of only approximately $0.05 t_{TSS}$ where none was observed in the default scenario. However, it reduces the overflow at NT to $0.84 t_{TSS}$. Combining the two measures (NT+&SA-) is able to completely eliminate the overflow at NT for this rain event.

The increase of the pumping capacity by 50% at CV is able to totally eliminate the overflow at CV and the same increase at JR reduces the overflow from 0.67 to $0.17 t_{TSS}$.

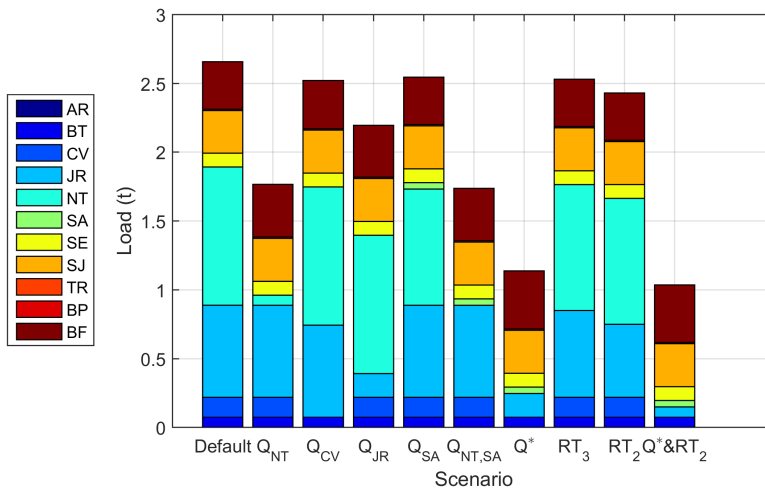
Since these are the smallest rain events analyzed, it is not surprising that none of the scenarios creates a by-pass of the biological treatment of the WRRF. The additional water sent to the WRRF creates only a slightly increased load of TSS at the outlet of BF.

Analysis Overall Impact on TSS Emissions

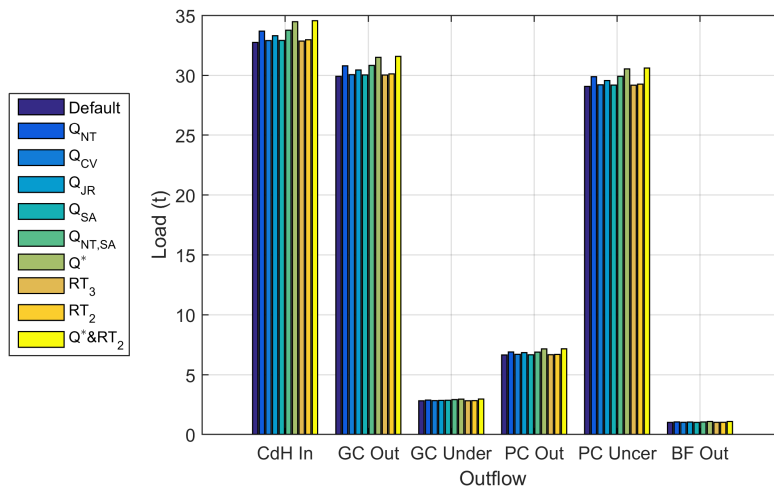
Figure 6.5b shows the total TSS load towards the receiving water. This analysis highlights that for these rain events the implementation of a simple RT control does not greatly reduce the overall TSS emissions to the receiving water. However, it should be remembered, that RE3 was more active on the left bank of the Garonne, and that two of the three RTs are placed on the right bank. The potential contribution of the RTs is thus limited. In addition, it should be remembered that the filling of the RTs only starts at three times the DWF (scenario RT₃),



(a) Single loads at selected locations



(b) Total TSS load for scenarios



(c) TSS load at WRRF

Figure 6.5: Total TSS loads for evaluation period RE5. The description of the scenarios is given in Table 6.3.

respectively 2 times the DWF (RT_2) and for such a minor rain event they are thus hardly activated. The effect of the control is thus limited.

Analysis TSS Loads on WRRF

Figure 6.5c shows that over the entire period RE5, the maximum overall emission reduction of approximately $1.5 t_{TSS}$ in scenario $Q^* \& RT_2$ (see Figure 6.5b) causes an increase of the same amount at the inlet of the WRRF. Relatively, however, this increase represents less than 5% of the total inload. Figure 6.5a already showed that the increase in the effluent of the BFs is marginal with 0.01 to $0.08 t_{TSS}$. The analysis in Figure 6.5c shows that the additional load arriving at the inlet of the WRRF is mostly removed at the PC, thus enabling the almost stable effluent load for the different scenarios.

For this evaluation period all tabulated results can be found in Table C.5.

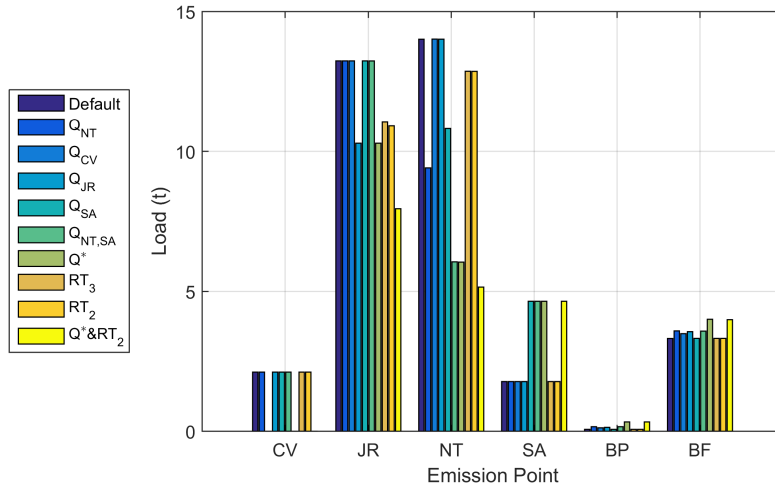
6.5.4 Analysis for Rain Event RE4, Return Period >24 months

Although the previously analyzed evaluation periods contained rain events of quite different magnitudes, the rain event in this period RE4 is, with a return period of over 24 months, a whole step bigger.

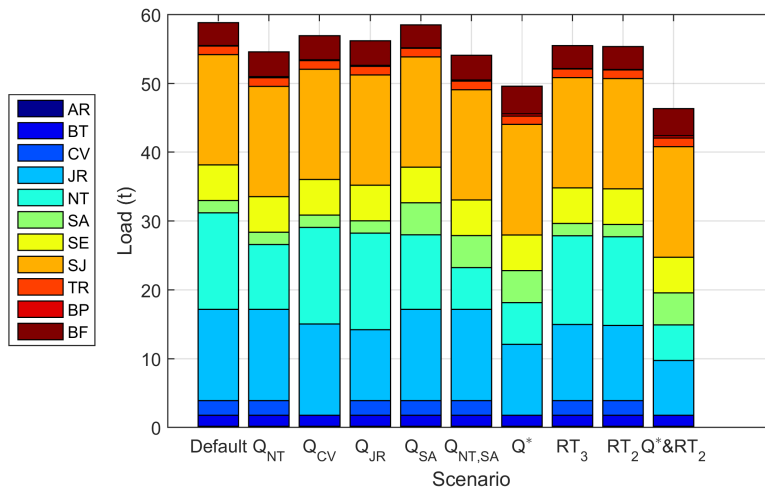
Analysis Selected Emission Points

Figure 6.6a shows that single measures (scenario Q_{NT} , Q_{CV} and Q_{JR}) can lead to important TSS emission reductions at the relevant overflow. With Q_{NT} , $4.6 t_{TSS}$ can be prevented to reach the receiving water at NT, with Q_{CV} , $2.1 t_{TSS}$ can be prevented at CV and with Q_{JR} , $3 t_{TSS}$ can be prevented at JR to reach the receiving water. For JR it should be noted that almost the same improvement can be achieved by implementing a simple control on the RTs. Since both the increased pumping capacity and the control of the RTs have a similar effect for the environment other factors, such as the costs, will play a more important role when evaluating the measures for practical implementation. It should be noted that all of the single measures prevented loads corresponding approximately to the total load of the previously analyzed smaller rain events with a return period smaller than 0.5 months (see Table C.3 for RE3, respectively Table C.5 for RE5). For NT, reducing the throttle capacity at SA is particularly important. For major rain events, it is especially favorable to overflow the less charged water at SA instead of transporting it further downstream and emit the more combined water at NT.

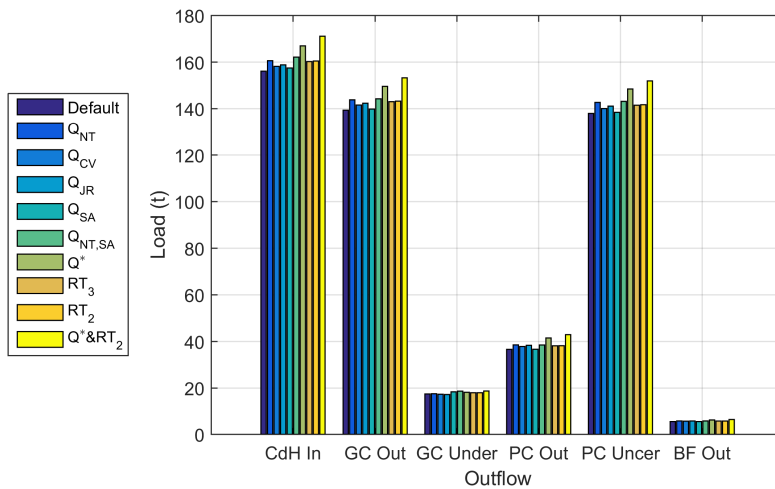
In comparison to the previous evaluation periods, Figure 6.6 shows for the first time the activation of the BP at the WRRF, with a comparably small load though ($0.067 t_{TSS}$ for the default scenario). The load from the BF remains remains comparably stable around the default load of $3.3 t_{TSS}$ with a maximum increase to $3.9 t_{TSS}$ for $Q^* \& RT_2$.



(a) Single loads at selected locations



(b) Total TSS load for scenarios



(c) TSS load at WRRF

Figure 6.6: Total TSS loads for evaluation period RE4. The description of the scenarios is given in Table 6.3.

Analysis Overall Impact on TSS Emissions

Figure 6.6b shows that for the default scenario a total of $59 t_{TSS}$ is emitted. By modifying all capacities (scenario Q^*) a reduction to $50 t_{TSS}$ can be achieved. By also implementing a simple control of the RTs, this number decreases to $46 t_{TSS}$. From the visual inspection of Figure 6.6b it can, however, also be observed that the overall improvement of the single measures (scenario Q_{NT} , Q_{CV} and Q_{JR}) is comparably small when all overflows are considered. A reduction to 93% to 97% of the default load is attained. Only scenarios combining different measures reach reductions to below 90% of the initial load. The relative performances of all scenarios in comparison to the default scenario are generally lower than for the previously analyzed evaluation periods with smaller rain events.

Analysis TSS Loads on WRRF

Figure 6.6c shows the loads on the WRRF, allowing to analyze what happens to the TSS that is prevented from reaching the receiving water. As for the previous evaluation periods, this load reaches the WRRF. The increase in load depends directly on the efficiency of the scenario. For the previous evaluation periods no increase in load at the underflow of the GC was observed, whereas for this evaluation period for the first time a slight increase is observed. As Figure 6.6c shows, the major part is, however, still removed at the PC. Although better visible in Figure 6.6a, the load from the BF to the receiving water stays comparably stable, with a slight increase for scenarios combining multiple measures.

For this evaluation period all tabulated results can be found in Table C.4.

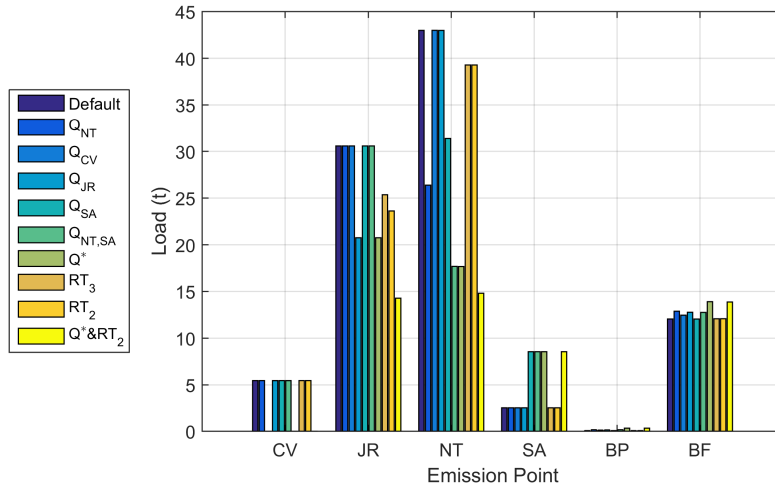
6.5.5 Analysis for 120 d

Analysis Selected Emission Points

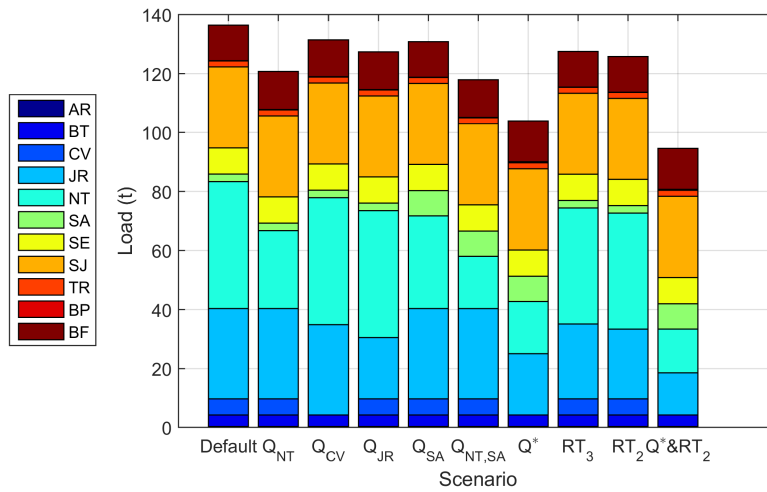
Figure 6.7 summarizes the performance of the different scenarios over the whole evaluation period from May to August 2017. Figure 6.7a shows very good performances of different scenarios at NT. The default load of $43 t_{TSS}$ can be reduced to $26 t_{TSS}$ for scenario Q_{NT} , to $18 t_{TSS}$ for $Q_{NT,SA}$ and to $15 t_{TSS}$ for $Q^* \& RT_2$.

Figure 6.7 also shows that increasing the pumping capacity at CV by 50% could eliminate the overflow at CV for all rain events occurring during the summer period of 2017.

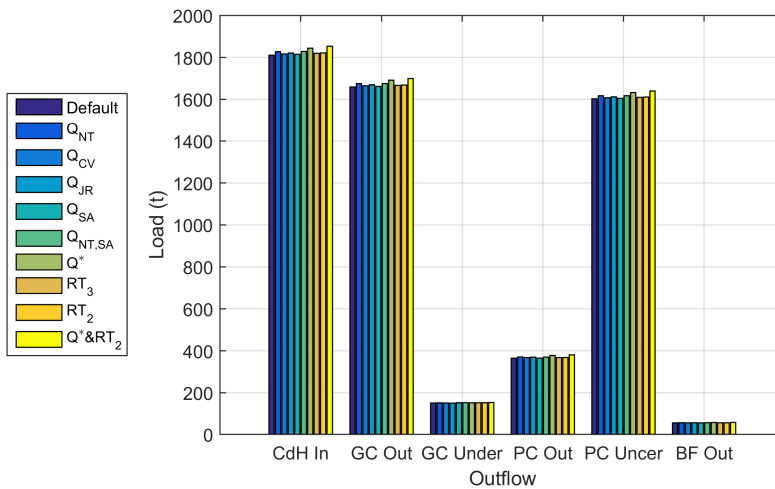
For JR it seems especially noteworthy that implementing a simple control of the upstream RTs leads to a similar improvement as increasing the pumping capacity. In the default scenario $31 t_{TSS}$ are emitted. Increasing the pumping capacity (scenario Q_{JR}) reduces this load to $21 t_{TSS}$, whereas with a control a reduction to $25 t_{TSS}$ (scenario RT_3), respectively $24 t_{TSS}$ (RT_2) can be achieved. For the decision on the measure to be implemented at JR, most likely the cost considerations will play an important role.



(a) Single loads at selected locations



(b) Total TSS load for scenarios



(c) TSS load at WRRF

Figure 6.7: Total TSS loads for 120 d. The description of the scenarios is given in Table 6.3.

Regarding the effect of the measures on the WRRF confirms the findings of the analysis of the individual rain events. Even though under certain conditions the increased flow towards the WRRF might create a by-pass and generally increases the TSS emitted over the effluent of the WRRF, considering the overall performance of the IUWS clearly shows that the total load emitted is considerably smaller in any case. Part of the explanation is certainly that under current conditions unexploited treatment capacities are available at the CdH WRRF.

Analysis Overall Impact on TSS Emissions

Figure 6.7b shows that from a total emission point of view, up to 40 t_{TSS} can be prevented from reaching the receiving water over the whole summer period. In the default scenario 136 t_{TSS} reaches the Garonne via CSOs and the flows from the WRRF. In the best case scenario ($Q^* \& RT_2$), the overall load is reduced to 94.6 t_{TSS} . This represents 70% of the default load, respectively a reduction of 30% of the TSS load to the Garonne over the entire summer period.

Analysis TSS Loads on WRRF

Figure 6.7c shows the loads at the WRRF over the entire summer period. In the big scheme of things, the differences in loads between the scenarios at the WRRF are hardly visible. A main reason for this finding is certainly that the loads at the WRRF over the entire summer period are mainly influenced by the DWF, as already discussed in Section 4.8. Of the roughly 1800 t_{TSS} arriving at the WRRF, the main share of approximately 1600 t_{TSS} is removed at the PC, a little bit less than 200 t_{TSS} at the GC and only roughly 50 t_{TSS} reaches the receiving water, of which approximately 15 t_{TSS} are caused by WWF, as indicated in Figure 6.7a. The importance of DWF at the WRRF is discussed in more detail in the previous Section 4.8.

For this evaluation period all tabulated results can be found in Table C.6.

Compliance Estimation for TSS Loads

The relevant regulations were introduced in Section Project-Relevant Regulations Regarding the Case Study CdH.

For the WRRF the regulation asks for a maximum daily average effluent concentration of TSS smaller than 35 mg/l. The average effluent concentration over the summer period is 7 mg/l with a standard deviation of 1 mg/l. These values clearly indicate that the effluent criterion for the WRRF is well-met.

For the sewer system compliance assessment, one out of three potential criteria is the pollutant load analysis over one year. The model calibration and validation, however, was carried out during the summer period (see Chapter 4). Additionally, rain data is available for the summer only and Bordeaux is known for the distinctive rain patterns for the summer and winter seasons (see Chapter 1). This means that the criteria regarding the pollutant load cannot be

Table 6.5: Compliance Estimation for the criterion based on pollutant load for TSS.

Scenario	CSOs	CdH In	Criterion
	F_{A1} (t_{TSS})	F_{A3} (t_{TSS})	$\frac{F_{A1}}{F_{A1}+F_{A3}} \cdot 100$ (%)
Default	124	1811	6.4
Q _{NT}	108	1827	5.6
Q _{CV}	119	1816	6.1
Q _{JR}	114	1821	5.9
Q _{SA}	119	1815	6.1
Q _{NT,SA}	105	1829	5.4
Q*	90	1844	4.6
RT ₃	115	1820	6.0
RT ₂	114	1821	5.9
Q*&RT ₂	80	1853	4.2

carried out over the whole year, but on the summer period only. Even if rain data over the entire year would be available, an evaluation of the yearly criterion would not be possible since model performance during winter season has not been evaluated.

In order to still have an estimation of the system performance for the different scenarios, the criterion is evaluated for the summer period. For the reason given previously, it is, however, advised to not extrapolate from the seasonal performance to the yearly compliance performance.

For the seasonal estimation of the compliance criterion, theoretically, three loads need to be compared: the pollutant load discharged over CSOs, the volume by-passed at the inlet of the WRRF and the volume entering the WRRF for treatment. To calculate the compliance, the load resulting from the CSO has to be compared to the sum of all loads. To comply with legislation, this ratio needs to be smaller than 5%. For the evaluation period, the by-passed load at the inlet of the WRRF, however, is irrelevant, since no by-pass occurred during the evaluation at this location. The results of the seasonal TSS load compliance estimation are listed in Table 6.5.

The results indicate that over the summer season the load criterion is not met for the default scenario. The results also show that all scenarios lead to an improvement of the criterion, but it is only met for two of them: scenario Q* and Q*&RT₂.

6.6 Conclusion

The detailed analysis showed that only a combination of different measures leads to an overall remarkable emission reduction, even though a single measure can already have quite an effect on a local basis. An example of this is the impact of an increase of the pumping capacity at NT

in scenario Q_{NT} . Over the evaluation of 120 days the total load is reduced locally to 60% of the default load. For the overall load this single measure reduces the load to approximately 90% of the default value. Generally, single measures reduce the overall load by approximately 5% to 10%, whereas scenarios with the implementation of multiple measures are able to reduce the overall load by 25% to 30%. The combination of the modifications of the pumping capacities leads to a reduction of roughly 15%. These improvements are generally possible because the WRRF is capable to remove the additional TSS load sent to the WRRF. Most of the TSS load is removed at the PC, independent of the scenario analyzed. The results of the effluent evaluation of the WRRF confirmed the good performance (Section 6.5.5). The results of the seasonal estimation of the yearly pollutant load criterion in Section 6.5.5 showed that only two scenarios (Q^* and $Q^* \& RT_2$) would lead to sewer system compliance. However, as stated in Section 6.5.5, a conclusion from this seasonal estimation to the yearly compliance is not possible.

The detailed analysis also showed that the effectiveness of the measures depends on the size of the rain events targeted. It is thus of particular importance to define whether it is desired to rather eliminate multiple overflows during smaller rain events or have a significant impact during heavier rain events.

Regarding the implementation of a simple control on the RTs, several conclusions can be drawn: First, the results generally indicate that the control has more potential on the right bank of the Garonne. This can be explained by the fact that the two RTs on the right bank cover a significant amount of the subcatchment of JR. The BG tank, however, covers only a small fraction of the subcatchment of NT. Hypothetically, it would thus be interesting to have the BG tank located further downstream, where a larger fraction of subcatchment could be covered. Secondly, the conclusion that the magnitude of the rain event targeted defines the usefulness of measures is of particular importance for the control of the RTs. By defining a threshold of 2 to 3 times the DWF for the filling of the RTs targets events with a return period of 2 to 8 months as the analysis showed. It means however, that the tanks are still not or only very little activated for smaller rain events and that their full capacity is reached before major rain events are over. For these measures it seems thus of particular interest to consider the potential of model predictive control, where the prediction of the meteorological forecast is considered. This means that the threshold for the filling, for example, could be based on the predicted flow.

The difference between JR and NT is however not only the location and number of the RTs, but also the fact that the subcatchment at JR is mainly serviced by a combined sewer system. The subcatchment of SA upstream of NT is, however, more influenced by WWF. This opens up the interesting measure to increase the overflow at this overflow and thus reduce the overflow at NT, where the water contains a larger fraction of sanitary wastewater.

For the overflow at CV the options of potential measures are limited since the subcatchment of CV is completely combined and thus does not have the same options as NT. In addition, no storage volume is available upstream of CV. The options for potential measures are thus limited. Further investigations could study the impact of a potential construction of a RT upstream of CV.

Comparing the results of this chapter with the results of the results in Section 5.6, where the effectiveness of different control handles was evaluated, confirms the general findings. The top four selected control handles Q_{NT} , Q_{CV} , Q_{JR} and Q_{SA} were indeed able to reduce the TSS emissions to the receiving water for a wide range of different rain events analyzed. From the previous results, it was however concluded that Q_{CV} generally has a greater impact than Q_{JR} . From the results over the 120 d in Figure 6.7 a slightly better performance of the same increase in pumping capacity at JR, respectively at CV, would result in more avoided emissions at JR. This leads to the last conclusion: Whereas the previous chapter was analyzed considering not only the uncertainty due to the variability in rain events, it also considered parameter uncertainty. The evaluation of this chapter was, however, only conducted for the default set of parameters. This clearly sets the results of this chapter in context. It should be remembered that the numbers only give an approximation and caution should be used when one scenario is considered better than another based on a small improvement. For future research it is thus suggested to also include parameter uncertainty analysis in the evaluation of the results.

Conclusions and Perspectives

Conclusions

The aim of this thesis was to advance the field of integrated urban wastewater quantity and quality modelling. This was accomplished on the one hand by achieving better understanding of the fate of solids in the integrated urban wastewater systems (IUWS) and, on the other hand, by developing tools to overcome barriers of integrated modelling (IM), thus making it more accessible. The research conducted is closely linked to the IUWS of the Clos de Hilde (CdH) water resource recovery facility (WRRF) in Bordeaux, France, since this site served as a case study. Even though the research is driven by the case study, the developed procedures are generally applicable and easily transferable to other case studies. Indeed, applying the developed theoretical procedures to a practical case study does not only validate the procedures as such, but also highlights their applicability. If one of the procedures is to be adopted for another case study, having an implemented example usually improves the transferability of the procedure greatly.

To better understand the transport and fate of solids in the IUWS, three measurement campaigns were carried out, the third of which was planned with model-based optimal experimental design (OED) to obtain the most information-rich data. The measurement campaigns allowed complementing the already available measurements of the utility. The measurement campaigns focused on online TSS measurements in the sewer system and ViCAs measurements both in the sewer system and on the WRRF. Building on the work of [Plana \(2015\)](#) for sensors in WRRFs, this research project allowed developing maintenance protocols for sensors deployed in the sewer systems ([Ledergerber et al., 2017b](#)).

The data obtained yielded the information necessary for successful modelling of solids with the PSVD approach. The proof of its usability was provided by the successful calibration and, especially, the powerful validation of the integrated model for the case study. This approach was implemented in the subsystems from the sewer down to the chemically enhanced primary treatment, including a model for retention tanks and the grit chamber. The retention tank model was simplified from its initial implementation to allow for faster calculations. Furthermore, the PSVD approach was extended with a catchment and a simple biofilter model

to cover the IUWS from the catchment down to the effluent of the WRRF. This allowed predicting the dynamics of both water quantity and quality for the entirety of the considered subsystems. It should be noted that quite detailed results throughout the IUWS can be obtained in less than 1 min calculation time per day simulated, including wet weather flow (WWF). Although the model of the case study includes TSS and the WRRF, and not only the water quantity of the sewer system as a detailed hydraulic model would, this model is considerably faster. This characteristic is of crucial importance in view of scenario and uncertainty analysis, as well as optimization questions or global sensitivity analysis (GSA) since all of these require multiple model evaluations.

The practical applicability of the PSVD approach was verified by studying various measures for the reduction of TSS emission towards the receiving water. Made possible by the integrated model, the performance of the measures could be compared and conclusions about the effectiveness of their potential implementation drawn. It was shown that at the level of individual combined sewer overflows, major improvements, up to the complete elimination of overflow during the summer period 2017, can be reached with single measures. The analysis of the total TSS emission over the summer period, however, showed that single measures reduce the emissions only by approximately 5% to 10% compared to the current situation. Nevertheless, combining different measures can lead to an overall flux reduction of 25% to 30% of the reference situation, which allows for approximately 40 t_{TSS} of the current total emission of 138 t_{TSS} to be prevented from reaching the environment in the case study. For two scenarios, compliance with the legislation regarding the total emitted flux through combined sewer overflows (CSO) could be achieved.

While developing the model of the case study, procedures were established which are applicable to a wider range of integrated models and make IM thus generally more feasible. The first procedure proposed governs the development of a conceptual water quantity model from its detailed hydraulic counterpart, making optimal reuse of already available data contained in the detailed model. This procedure provides guidance if a detailed hydraulic model is available and it has to be emulated with a fast running conceptual model. Such a model can be extended with a water quality model, as for the case study, but this is not necessary for the applicability of the procedure. Applying the procedure to two independent case studies (Ottawa, ON, Canada and Bordeaux, France) provided conceptual models with the aimed accuracy at the locations where flow predictions were desired (calibration: $\text{NSE} > 0.8$ and validation: $\text{NSE} > 0.65$), with a reduction of calculation time by a factor of 10 to 80 in comparison to the detailed hydraulic model.

Similarly to the first, the second procedure is also related to the vast amount of data necessary for IM. Thus, a procedure is provided that makes model-based OED applicable to the complex sewer environment. With the explicit use of the measurement error of the installed equipment, the most information-rich location and periods were evaluated. Regarding the location of the

online measurements, NT was confirmed as the optimal of the feasible placements. Regarding the timing of the TSS measurements, it was found that the beginning of rain events is by factors the most relevant time to measure. This finding was also very important from a practical point of view, since a failure of sensors during a rain event is unfortunately common and an intervention in the field to repair the equipment is usually hardly possible due to security restrictions. Hence, it is fortunate that measurements are paramount in the beginning when the sensor is still likely to function well.

The third developed procedure addresses uncertainty and allows including rain variability and parameter uncertainty in the selection of the most effective control handles in the IUWS. This ensures that potential deviations between model and reality do not cause unfortunate management decisions. For the case study it was found that the top three control handles are most likely part of a no-regret selection, since they are ranked high regardless of the rain event chosen or the parameter set analyzed. The procedure, however, also allowed to detect potential regret control handles. Fortunately, the potential regret control handles were generally low-ranked and thus seemed a less reasonable choice, not only due to the potential deviations between model and reality but also due to their potential low impact on the environment, given comparable investments.

Perspectives

The developed integrated model allows estimating the TSS emissions towards the receiving water. In order to directly evaluate the impact, it is suggested to include a river water quality submodel in the model of the case study. This would allow not only evaluating the emission, but tackling the actual immissions (Fronteau et al., 1996; Erbe and Schütze, 2005). In this way, the evaluation of different measures could include the full flexibility and the complexity of IUWS (Benedetti et al., 2008).

A second extension to the developed integrated model is desirable. The sustainability aspect of the model could be broadened by expanding the modelling approach to include more water quality parameters. The developed model allows to predict the transport and fate of solids in the IUWS providing a tool for the protection of the receiving water, which, in the end, serves as a source for drinking water. As mentioned in the Rationale, it fits thus perfectly well with the sustainable development goals. To broaden the sustainability aspects by including, for example, resource recovery, it would be invaluable to include components such as nitrogen and phosphate. This would allow designing measures that close the nutrient cycle by, for example, developing fertilizers from wastewater. This promotes wastewater rather as a resource than a waste (Vaneckhaute et al., 2013). The inclusion of new parameters could, however, go beyond additional water parameters to include further sustainability aspects, such as energy and cost, which seems advantageous when evaluating different measures to improve the receiv-

ing water quality. Energy plays a major role in the aeration of the biological treatment and the pumping activity since these processes consume energy, while anaerobic digestion provides energy. This is, of course, related to cost, respectively revenues. Another process related to cost is the chemical addition which could be optimized as demonstrated by Tik and Vanrolleghem (2017). Incorporating such aspects would thus broaden the sustainability evaluation of different mitigation measures.

Even though the challenge of the tremendous data need of integrated models was addressed, further work in this field is required. Especially in the field of sewers, water quality data are still scarce, which limits not only the model calibration and validation of the case studies, but also limits the development of the modelling approaches itself. For this thesis the PSVD sewer model had to be calibrated and validated with quite scarce data. It would thus be worthwhile to validate it on a comparatively short, but well characterized sewer stretch. This would, for example, allow monitoring particle settling and resuspension in detail and thus further increase the credibility of the approach.

Model uncertainty and the deviation between model and reality were addressed during the selection of the control handles. For a more realistic evaluation, it would, however, also be advantageous to include such reflections during model simulation. As the modelling approach chosen is a deterministic approach, a promising extension could thus be the inclusion of probabilistic components in the model input or in the models themselves. A potential extension to the current modelling approach could, for example, include probabilistic TSS generation characteristics. This would provide more realistic pollution load estimations and thus enhance the evaluation of TSS mitigation measures (Leutnant et al., 2018).

With respect to the case study, perspectives could include further measures to mitigate TSS emissions. A promising development would constitute, for example, the inclusion of water quality based RTC (Erbe et al., 2002; Vanrolleghem et al., 2005b; Tik et al., 2016b; Ly, 2019) or the implementation of a model predictive control that was proven successful in other case studies (Duchesne et al., 2004; Lund et al., 2018).

Generally, it can be concluded that, although considerable progress has been made in the field of IM, further developments are required not only with respect to the submodels, the pollutants considered and the potential measures implemented, but also with respect to data availability and the consideration of potential deviations between model and reality to fully support the sustainable development of the IUWS, as this is and should remain the principal driver of this crucial endeavor.

Appendix A

Tabulated Performance Conceptual Models in Comparison to Detailed Models

Table A.1: Performance Ottawa case study. Calibration and validation results of both the less aggregated (V1) and the maximally aggregated conceptual model (V2) in comparison with the detailed model.

Comp Point	DWF Calibration					WWF Calibration					WWF Validation				
	Average Flow	Peak Flow	PVE	PEP	NSE	Event volume	Peak Flow	PVE	PEP	NSE	Event volume	Peak Flow	PVE	PEP	NSE
	(1/s)	(1/s)	(%)	(%)	(-)	(10 ³ m ³)	(1/s)	(%)	(%)	(-)	(10 ³ m ³)	(1/s)	(%)	(%)	(-)
Ottawa Detailed Model															
Z1	246	307				101	1080				90	880			
Z3	570	683				261	2738				229	2106			
Z4	192	273				98	1239				83	1735			
Z5	112	146				67	805				55	1161			
Z6	683	825				328	3539				284	2628			
Z9	939	1124				459	4708				401	4833			
Z10	977	1171				475	4880				415	4662			
Z12	1230	1499				615	6910				543	7026			
Z15	590	741				314	3684				267	3919			
Z16	645	808				349	4104				295	4202			
Z17	2004	2388				979	8801				879	8251			
Ottawa - Conceptual V1															
Z1	248	323	-1	-5	1.00	107	1080	-6	0	0.97	100	979	-11	-11	0.95
Z3	561	689	2	-1	1.00	268	2738	-3	0	0.99	253	2474	-11	-17	0.97
Z4	191	274	1	-1	0.99	98	1167	1	6	0.96	91	1011	-9	42	0.84
Z5	111	151	1	-3	1.00	66	808	0	0	0.97	55	604	0	48	1.00

Comp Point	DWF Calibration					WWF Calibration					WWF Validation				
	Average Flow (1/s)	Peak Flow (1/s)	PVE (%)	PEP (%)	NSE (-)	Event volume (10 ³ m ³)	Peak Flow (1/s)	PVE (%)	PEP (%)	NSE (-)	Event volume (10 ³ m ³)	Peak Flow (1/s)	PVE (%)	PEP (%)	NSE (-)
Z6	672	837	2	-1	1.00	335	3539	-2	0	0.99	308	3016	-9	-15	0.98
Z9	921	1147	2	-2	1.00	466	4729	-2	0	0.91	436	4753	-9	2	0.88
Z10	956	1194	2	-2	1.00	486	4880	-2	0	0.89	452	4880	-9	-5	0.94
Z12	1198	1504	3	0	1.00	615	6936	0	0	0.96	586	6936	-8	1	0.92
Z15	594	723	-1	2	1.00	320	3779	-2	-3	0.99	289	3530	-8	10	0.95
Z16	654	801	-1	1	1.00	365	4404	-5	-7	0.98	329	4037	-11	4	0.99
Z17	1988	2434	1	-2	1.00	984	8801	-1	0	0.99	944	8801	-7	-7	0.99
Ottawa - Conceptual V2															
Z1	248	325	-1	-6	1.00	106	1080	-4	0	0.97	98	1002	-9	-14	0.87
Z3	555	694	3	-2	1.00	268	2738	-2	0	0.99	251	2433	-10	-16	0.87
Z4	190	271	1	0	1.00	99	1231	-1	1	0.97	91	1029	-10	41	0.68
Z5	111	146	1	0	1.00	68	852	-2	-6	0.98	62	650	-13	44	0.77
Z6	667	831	2	-1	1.00	335	3539	-2	0	0.99	313	3080	-10	-17	0.86
Z9	913	1127	3	0	1.00	467	4643	-2	1	0.95	442	4751	-10	2	0.74
Z10	949	1178	3	-1	1.00	486	4880	-2	0	0.92	458	4880	-10	-5	0.74
Z12	1194	1495	3	0	1.00	615	6936	0	0	0.98	591	6936	-9	1	0.80
Z15	591	725	0	2	1.00	319	3711	-1	-1	0.99	286	3555	-7	9	0.87
Z16	652	803	-1	1	1.00	363	4272	-4	-4	0.99	326	3974	-10	5	0.83
Z17	2003	2444	0	-2	1.00	986	8801	-1	0	0.99	947	8801	-8	-7	0.91

Table A.2: Performance CdH case study. Calibration and validation results of the conceptual model in comparison to the detailed model.

Comp Point	DWF Calibration					WWF Calibration					WWF Validation				
	Average Flow (l/s)	Peak Flow (l/s)	PVE (%)	PEP (%)	NSE (-)	Event volume (10 ³ m ³)	Peak Flow (l/s)	PVE (%)	PEP (%)	NSE (-)	Event volume (10 ³ m ³)	Peak Flow (l/s)	PVE (%)	PEP (%)	NSE (-)
Bordeaux - Detailed															
AB1	42	49				11.74	192.23				14	375			
AB2	60	69				16.35	229.67				19	431			
AB3	142	162				39.81	558.11				46	1072			
AB4	58	67				16.64	274.78				20	538			
AB6	163	186				45.07	581.02				52	1101			
AC1	9	12				3.05	90.37				4	176			
BL1	22	26				6.05	55.64				7	96			
RD1	9	11				3.67	441.28				5	979			
RD4	56	65				21.37	1114.45				30	2608			
RD6	34	39				17.84	1568.53				31	3390			
RG3	124	130				37.51	448.22				42	563			
RG4	163	174				58.36	2470.28				76	4898			
RG5	439	491				119.03	775.66				123	820			
BG1	5	6				2.58	383.10				4	850			
Bordeaux - Conceptual															
AB1	42	48	0	-1	0.98	11.62	200.10	-1	4	0.97	14	491	5	31	0.91
AB2	60	69	0	0	1.00	16.28	241.06	0	5	0.98	20	570	5	32	0.90

Comp Point	DWF Calibration					WWF Calibration					WWF Validation				
	Average Flow	Peak Flow	PVE	PEP	NSE	Event volume	Peak Flow	PVE	PEP	NSE	Event volume	Peak Flow	PVE	PEP	NSE
	(l/s)	(l/s)	(%)	(%)	(-)	(10 ³ m ³)	(l/s)	(%)	(%)	(-)	(10 ³ m ³)	(l/s)	(%)	(%)	(-)
AB3	142	162	0	0	0.97	39.77	559.35	0	0	0.99	49	1316	7	23	0.93
AB4	58	66	0	-1	1.00	16.81	274.88	1	0	0.99	22	667	11	24	0.88
AB6	163	186	0	0	0.97	45.00	579.03	0	0	0.99	55	1334	6	21	0.93
AC1	9	12	0	-4	0.99	2.97	70.00	-3	-23	0.92	4	186	7	6	0.79
BL1	22	26	0	-1	0.99	5.93	58.06	-2	4	0.92	7	124	1	29	0.91
RD1	9	11	1	0	0.91	3.38	434.36	-8	-2	0.96	6	1282	3	31	0.94
RD4	57	67	2	3	0.94	22.06	1226.26	3	10	0.86	35	3266	16	25	0.71
RD6	34	38	-2	-1	0.90	18.29	1671.09	3	7	1.00	36	4747	15	40	0.91
RG3	124	132	0	2	0.84	36.71	450.00	-2	0	0.92	43	450	2	-20	0.72
RG4	163	177	0	2	0.84	57.49	2769.44	-1	12	0.99	83	7271	10	48	0.88
RG5	442	478	1	-2	0.84	118.37	765.85	-1	-1	0.84	123	770	0	-6	0.88
BG1	5	6	0	2	0.89	2.43	396.42	-6	3	0.97	5	1169	11	38	0.89

Appendix B

Tabulated Parameter Values, Calibration and Validation Results

Table B.1: Calibrated water quality parameter values for all the submodels.

Parameter	Description	Value	Unit
<i>Catchment</i>			
$TSS_{DWF,CdH}$	Mean DWF conc. excluding NT	350	mg/l
$TSS_{DWF,NT}$	Mean DWF conc. subcatchment NT	440	mg/l
$TSS_{Ind,CdH}$	Mean conc. infiltration water excluding NT	80	mg/l
$TSS_{Ind,NT}$	Mean conc. infiltration water subcatchment NT	140	mg/l
$TSS_{WWF,CdH}$	Event mean conc. WWF excluding NT	50	mg/l
$TSS_{WWF,NT}$	Event mean conc. WWF subcatchment NT	80	mg/l
<i>Sewer</i>			
$r_{resusp,max,CdH}$	Max. resuspension rate excluding NT	24	d ⁻¹
$r_{resusp,max,NT}$	Max. resuspension rate subcatchment NT	48	d ⁻¹
n_{CdH}	Steepness around Q_{half} excluding NT	4	-
n_{NT}	Steepness around Q_{half} subcatchment NT	8	-
$f_{Qhalf,CdH}$	Factor for Q_{half} as function of max. DWF excluding NT	1.4	-
$f_{Qhalf,NT}$	Factor for Q_{half} as function of max. DWF subcatchment NT	1.5	-
<i>Grit Chamber</i>			
k_d^{5-l}	Factor airflow induced velocity decrease in layer l	0.9	-
Q_{air}	Upstream air flow	4 500	m ³ /d
<i>Primary Clarifier</i>			
A	Projected surface area	6 000	m ²
<i>Biofilter</i>			
RE	Removal efficiency	0.85	-

Table B.2: Detailed calibration results, indicating the root mean square error (RMSE), the relative RMSE (rel. RMSE) with respect to the mean measured value, the mean modelled and the mean measured value over the whole period.

<i>Calibration Day 65 - 75</i>				
Comparison Point	RMSE	rel. RMSE	Mean Flow	
			Model	Meas
Quantity	(m ³ /s)	(%)	(m ³ /s)	(m ³ /s)
CdH total	0.087	12	0.74	0.71
CdH Tributary 1	0.032	12	0.27	0.26
CdH Tributary 2	0.063	16	0.42	0.40
CdH Tributary 3	0.007	19	0.03	0.03
CdH Tributary 4	0.004	21	0.02	0.02
Jourde Outflow	0.022	19	0.11	0.12
Jourde Overflow	0.092	436	0.02	0.02
C. Vernet Outflow	0.034	26	0.14	0.13
Noutary Inflow	0.222	91	0.19	0.24
	RMSE	rel. RMSE	Mean Conc	
Quality	(mg/l)	(%)	Model	Meas
CdH Tributary 2	40	26	170	153
Noutary Inflow	38	22	180	172
PC Out	10	22	43	45
BF Out	2	35	7	7

Table B.3: Detailed validation results, indicating the root mean square error (RMSE), the relative RMSE (rel. RMSE) with respect to the mean measured value, the Janus coefficient (Janus) comparing the RMSE of the validation period with the calibration period, the mean modelled and the mean measured value over the whole period.

<i>Validation 1 Day 8-12</i>					
Comparison Point	RMSE	rel. RMSE	Janus	Mean Flow	
				Model	Meas
Quantity	(m ³ /s)	(%)	(-)	(m ³ /s)	(m ³ /s)
CdH total	0.076	10	0.9	0.73	0.75
CdH Tributary 1	0.024	9	0.8	0.26	0.27
CdH Tributary 2	0.056	13	0.9	0.41	0.43
CdH Tributary 3	0.004	13	0.5	0.03	0.03
CdH Tributary 4	0.004	20	1.1	0.02	0.02
Jourde Outflow	0.023	19	1.0	0.12	0.12
Jourde Overflow	0.010	N/A	0.1	0.00	0.00
C. Vernet Outflow	0.024	17	0.7	0.14	0.14
Noutary Inflow	0.033	19	0.1	0.16	0.18
	RMSE	rel. RMSE	Janus	Mean Conc	
Quality	(mg/l)	(%)	(-)	Model	Meas
CdH Tributary 2	47	24	1.2	175	194
Noutary Inflow	N/A	N/A	N/A	N/A	N/A
PC Out	10	25	1.0	44	39
BF Out	4	50	1.5	7	7
<i>Validation 4 Day 55-67</i>					
Comparison Point	RMSE	rel. RMSE	Janus	Mean Flow	
				Model	Meas
Quantity	(m ³ /s)	(%)	(-)	(m ³ /s)	(m ³ /s)
CdH total	0.108	12	1.2	0.92	0.90
CdH Tributary 1	0.063	19	2.0	0.31	0.33
CdH Tributary 2	0.107	21	1.7	0.55	0.50
CdH Tributary 3	0.014	33	2.2	0.03	0.04
CdH Tributary 4	0.016	48	4.0	0.02	0.03
Jourde Outflow	0.084	68	3.8	0.17	0.12
Jourde Overflow	0.274	114	3.0	0.17	0.24
C. Vernet Outflow	0.053	30	1.6	0.17	0.18
Noutary Inflow	0.167	51	0.7	0.31	0.33
	RMSE	rel. RMSE	Janus	Mean Conc	
Quality	(mg/l)	(%)	(-)	Model	Meas
CdH Tributary 2	50	35	1.3	155	144
Noutary Inflow	N/A	N/A	N/A	N/A	N/A
PC Out	10	23	1.0	43	44
BF Out	4	43	1.7	7	10

Appendix C

Tabulated Results Analysis Scenarios

Table C.1: Evaluation period RE1. The fluxes towards the receiving water are calculated for every scenario at every overflow. The total flux, calculated as the sum of all overflows, is also indicated. The performance of a specific scenario is calculated by dividing the flux of that specific scenario by the flux of the default scenario. A value <1 thus indicates an improvement in comparison to the default scenario.

	Scenario	AR	BT	CV	JR	NT	SA	SE	SJ	TR	BP	BF	Total
Flux (t)	Default	$2.8 \cdot 10^{-3}$	0.21	0.42	1.6	3.1	0.058	0.4	1.2	0.081	0	0.93	8.0
	Q _{NT}	$2.8 \cdot 10^{-3}$	0.21	0.42	1.6	1.9	0.058	0.4	1.2	0.081	0	0.99	6.8
	Q _{CV}	$2.8 \cdot 10^{-3}$	0.21	0	1.6	3.1	0.058	0.4	1.2	0.081	0	0.96	7.6
	Q _{JR}	$2.8 \cdot 10^{-3}$	0.21	0.42	0.97	3.1	0.058	0.4	1.2	0.081	0	0.98	7.4
	Q _{SA}	$2.8 \cdot 10^{-3}$	0.21	0.42	1.6	2.2	0.51	0.4	1.2	0.081	0	0.93	7.6
	Q _{NT,SA}	$2.8 \cdot 10^{-3}$	0.21	0.42	1.6	1.1	0.51	0.4	1.2	0.081	0	0.99	6.5
	Q*	$2.8 \cdot 10^{-3}$	0.21	0	0.97	1.1	0.51	0.4	1.2	0.081	0	1.1	5.6
	RT ₃	$2.8 \cdot 10^{-3}$	0.21	0.42	1.3	2.8	0.058	0.4	1.2	0.081	0	0.94	7.5
	RT ₂	$2.8 \cdot 10^{-3}$	0.21	0.42	1.2	2.8	0.058	0.4	1.2	0.081	0	0.94	7.4
	Q*&RT ₂	$2.8 \cdot 10^{-3}$	0.21	0	0.61	0.91	0.51	0.4	1.2	0.081	0	1.1	5.0
Perf (-)	Q _{NT}	0.99	1.0	1.0	1.0	0.6	1.0	1.0	1.0	1.0	N/A	1.1	0.85
	Q _{CV}	1.0	1.0	0	1.0	1.0	1.0	1.0	1.0	1.0	N/A	1.0	0.95
	Q _{JR}	0.99	1.0	1.0	0.6	1.0	1.0	1.0	1.0	1.0	N/A	1.1	0.93
	Q _{SA}	0.99	1.0	1.0	1.0	0.72	8.8	1.0	1.0	1.0	N/A	1.0	0.95
	Q _{NT,SA}	0.99	1.0	1.0	1.0	0.36	8.8	1.0	1.0	1.0	N/A	1.1	0.82
	Q*	1.0	1.0	0	0.6	0.36	8.8	1.0	1.0	1.0	N/A	1.2	0.7
	RT ₃	0.99	1.0	1.0	0.84	0.92	1.0	1.0	1.0	1.0	N/A	1.0	0.94
	RT ₂	0.99	1.0	1.0	0.75	0.92	1.0	1.0	1.0	1.0	N/A	1.0	0.92
	Q*&RT ₂	0.99	1.0	0	0.38	0.29	8.8	1.0	1.0	1.0	N/A	1.2	0.63

Table C.2: Evaluation period RE2. The fluxes towards the receiving water are calculated for every scenario at every overflow. The total flux, calculated as the sum of all overflows, is also indicated. The performance of a specific scenario is calculated by dividing the flux of that specific scenario by the flux of the default scenario. A value <1 thus indicates an improvement in comparison to the default scenario.

	Scenario	AR	BT	CV	JR	NT	SA	SE	SJ	TR	BP	BF	Total
Flux (t)	Default	0.047	0.5	0.77	3.9	5.8	0.4	1.2	3.6	0.25	0	1.6	18.0
	Q _{NT}	0.047	0.5	0.77	3.9	3.9	0.4	1.2	3.6	0.25	0	1.7	16.0
	Q _{CV}	0.047	0.5	0	3.9	5.8	0.4	1.2	3.6	0.25	0	1.6	17.0
	Q _{JR}	0.047	0.5	0.77	2.5	5.8	0.4	1.2	3.6	0.25	0	1.7	17.0
	Q _{SA}	0.047	0.5	0.77	3.9	4.3	1.3	1.2	3.6	0.25	0	1.6	17.0
	Q _{NT,SA}	0.047	0.5	0.77	3.9	2.4	1.3	1.2	3.6	0.25	0	1.7	16.0
	Q*	0.047	0.5	0	2.5	2.4	1.3	1.2	3.6	0.25	0	1.9	14.0
	RT ₃	0.047	0.5	0.77	3.2	5.3	0.4	1.2	3.6	0.25	0	1.6	17.0
	RT ₂	0.048	0.5	0.77	2.8	5.3	0.4	1.2	3.6	0.25	0	1.6	17.0
	Q*&RT ₂	0.047	0.5	0	1.5	2.0	1.3	1.2	3.6	0.25	0	1.9	12.0
Perf (-)	Q _{NT}	1.0	1.0	1.0	1.0	0.66	1.0	1.0	1.0	1.0	N/A	1.1	0.9
	Q _{CV}	1.0	1.0	0	1.0	1.0	1.0	1.0	1.0	1.0	N/A	1.0	0.96
	Q _{JR}	1.0	1.0	1.0	0.64	1.0	1.0	1.0	1.0	1.0	N/A	1.1	0.93
	Q _{SA}	1.0	1.0	1.0	1.0	0.74	3.2	1.0	1.0	1.0	N/A	1.0	0.96
	Q _{NT,SA}	1.0	1.0	1.0	1.0	0.42	3.2	1.0	1.0	1.0	N/A	1.1	0.87
	Q*	1.0	1.0	0	0.64	0.42	3.2	1.0	1.0	1.0	N/A	1.2	0.76
	RT ₃	1.0	1.0	1.0	0.82	0.92	1.0	1.0	1.0	1.0	N/A	1.0	0.93
	RT ₂	1.0	1.0	1.0	0.74	0.92	1.0	1.0	1.0	1.0	N/A	1.0	0.92
	Q*&RT ₂	1.0	1.0	0	0.4	0.35	3.2	1.0	1.0	1.0	N/A	1.2	0.68

Table C.3: Evaluation period RE3. The fluxes towards the receiving water are calculated for every scenario at every overflow. The total flux, calculated as the sum of all overflows, is also indicated. The performance of a specific scenario is calculated by dividing the flux of that specific scenario by the flux of the default scenario. A value <1 thus indicates an improvement in comparison to the default scenario.

	Scenario	AR	BT	CV	JR	NT	SA	SE	SJ	TR	BP	BF	Total
Flux (t)	Default	0	0.041	0.01	0	0.91	$6.1 \cdot 10^{-3}$	0	0.022	0	0	0.26	1.3
	Q _{NT}	0	0.041	0.01	0	0.13	$6.1 \cdot 10^{-3}$	0	0.022	0	0	0.29	0.5
	Q _{CV}	0	0.041	0	0	0.92	$6.1 \cdot 10^{-3}$	0	0.022	0	0	0.26	1.2
	Q _{JR}	0	0.041	0.01	0	0.92	$6.1 \cdot 10^{-3}$	0	0.022	0	0	0.26	1.3
	Q _{SA}	0	0.041	0.01	0	0	0.25	0	0.022	0	0	0.26	0.59
	Q _{NT,SA}	0	0.041	0.01	0	0	0.25	0	0.022	0	0	0.26	0.59
	Q*	0	0.041	0	0	0	0.25	0	0.022	0	0	0.26	0.58
	RT ₃	0	0.041	0.01	0	0.91	$6.1 \cdot 10^{-3}$	0	0.022	0	0	0.26	1.3
	RT ₂	0	0.041	0.01	0	0.91	$6.1 \cdot 10^{-3}$	0	0.022	0	0	0.26	1.3
	Q*&RT ₂	0	0.041	0	0	0	0.25	0	0.022	0	0	0.26	0.58
Perf (-)	Q _{NT}	N/A	1.0	1.0	N/A	0.14	1.0	N/A	1.0	N/A	N/A	1.1	0.4
	Q _{CV}	N/A	1.0	0	N/A	1.0	1.0	N/A	1.0	N/A	N/A	1.0	0.99
	Q _{JR}	N/A	1.0	1.0	N/A	1.0	1.0	N/A	1.0	N/A	N/A	1.0	1.0
	Q _{SA}	N/A	1.0	1.0	N/A	0	41.0	N/A	1.0	N/A	N/A	1.0	0.47
	Q _{NT,SA}	N/A	1.0	1.0	N/A	0	41.0	N/A	1.0	N/A	N/A	1.0	0.47
	Q*	N/A	1.0	0	N/A	0	41.0	N/A	1.0	N/A	N/A	1.0	0.46
	RT ₃	N/A	1.0	1.0	N/A	1.0	1.0	N/A	1.0	N/A	N/A	1.0	1.0
	RT ₂	N/A	1.0	1.0	N/A	1.0	1.0	N/A	1.0	N/A	N/A	1.0	1.0
	Q*&RT ₂	N/A	1.0	0	N/A	0	41.0	N/A	1.0	N/A	N/A	1.0	0.46

Table C.4: Evaluation period RE4. The fluxes towards the receiving water are calculated for every scenario at every overflow. The total flux, calculated as the sum of all overflows, is also indicated. The performance of a specific scenario is calculated by dividing the flux of that specific scenario by the flux of the default scenario. A value <1 thus indicates an improvement in comparison to the default scenario.

	Scenario	AR	BT	CV	JR	NT	SA	SE	SJ	TR	BP	BF	Total
Flux (t)	Default	0.15	1.7	2.1	13.0	14.0	1.8	5.2	16.0	1.3	0.069	3.3	59.0
	Q _{NT}	0.15	1.7	2.1	13.0	9.4	1.8	5.2	16.0	1.3	0.16	3.5	55.0
	Q _{CV}	0.15	1.7	0	13.0	14.0	1.8	5.2	16.0	1.3	0.12	3.4	57.0
	Q _{JR}	0.15	1.7	2.1	10.0	14.0	1.8	5.2	16.0	1.3	0.14	3.5	56.0
	Q _{SA}	0.15	1.7	2.1	13.0	11.0	4.7	5.2	16.0	1.3	0.069	3.2	58.0
	Q _{NT,SA}	0.15	1.7	2.1	13.0	6.1	4.7	5.2	16.0	1.3	0.16	3.5	54.0
	Q*	0.15	1.7	0	10.0	6.0	4.7	5.2	16.0	1.3	0.33	3.9	50.0
	RT ₃	0.15	1.7	2.1	11.0	13.0	1.8	5.2	16.0	1.3	0.069	3.2	55.0
	RT ₂	0.15	1.7	2.1	11.0	13.0	1.8	5.2	16.0	1.3	0.068	3.2	55.0
	Q*&RT ₂	0.15	1.7	0	8.0	5.2	4.7	5.2	16.0	1.3	0.33	3.9	46.0
Perf (-)	Q _{NT}	1.0	1.0	1.0	1.0	0.67	1.0	1.0	1.0	1.0	2.4	1.1	0.93
	Q _{CV}	1.0	1.0	0	1.0	1.0	1.0	1.0	1.0	1.0	1.8	1.1	0.97
	Q _{JR}	1.0	1.0	1.0	0.78	1.0	1.0	1.0	1.0	1.0	2.0	1.1	0.96
	Q _{SA}	1.0	1.0	1.0	1.0	0.77	2.6	1.0	1.0	1.0	1.0	1.0	0.99
	Q _{NT,SA}	1.0	1.0	1.0	1.0	0.43	2.6	1.0	1.0	1.0	2.4	1.1	0.92
	Q*	1.0	1.0	0	0.78	0.43	2.6	1.0	1.0	1.0	4.8	1.2	0.84
	RT ₃	1.0	1.0	1.0	0.83	0.92	1.0	1.0	1.0	1.0	1.0	1.0	0.94
	RT ₂	1.0	1.0	1.0	0.82	0.92	1.0	1.0	1.0	1.0	1.0	1.0	0.94
	Q*&RT ₂	1.0	1.0	0	0.6	0.37	2.6	1.0	1.0	1.0	4.8	1.2	0.79

Table C.5: Evaluation period RE5. The fluxes towards the receiving water are calculated for every scenario at every overflow. The total flux, calculated as the sum of all overflows, is also indicated. The performance of a specific scenario is calculated by dividing the flux of that specific scenario by the flux of the default scenario. A value <1 thus indicates an improvement in comparison to the default scenario.

	Scenario	AR	BT	CV	JR	NT	SA	SE	SJ	TR	BP	BF	Total
Flux (t)	Default	0	0.076	0.14	0.67	1.0	0	0.1	0.31	$9.4 \cdot 10^{-3}$	0	0.34	2.7
	Q _{NT}	0	0.076	0.14	0.67	0.073	0	0.1	0.31	$9.4 \cdot 10^{-3}$	0	0.38	1.8
	Q _{CV}	0	0.076	0	0.67	1.0	0	0.1	0.31	$9.4 \cdot 10^{-3}$	0	0.35	2.5
	Q _{JR}	0	0.076	0.14	0.17	1.0	0	0.1	0.31	$9.4 \cdot 10^{-3}$	0	0.38	2.2
	Q _{SA}	0	0.076	0.14	0.67	0.84	0.046	0.1	0.31	$9.4 \cdot 10^{-3}$	0	0.35	2.5
	Q _{NT,SA}	0	0.076	0.14	0.67	0	0.046	0.1	0.31	$9.4 \cdot 10^{-3}$	0	0.38	1.7
	Q*	0	0.076	0	0.17	0	0.046	0.1	0.31	$9.4 \cdot 10^{-3}$	0	0.42	1.1
	RT ₃	0	0.076	0.14	0.63	0.91	0	0.1	0.31	$9.4 \cdot 10^{-3}$	0	0.35	2.5
	RT ₂	0	0.076	0.14	0.53	0.91	0	0.1	0.31	$9.4 \cdot 10^{-3}$	0	0.35	2.4
	Q*&RT ₂	0	0.076	0	0.075	0	0.046	0.1	0.31	$9.4 \cdot 10^{-3}$	0	0.42	1.0
Perf (-)	Q _{NT}	N/A	1.0	1.0	1.0	0.073	N/A	1.0	1.0	1.0	N/A	1.1	0.66
	Q _{CV}	N/A	1.0	0	1.0	1.0	N/A	1.0	1.0	1.0	N/A	1.0	0.95
	Q _{JR}	N/A	1.0	1.0	0.26	1.0	N/A	1.0	1.0	1.0	N/A	1.1	0.83
	Q _{SA}	N/A	1.0	1.0	1.0	0.84	N/A	1.0	1.0	1.0	N/A	1.0	0.96
	Q _{NT,SA}	N/A	1.0	1.0	1.0	0	N/A	1.0	1.0	1.0	N/A	1.1	0.65
	Q*	N/A	1.0	0	0.26	0	N/A	1.0	1.0	1.0	N/A	1.2	0.43
	RT ₃	N/A	1.0	1.0	0.94	0.91	N/A	1.0	1.0	1.0	N/A	1.0	0.95
	RT ₂	N/A	1.0	1.0	0.79	0.91	N/A	1.0	1.0	1.0	N/A	1.0	0.91
	Q*&RT ₂	N/A	1.0	0	0.11	0	N/A	1.0	1.0	1.0	N/A	1.2	0.39

Table C.6: Evaluation period 120d. The fluxes towards the receiving water are calculated for every scenario at every overflow. The total flux, calculated as the sum of all overflows, is also indicated. The performance of a specific scenario is calculated by dividing the flux of that specific scenario by the flux of the default scenario. A value <1 thus indicates an improvement in comparison to the default scenario.

	Scenario	AR	BT	CV	JR	NT	SA	SE	SJ	TR	BP	BF	Total
Flux (t)	Default	0.281	4.02	5.46	30.6	43.0	2.55	8.88	27.5	2.02	0.0686	12.1	136.0
	Q _{NT}	0.281	4.02	5.46	30.6	26.4	2.55	8.88	27.5	2.02	0.162	12.9	121.0
	Q _{CV}	0.281	4.02	0	30.6	43.0	2.55	8.88	27.5	2.02	0.123	12.5	131.0
	Q _{JR}	0.281	4.02	5.46	20.7	43.0	2.55	8.88	27.5	2.02	0.14	12.8	127.0
	Q _{SA}	0.281	4.02	5.46	30.6	31.4	8.55	8.88	27.5	2.02	0.0688	12.1	131.0
	Q _{NT,SA}	0.281	4.02	5.46	30.6	17.7	8.55	8.88	27.5	2.02	0.162	12.8	118.0
	Q*	0.281	4.02	0	20.8	17.7	8.55	8.88	27.5	2.02	0.333	13.9	104.0
	RT ₃	0.281	4.02	5.46	25.4	39.3	2.55	8.88	27.5	2.02	0.0687	12.1	128.0
	RT ₂	0.281	4.02	5.46	23.6	39.3	2.55	8.88	27.5	2.02	0.0685	12.1	126.0
	Q*&RT ₂	0.281	4.02	0	14.3	14.8	8.55	8.88	27.5	2.02	0.333	13.9	94.6
Perf (-)	Q _{NT}	1.0	1.0	1.0	1.0	0.614	1.0	1.0	1.0	1.0	2.36	1.07	0.885
	Q _{CV}	1.0	1.0	0	1.0	1.0	1.0	1.0	1.0	1.0	1.79	1.03	0.963
	Q _{JR}	1.0	1.0	1.0	0.679	1.0	1.0	1.0	1.0	1.0	2.03	1.06	0.934
	Q _{SA}	1.0	1.0	1.0	1.0	0.73	3.36	1.0	1.0	1.0	1.0	1.0	0.959
	Q _{NT,SA}	1.0	1.0	1.0	1.0	0.411	3.36	1.0	1.0	1.0	2.35	1.06	0.864
	Q*	1.0	1.0	0	0.679	0.411	3.36	1.0	1.0	1.0	4.85	1.15	0.762
	RT ₃	1.0	1.0	1.0	0.829	0.914	1.0	1.0	1.0	1.0	1.0	1.0	0.935
	RT ₂	1.0	1.0	1.0	0.772	0.914	1.0	1.0	1.0	1.0	0.998	1.0	0.922
	Q*&RT ₂	1.0	1.0	0	0.467	0.345	3.36	1.0	1.0	1.0	4.85	1.15	0.693

Bibliography

- Achleitner, S., Möderl, M., and Rauch, W. (2007). CITY DRAIN[©] - An open source approach for simulation of integrated urban drainage systems. *Environ. Model. Softw.*, 22(8):1184–1195.
- Ahyerre, M. and Chebbo, G. (2002). Identification of in-sewer sources of organic solids contributing to combined sewer overflows. *Environ. Technol.*, 23(9):1063–1073.
- Alferes, J., Poirier, P., Lamarie-Chad, C., Sharma, A. K., Mikkelsen, P. S., and Vanrolleghem, P. A. (2013a). Data quality assurance in monitoring of wastewater quality: Univariate on-line and off-line methods. In *Proceedings of the 11th IWA Conference on Instrumentation, Control and Automation ICA 2013*, Narbonne, France, September 18-20 2013.
- Alferes, J., Tik, S., Copp, J., and Vanrolleghem, P. A. (2013b). Advanced monitoring of water systems using in situ measurement stations: Data validation and fault detection. *Water Sci. Technol.*, 68(5):1022–1030.
- Andréa, G., Ahyerre, M., Pleau, M., Pérarnaud, J.-J., Komorowski, F., and Schoorens, J. (2013). Louis Fargue catchment area in Bordeaux - real time control of CSO's: Implementation and first operational results. In *Proceedings of the 8th International Conference NOVATECH*, Lyon, France, June 23-27 2013.
- Ashley, R. M., Arthur, S., Coghlan, B. P., and McGregor, I. (1994). Fluid sediment in combined sewers. *Water Sci. Technol.*, 29(1–2):113–123.
- Ashley, R. M., Bertrand-Krajewski, J.-L., Hvitved-Jacobsen, T., and Verbanck, M. (2004). *Solids in Sewers – Characteristics, Effects and Control of Sewer Solids and Associated Pollutants*. Number 14. IWA Publishing, London, U.K.
- Bach, P. M., Rauch, W., Mikkelsen, P. S., McCarthy, D. T., and Deletic, A. (2014). A critical review of integrated urban water modelling – Urban drainage and beyond. *Environ. Model. Softw.*, 54:88–107.
- Bachis, G., Maruéjols, T., Tik, S., Amerlinck, Y., Melcer, H., Nopens, I., Lessard, P., and Vanrolleghem, P. A. (2015). Modelling and characterization of primary settlers in view of whole plant and resource recovery modelling. *Water Sci. Technol.*, 72(12):2251–2261.

- Bauwens, W., Vanrolleghem, P. A., and Smeets, M. (1996). An evaluation of the efficiency of the combined sewer - wastewater treatment system under transient conditions. *Water Sci. Technol.*, 33(2):199–208.
- Beck, M. B. (1976). Dynamic modelling and control applications in water quality maintenance. *Water Res.*, 10(7):575–595.
- Beck, M. B. (1981). *Operational Water Quality Management: Beyond Planning and Design*. International Institute for Applied Systems Analysis, Laxenburg, Austria.
- Beck, M. B. (1987). Water quality modeling: A review of the analysis of uncertainty. *Water Resour. Res.*, 23(8):1393–1442.
- Beck, M. B., Adeloje, A. J., Finney, B. A., and Lessard, P. (1991). Operational water quality management: Transient events and seasonal variability. *Water Sci. Technol.*, 24(6):257–265.
- Beck, M. B. and Reda, A. (1994). Identification and application of a dynamic model for operational management of water quality. *Water Sci. Technol.*, 30(2):0.
- Belia, E., Amerlinck, Y., Benedetti, L., Johnson, B., Sin, G., Vanrolleghem, P. A., Gernaey, K. V., Gillot, S., Neumann, M. B., Rieger, L., Shaw, A., and Villez, K. (2009). Wastewater treatment modelling: Dealing with uncertainties. *Water Sci. Technol.*, 60(8):1929–1941.
- Benedetti, L., Batstone, D. J., De Baets, B., Nopens, I., and Vanrolleghem, P. A. (2012). Uncertainty analysis of WWTP control strategies made feasible. *Water Qual. Res. J. Can.*, 47(1):14–29.
- Benedetti, L., Bixio, D., Claeys, F., and Vanrolleghem, P. A. (2008). Tools to support a model-based methodology for emission/immission and benefit/cost/risk analysis of wastewater systems that considers uncertainty. *Environ. Model. Softw.*, 23(8):1082–1091.
- Benedetti, L., Langeveld, J., Comeau, A., Corominas, L., Daigger, G., Martin, C., Mikkelsen, P. S., Vezzaro, L., Weijers, S., and Vanrolleghem, P. A. (2013a). Modelling and monitoring of integrated urban wastewater systems: Review on status and perspectives. *Water Sci. Technol.*, 68(6):1203–1215.
- Benedetti, L., Langeveld, J., van Nieuwenhuijzen, A. F., de Jonge, J., de Klein, J., Flameling, T., Nopens, I., van Zanten, O., and Weijers, S. (2013b). Cost-effective solutions for water quality improvement in the Dommel river supported by sewer-WWTP-river integrated modelling. *Water Sci. Technol.*, 68(5):965–973.
- Benedetti, L., Meirlaen, J., and Vanrolleghem, P. A. (2004). Model connectors for integrated simulations of urban wastewater systems. In Bertrand-Krajewski, J.-L., Almeida, M.,

- Matos, J., and Abdul-Talib, S., editors, *Sewer Networks and Processes within Urban Water Systems*, pages 13–21, IWA Publishing, London, UK.
- Bennett, N. D., Croke, B. F., Guariso, G., Guillaume, J. H., Hamilton, S. H., Jakeman, A. J., Marsili-Libelli, S., Newham, L. T., Norton, J. P., Perrin, C., Pierce, S. A., Robson, B., Seppelt, R., Voinov, A. A., Fath, B. D., and Andreassian, V. (2013). Characterising performance of environmental models. *Environ. Model. Softw.*, 40:1–20.
- Berrouard, E. (2010). Caractérisation de la décantabilité des eaux pluviales. Master’s thesis, Université Laval, Québec, QC, Canada.
- Bertrand-Krajewski, J.-L. (2007). Stormwater pollutant loads modelling: Epistemological aspects and case studies on the influence of field data sets on calibration and verification. *Water Sci. Technol.*, 55(4):1–17.
- Bertrand-Krajewski, J.-L., Chebbo, G., and Saget, A. (1998). Distribution of pollutant mass vs volume in stormwater discharges and the first flush phenomenon. *Water Res.*, 32(8):2341–2356.
- Bilodeau, K., Pelletier, G., and Duchesne, S. (2018). Real-time control of stormwater detention basins as an adaptation measure in mid-size cities. *Urban Water J.*, 15(9):858–867.
- Blöch, H. (1999). The European Union Water Framework Directive: Taking European water policy into the next millennium. *Water Sci. Technol.*, 40(10):67–71.
- Blumensaat, F., Stauer, P., Heusch, S., Reußner, F., Schütze, M., Seiffert, S., Gruber, G., Zawilski, M., and Rieckermann, J. (2012). Water quality-based assessment of urban drainage impacts in Europe - where do we stand today? *Water Sci. Technol.*, 66(2):304–313.
- Blumensaat, F., Tränckner, J., Hoefft, S., Jardin, N., and Krebs, P. (2009). Quantifying effects of interacting optimisation measures in urban drainage systems. *Urban Water J.*, 6(2):93–105.
- “Bordeaux” (2019). Wikipedia. Retrieved October 04, 2019, from <https://fr.wikipedia.org/wiki/Bordeaux>.
- Butler, D. and Schütze, M. (2005). Integrating simulation models with a view to optimal control of urban wastewater systems. *Environ. Model. Softw.*, 20(4):415–426.
- CCME (2009). Canada-wide Strategy for the Management of Municipal Wastewater Effluent.
- CEC (2000). Directive 2000/60/EC of the European Parliament and of the Council of 23 October 2000 establishing a framework for Community action in the field of water policy. *Official Journal of the European Communities*, 43(L 327):1–73.

- Chancelier, J. P., Chebbo, G., and Lucas-Aiguier, E. (1998). Estimation of settling velocities. *Water Res.*, 32(11):3461–3471.
- Chebbo, G. and Gromaire, M.-C. (2009). VICAS – An operating protocol to measure the distributions of suspended solid settling velocities within urban drainage samples. *J. Environ. Eng.*, 135(9):768–775.
- Cherqui, F., Belmeziti, A., Granger, D., Sourdril, A., and Gauffre, P. L. (2015). Assessing urban potential flooding risk and identifying effective risk-reduction measures. *Sci. Total Environ.*, 514:418–425.
- Copp, J. B., editor (2002). *The COST Simulation Benchmark: Description and Simulator Manual*. Office for Official Publications of the European Communities, Luxembuorg.
- Corominas, L. and Neumann, M. B. (2014). Ecosystem-based management of a mediterranean urban wastewater system: A sensitivity analysis of the operational degrees of freedom. *J. Environ. Manage.*, 143:80–87.
- Cosenza, A., Mannina, G., Vanrolleghem, P. A., and Neumann, M. B. (2013). Global sensitivity analysis in wastewater applications: A comprehensive comparison of different methods. *Environ. Model. Softw.*, 49:40–52.
- Davidson, S., Löwe, R., Thrysoe, C., and Arnbjerg-Nielsen, K. (2017). Simplification of one-dimensional hydraulic networks by automated processes evaluated on 1D/2D deterministic flood models. *J. Hydroinform.*, 19(5):686–700.
- De Pauw, D. J. W. and Vanrolleghem, P. A. (2006a). Designing and performing experiments for model calibration using an automated iterative procedure. *Water Sci. Technol.*, 53(1):117–127.
- De Pauw, D. J. W. and Vanrolleghem, P. A. (2006b). Practical aspects of sensitivity function approximation for dynamic models. *Math. Comput. Modell. Dyn. Syst.*, 12(5):395–414.
- Deletic, A., Dotto, C., McCarthy, D., Kleidorfer, M., Freni, G., Mannina, G., Uhl, M., Heinrichs, M., Fletcher, T., Rauch, W., Bertrand-Krajewski, J.-L., and Tait, S. (2012). Assessing uncertainties in urban drainage models. *Phys. Chem. Earth*, 42-44:3–10.
- Devesa, F., Comas, J., Turon, C., Freixó, A., Carrasco, F., and Poch, M. (2009). Scenario analysis for the role of sanitation infrastructures in integrated urban wastewater management. *Environ. Model. Softw.*, 24(3):371–380.
- Dochain, D. and Vanrolleghem, P. A. (2001). *Dynamical Modelling and Estimation in Wastewater Treatment Processes*. IWA Publishing, London, UK.

- Dominguez, D. and Gujer, W. (2006). Evolution of a wastewater treatment plant challenges traditional design concepts. *Water Res.*, 40(7):1389–1396.
- Dong, X., Zeng, S., Chen, J., and Zhao, D. (2012). An integrated urban drainage system model for assessing renovation scheme. *Water Sci. Technol.*, 65(10):1781–1788.
- Duchesne, S., Beck, M. B., and Reda, A. L. (2001). Ranking stormwater control strategies under uncertainty: The River Cam case study. *Water Sci. Technol.*, 43(7):311–320.
- Duchesne, S., Mailhot, A., and Villeneuve, J. (2004). Global predictive real-time control of sewers allowing surcharged flows. *J. Environ. Eng.*, 130(5):526–534.
- EPA (2002). Federal Water Pollution Control Act (Clean Water Act).
- Erbe, V., Frehmann, T., Geiger, W. F., Krebs, P., Londong, J., Rosenwinkel, K.-H., and Seggelke, K. (2002). Integrated modelling as an analytical and optimisation tool for urban watershed management. *Water Sci. Technol.*, 46(6-7):141–150.
- Erbe, V. and Schütze, M. (2005). An integrated modelling concept for immission-based management of sewer system, wastewater treatment plant and river. *Water Sci. Technol.*, 52(5):95–103.
- Euler, G. (1983). Ein hydrologisches Näherungsverfahren für die Berechnung des Wellenablaufs in Kreisrohren. *Wasser und Boden*, (Heft 2):85–88 (in German).
- Exall, K., Marsalek, J., and Krishnappan, B. G. (2009). Hydraulic fractionation of conventional water quality constituents in municipal dry- and wet-weather flow samples. *Water Sci. Technol.*, 59(6):1159–1167.
- Freni, G., Maglionico, M., Mannina, G., and Viviani, G. (2008). Comparison between a detailed and a simplified integrated model for the assessment of urban drainage environmental impact on an ephemeral river. *Urban Water J.*, 5(2):87–96.
- Freni, G. and Mannina, G. (2012). The identifiability analysis for setting up measuring campaigns in integrated water quality modelling. *Phys. Chem. Earth*, 42-44:52–60.
- Freni, G., Mannina, G., and Viviani, G. (2011). Assessment of the integrated urban water quality model complexity through identifiability analysis. *Water Res.*, 45(1):37–50.
- Friedler, E., Brown, D. M., and Butler, D. (1996). A study of WC derived sewer solids. *Water Sci. Technol.*, 33(9):17–24.
- Fronteau, C., Bauwens, W., and Vanrolleghem, P. (1997). Integrated modelling: Comparison of state variables, processes and parameters in sewer and wastewater treatment plant models. *Water Sci. Technol.*, 36(5):373–380.

- Fronteau, C., Bauwens, W., Vanrolleghem, P., and Smeets, M. (1996). An immission based evaluation of the efficiency of the sewer-WWTP-river system under transient conditions. In *Proceedings of the 7th International Conference on Urban Storm Drainage*, pages 9–13, Hannover, Germany, September 9-13, 1996.
- Fryd, O., Jensen, M. B., Ingvertsen, S. T., Jeppesen, J., and Magid, J. (2010). Doing the first loop of planning for sustainable urban drainage system retrofits: A case study from Odense, Denmark. *Urban Water J.*, 7(6):367–378.
- Gamerith, V., Neumann, M. B., and Muschalla, D. (2013). Applying global sensitivity analysis to the modelling of flow and water quality in sewers. *Water Res.*, 47(13):4600–4611.
- “Garonne” (2019). Wikipedia. Retrieved October 04, 2019, from <https://fr.wikipedia.org/wiki/Garonne>.
- Gernaey, K. V., van Loosdrecht, M. C., Henze, M., Lind, M., and Jørgensen, S. B. (2004). Activated sludge wastewater treatment plant modelling and simulation: state of the art. *Environ. Model. Softw.*, 19(9):763–783.
- Gujer, W., Krejci, V., Schwarzenbach, R., and Zobrist, J. (1982). Von der Kanalisation ins Grundwasser – Charakterisierung eines Regenereignisses im Glattal. *Gas-Wasser-Abwasser*, 62(7):298–311 (in German).
- Guo, L., Tik, S., Ledergerber, J. M., Santoro, D., Elbeshbishy, E., and Vanrolleghem, P. A. (2019). Conceptualizing the sewage collection system for integrated sewer-WWTP modelling and optimization. *J. Hydrol.*, 573:710–716.
- Gustafsson, L.-G., Lumley, D. J., Lindeborg, C., and Haraldsson, J. (1993). Integrating a catchment simulator into wastewater treatment plant operation. *Water Sci. Technol.*, 28(11-12):45–54.
- Haboub, K., Zhu, X., Maruéjols, T., Bertrand-Krajewski, J.-L., and Vanrolleghem, P. (2019). A new approach of measuring TSS settling velocity based on turbidity measurements. In *Proceedings of the 9th International Conference on Sewer Processes and Networks (SPN)*, Aalborg, Denmark, August 27-31 2019.
- Harremoës, P. and Rauch, W. (1996). Integrated design and analysis of drainage systems, including sewers, treatment plant and receiving waters. *J. Hydraul. Res.*, 34(6):815–826.
- Hauduc, H., Neumann, M., Muschalla, D., Gamerith, V., Gillot, S., and Vanrolleghem, P. A. (2015). Efficiency criteria for environmental model quality assessment: A review and its application to wastewater treatment. *Environ. Model. Softw.*, 68:196–204.

- Henze, M., Gujer, W., Mino, T., and van Loosedrecht, M. (2006). *Activated Sludge Models ASM1, ASM2, ASM2d and ASM3*. Scientific and Technical Report. IWA Publishing, London, UK.
- Holzer, P. and Krebs, P. (1998). Modelling the total ammonia impact of CSO and WWTP effluent on the receiving water. *Water Sci. Technol.*, 38(10):31–39.
- Jefferies, C. and Ashley, R. M. (1994). Gross solids in sewer systems: Temporal and catchment based relationships. *Water Sci. Technol.*, 30(1):63–71.
- JORF (2015). Arrêté du 21 juillet 2015 relatif aux systèmes d’assainissement collectif et aux installations d’assainissement non collectif, à l’exception des installations d’assainissement non collectif recevant une charge brute de pollution organique inférieure ou égale à 1,2 kg/j de DBO₅. Journal Officiel de la République Française (in French).
- Krebs, P., Holzer, P., Huisman, J. L., and Rauch, W. (1999). First flush of dissolved compounds. *Water Sci. Technol.*, 39(9):55–62.
- Kroll, S., Fenu, A., Wambecq, T., Weemaes, M., Impe, J. V., and Willems, P. (2018). Energy optimization of the urban drainage system by integrated real-time control during wet and dry weather conditions. *Urban Water J.*, 15(4):362–370.
- Kroll, S., Wambecq, T., Weemaes, M., Impe, J. V., and Willems, P. (2017). Semi-automated buildup and calibration of conceptual sewer models. *Environ. Model. Softw.*, 93:344–355.
- Langeveld, J., Clemens, F., and van der Graaf, J. (2002). Increasing wastewater system performance – the importance of interactions between sewerage and wastewater treatment. *Water Sci. Technol.*, 45(3):45–52.
- Langeveld, J., Nopens, I., Schilperoort, R., Benedetti, L., de Klein, J., Amerlinck, Y., and Weijers, S. (2013a). On data requirements for calibration of integrated models for urban water systems. *Water Sci. Technol.*, 68(3):728–736.
- Langeveld, J. G., Benedetti, L., de Klein, J. J. M., Nopens, I., Amerlinck, Y., van Nieuwenhuijzen, A., Flameling, T., van Zanten, O., and Weijers, S. (2013b). Impact-based integrated real-time control for improvement of the Dommel river water quality. *Urban Water J.*, 10(5):312–329.
- Lau, J., Butler, D., and Schütze, M. (2002). Is combined sewer overflow spill frequency/volume a good indicator of receiving water quality impact? *Urban Water*, 4(2):181–189.
- Le LyRE (2016). QualiDO – Evaluation de la qualité des rejets du bassin versant Louis Fargue. Technical report, Le LyRE, Bordeaux, France (in French).

- Ledergerber, J., Pieper, L., Binet, G., Comeau, A., Maruéjols, T., Muschalla, D., and Vanrolleghem, P. (2019a). An efficient and structured procedure to develop conceptual catchment and sewer models from their detailed counterparts. *Water*, 11(10):2000.
- Ledergerber, J. M., Leray, É., Maruéjols, T., and Vanrolleghem, P. A. (2017a). Optimization of installation and maintenance of water quality sensors in combined sewers. In *Proceedings of the 14th IWA/IHAR International Conference on Urban Drainage (ICUD2017)*, Prague, Czech Republic, September 10-15 2017.
- Ledergerber, J. M., Maruéjols, T., and Vanrolleghem, P. A. (2019b). No-regret selection of effective control handles for integrated urban wastewater systems management under parameter and input uncertainty. In *Proceedings of the 10th IWA Symposium on Modelling and Integrated Assessment (Watermatex 2019)*, Copenhagen, Denmark, September 1-4 2019.
- Ledergerber, J. M., Maruéjols, T., and Vanrolleghem, P. A. (2019c). Optimal experimental design for calibration of a new sewer water quality model. *J. Hydrol.*, 574:1020–1028.
- Ledergerber, J. M., Maruéjols, T., Aaron, C., Alferes, J., Plana, Q., Tik, S., and Vanrolleghem, P. A. (2017b). Validation of an online water quality monitoring methodology for sewer systems of mid-size cities. In *Proceedings of the 23rd EJSW – Monitoring urban drainage systems*, Chichilianne, France, May 15-20 2017.
- Ledergerber, J. M., Tik, S., Maruéjols, T., and Vanrolleghem, P. A. (2019d). A validated conceptual sewer water quality model based on the particle settling velocity distribution. In *Proceedings of the 9th International Conference on Sewer Processes and Networks (SPN)*, Aalborg, Denmark, August 27-31 2019.
- Lessard, P. (1989). *Operational water quality management: Control of stormwater discharges*. PhD thesis, Imperial College London, London, UK.
- Lessard, P. and Beck, M. B. (1990). Operational water quality management: Control of storm sewage at a wastewater treatment plant. *Res. J. Water Pollut. Control*, 62(6):810–819.
- Leutnant, D., Muschalla, D., and Uhl, M. (2018). Statistical distribution of TSS event loads from small urban environments. *Water*, 10(6):769.
- Lijklema, L., Tyson, J., and Lesouef, A. (1993). Interactions between sewers, treatment plants and receiving waters in urban areas: A summary of the INTERURBA '92 workshop conclusions. *Water Sci. Technol.*, 27(12):1–29.
- Lin, H. (2003). *Granulometry, chemistry and physical interactions of non-colloidal particulate matter transported by urban storm water*. PhD thesis, Louisiana State University, USA.
- Lindholm, O. (1985). May retention basins have an overall negative effect? *Vatten*, 41:214–217.

- Lund, N. S. V., Falk, A. K. V., Borup, M., Madsen, H., and Mikkelsen, P. S. (2018). Model predictive control of urban drainage systems: A review and perspective towards smart real-time water management. *Crit. Rev. Env. Sci. Tec.*, 48(3):279–339.
- Ly, D. K. (2019). *Water Quality-Based Real Time Control of Combined Sewer Systems*. PhD thesis, Université de Lyon - INSA Lyon, France.
- Machac, D., Reichert, P., and Albert, C. (2016). Emulation of dynamic simulators with application to hydrology. *J. Comput. Phys.*, 313:352–366.
- Mahmoodian, M., Delmont, O., and Schutz, G. (2017). Pollution-based model predictive control of combined sewer networks, considering uncertainty propagation. *Int. J. Sus. Dev. Plann.*, 12(1):98–111.
- Maidment, D. R. (1993). *Handbook of Hydrology*. McGraw-Hill, New York, USA.
- Männig, F. and Lindenberg, M. (2013). Betriebserfahrungen mit der Abflusssteuerung des Dresdner Mischwassernetzes. *Korrespondenz Abwasser*, 12:1036–1043 (in German).
- Mannina, G., Butler, D., Benedetti, L., Deletic, A., Fowdar, H., Fu, G., Kleidorfer, M., McCarthy, D., Mikkelsen, P. S., Rauch, W., Sweetapple, C., Vezzaro, L., Yuan, Z., and Willems, P. (2018). Greenhouse gas emissions from integrated urban drainage systems: Where do we stand? *J. Hydrol.*, 559:307–314.
- Mannina, G. and Viviani, G. (2010). An urban drainage stormwater quality model: Model development and uncertainty quantification. *J. Hydrol.*, 381:248–265.
- Maruėjouls, T., Lessard, P., and Vanrolleghem, P. A. (2014). Calibration and validation of a dynamic model for water quality in combined sewer retention tanks. *Urban Water J.*, 11(8):668–677.
- Maruėjouls, T., Lessard, P., and Vanrolleghem, P. A. (2015). A particle settling velocity-based integrated model for dry and wet weather wastewater quality modeling. In *Proceedings of the WEF Collection Systems Conference*, Cincinnati, Ohio, United States, April 19-22 2015.
- Maruėjouls, T., Lessard, P., Wipliez, B., Pelletier, G., and Vanrolleghem, P. A. (2011). Characterization of the potential impact of retention tank emptying on wastewater primary treatment: a new element for cso management. *Water Sci. Technol.*, 64(9):1898–1905.
- Maruėjouls, T., Vanrolleghem, P. A., Pelletier, G., and Lessard, P. (2012). A phenomenological retention tank model using settling velocity distributions. *Water Res.*, 46(20):6857–6867.
- Mattsson, J., Hedström, A., Ashley, R. M., and Viklander, M. (2015). Impacts and managerial implications for sewer systems due to recent changes to inputs in domestic wastewater – a review. *J. Environ. Manage.*, 161:188–197.

- Mehler, R. (2000). Mischwasserbehandlung – Verfahren und Modellierung. *Mitteilungen des Institutes für Wasserbau und Wasserwirtschaft, TU Darmstadt*, Heft 113 (in German).
- Mehra, R. K. (1974). Optimal input signals for parameter estimation in dynamic systems—survey and new results. *IEEE Transactions on Automatic Control*, 19(6):753–768.
- Meirlaen, J. (2002). *Immission based real-time control of the integrated urban wastewater system*. PhD thesis, Universiteit Gent, Belgium.
- Meirlaen, J., Van Assel, J., and Vanrolleghem, P. A. (2002). Real time control of the integrated urban wastewater system using simultaneously simulating surrogate models. *Water Sci. Technol.*, 45(3):109–116.
- Michelbach, S. (1995). Origin, resuspension and settling characteristics of solids transported in combined sewage. *Water Sci. Technol.*, 31(7):69–76.
- Milina, J., Sægrov, S., Lei, J., König, A., Nilssen, O., Ellingsson, A., Alex, J., and Schilling, W. (1999). Improved interception of combined sewage in the Trondheim-Høvringen wastewater system. *Water Sci. Technol.*, 39(2):159–168.
- Mohtar, W. H. M. W., Afan, H., El-Shafie, A., Bong, C. H. J., and Ghani, A. A. (2018). Influence of bed deposit in the prediction of incipient sediment motion in sewers using artificial neural networks. *Urban Water J.*, 15(4):296–302.
- Mollerup, A. L., Grum, M., Muschalla, D., Van Velzen, E., Vanrolleghem, P., Mikkelsen, P., and G., S. (2013). Integrated control of the wastewater system: Potential and barriers. *Water 21*, pages 39–41.
- “Météo France” (2019). Pluies extrêmes en france métropolitaine. Retrieved November 11, 2019, from <http://pluiesextremes.meteo.fr/france-metropole/-Evenements-memorables.html>.
- Mugume, S. N., Diao, K., Astaraie-Imani, M., Fu, G., Farmani, R., and Butler, D. (2015). Enhancing resilience in urban water systems for future cities. *Water Sci. Technol.*, 15(6):1343–1352.
- Murali, M. K., Hipsey, M. R., Ghadouani, A., and Yuan, Z. (2019). The development and application of improved solids modelling to enable resilient urban sewer networks. *J. Environ. Manage.*, 240:219–230.
- Muschalla, D. (2008). Optimization of integrated urban wastewater systems using multi-objective evolution strategies. *Urban Water J.*, 5(1):59–67.
- Muschalla, D., Hofer, T., Maier, R., Rieger, L., Schraa, O., and Gruber, G. (2015a). Development of an innovative concept for building integrated urban water models. In *Proceedings*

- of the 10th International Conference on Urban Drainage Modelling, Quebec, Canada, September 20-23 2015.
- Muschalla, D., Leimgruber, J., Maier, R., Tscheikner-Gratl, F., Kleidorfer, M., Wolfgang, R., Ertl, T., Kretschmer, F., Sulzbacher, R., and Neunteufel, R. (2015b). *DATMOD - Sanierungs- und Anpassungsplanung von kleinen und mittleren Kanalnetzen*. Bundesministerium für Land- und Forstwirtschaft, Umwelt und Wasserwirtschaft, Österreich. (in German).
- Muschalla, D., Schütze, M., Schroeder, K., Bach, M., Blumensaat, F., Gruber, G., Klepizewski, K., Pabst, M., Pressl, A., Schindler, N., Solvi, A.-M., and Wiese, J. (2009). The HSG procedure for modelling integrated urban wastewater systems. *Water Sci. Technol.*, 60(8):2065–2075.
- Muschalla, D., Vallet, B., Anctil, F., Lessard, P., Pelletier, G., and Vanrolleghem, P. A. (2014). Ecohydraulic-driven real-time control of stormwater basins. *J. Hydrol.*, 511:82–91.
- Neumann, M. B., Rieckermann, J., Hug, T., and Gujer, W. (2015). Adaptation in hindsight: Dynamics and drivers shaping urban wastewater systems. *J. Environ. Manage.*, 151:404–415.
- Nopens, I., Benedetti, L., Jeppsson, U., Pons, M.-N., Alex, J., Copp, J. B., Gernaey, K. V., Rosen, C., Steyer, J.-P., and Vanrolleghem, P. A. (2010). Benchmark Simulation Model No 2: Finalisation of plant layout and default control strategy. *Water Sci. Technol.*, 62(9):1967–1974.
- Penn, R., Schütze, M., Jens, A., and Friedler, E. (2018). Tracking and simulation of gross solids transport in sewers. *Urban Water J.*, 15(6):1–8.
- Philippe, R. (2019). Outils automatiques d'évaluation de la qualité des données pour le suivi en continu de la qualité des eaux usées. Master's thesis, Université Laval, Québec, QC, Canada (in French).
- Pieper, L. (2017). Development of a model simplification procedure for integrated urban water system models - conceptual catchment and sewer modelling. Master's thesis, Université Laval, Québec, QC, Canada.
- Pikaar, I., Sharma, K. R., Hu, S., Gernjak, W., Keller, J., and Yuan, Z. (2014). Reducing sewer corrosion through integrated urban water management. *Science*, 345(6198):812–814.
- Plana, Q. (2015). Automated data collection and management at enhanced lagoons for wastewater treatment. Master's thesis, Université Laval, Québec, Canada.
- Plana, Q. (2019). *Characterization and modelling of grit chambers based on particle settling velocity distributions*. PhD thesis, Université Laval, Québec, Canada.

- Plana, Q., Carpentier, J., Tardif, F., Pauleat, A., Gadbois, A., Lessard, P., and Vanrolleghem, P. A. (2018). Grit particle characterization: Study of the settleability. In *Proceedings 91st Annual WEF Technical Exhibition and Conference (WEFTEC2018)*, New Orleans, LA, USA, September 29 - October 3 2018.
- Pleau, M., Colas, H., Lavallée, P., Pelletier, G., and Bonin, R. (2005). Global optimal real-time control of the Québec urban drainage system. *Environ. Modell. Softw.*, 20(4):401–413.
- Prat, P., Benedetti, L., Corominas, L., Comas, J., and Poch, M. (2012). Model-based knowledge acquisition in environmental decision support system for wastewater integrated management. *Water Sci. Technol.*, 65(6):1123–1129.
- Puig, V., Cembrano, G., Romera, J., Quevedo, J., Aznar, B., Ramón, G., and Cabot, J. (2009). Predictive optimal control of sewer networks using CORAL tool: Application to Riera Blanca catchment in Barcelona. *Water Sci. Technol.*, 60(4):869–878.
- Qasim, S. R. (2017). *Wastewater treatment plants: planning, design, and operation*. Routledge, Abingdon, UK.
- Rauch, W., Aalderink, H., Krebs, P., Schilling, W., and Vanrolleghem, P. (1998). Requirements for integrated wastewater models - driven by receiving water objectives. *Water Sci. Technol.*, 38(11):97–104.
- Rauch, W., Bertrand-Krajewski, J.-L., Krebs, P., Mark, O., Schilling, W., Schütze, M., and Vanrolleghem, P. A. (2002). Deterministic modelling of integrated urban drainage systems. *Water Sci. Technol.*, 45(3):81–94.
- Rauch, W., Seggelke, K., Brown, R., and Krebs, P. (2005). Integrated approaches in urban storm drainage: Where do we stand? *Environ. Manage.*, 35(4):396–409.
- Refsgaard, J. C., Henriksen, H. J., Harrar, W. G., Scholten, H., and Kassahun, A. (2005). Quality assurance in model based water management - review of existing practice and outline of new approaches. *Environ. Model. Softw.*, 20(10):1201–1215.
- Refsgaard, J. C., van der Sluijs, J. P., Højberg, A. L., and Vanrolleghem, P. A. (2007). Uncertainty in the environmental modelling process - a framework and guidance. *Environ. Model. Softw.*, 22(11):1543–1556.
- Regneri, M., Klepiszewski, K., Ostrowski, M., and Vanrolleghem, P. A. (2010). Fuzzy decision making for multi-criteria optimization in integrated wastewater system management. In *Proceedings of the 6th International Conference on Sewer Processes and Networks (SPN)*, Surfers Paradise, Gold Coast, Australia, November 7-10 2010.
- Rieger, L., Gillot, S., Langergraber, G., Ohtsuki, T., Shaw, A., Takacs, I., and Winkler, S. (2012). *Guidelines for Using Activated Sludge Models*. IWA Publishing, London, UK.

- Rieger, L. and Vanrolleghem, P. A. (2008). mon*EAU*: A platform for water quality monitoring networks. *Water Sci. Technol.*, 57(7):1079–1086.
- Rogerson, P. A. (2014). *Statistical methods for geography: a student's guide*. Sage Publications, London, UK.
- Rosen, C., Jeppsson, U., and Vanrolleghem, P. (2004). Towards a common benchmark for long-term process control and monitoring performance evaluation. *Water Sci. Technol.*, 50(11):41–49.
- Ruban, G., Mabilais, D., and Lemaire, K. (2015). Particle characterization of urban wet-weather discharges: Methods and related uncertainties. *Urban Water J.*, 12(5):404–413.
- Saagi, R., Flores-Alsina, X., Kroll, S., Gernaey, K., and Jeppsson, U. (2017). A model library for simulation and benchmarking of integrated urban wastewater systems. *Environ. Model. Softw.*, 93:282–295.
- Saagi, R., Kroll, S., Flores-Alsina, X., Gernaey, K. V., and Jeppsson, U. (2018). Key control handles in integrated urban wastewater systems for improving receiving water quality. *Urban Water J.*, 15(8):790–800.
- Saltelli, A., Ratto, M., Andres, T., Campolongo, F., Cariboni, J., Gatelli, D., Saisana, M., and Tarantola, S. (2008). *Global Sensitivity Analysis: The Primer*. John Wiley & Sons, West Sussex, UK.
- Schmitt, T. and Huber, W. (2006). The scope of integrated modelling: System boundaries, sub-systems, scales and disciplines. *Water Sci. Technol.*, 54(6-7):405–413.
- Scholten, H., Kassahun, A., Refsgaard, J. C., Kargas, T., Gavardinas, C., and Beulens, A. J. (2007). A methodology to support multidisciplinary model-based water management. *Environ. Model. Softw.*, 22(5):743–759.
- Schütze, M., Lange, M., Pabst, M., and Haas, U. (2018). Astlingen – a benchmark for real time control (RTC). *Water Sci. Technol.*, 2017(2):552–560.
- Schütze, M., Seidel, J., Chamorro, A., and León, C. (2019). Integrated modelling of a megacity water system – the application of a transdisciplinary approach to the lima metropolitan area. *J. Hydrol.*, 573:983–993.
- Schulz, N., Baur, R., and Krebs, P. (2005). Integrated modelling for the evaluation of infiltration effects. *Water Sci. Technol.*, 52(5):215–223.
- Schütze, M., Butler, D., and Beck, M. B. (1999). Optimisation of control strategies for the urban wastewater system – An integrated approach. *Water Sci. Technol.*, 39(9):209–216.

- Seggelke, K., Fuchs, L., Alt, K., Wu, X., and Hennings, J. (2017). Systemoptimierung versus Neubau von Beckenvolumen auf der Zentralkläranlage Lemgo. *Korrespondenz Abwasser*, 64(1):33–39 (in German).
- Seggelke, K., Löwe, R., Beeneken, T., and Fuchs, L. (2013). Implementation of an integrated real-time control system of sewer system and waste water treatment plant in the city of Wilhelmshaven. *Urban Water J.*, 10(5):330–341.
- Seggelke, K., Rosenwinkel, K., Vanrolleghem, P. A., and Krebs, P. (2005). Integrated operation of sewer system and WWTP by simulation-based control of the WWTP inflow. *Water Sci. Technol.*, 52(5):195–203.
- Sharma, A., Alferes, J., Vezzaro, L., Lamaire-Chad, C., Thirsing, C., Vanrolleghem, P., and Mikkelsen, P. (2013). Effect of on/off pumping strategy on sewer sediment behaviour elucidated by high frequency monitoring at the treatment plant inlet. In *Proceedings of the 7th International Conference on Sewer Processes and Networks (SPN)*, Sheffield, United Kingdom, August 28-30 2013.
- Sharma, K. R., Corrie, S., and Yuan, Z. (2012). Integrated modelling of sewer system and wastewater treatment plant for investigating the impacts of chemical dosing in sewers. *Water Sci. Technol.*, 65(8):1399–1405.
- Shishegar, S., Duchesne, S., and Pelletier, G. (2019). An integrated optimization and rule-based approach for predictive real time control of urban stormwater management systems. *J. Hydrol.*, 577:983–993.
- Sin, G., De Pauw, D. J., Weijers, S., and Vanrolleghem, P. A. (2008). An efficient approach to automate the manual trial and error calibration of activated sludge models. *Biotechnol. Bioeng.*, 100(3):516–528.
- Solvi, A.-M. (2006). *Modelling the Sewer-Treatment-Urban River System in View of the EU Water Framework Directive*. PhD thesis, Ghent University, Belgium.
- Solvi, A. M., Schosseler, P. M., and Vanrolleghem, P. (2008). Combined immission-emission based evaluation of integrated urban wastewater system scenarios. In *Proceedings of the 11th International Conference on Urban Drainage (ICUD2008)*, Edinburgh, Scotland, United Kingdom, August 31 - September 5, 2008.
- Sweetapple, C., Fu, G., and Butler, D. (2014). Identifying sensitive sources and key control handles for the reduction of greenhouse gas emissions from wastewater treatment. *Water Res.*, 62:249–259.
- Takács, I., Patry, G. G., and Nolasco, D. (1991). A dynamic model of the clarification-thickening process. *Water Res.*, 25(10):1263–1271.

- Tchobanoglous, G., Burton, F. L., and Stensel, H. D. (2004). *Wastewater Engineering: Treatment and Reuse*. McGraw-Hill, New York, USA, 4th edition.
- Tik, S., Bachis, G., Maruéjols, T., Charette, S., Lessard, P., and Vanrolleghem, P. A. (2016a). A CEPT model based on particle settling velocity distributions. In *Proceedings of the IWA Particle Separation Conference (PS 2016)*, Oslo, Norway, June 22-24 2016.
- Tik, S., Maruéjols, T., Bachis, G., Vallet, B., Lessard, P., and Vanrolleghem, P. A. (2014a). Using particle settling velocity distribution to better model the fate of stormwater TSS throughout the integrated urban wastewater system. *Influents*, 9:48–52.
- Tik, S., Maruéjols, T., Lessard, P., and Vanrolleghem, P. A. (2014b). Optimising wastewater management during wet weather using an integrated model. In *Proceedings of the 13th International Conference on Urban Drainage (ICUD2014)*, Kuching, Sarawak, Malaysia, September 7-12 2014.
- Tik, S., Maruéjols, T., Lessard, P., and Vanrolleghem, P. A. (2015). Gestion optimale de la vidange des bassins de rétention en réseau unitaire à l'aide d'un modèle intégré. *Houille Blanche*, -(3):44–50 (in French).
- Tik, S., Maruéjols, T., Lessard, P., and Vanrolleghem, P. A. (2016b). Estimating and minimizing both cso and wrrf discharge impact by water quality based control. In *Proceedings of the WEF Collection Systems Conference 2016*, Atlanta, GA, USA, May 1-4 2016.
- Tik, S. and Vanrolleghem, P. A. (2017). Chemically enhancing primary clarifiers: model-based development of a dosing controller and full-scale implementation. *Water Sci. Technol.*, 75(5):1185–1193.
- Tränckner, J., Bönisch, G., Gebhard, V. R., Dirckx, G., and Krebs, P. (2008). Model-based assessment of sediment sources in sewers. *Urban Water J.*, 5(4):277–286.
- Tränckner, J., Franz, T., Seggelke, K., and Krebs, P. (2007). Dynamic optimisation of WWTP inflow to reduce total emission. *Water Sci. Technol.*, 56(10):11–18.
- United Nations (2019). "Sustainable Development Goals". Retrieved September 27, 2019, from <https://www.un.org/sustainabledevelopment/sustainable-development-goals/>.
- Vallet, B., Lessard, P., and Vanrolleghem, P. A. (2016). A storm water basin model using settling velocity distribution. *J. Environ. Eng. Sci.*, 11:84–95.
- van Daal, P., Gruber, G., Langeveld, J., Muschalla, D., and Clemens, F. (2017). Performance evaluation of real time control in urban wastewater systems in practice: Review and perspective. *Environ. Model. Softw.*, 95:90–101.

- Vaneeckhaute, C., Meers, E., Michels, E., Ghekiere, G., Accoe, F., and Tack, F. (2013). Closing the nutrient cycle by using bio-digestion waste derivatives as synthetic fertilizer substitutes: A field experiment. *Biomass Bioenerg.*, 55:175–189.
- Vanrolleghem, P., Rosen, C., Zaher, U., Copp, J., Benedetti, L., Ayesa, E., and Jeppsson, U. (2005a). Continuity-based interfacing of models for wastewater systems described by Petersen matrices. *Water Sci. Technol.*, 52(1-2):493–500.
- Vanrolleghem, P. A., Benedetti, L., and Meirlaen, J. (2005b). Modelling and real-time control of the integrated urban wastewater system. *Environ. Model. Softw.*, 20(4):427–442.
- Vanrolleghem, P. A. and Coen, F. (1995). Optimal design of in-sensor-experiments for on-line modelling of nitrogen removal processes. *Water Sci. Technol.*, 31(2):149–160.
- Vanrolleghem, P. A., Daele, M. V., and Dochain, D. (1995). Practical identifiability of a biokinetic model of activated sludge respiration. *Water Res.*, 29(11):2561–2570.
- Vanrolleghem, P. A., Fronteau, C., and Bauwens, W. (1996). Evaluation of design and operation of the sewage transport and treatment system by an EQO/EQS based analysis of the receiving water immission characteristics. In *Proceedings WEF Speciality Conference Series – Urban Wet Weather Pollution – Controlling Sewer Overflows and Stormwater Runoff*, Québec, Québec, Canada, June 16-19 1996.
- Vanrolleghem, P. A., Kamradt, B., Solvi, A.-M., and Muschalla, D. (2009). Making the best of two hydrological flow routing models: Nonlinear outflow-volume relationships and backwater effects model. In *Proceedings of the 8th International Conference on Urban Drainage Modelling*, Tokyo, Japan, September 7-11 2009.
- Vanrolleghem, P. A., Mannina, G., Cosenza, A., and Neumann, M. B. (2015). Global sensitivity analysis for urban water quality modelling: Terminology, convergence and comparison of different methods. *J. Hydrol.*, 522:339–352.
- Vanrolleghem, P. A., Schilling, W., Rauch, W., Krebs, P., and Aalderink, H. (1999). Setting up measuring campaigns for integrated wastewater modelling. *Water Sci. Technol.*, 39(4):257–268.
- Vanrolleghem, P. A., Tik, S., and Lessard, P. (2018). Advances in modelling particle transport in urban storm- and wastewater systems. In *Proceedings of the 11th International Conference on Urban Drainage*, Palermo, Italy, September 23-26 2018.
- Vezzaro, L. and Grum, M. (2014). A generalised dynamic overflow risk assessment (DORA) for real time control of urban drainage systems. *J. Hydrol.*, 515:292–303.
- Weinreich, G., Schilling, W., Birkely, A., and Moland, T. (1997). Pollution based real time control strategies for combined sewer systems. *Water Sci. Technol.*, 36(8-9):331–336.

- Willems, P. (2008). Quantification and relative comparison of different types of uncertainties in sewer water quality modeling. *Water Res.*, 42(13):3539–3551.
- Wolfs, V. (2016). *Conceptual model structure identification and calibration for river and sewer systems*. PhD thesis, KU Leuven, Belgium.
- Wolfs, V., Meert, P., and Willems, P. (2015). Modular conceptual modelling approach and software for river hydraulic simulations. *Environ. Model. Softw.*, 71:60–77.
- Wolfs, V., Villazon, M. F., and Willems, P. (2013). Development of a semi-automated model identification and calibration tool for conceptual modelling of sewer systems. *Water Sci. Technol.*, 68(1):167–175.
- Wong, K. B. and Piedrahita, R. H. (2000). Settling velocity characterization of aquacultural solids. *Aquacult. Eng.*, 21(4):233–246.
- World Commission on Environment and Development (WCED), United Nations (1987). Our common future.
- Zhu, Z., Oberg, N., Morales, V. M., Quijano, J. C., Landry, B. J., and Garcia, M. H. (2016). Integrated urban hydrologic and hydraulic modelling in Chicago, Illinois. *Environ. Model. Softw.*, 77:63–70.